Genetic Control of Photoperiod Responsiveness in Pea

By

Lim Chee Liew

B. Biotech. (Hons)

Submitted in the fulfilment of the requirements for

the Degree of Doctor of Philosophy

June 2011

University of Tasmania

Declaration and statements

Declaration of originality

This thesis contains no material which has been accepted for a degree or diploma by the University or any other institution, except by way of background information and duly acknowledged in the thesis, and to the best of the my knowledge and belief no material previously published or written by another person except where due acknowledgement is made in the text of the thesis, nor does the thesis contain any material that infringes copyright.

Access statement

This thesis may be made available for loan. Copying of any part of this thesis is prohibited for two years from the date this statement was signed; after that time limited copying is permitted in accordance with the Copyright Act 1968.

Statement regarding published work

The publishers of the papers comprising part of Chapters 3 and 4 hold the copyright for that content, and access to the material should be sought from the respective journals. The full publications are included at the back of this thesis as references. Contribution of peoples and institutions to specific experiments are outlined in individual chapters.

Lim Chee Liew Date

Acknowledgement

I would like to sincerely thank all the people who made this thesis possible. I wish to express my deepest gratitude, first and foremost, to my supervisors Dr. Jim Weller and Dr. Valérie Hecht. It has been an honour to be their PhD student, they has made their continuous support of my PhD study. I am indebted to Dr. Jim Weller for his patience, motivation, and enthusiasm throughout the research and during the writing of the thesis. I would like to thank my enthusiastic supervisor, Dr. Valérie Hecht, whose guidance and support in the lab enabled me to develop skills and interests to molecular works.

I am grateful to Jackie Vander Schoor for her support as a friend and assistance in the glasshouse. I would also like to acknowledge the help of Ian Cummings and Tracey Winterbottom for glasshouse maintenance and plant husbandry, and Adam Smolenski for his technical support in the Genetics lab. Clancy Carver, Catherine Jones, and Jodi Noble are thanked for their administrative assistance in the School of Plant Science. It is a pleasure to thank everyone from School of Plant Science who has made it a happy and pleasant place to work. In addition, I would like to specially thank Prof. David Bowman, Assoc. Prof. Réne Vaillancourt, and Dr. Rob Wiltshire who gave me the opportunity to work with them in research and teaching.

I wish to thank my family who have given me the chance to further my education overseas and have forgiven my absence from many family events. I have to say a warm thank you to my fellow students and friends for their company to make my PhD journey not a lonely one. I dedicate this thesis to my beloved partner, Jeffrey Ong for his endless support and encouragement and always believing in me.

The last but not least, the financial support of Endeavour International Postgraduate Research Scholarship and School of Plant Science is greatly acknowledged.

Abbreviations

Acronym	Full-name
ACT	*ACTIN*
AGL24	*AGAMOUS-LIKE 24*
AP1	*APETALA*
ATC	*ARABIDOPSIS THALIANA CENTRORADIALIS*
BFT	*BROTHER OF FT AND TFL1*
CAB9	*CHLOROPHYLL-A-BINDING PROTEIN 9*
CAL	*CAULIFLOWER*
CCA1	*CIRCADIAN CLOCK-ASSOCIATED 1*
CCL	*CCR-LIKE*
CCR2	*COLD CIRCADIAN RHYTHM RNA BINDING 2*
CCT	Constans, Constans-like, TOC1
CDF1	*CYCLING DOF FACTOR 1*
cDNA	Complementary Deoxyribonucleic acid
CHE	*CCA1 HIKING EXPEDITION*
CO	*CONSTANS*
COP1	*CONSTITUTIVE PHOTOMORPHOGENIC 1*
CRY	Crytochromes
CTAB	Cetyl trimethylammonium bromide
DD	Constant dark
DNA	Deoxyribonucleic acid
DNE	*DIE NEUTRALIS*
E	*EARLY INITIATING*
ELF3	*EARLY FLOWERING 3*
ELF4	*EARLY FLOWERING 4*
EMS	Ethyl methanesulfonate

EST	Expressed Sequence Tag
FIO1	*FIONA1*
FKF1	*FLAVIN BINDING KELCH F BOX 1*
FLC	*FLOWERING LOCUS C*
FLD	*FLOWERING LOCUS D*
FLK	*FLOWERING LATE WITH KH MOTIFS*
FRI	*FRIGIDA*
FT	*FLOWERING LOCUS T*
FTL	*FT*-like
FUL	*FRUITFULL*
FUN1	*FAR-RED UNRESPONSIVE*
GA	GIBBERELLINS
GAI	*GIBBERELLIC ACID INSENSITIVE*
GI	*GIGANTEA*
Hd1	*HEADING DATE 1*
Hd3a	*HEADING DATE 3a*
HOS1	*HIGH EXPRESSION OF OSMOTICALLY RESPONSIVE GENE 1*
HR	*HIGH RESPONSE*
L1-9	Internode length between node 1 and node 9
LATE	*LATE BLOOMER*
LD	Long day
LD	*LUMINIDEPENDENS*
LF	*LATE FLOWERING*
LFY	*LEAFY*
LHP1	*LIKE HETEROCHROMATIN PROTEIN 1*
LHY	*ELONGATED HYPOCOTYL*
LIP1	*LIHGT INSENSITIVE PERIOD 1*
LKP2	*LOV KELCH PROTEIN 2*
LL	Constant light

LUX	*LUX ARRHYTHMO*
MFT	*MOTHER OF FT AND TFL1*
miRNA	MicroRNA
NFI	Node of first flower initiation
PCR	Polymerase Chain Reaction
PHOT	Phototrophins
PHY	Phytochromes
PIE	*PHOTOPERIOD-INDEPENDENT EARLY FLOWERING 1*
PIF3	*PHYTOCHROME INTERACTING FACTOR 3*
PIM	*PROLIFERATING INFLORESCENCE MERISTEM*
PPD	*PHOTOPERIOD*
PR	Pseudo Receiver
PRR	*PREUDO RESPONSE REGULATOR*
RACE	Rapid Amplification of cDNA Ends
RFI2	*RED AND FAR-RED INSENSITIVE 2*
RGA	*REPRESSOR OF GAI-3*
RN	Reproductive node
RNA	Ribonucleic acid
RT-PCR	Real time PCR
SD	Short day
SEN1	*SENESCENCE ASSOCIATED GENE 1*
SN	*STERILE NODE*
SOC1	*SUPPRESSOR OF OVEREXPRESSION OF CO 1*
SPA1	*SUPPRESSOR OF PHYA 1*
SPY	*SPINDLY*
SRR1	*SENSITIVITY TO RED LIGHT INDUCED*
SVP	*SHORT VEGETATIVE PHASE*
TBL	Total lateral branch length
TFL1	*TERMINAL FLOWER 1*

TIC	*TIME FOR COFFEE*
TN	Total number of nodes
TOC1	*TIMING OF CAB EXPRESSION 1*
TPH	Total plant height
TSF	*TWIN SISTER OF FT*
VEG1	*VEGETATIVE 1*
VEG2	*VEGETATIVE 2*
VGT1	*VEGETATIVE TO GENERATIVE TRANSITION 1*
VIN3	*VERNALISATION INSENSITIVE 3*
VIP	*VERNALISATION INDEPENDENCE*
VRN1	*VERNALISATION 1*
VRN2	*VERNALISATION 2*
WT	Wild type
XCT	*XAP5 CIRCADIAN TIMEKEEPER*
ZT	Zeitgeber time
ZTL	*ZELTLUPE*

Abstract

The change from vegetative to reproductive growth is one of the most important transitions in the life of a plant, and the precise timing of flowering is critical to maximise reproductive success. Flowering time is therefore regulated by many different environmental cues, including daylength and temperature, and responsiveness to these factors determines the geographic and seasonal range of many crop species. The genetic control of flowering time has been well-characterised in the model species, *Arabidopsis thaliana* and this has identified many of the molecular mechanisms by which flowering time is regulated by environmental and endogenous signals. More recently, research on other species has begun to show how these mechanisms differ in different species and varieties that respond differently to photoperiod changes.

The legumes are a large and agriculturally important plant group that includes crop species such as lentils, beans, chickpea, peanut, clover, alfalfa, and soybean. In several of these species, genetic loci have been identified with a function in regulation of flowering time and photoperiod responsiveness and in many cases, natural allelic variation at these loci are important in classical breeding programs to improve crop performance. In garden pea (*Pisum sativum* L.), recessive alleles at several different loci result in early flowering and a loss of photoperiod sensitivity. These include two loci, *STERILE NODE* (*SN*) and *HIGH RESPONSE* (*HR*) first defined in studies of naturally-occurring variation, and two others, *DIE NEUTRALIS* (*DNE*) and *PHOTOPERIOD* (*PPD*), defined by studies of induced mutants. Phenotypic

comparisons with Arabidopsis photoperiod-response mutants suggested that all four loci might participate in circadian clock function, a conclusion supported by a preliminary analysis of diurnal rhythms of gene expression.

The overall aim of the research in this thesis was to discover the molecular identity of *DNE, SN, PPD,* and *HR* and hence to better understand their roles in the circadian clock and photoperiodic control of flowering. A 'positional candidate' approach was taken, in which pea homologs of Arabidopsis circadian clock-related genes were isolated and assessed as candidates on the basis of map position and through phenotypic comparisons with Arabidopsis. The availability of extensive *Medicago truncatula* genome sequence and the close synteny between Medicago and pea greatly assisted the identification process of pea clock gene isolation, and the use of primers directly based on Medicago sequence proved to be highly successful for pea gene isolation.

Using this approach, pea sequence of several clock-related genes were isolated or extended, including *EARLY FLOWERING 4* (*ELF4*), *EARLY FLOWERING 3* (*ELF3*), *LUX ARRHYTHMO* (*LUX*), and *TIME FOR COFFEE* (*TIC*), and components of gene families of *CIRCADIAN CLOCK-ASSOCIATED 1* (*CCA1*) /*ELONGATED HYPOCOTYL* (*LHY*) and *PSEUDO RESPONSE REGULATOR* (*PRR*). This demonstrates that the majority of Arabidopsis clock-related genes are present in pea, although in some cases gene families differ in size. Most pea genes show diurnal expression patterns similar to their Arabidopsis homologs suggesting they may function in a similar way. Map positions ruled out several genes as candidates for the photoperiod loci, but identified several others as strong candidates. Further analysis

resulted in identification of *DNE*, *SN*, and *HR* as orthologs of Arabidopsis clock genes, *ELF4*, *LUX*, and *ELF3* respectively.

The *HR* locus in particular is considered to be to be one of the most important loci controlling photoperiod responsiveness in cultivated pea germplasm, and sequence diversity at *HR* was examined across a range of accessions. A single-nucleotide indel in *HR* was correlated with photoperiod responsiveness and the difference between spring and winter pea cultivars. Analysis of circadian rhythms of clock gene expression in our standard wild-type, NGB5839 revealed damped circadian rhythms under constant light but not constant dark. This line, likes many other spring cultivars carries loss-of-function alleles at *HR/PsELF3*. This demonstrates that other flowering mutants in the NGB5839 background, including *dne*, *sn*, and *ppd*, are all effectively double mutants, which is likely to explain the subtle effects on diurnal and circadian rhythms of clock gene expression in these mutants. Finally, the pathway through which *DNE*, *SN*, *PPD* and *HR* act to control flowering was also investigated by grafting experiments and expression analysis of genes in the *CO* and *FT* families. In *dne*, *sn*, and *ppd* mutants, the early flowering phenotypes were found to be associated with elevated expression of several *FT* genes, but these mutants showed no alterations on diurnal expression of *CO*-like genes.

Collectively, these detailed physiological, genetic and molecular analyses of *DNE*, *SN*, *PPD*, and *HR* have revealed the importance of the circadian clock for photoperiodic responsiveness in pea.

Contents

DECLARATION AND STATEMENTS I

ACKNOWLEDGEMENT II

ABBREVIATIONS III

ABSTRACT VII

CHAPTER 1 GENERAL INTRODUCTION: GENETIC CONTROL OF FLOWERING TIME

1.1. Importance of flowering time **1**

1.2. Environmental regulation of flowering **2**

1.2.1. Florigen and the FT gene family *4*

1.2.2. Photoperiod pathway *6*

1.2.3. Vernalisation and autonomous pathway *6*

1.2.4. Gibberellins pathway *9*

1.2.5. Other integrators *10*

1.3. The circadian clock and the response to photoperiod in Arabidopsis **12**

1.3.1. The core oscillator *15*

1.3.2. Input pathways *20*

1.3.3. Output pathways: Photoperiodic control of flowering by circadian clock via CONSTANS *24*

1.3.4. Regulation of other output pathways *28*

1.4. Flowering and circadian clock genes in other species **30**

1.5. Flowering regulatory pathways in *Pisum sativum* **33**

1.6. Aims **38**

CHAPTER 2 GENERAL MATERIALS AND METHODS **39**

2.1. Plant materials **39**

2.2. Plant growth conditions and general husbandry 39

2.3. Scoring of phenotypic traits 40

2.4. Grafting 42

2.5. Bioinformatics and genetics analysis 42

2.6. Primers 43

2.7. Gene isolation 43

2.7.1. DNA extraction 43
2.7.2. DNA Quantification 44
2.7.3. Polymerase Chain Reaction (PCR) 44
2.7.4. Cloning 45
2.7.5. Colony PCR 45
2.7.6. Plasmid DNA extraction 45
2.7.7. Rapid Amplification of cDNA Ends (RACE) PCR 46
2.7.8. Genome walking 46
2.7.9. Sequencing 47

2.8. Gene expression 47

2.8.1. RNA extraction 47
2.8.2. Quantification 47
2.8.3. Reverse transcription 47
2.8.4. Real-time quantitative PCR (RT-PCR) 48

2.9. Molecular markers, genotyping, and mapping 50

2.9.1. Mapping 50
2.9.2. Genotyping 50

CHAPTER 3 ISOLATION AND CHARACTERIZATION OF CIRCADIAN CLOCK-RELATED GENES IN PEA

3.1. Introduction 51

3.1.1. Aims 53

3.2. Materials and methods 53

3.2.1. Gene expression experiments 53

3.3. Results 54

3.3.1. Identification of circadian clock-related genes in Medicago 54
3.3.2. Isolation of circadian clock-related genes from pea 58
3.3.3. Characterizations of pea orthologs of circadian clock-related genes . 60
3.3.3.1. ELF3 61
3.3.3.2. *ELF4* 63
3.3.3.3. MYB1 and MYB2 65
3.3.3.4. TOC1 68
3.3.3.5. PRR37 and PRR59 70
3.3.3.6. LUX 73
3.3.3.7. TIC 75
3.3.4. Mapping of circadian clock related genes in pea 76
3.4. Discussion 80
3.4.1. Pea circadian clock gene orthologs are amplified using information collected from Medicago database 80
3.4.2. Arabidopsis circadian clock genes are conserved in pea 82
3.4.3. Potential candidate gene relationship suggested by comparative mapping 84

CHAPTER 4 CHARACTERIZATION OF THE FLOWERING LOCUS *DIE NEUTRALIS* (*DNE*)

4.1. Introduction 86
4.2. Materials and methods 87
4.2.1. Gene expression experiments 87
4.2.2. Real-time analysis 89
4.2.3. Complementation studies 89
4.3. Results 90
4.3.1. The dne mutant shows early, photoperiod-insensitive flowering 90
4.3.2. The dne mutant shows altered rhythms of gene expression under light/dark cycles 91
4.3.3. DNE affects rhythms of clock gene expression in constant light 94
4.3.4. DNE also affects rhythms of clock gene expression in constant darkness 96
4.3.5. DNE is the likely pea ortholog of Arabidopsis ELF4 98
4.3.6. Genetic and physiological interaction of DNE and LATE1 in the

control of flowering and clock gene expression *102*
4.3.7. Effects of DNE on CO and FT expression *107*
4.3.8. DNE also regulates stem elongation *111*
4.4. Discussions **113**
4.4.1. Rhythmic expression of pea clock genes *113*
4.4.2. Roles of DNE in diurnal and circadian rhythms *116*
4.4.3. Coupling of DNE and LATE1 to flowering output pathways *118*

CHAPTER 5 CHARACTERIZATION OF THE FLOWERING LOCUS *STERILE NODES* (*SN*)

5.1. Introduction **121**
5.1.1. Pea sn mutant *121*
5.2. Materials and methods **123**
5.2.1. Gene expression experiments *123*
5.2.2. Generation of the mapping population of sn4 x Terese *123*
5.2.3. Genotyping using High Resolution Melting (HRM) *124*
5.3. Results **124**
5.3.1. The sn mutant shows early, photoperiod-insensitive flowering *124*
5.3.2. SN affect seedling photomorphogenesis *126*
5.3.3. The sn mutant shows altered expression rhythms of circadian clock gene homologs under light/dark cycles *128*
5.3.4. SN affect rhythms of clock gene expression in constant darkness *131*
5.3.5. Comparative mapping provides a refined map position for SN *132*
5.3.6. SN is the pea ortholog of Arabidopsis LUX *138*
5.3.7. SN regulation of the CO- and FT-like genes expression *142*
5.3.8. Genetic and physiological interaction of SN, DNE and LATE1 in the control of flowering *145*
5.3.8.1. *sn dne* double mutant 145
5.3.8.2. *sn late1 double mutant* 147
5.3.8.3. *sn dne late1* triple mutant 149
5.3.9. Genetic and physiological interaction of SN and HR in the control of flowering *150*
5.4. Discussion **152**
5.4.1. Comparative mapping and candidate gene approach in identifying

SN as ortholog of Arabidopsis LUX *153*
5.4.2. Roles of SN in the circadian clock *154*
5.4.3. Photomorphogenic effect of SN *156*
5.4.4. Effect of SN in flowering output pathway and the interaction with DNE and LATE1 ..... *157*

CHAPTER 6 CHARACTERIZATION OF THE FLOWERING LOCUS *PHOTOPERIOD* (*PPD*)

6.1. Introduction **159**

6.2. Materials and methods **160**

6.2.1. Gene expression experiments *160*
6.2.2. Generation of the mapping population of ppd-3 x Terese *161*

6.3. Results **161**

6.3.1. The ppd mutant shows early, photoperiod insensitive flowering *161*
6.3.2. PPD affect seedling photomorphogenesis *164*
6.3.3. The ppd-3 mutant shows altered expression rhythms of circadian clock gene homologs under light/dark cycles *165*
6.3.4. PPD affects rhythms of clock gene expression in constant darkness *168*
6.3.5. Comparative mapping between pea and Medicago refine PPD map position *169*
6.3.6. PPD regulation on CO and FT expression *173*

6.4. Discussion **176**

6.4.1. Physiological Role of PPD on flowering *176*
6.4.2. Roles of PPD on diurnal and circadian rhythms *178*
6.4.3. The map position of PPD locus was refined using comparative mapping *178*

CHAPTER 7 CHARACTERIZATION OF THE FLOWERING LOCUS *HIGH RESPONSE* (*HR*)

7.1. Introduction **180**

7.2. Materials and methods **182**

7.2.1. Gene expression experiments *182*

7.2.2. Pisum germplasm collection study 183
7.2.3. Frost tolerance study 183
7.3. Results 184
7.3.1. Circadian rhythms restored in NGB5839 on transfer from constant light to constant dark 184
7.3.2. The HR locus affects rhythms of clock gene expression under constant conditions 186
7.3.3. Comparative mapping between pea and Medicago refine the HR map position 188
7.3.4. HR is the likely pea ortholog of Arabidopsis ELF3 192
7.3.5. Distribution of HR alleles and its correlation with photoperiod responsiveness 194
7.3.6. The hr mutant shows early, photoperiod-dependent flowering 199
7.3.7. Effect of HR on CO and FT expression 200
7.3.8. Effect of HR on cold tolerance 203
7.3.9. Effect of sn on circadian rhythms in HR background 205
7.4. Discussions 208
7.4.1. Roles of HR in circadian clock 208
7.4.2. Pleiotropic effect of HR 211

CHAPTER 8 GENERAL DISCUSSION

8.1. Concluding remarks 215
8.2. Improvement on techniques 218
8.3. Future works 219
8.4. Implication for other legumes 220

REFERENCES

APPENDIX

Appendix 1 – Primers

Appendix 2 – Referred publications

Chapter 1 General introduction: Genetic control of flowering time

1.1. Importance of flowering time

During their life cycle plants shift their energy from vegetative growth to reproductive growth (transition to flowering) in response to stress, nutrient and environment and most commonly occur in favourable conditions in order to maximise their reproductive success and hence enhance their fitness and survival. The geographical distribution of plants is in part determined by natural selection on flowering time control which confers adaptation to different geographical conditions and environmental conditions such as light and temperature. Other than this, differences in flowering time can also form a reproductive barrier for out-crossing or conversely, increase outcrossing rate by synchronisation of flowering time. Natural variation for flowering time in different species or within the same species has been reported where plants adapt to different latitudinal changes by regulating photoperiod or cold responsiveness and requirement.

Besides its importance for natural distribution, flowering time is an important trait in crop plants. Many crops have spring and winter varieties in which spring cultivars flower early to avoid summer heat and have short-growing season while winter varieties flower late to escape winter frost and have long-growing season. For example, barley has photoperiod-responsive and non-responsive cultivars which are distributed in southern Europe and northern Europe respectively (Turner et al., 2005). Early and late cultivars of rice are also widespread in Asia (Takahashi et al., 2009). High frequency of early-flowering varieties of Maize is present in northern Europe

(Ducrocq et al., 2008). The timing of flowering is an important trait being manipulated in many breeding programs to maximise crop production in relation to regional climatic differences and seasonal changes. Furthermore, in different types of crops, the desired flowering characteristics depend on the nature of the crop. Delayed flowering can improve yield in crops grown for vegetative biomass whereas in many cases early flowering is desirable in seed crops and diverts energy for seed development. Recent evidence has shown that flowering time may also interact with other factors such as stress tolerance, frost sensitivity, and survival which will likely to have an impact on yield (Michael et al., 2003; Dodd et al., 2005). It is therefore essential to understand flowering regulatory pathways in order to fully utilise the genetics behind it to improve plant breeding and modify the elements in the pathways to make suitable adaptation to climate changes.

1.2. Environmental regulation of flowering

The first detailed report on environmental regulation of flowering time was made by Garner and Allard in the 1920s (Garner and Allard, 1920). They tested the flowering response of several species under different day lengths and observed a correlation between flowering time and day length in many of these species. They introduced the term 'photoperiod' to denote relative length of the day and 'photoperiodism' to denote response of plants to photoperiod. On the basis of photoperiodic response of flowering, they categorised plants into three main groups. Long-day plants (LDP) flower only when exposed to the daylength which is longer than a certain critical length (e.g. spinach and radish) whereas short-day plants (SDP) flower when the daylength become shorter (e.g. tobacco and soybean) and day-neutral plants flower at a similar time regardless of daylength (e.g. tomato and sunflower).

This discovery provided the first insight into the importance of daylength for natural distribution of plants, with plants at higher latitudes often flowering in LD of spring or summer and those from lower latitudes flowering in SD.

In addition to photoperiod, plants native to higher latitudes also display specific response to temperature. The work of Gassner (1918) was one of the first to demonstrate that flowering in cereal crops was accelerated by a period of low temperature. He also classified plants according their requirement to cold exposure in two main categories; 'winter annual', which require cold exposure to flower, and 'summer annual' which have no cold requirement for flowering (Chouard, 1960). This phenomenon was subsequently called 'vernalisation' (Chouard, 1960).

Early studies also investigated the sites within the plant important for regulation of flowering. In 1934, James Knott showed that exposure of single leaf of a spinach plant to inductive LD is enough to induce flowering (Knott, 1934) indicating that that daylength perception can occur in leaves and induces flowering at the shoot apical meristem. Subsequent grafting experiments demonstrated the existence of a mobile flowering signal termed "florigen" that was exchangeable between related species of different photoperiodic response type (LDP or SDP) (Chaïlakhyan, 1985).

In late 20th century, *Arabidopsis thaliana* emerged as a model research organism for genetics due to its rapid life cycle and small genome size, and has since been used in intensive studies of flowering time control. Nowadays, due to availability of full genome sequence and flowering mutant lines, the genetic pathways involved in flowering regulation have been well characterised in *Arabidopsis thaliana* (Mouradov et al., 2002; Simpson and Dean, 2002; Boss et al., 2004; Putterill et al., 2004; Bernier and Périlleux, 2005; Baurle and Dean, 2006). Four main pathways have been proposed to regulate flowering time in Arabidopsis: autonomous, vernalisation,

gibberellins, and photoperiod pathways (Figure 1.1). Figure 1.1 summarises the key genes involved in the four major flowering regulatory pathways in the model species, Arabidopsis.

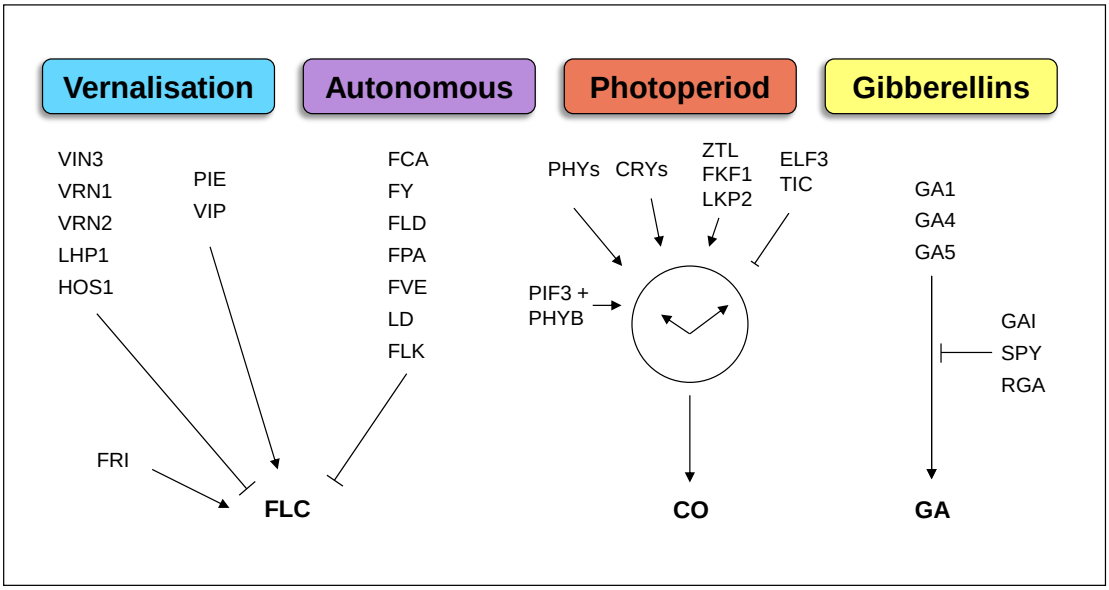

Figure 1.1 Summary of genes involved in the four major flowering regulatory pathways in *Arabidopsis thaliana*. The four major pathways are vernalisation, autonomous, photoperiod, and Gibberellins pathways. Arrows represent a promoting effect whereas perpendicular lines represent a repressive effect. The main components regulated by each pathway are highlighted in bold. The full names of the genes are included in the text. Besides these four major pathways, ambient temperature and light quality are also known to affect flowering time.

1.2.1. Florigen and the FT gene family

Numerous studies have focused on how flowering pathways are integrated, and an important role has emerged for the *FLOWERING LOCUS T* (*FT*) gene. *FT* is expressed in vascular tissue of leaves and is strongly regulated by the photoperiod pathway (Kardailsky et al., 1999). Recent evidence indicates that the FT protein acts as a mobile signal, which translocates from leaves to apex and triggers flowering in the shoot apical meristem (Corbesier et al., 2007; Jaeger and Wigge, 2007). In the shoot apex, FT interacts directly with a bZIP protein FD to induce expression of floral

meristem identity genes (Abe et al., 2005). In addition to regulation by the photoperiod pathway, *FT* expression is also influenced by vernalisation, autonomous, GA pathways, and microRNAs.

Furthermore, FT is a member of the phosphatidylethanolamine-binding protein (PEBP) gene family, which also includes *TERMINAL FLOWER 1* (*TFL1*), *MOTHER OF FT AND TFL1* (MFT), *BROTHER OF FT AND TFL1* (BFT), *TWIN SISTER OF FT* (TSF), and *ARABIDOPSIS THALIANA CENTRORADIALIS* (*ATC*). *TSF* is a close homolog of *FT* and is also regulated by photoperiod and vernalisation pathways in a similar way (Yamaguchi et al., 2005). This suggests *TSF* may act redundantly with *FT* as floral integrator in Arabidopsis. In contrast, *TFL1* antagonises *FT* action to delay flowering (Kobayashi et al., 1999).

Genes similar to *FT* have now been characterised in many other species. For example, 13 *FT*-like (*FTL*) genes have been identified in rice of which *Hd3a* is the most similar to Arabidopsis *FT* (Tamaki et al., 2007). Similarly, 5 *FTL* genes have been found in barley with *HvFT1* mainly involved in flowering transition (Faure et al., 2007). 6 *FT* genes were found in *Brassica napus* which is in the same genus as Arabidopsis (Wang et al., 2009). Even in non-photoperiodic species, tomato, the ortholog of Arabidopsis *FT*, *SINGLE-FLOWER TRUSS* (*SFT*) are found to induce flowering in tomato by generating graft-transmissible signal (Lifschitz and Eshed, 2006; Lifschitz et al., 2006). Flowering in trees also seems to be regulated by *FTL* genes, there are at least 9 *FTL* have been isolated in the perennial woody plant, poplar where two *FT*-like genes, *PnFT1* and *PnFT2* are suggested to have a role on flowering promotion (Hsu et al., 2006; Igasaki et al., 2008). All these research studies in different species suggest the general functions of *FT* are likely to be conserved across a wide range of different species.

1.2.2. Photoperiod pathway

Photoperiod or daylength changes are one of the major environmental cues that determine the transition to flowering in many species and are thought to act predominantly by influencing the expression of *FT*- like genes. However, it has long been of interest to determine the mechanisms that underlie this regulation.

The study of late-flowering photoperiod-insensitive Arabidopsis mutants for the B-box zinc finger protein CONSTANS (CO), has suggested that *CO* is a critical component in the photoperiod pathway (Putterill et al., 1995). Its expression peaks at a specific time of the day as a result of interaction between circadian clock and light. Furthermore, it is expressed in the phloem tissue of leaves coincident with *FT* expression. It is the temporal and spatial regulation of *CO* transcript and protein level which is believed to induce *FT* expression in the leaves. However, *FT* expression is also regulated by microRNA such as miR172 which able to promote flowering in response to photoperiod in the absence of functional CO (Jung et al., 2007). This suggests *FT* can also be regulated via CO-independent pathway. The regulation of *CO* will be further discussed in the following sections.

1.2.3. Vernalisation and autonomous pathway

Flowering can also be accelerated by exposure to a long period of cold. This process is known as vernalisation. The requirement of period and degree of cold are depend on species and cultivars. Vernalisation is an adaptation process developed by plants to prevent flowering occur in winter otherwise flower might be damaged by cold and ensure flowering occurs at favourable condition of spring. By manipulating vernalisation, flowering can be induced earlier with suitable cold treatment and also enhance vegetative growth in some forage crops (Slotte et al., 2007). Unlike

photoperiod pathway, vernalisation pathway actually inhibits *FT* expression until sufficient cold is perceived by the plants.

In Arabidopsis, dominant alleles at two loci, *FLOWERING LOCUS C* (*FLC*) and *FRIGIDA* (*FRI*) are required to confer vernalisation requirement and accounts for most of the flowering time difference between winter annual and summer annual varieties in Arabidopsis (Johanson et al., 2000; Edwards et al., 2006). *FLC* encodes a MADS-box transcription factor which acts as a repressor of floral transition. FRI is a coiled-coil domain protein that serves as an activator of *FLC*. By promoting expression of *FLC*, *FRI* repress flowering transition during winter and thus confers the requirement for vernalisation. The *FLC* mRNA and protein levels are higher in winter annual when compared to summer annual varieties in Arabidopsis. The stability of *FLC* expression can be passed on through mitotic cell division once the plant exposed to cold but reset after meiosis around early embryogenesis. This suggests an epigenetic basis for vernalisation and the characterization of genes involved further emphasises this concept. *PHOTOPERIOD-INDEPENDENT EARLY FLOWERING1* (*PIE1*) (Noh and Amasino, 2003) and *VERNALIZATION INDEPENDENCE* (*VIP*) (Zhang et al., 2003) genes function in a chromatin-modifying complex to maintain *FLC* chromatin in an active state (euchromatin) before vernalisation. This ensures the vernalisation requirement of plants because *FLC* is expressed to inhibit flowering before plant get vernalised.

The repression of flowering by *FLC* can be overcome by vernalisation through a cascade of regulatory process starting from *VERNALIZATION INSENTIVE 3* (*VIN3*) to gradually reduce *FLC* expression during the cold and stabilise in the warm and hence promote flowering in spring (Sung and Amasino, 2004). *VIN3* encodes for a plant homeodomain protein which required for histone deacetylation of

FLC. However, *VIN3* only expressed after a period of cold exposure implies it is involved in establishment of *FLC* reduction but it is not responsible for the initiation of the reduction (Bond et al., 2009). It is not clear which molecules are involved in the initiation of *FLC* reduction in the cold but research suggests *HIGH EXPRESSION OF OSMOTICALLY RESPONSIVE GENES 1* (*HOS1*) might be the genes involved as *hos1* mutant showed reduced *FLC* expression and enhanced cold-induced genes expression(Lee et al., 2001). *VERNALISATION 1* (*VRN1*) (Levy et al., 2002), *VERNALISATION 2* (*VRN2*) (Gendall et al., 2001), and *LIKE HETEROCHROMATIN PROTEIN 1* (*LHP1*) (Mylne et al., 2006) are thought to maintain the repression of *FLC* by maintaining *FLC* chromatin in the repressed state (heterochromatin) which is incompatible to transcription. *VRN1* encodes for a DNA-binding protein which may function with VRN2, a Polycomb Group protein to target *FLC* gene histone methylation whereas LHP1 is thought to stabilise the methylation mark required for the formation of heterochromatin.

Vernalisation is an important process to regulate flowering, permitting initiation of flowering after sufficient duration of cold by releasing FT inhibition by FLC through repressing *FLC* expression progressively. Nevertheless, vernalisation might have a role in promoting flowering independently of *FLC* because vernalisation can still accelerate flowering in *flc* null mutant (Sung and Amasino, 2004). This is an exciting area of research, however, little is known about the initiation of *FLC* repression by vernalisation pathway in response to cold and also the resetting of *FLC* expression during seed development.

The autonomous pathway comprises a group of negative regulators of *FLC* identified through analysis of late-flowering mutants with higher levels of *FLC* mRNA that still responds to environmental signals. So far seven genes (*FCA*, *FY*,

FLD, *FPA*, *FVE*, *LD*, and *FLK*) have been identified as components of autonomous pathway. They are either RNA binding proteins or chromatin-associated proteins suggesting post-transcriptional and epigenetic regulation of autonomous pathway in control of *FLC* repression. However, they do not appear to repress *FLC* in a linear pathway but instead form sub-pathways influencing *FLC* expression via different mechanisms (Lee et al., 1994; Macknight et al., 1997; Schomburg et al., 2001; He et al., 2003; Quesada et al., 2003; Simpson et al., 2003; Kim et al., 2004; Lim et al., 2004).

Vernalisation and autonomous pathways regulate *FT* expression mainly via *FLC* through several different ways. *FLC* can antagonise CO activity by repressing *FT* expression in leaves (Searle et al., 2006). *FLC* has also been shown to repress expression of *FD* in shoot apex, possible preventing FD to recruit FT for floral meristem identity gene activation (Searle et al., 2006).

1.2.4. Gibberellins pathway

Gibberellins (GA) is one of the phytohormones which has a role in flowering regulation and best studied in Arabidopsis. It was first discovered by application of exogenous GA which promotes flowering. Recently, studies on GA biosynthesis and GA signalling pathways has revealed mutants with decreased GA levels or impaired sensitivity have delayed flowering and *vice versa* (Davis, 2009). *GA1* is a biosynthesis gene in the very first step of the biosynthesis pathway of GA. The *ga1* mutant is unable to flower under SD and flower late in LD. *GA4* and *GA5* encode for GA 3β-hydroxylase and GA 20-oxidase respectively, which both regulate other steps in the GA biosynthesis pathway. Mutations in these two genes have less severe effects on flowering but overexpression of these genes leads to early flowering.

This may imply GA is not an essential factor for the initial flowering transition but a may be a limiting factor on flowering time. Redundancy of gene functions can also explain this lesser response in mutants. On the other hand, genes involved in GA signalling such as *GIBBERELLIC ACID INSENSITIVE* (*GAI*) (Willige et al., 2007), *SPINDLY* (*SPY*) (Jacobsen and Olszewski, 1993), and *REPRESSOR OF GA1-3* (*RGA*) (Silverstone et al., 1997) when mutated will enhance the GA signalling and produce early-flowering plants. Interestingly, all of these effects of GA on flowering regulation in Arabidopsis are more predominant in non-inductive SD condition. This suggest interaction of GA pathway with other flowering regulatory pathway especially photoperiod pathway in regulating timing of flowering. GA pathway might influence *FT* expression as well especially in non-inductive SD but GA effect on *FT* transcript level appears to be species-specific (Mutasa-Gottgens and Hedden, 2009).

1.2.5. Other integrators

As discussed in the previous sections, flowering time is controlled by four major pathways in which autonomous and GA pathways mainly response to endogenous signals whereas vernalisation and photoperiod pathways response to cold and daylength respectively (Figure 1.1). In addition to these pathways, light quality and ambient temperature were also found to affect flowering time (Cerdan and Chory, 2003; Thines and Harmon, 2010). Flowering occurs in shoot apical meristem where flower primordia emerge after activation of floral meristem identity genes. The *FT* gene has been discovered to have a role in converging the signals from different pathways to initiate flowering by activating expression of floral meristem identity genes such as *APETALA* (*AP1*), *CAULIFLOWER* (*CAL*), and *FRUITFULL* (*FUL*).

Besides *FT*, two other genes have been identified as floral integrators whose

expression and function are regulated by more than one flowering pathway and are hence able to integrate signals from different pathways to induce floral meristem identity gene expression. They are *LEAFY* (*LFY*) and *SUPPRESSOR OF OVEREXPRESSION OF CO 1* (*SOC1*). *LFY* is expressed mainly in shoot apex and its expression is regulated by photoperiod and GA pathways independently (Blazquez et al., 2002). A recent study has revealed LFY is a transcription factor with DNA-binding domain and bind directly to pseudo-palindromic sequence elements (CCANTGT/G) in the promoter of floral meristem identity gene *AP1*. Protein structure analysis showed high similarity of LFY protein to helix-turn-helix protein which is known to be homeodomain protein for morphogenesis regulation (Hames et al., 2008). This implies *LFY* might have dual role as floral integrator and floral meristem identity gene. SOC1 (or AGL20) is a MADS box transcription factor which promote flowering. It was first identified as a late mutant when screening for suppressors of overexpression of *CO* (Onouchi et al., 2000). *SOC1* is expressed mainly in leaves and shoot apex and its expression is known to be regulated by four of the regulatory pathways. *SOC1* expression is up-regulated by photoperiod pathway and GA pathway whereas downregulated by vernalisation and autonomous pathway (Samach et al., 2000; Lee and Lee, 2010).

As outlined, even if the three floral integrators are differentially regulated by photoperiod, vernalisation, autonomous, and GA pathways, *CO* and *FLC* seem to be the critical components which serve as inputs for these floral integrators. In order to precisely regulate flowering time, one might expect interaction between floral integrators and predominance of one over another in different environments. Two MADS box transcription factor, *AGAMOUS-LIKE 24* (*AGL24*) and *SHORT VEGETATIVE PHASE* (*SVP*) were proposed to act as important link between floral

integrators (Hartmann et al., 2000; Michaels et al., 2003; Liu et al., 2008a).

1.3. The circadian clock and the response to photoperiod in Arabidopsis

Among the four major pathways, photoperiod pathway is best understood. According to the external and internal coincidence model, the circadian clock plays a key role in the photoperiodic measurement of flowering. The circadian clock is an internal timekeeping system which generates daily biological rhythms to keep track of the passage of time. The rhythms generated by circadian clock are referred as 'circadian rhythms' and have three distinct characteristics (Yanovsky and Kay, 2003; Montaigu et al., 2010). First, the rhythms persist even in the absence of external signals such as light or temperature (constant environments of continuous light or darkness). This shows circadian rhythms are truly intrinsic and able to maintain the duration of each cycle ('free-running period') at approximately 24 hours under constant conditions. Secondly, circadian rhythms are temperature compensated so that they maintain an approximate 24 hours periodicity over a wide range of temperatures. Thirdly, the circadian rhythm can be entrained by external signals in order to synchronise the internal timing with the environment. The external signals that entrain circadian rhythm are known as 'zeitgeber' (*time giver* in German) and the phase after onset of zeitgeber is referred as 'zeitgeber time'.

These three properties not only ensure circadian rhythms are stable and reliable in co-ordinating internal pathways in an appropriate and efficient manner but also allow plants to anticipate different environmental changes in order to precisely program temporal biological events. Analysis suggests that up to 40% of the transcriptome in Arabidopsis estimated is regulated by circadian clock (Harmer et al.,

2000; Covington et al., 2008). This further emphasises the importance of circadian clock in regulation of huge varieties of biological activities including flowering. Recently, studies also showed the contribution of circadian clock to enhance adaptation, fitness, and survival of plants (Green et al., 2002; Michael et al., 2003; Dodd et al., 2005).

In order to understand the mechanism for photoperiod control of flowering by circadian clock, three main models have been proposed (Yanovsky and Kay, 2003). The *hourglass* model assumes the gradual accumulation of some key regulatory product in response to the duration of light or darkness. When the key regulatory product reaches a critical threshold, certain physiological responses will be triggered. However, various experiments have showed this is not the case for flowering control, as light/dark cycles longer than 24h and cycles in which dark is interrupted by brief light pulses will still affect flowering. This leads to two other more sophisticated models, the external coincidence model and the internal coincidence model (Yanovsky and Kay, 2003).

The *external coincidence* model was first developed by Erwin Bünning in from observations that daily rhythms of leaf movement in bean persisted even in plants transferred to complete darkness (Halaban, 1968; Satter and Galston, 1981). This suggested the presence of some form of endogenous time-keeping mechanism (circadian clock) that generates internal rhythms (circadian rhythm) independently of day/night cycles. The external coincidence model proposed that a photoperiodic response is induced when the level the circadian clock enters a phase permitting the induction of some key regulatory molecule by external light signals. In this model, light acts both to synchronise the circadian clock to the light-dark cycle and also to directly induce formation of the key regulatory product (Eriksson and Millar, 2003).

In the alternative *internal coincidence* model, light is only required to synchronise the circadian clock with external signals (light and darkness) to produce internal rhythms (Pittendrigh, 1972), and a photoperiodic response would be triggered only when two or more internal rhythms are in a certain phase relationship. These rhythms could be produced by single circadian clock or by distinct circadian clocks in different tissues.

The hourglass model thus depends on the amount of light to regulate the photoperiodic response, whereas the external coincidence model and internal coincidence model both depend on circadian clock synchronisation of light/dark signals. The external coincidence model requires precise presence of light in specific time of a day whereas the internal coincidence model depends on differentially entrained rhythms. In recent years it has become possible to relate these theoretical possibilities to actual data derived from studies of key photoperiod and clock-regulated genes. While the temporal pattern of expression of circadian clock-regulated genes does provide evidence in support of the internal coincidence model, the external coincidence model is generally believed to be the most appropriate model as it is consistent with the majority of the genetic evidence so far.

These sophisticated and multifaceted functions of circadian rhythms make us to believe the underlying regulatory mechanisms by circadian clock could be complicated. A simple linear pathway for clock function comprising three parts (input pathways, a core oscillator, and output pathways) was first suggested by early researchers to explain the generation of circadian rhythms in Arabidopsis (Dunlap, 1999; Barak et al., 2000). Each of the components of circadian clock will be elucidated in the following sections based on information from the model species Arabidopsis and further discussion will be focused on photoperiodic control of

flowering as an output pathway.

1.3.1. The core oscillator

The core oscillator is the central part of circadian clock which is responsible to generate endogenous rhythms, entrain the rhythms to external signals (via input pathways), and produce entrained rhythms to control wide range of biological processes (via output pathway). The first consistent model described in Arabidopsis for the core oscillator is a single transcriptional-translational negative feedback loop comprise of *TIMING OF CAB EXPRESSION 1* (*TOC1*) and partially redundant genes *CIRCADIAN CLOCK-ASSOCIATED 1* (*CCA1*) and *ELONGATED HYPOCOTYL* (*LHY*) in which they reciprocally regulate each other (Alabadi et al., 2001). This observation was based on the opposite expression phase of *TOC1* and *CCA1/LHY* around dusk and dawn respectively. The model proposed that in the late evening, TOC1 activates the transcription of *CCA1/LHY* which results in peaking of their mRNA and protein level around dawn. The increased CCA1/LHY proteins bind directly to an 'evening element' (EE, AAAATATCT) in the promoter of *TOC1* and represses the transcription of *TOC1*. This in turn leads to decreasing of CCA1/LHY protein level as TOC1 acts as a positive activator of *CCA1/LHY*. Evidence supporting this model includes the fact that the expression of *TOC1* suppressed in constitutively expressed *CCA1* or *LHY* plants (Alabadi et al., 2002) whereas *lhy cca1* double mutants have increased *TOC1* mRNA level (Mizoguchi et al., 2002). Reciprocally, the loss of function of *TOC1* in *toc1* mutant reduces the level of *CCA1* and *LHY* and shorter period length in transcription rhythms (Más et al., 2003b).

However, this single loop model was inadequate to account for some aspect of the core oscillator such as *toc1-2* but not *toc1-1* reduces *LHY*/*CCA1* expression

(Alabadi et al., 2001), *cca1lhy* double mutant is not completely arrhythmic (Mizoguchi et al., 2002), and overexpression mutants of *TOC1* reduce *CCA1*/*LHY* expression (Más et al., 2003b). Additionally, there are more genes discovered to affect rhythmicity of clock genes and are not yet fitted into the single loop model (Locke et al., 2005).

In order to explain these experimental data, two recent mathematical modelling studies (Locke et al., 2006; Zeilinger et al., 2006) have extended the 'single loop model' into 'three-loop model' (Figure 1.3). The three-loop model consists of the existing TOC1-CCA1/LHY loop as a core loop and two loops occur in the morning and evening respectively. In the core loop, a hypothetical component '*X'* was also proposed to act in between *TOC1* and *CCA1*/*LHY* for *CCA1*/*LHY* induction as no evidence has shown direct binding of TOC1 to *CCA1*/*LHY*. A recent identified TCP (TB1, CYC, PCFs) transcription factor, CHE (CCA1 HIKING EXPEDITION) was identified as a component for this core loop (Pruneda-Paz et al., 2009). CHE physically interacts with TOC1 and recruits TOC1 to TCP binding site in the promoter of *CCA1* and activates *CCA1* transcription. CCA1 then negatively feeds back on *CHE* expression.

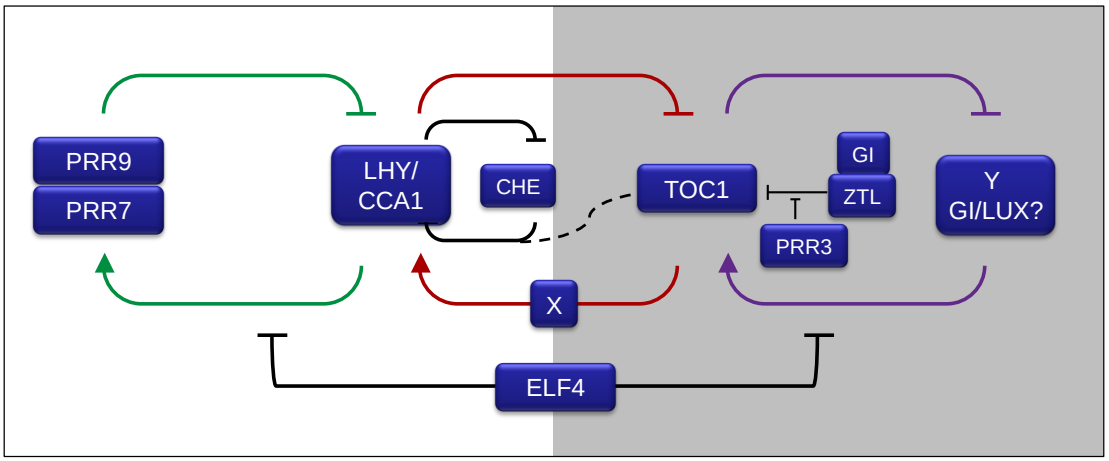

Figure 1.2 Core oscillator in Arabidopsis consists of the proposed three-interlocking loops. The three negative feedback loops are represented by three different colours. The white and gray background represent day and night respectively. In the central loop (red), LHY and CCA1 bind to *TOC1* promoter in the morning to repress *TOC1* expression. *LHY* and *CCA1* expression decreased throughout the day which leads to increased *TOC1* expression. Elevated TOC1 level activates *LHY* and *CCA1* expression via an unknown factor 'X'. Another recently identified component in the central loop is *CHE*. CHE physically interacts with TOC1 and activate *CCA1* expression. The morning loop (green) includes activation of *PRR9*/*PRR7* expression by LHY/CCA1 while PRR9/PRR7 negatively feedback on *LHY*/*CCA1* expression. In the evening loop (purple), a hypothetical element 'Y' (whose activity can be explained by *GI* or *LUX*) will promote *TOC1* expression in the evening whereas TOC1 will negatively feedback on '*Y*' expression. Additionally, ZTL was suggested to inhibit TOC1 level by protein degradation. This proteasome-mediated degradation is suspected to be stabilised by GI and disrupted by PRR3. Besides this three interlocking loop, ELF4 is hypothesised to inhibit the morning and the evening loops. (Modified from Montaigu et. al. 2010).

In this new model, a morning loop comprised of *PSEUDO RESPONSE REGULATOR 7* (*PRR7*) and *PSEUDO RESPONSE REGULATOR 9* (*PRR9*) is activated by CCA1/LHY and PRR7/PRR9 then negatively feed back to regulate *CCA1*/*LHY* expression. *PRR7*/*PRR9* are part of the *Pseudo Response Regulator* (*PRR*) gene family which includes *TOC1* (*PRR1)*, and all members of the family contain two characteristic domains of C-terminal Pseudo-Receiver (PR) domain and N-terminal Constans, Constans-like, TOC1 (CCT) domain(Matsushika et al., 2000). The members of this family show sequentially expression peaks every 2 hours after dawn in the order of *PRR9*, *PRR7*, *PRR5*, and *PRR3* and until *TOC1* is eventually expressed in the evening (Matsushika et al., 2000). Experimental data which supports this

morning loop includes the CCA1 binding directly to CBS (*CCA1*-binding site) in *PRR7* and *PRR9* promoters and a later phase shift in *CCA1* and *LHY* expression in *prr7prr9* double mutant (Farré et al., 2005). Moreover, *PRR7* and *PRR9* were found to be essential for temperature sensitivity of circadian clock (Salome and McClung, 2005b). Therefore, *PRR7* and *PRR9* could be important components that respond to light and temperature input signals.

Separately, a hypothetical component 'Y' was proposed to induce *TOC1* expression in an evening loop and *ZEITLUPE* (*ZTL*) was suggested to repress *TOC1* expression. The expression of *Y* is in turn negatively regulated by TOC1. *ZTL* encodes a blue light photoreceptor which involved in the input pathways. ZTL interacts with TOC1 *in vivo* and target TOC1 for proteasome-mediated degradation in the dark. This finding is consistent with the observation that *ztl* mutant has elevated TOC1 protein level (Más et al., 2003a). *GIGANTEA* (*GI*) (Fowler et al., 1999; Park et al., 1999) and *LUX ARRHYTHMO* (*LUX*) (Hazen et al., 2005; Onai and Ishiura, 2005) are possible candidates for Y component. *GI* encodes a nuclear protein with several membrane-spanning domains. *GI* transcript is regulated by clock and peaks around late afternoon supporting a role for GI in the feedback loop as a positive regulator of *TOC1* expression. Furthermore, decreased *CCA1*/*LHY* expression is observed in *gi* mutant that might due to the reduced TOC1 levels in the mutant (Fowler et al., 1999). GI was also found to stabilise ZTL in the blue light to ensure robust rhythm of *TOC1* (Kim et al., 2007). Interestingly, PRR3 was found to disrupt TOC1 degradation by ZTL by binding to TOC1 (Para et al., 2007). Besides its role in circadian clock, *GI* was also found to function in phytochromeA-mediated photomorphogenesis (Oliverio et al., 2007), temperature compensation (Gould et al., 2006), and also interact with SPY in the GA signalling pathway (Tseng et al., 2004). *LUX* encodes for a MYB

transcription factor which expressed at the same time during the day as *TOC1* and mutation in *LUX* cause arrhythmia in both *TOC1* and *CCA1*/*LHY* expression rhythms (Onai and Ishiura, 2005).

In addition to this 'three-loop model', *EARLY FLOWERING 4* (*ELF4*) was integrated into this model via recent structural and functional analysis (Kolmos et al., 2009). *ELF4* encodes a novel protein with no known domains and its transcript is clock regulated with a peak at dusk (Doyle et al., 2002). Furthermore, *elf4* mutant has reduced *CCA1*/*LHY* expression and elevated *TOC1* expression (Kikis et al., 2005). Recently, *ELF4* was found to repress *PRR7*/*PRR9* expression in the morning loop and *GI*/*LUX* expression in the evening loop (Kolmos et al., 2009). This suggests *ELF4* may be part of the core oscillator. Moreover, several genes known to affect rhythmicity under constant conditions have not yet placed into this model such as *FIONA1* (*FIO1*) (Kim et al., 2008), *TEJ* (Panda et al., 2002), and *PRR5* (Ito et al., 2008).

Besides transcriptional feedback loop, core oscillator is also regulated by other mechanisms. Histone acetylation in *TOC1* chromatin regulates the transcription activation or repression of *TOC1* (Más, 2008). Post-translational phosphorylation of CCA1 by CK2 regulates stability and activities of CCA1 (Daniel et al., 2004). In addition to TOC1, several other components of core oscillator are also regulated by proteasome-dependent degradation such as PRR3 by WNK1 (Murakami et al., 2002). Therefore, it is highly likely that the 'three-loop model' is not enough to explain the operation of core oscillator and will need to be repeatedly revised after exploring relationship of different components using either experimental or modelling approaches.

1.3.2. Input pathways

The input pathway involved perception of environmental signals, transduction of the signal to core oscillator and entrainment of circadian clock. The two main zeitgeber are light and temperature. The mechanism of temperature signalling pathways are less well studied as no temperature sensor is identified so far. However, several circadian clock genes expressions are known to be entrained by temperature cycle. On the other hand, circadian clock mutant was found not entrain to temperature cycle and does not response to temperature changes. In addition, photoreceptor signalling pathway is temperature sensitive which suggests light and temperature signalling pathway are interdependent (Michael and McClung, 2002; Salome and McClung, 2005a).

The effect of light to circadian clock and its roles in input pathways are better studied in plants especially in Arabidopsis. Four main classes of photoreceptors have been characterised in Arabidopsis: phytochromes, crytochromes, phototropins, and ZTL family. Phytochromes are responsible for perceiving red or far red light while crytochromes and phototropins perceive UV or blue light. ZTL family are also involved in perception of blue light and in entrainment of the clock. However, only phytochromes and crytochromes but not phototropins have a role in clock entrainment (Somers et al., 1998a; Salome and McClung, 2005a). Based on mutant studies in Arabidopsis, PHYA and PHYB are the two major phytochromes which are responsible for low fluence red light and high fluence red light respectively whereas CRY1 and CRY2 are responsible to perceive blue light. However, no single photoreceptor alone is crucial for entrainment of circadian clock as all the single photoreceptor mutants display weaker effect in white light and the *phyA phyB cry1 cry2* quadruple mutant still shows robust rhythms for leaf movement in white light

(Yanovsky et al., 2000). These findings imply that either other known photoreceptor (PHYC, PHYD, PHYE, CRY3) or unidentified novel photoreceptors can function for clock entrainment.

The identification of a small gene family consist of *ZTL* (Somers et al., 2000), *FLAVIN BINDING KELCH F BOX 1* (*FKF1*) (Mizoguchi and Coupland, 2000), and *LOV KELCH PROTEIN 2* (*LKP2*) (Schultz et al., 2001) has advanced our understanding of the input pathway. These three blue light photoreceptors share high protein similarity and contain N-terminal LOV domain, F-box domain in the middle, and six Kelch repeats at C-terminal. The LOV domain is a common motif found in Arabidopsis phototrophins (PHOT1 and PHOT2) which is a light sensitive domain, the F-box is a motif found in protein involved in ubiquitin-proteasome degradation, and the Kelch domain is a protein-protein interaction domain. These three distinct domains together speculate the role of this gene family in facilitating light-dependent degradation of clock components. As mentioned before, TOC1 was showed to be one of the substrate of ZTL for ubiquitin-mediated degradation (Más et al., 2003a). This process is somehow repressed by light. One possible explanation is the LOV domain in ZTL undergoes light-induced conformational changes and blocks the interaction with TOC1 in the light. Recent studies revealed another core oscillator component PRR5 is also targeted for degradation by ZTL in the similar way as TOC1 (Kiba et al., 2007). There is a recent study suggest FKF1 and LKP2 might work together with ZTL in regulating TOC1 and PRR5 degradation (Baudry et al., 2010). Moreover, FKF1 might have an additional role in the output pathway to regulate flowering (Sawa et al., 2007).

EARLY FLOWERING 3 (*ELF3*) was recently identified as an additional component in the input pathway. The phenotype of *elf3* mutant is similar to *phyB*

mutant as in early flowering, long hypocotyls, and defective responses under red light condition (Hicks et al., 1996). However, *phyB elf3* double mutant show additive phenotype indicating ELF3 acts independently of PHYB (Reed et al., 2000; Liu et al., 2001b). Moreover, mutations in *ELF3* result in arrhythmia of circadian clock gene expression only in light but not in darkness (Hicks et al., 1996). This conditional arrhythmicity suggests ELF3 negatively regulate light input to circadian clock (circadian 'gating' of light) during the night. 'Gating' is a mechanism hypothesised to regulate rhythmic sensitivity of clock to light where clock-regulated gene (such as *ELF3*) feed back to regulate light input to oscillator. This finding was further supported by the fact that *ELF3* transcript and protein level peak around the dusk when it is required to gate the light input (McWatters et al., 2000; Covington et al., 2001; Hicks et al., 2001; Carre, 2002). Recently, another gene, *TIME FOR COFFEE* (*TIC*) with similar functions as *ELF3* was identified (Hall et al., 2003). *TIC* was shown to have partial defect in circadian gating and affect circadian rhythm of several clock-regulated gene especially during the day. Furthermore, *tic elf3* double mutant lost the circadian rhythmicity in both light and dark suggesting ELF3 and TIC work at different phase of a day and a possible role for TIC to gate light input during the day (Ding et al., 2007).

Another gene *PHYTOCHROME INTERACTING FACTOR 3* (*PIF3*) which encodes for a transcription factor containing basic helix-loop-helix (bHLH) domain was found to have an important role in light transduction to circadian clock (Ni et al., 1998). PIF3 was found to bind to G-box motifs (CACGTG) in the promoter of two essential core oscillator components *CCA1* and *LHY* (Ni et al., 1999). When light activates PHYB from inactive Pr form to active Pfr form, PHYB will translocate into the nucleus and interact with the PIF3-G-box complex and trigger the transcription of

CCA1 or *LHY*. This interaction was found to be reversible when PHYB reconvert from Pfr to Pr form. This finding provides a possible molecular link between the input pathways and the core oscillator.

There are a few more proteins have been identified to have a role in the input pathway of circadian clock such as SENSITIVITY TO RED LIGHT INDUCED (SRR1) (Staiger et al., 2003b), LIGHT INSENSITIVE PERIOD 1 (LIP1) (Kevei et al., 2007), and XAP5 CIRCADIAN TIMEKEEPER (XCT) (Martin-Tryon and Harmer, 2008) but the action of these proteins remain undefined. SRR1 positively regulate light input particularly to red and white light and the *srr1* mutant has shown to affect core oscillator and output genes expression. *LIP1* encodes for a small GTPase protein which was thought to have a negative role in light input and entrainment of clock. XCT was found to specifically regulate red light input to circadian clock and showed to have shortened period for many clock output genes. It is therefore pretty clear that there are more components of circadian clock input pathway to be identified.

In brief, the components in the input pathways were identified to perceive light and transmit the information for clock entrainment through several mechanisms (Figure 1.3). First mechanism is the rhythmic regulation of light input. The phytochromes and crytochromes are responsible to perceive light at different wavelength and their transcription are also found to be clock-regulated and peak at different phase during the day to ensure resetting cues are perceived at the right time of a day. ELF3 and possibly TIC are involved in circadian 'gating' mechanism which rhythmically regulate light input and ensure sensitivity to light at certain phase of a day. Secondly, PIF3-PHYB interaction with core oscillator component establishes a direct link between photoreceptor and transcriptional regulation of core oscillator to allow precise entrainment of clock by light. Thirdly, light-regulated post-translational

regulation of core oscillator component by ZTL through the proteasome pathway provides a further mechanism for clock entrainment via regulation of protein stability.

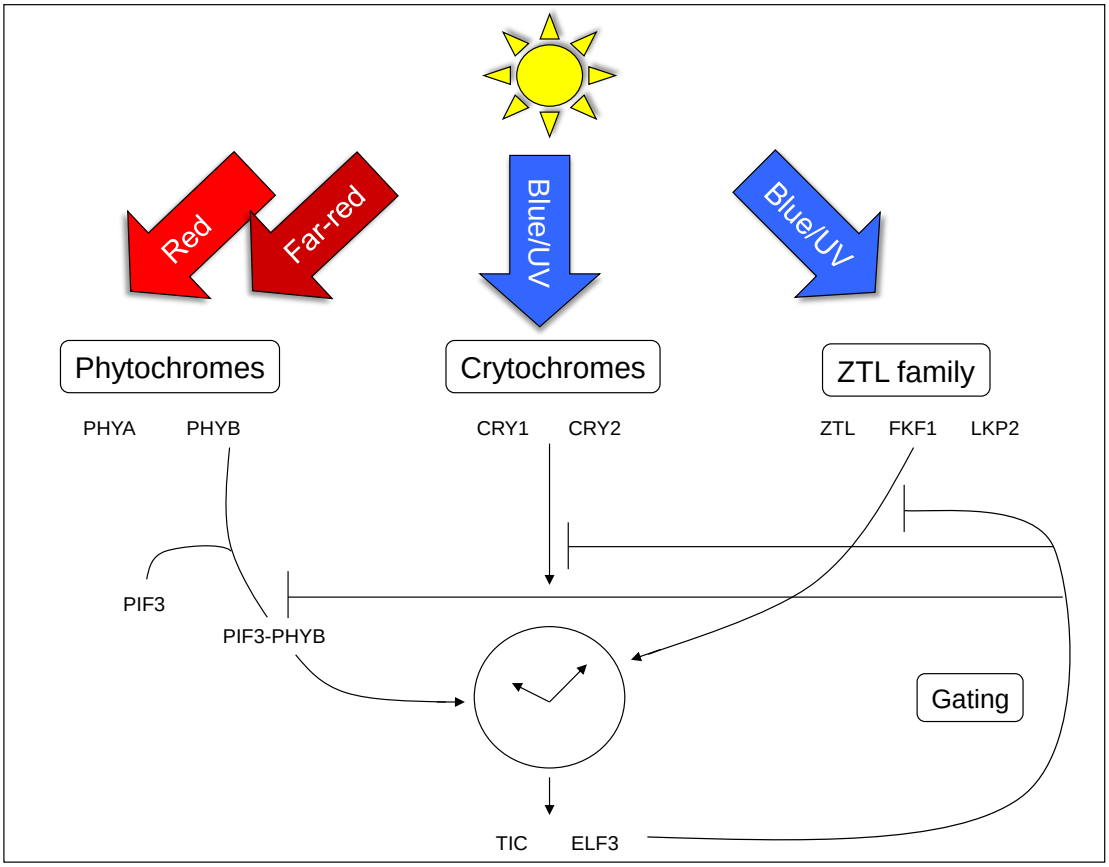

Figure 1.3 Summary of input pathway in Arabidopsis. Three types of photoreceptors, phytochromes, crytochromes, and *ZTL* family are responsible to perceive red, far-red, blue/UV lights for entrainment of circadian clock. *PIF3* was found to interact with *PHYB* and translocate it to target clock genes expression. *ELF3* and *TIC* were found to gate the light transduction to circadian clock.

1.3.3. Output pathways: Photoperiodic control of flowering by circadian clock via CONSTANS

The output pathways are the link between the core oscillator and biological processes regulated by the rhythms generated. In plants, the circadian clock controls a wide range of processes including developmental processes from germination to reproduction and cellular process such as stomatal opening, leaf movement, photosynthesis, and stress responsiveness (Yakir et al., 2007). One of the best understood examples of a circadian clock output pathway is regulation of

photoperiodic control of flowering time through CO.

CO mRNA shows rhythmic expression under both LD and SD and accumulates to maximum level during the night. However, an additional evening peak is present only in the LD which is thought to be critical to induce flowering of Arabidopsis in LD (Figure 1.4). The *CO* mRNA abundance is regulated by a transcriptional repressor *CYCLING DOF FACTOR 1* (*CDF1*). CDF1 bind directly to the Dof binding sites (AAAG) in the *CO* promoter to repress *CO* transcription (Imaizumi et al., 2005; Fornara et al., 2009). This CDF1-mediated repression of CO can be destabilised by FKF1-GI complex and hence release *CO* for transcription (Sawa et al., 2007). As mentioned before, FKF1 and GI are both part of the circadian clock where FKF1 is a blue light photoreceptor involved in light dependent degradation and GI is a component of the core oscillator. The transcription of *FKF1*, *GI* and *CDF1* are all regulated by circadian clock in which *FKF1* and *GI* expressed 8-12h after dawn and *CDF1* expression peak at dawn. The LD-specific peak of *CO* mRNA can be explained by light dependent interaction of FKF1 and GI. It is because this complex will only form in the late afternoon in LD when *FKF1* and *GI* are expressed in the light. This complex will then target CDF1 for ubiquitin-proteasome degradation and release *CO* for transcription to produce LD-specific daytime peak of *CO* expression. Nevertheless, ELF3 might act as repressor to *CO* transcription independent to CDF1 mechanism. In *elf3* mutant, *FKF1* and *GI* expression is elevated and so does *CO* expression (Kim et al., 2005). It is possible that ELF3 repress *CO* expression through down regulating *FKF1* and *GI* expression (Yu et al., 2008). On the other hand, in SD, *FKF1* and *GI* expressions peak at night and FKF1-GI complex is unable to form due to absence of light (Imaizumi et al., 2005; Sawa et al., 2007). This will eventually result in *CO* mRNA only has a night time peak in SD (Figure 1.4).

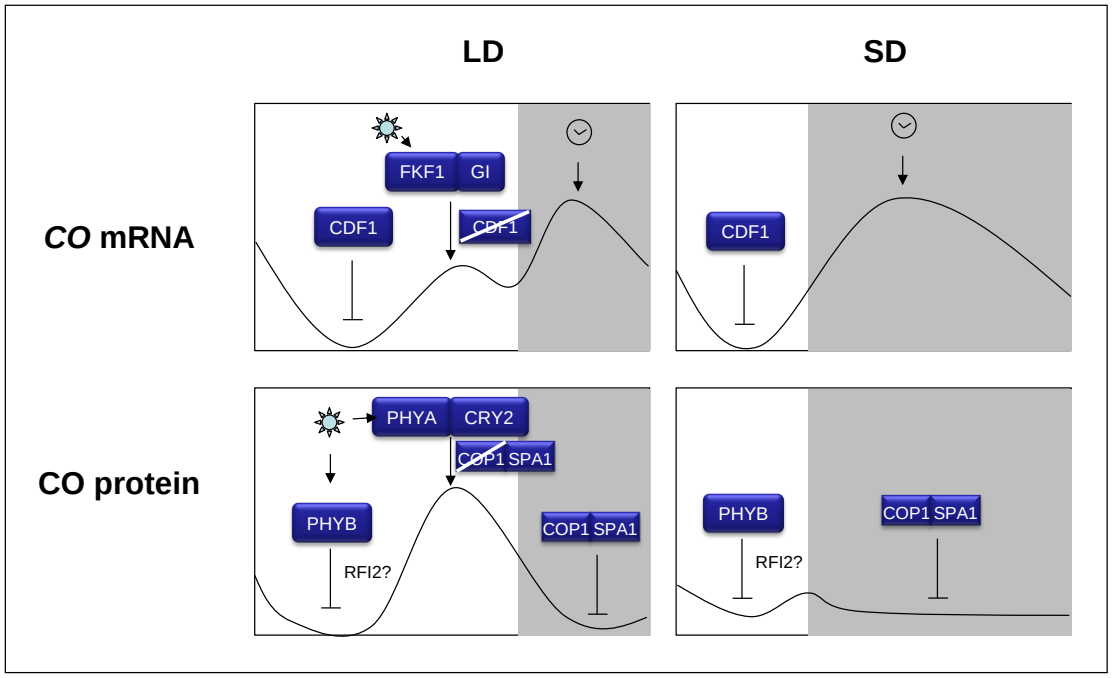

Figure 1.4 CO mRNA and protein regulation by daylength in Arabidopsis. *CO* mRNA level shows diurnal expression rhythms in response to LD and SD. CDF1 act as a transcriptional repressor of *CO* in the early morning of both LD and SD. FKF1 protein abundance exhibits diurnal rhythm and peak in the mid day. In LD, FKF1 is induced by light to form a FKF1-GI complex to target CDF1 for degradation which eventually releases *CO* transcriptional inhibition by CDF1 and facilitate the formation of LD-specific daytime peak for *CO* mRNA. On the other hand, CO protein is stable in light and degraded in the darkness. In the daytime, CO protein is destabilised by PHYB while stabilised by PHYA and CRY2. In the night time, CO protein is degraded by COP1-SPA1 complex but COP1 protein is inhibited by PHYA and CRY2 in the day time. PHYB inhibit CO protein in the daytime through COP1-independent mechanism and maybe via RFI2. In SD, FKF1 expression peaks in the evening which fails to be induced by light and result in only the night time peak of CO mRNA. The translated CO protein in SD is degraded by COP1-SPA1 mediated degradation in the night.

Besides transcriptional regulation of *CO* mRNA, post-translational regulation of CO protein by light is also essential for control of flowering. CO protein is only stable in the presence of light and rapidly degraded in the dark (Suarez-Lopez et al., 2001). The CO protein stability has been shown to be regulated by photoreceptors. There is an increased abundance of CO protein when flowering is promoted in far-red and blue light which is perceived by PHYA and CRY1/CRY2 respectively (Cerdan and Chory, 2003). However, *PHYB* is known to delay flowering and no accumulation of CO protein is detected in the red light. Consistent with this idea, *phyA* and *cry1cry2*

mutants are late-flowering (Johnson et al., 1994; Devlin and Kay, 2000; Imaizumi et al., 2003) mutants and showed to reduce in CO protein level in the morning and evening of LD. Conversely, *phyB* early-flowering mutant showed to have increase CO protein abundance (Valverde et al., 2004). Recently, *CONSTITUTIVE PHOTOMORPHOGENIC 1* (*COP1*) (Jang et al., 2008) and *SUPPRESSOR OF PHYA 1* (*SPA1*) (Ishikawa et al., 2006) has been shown to form an ubiquitin-ligase complex to ubiquitinate CO protein and promote CO degradation in the darkness. This ubiquitin-mediated degradation of CO protein is inhibited by light through repression of COP1 by PHYA, CRY1, and CRY2 (Wang et al., 2001; Liu et al., 2008b). However, PHYB has shown to promote degradation of CO protein in the morning via COP1-SPA1 independent mechanism but the underlying mechanism is unclear. *RED AND FAR-RED INSENSITIVE 2* (*RFI2*) encodes for a protein contains RING-finger domain which was normally found in protein involved in protein degradation suggests RFI2 might affects CO protein stability (Chen and Ni, 2006b, a). The *rfi2* mutant has increased *CO* expression and *RFI2* expression is reduced in *phyB* mutant when compared to wild-type plants. This suggests RFI2 might have a role in transcriptional regulation of *CO* via *PHYB*. As a result of post-transcriptional regulation of CO, CO protein accumulate in the evening of LD. Reciprocally, no CO protein is produced in SD because *CO* transcript peak in the night and the translated CO protein is degraded by COP1-SPA1 ubiquitin-ligase complex (Figure 1.4).

The regulation of *CO* can be explained as a result of external coincidence model in which the circadian clock acts in concert with light to transcriptionally and post-translationally regulate *CO* activity. As a LD plant, the circadian clock in Arabidopsis regulates the oscillations of most of the genes involved in monitoring *CO* mRNA and CO protein to ensure they coincide with the light inducible phase in LD

but not SD (Suarez-Lopez et al., 2001). This also emphasises the importance of circadian clock in the photoperiod pathway of flowering by synchronising endogenous signals (CO protein level) with external signals (light).

1.3.4. Regulation of other output pathways

Besides flowering, circadian clock is known to regulate wide range of processes physiological, developmental and metabolic processes. Output pathway is best studied through transcriptomics. As mentioned before, microarray and luciferase-based enhancer-trapping approaches have revealed that up to 40% of the Arabidopsis transcriptome is regulated by circadian clock (Harmer et al., 2000; Schaffer et al., 2001; Michael and McClung, 2003; Covington et al., 2008; MIchael et al., 2008; Hazen et al., 2009). As expected, the microarray analyses identified many genes already shown in individual analyses to be clock-regulated, such as those involved in the photoperiodic control of flowering (Mouradov et al., 2002; Yanovsky and Kay, 2003; Searle and Coupland, 2004; Zhou et al., 2007), leaf movement (Satter and Galston, 1981; Edwards and Millar, 2007), stomatal opening (Webb, 1998), and hypocotyl (or cell) elongation (Dowson-Day and Millar, 1999). The microarray analyses also identified a broad range of other genes, including genes implicated in sugar metabolism, hormone signalling, and stress response. Several reviews provide detailed information on a few of these output pathways (Webb, 2003; Yakir et al., 2007; Montaigu et al., 2010; Thines and Harmon, 2011).

However, unlike the input pathways and the core oscillator, the mechanisms for regulating output pathways are less studied and little is known about the components involved. Several sequence-specific motifs have been identified in the promoters of clock regulated genes and discovered to associate with phase-specific

gene expression. The evening element (EE) that present in the promoter of *TOC1* is also found in *GI* and *LUX* and is thought to be bound by CCA1/LHY protein to induce evening-phased expression (Michael and McClung, 2002). Other than this, several other motifs have been identified to have a role in phase-specific expression such as morning element (ME; AACCACGAAAAT) found in morning-phased genes, G-box (CACGTG) found in light-activated genes, and protein box (PBX; ATGGGCC) found in night-phased genes (Martinez-Garcia et al., 2002; Harmer and Kay, 2005; Covington et al., 2008; MIchael et al., 2008). In addition to direct regulation of gene expression of genes involved in biological processes, the circadian clock might regulate some process through regulating one or more master genes which in turn initiate cascades of regulatory pathways.

The core oscillator also regulates output pathways post-transcriptionally through regulation of the stability, splicing, and transport of mRNA. RNA binding protein, COLD CIRCADIAN RHYTHM RNA BINDING 2 (CCR2, also called AtGRP7) regulates a closely-related *CCR1* gene and its own mRNA abundance by alternate splicing the mRNA (Heintzen et al., 1997; Staiger et al., 2003a). Furthermore, transcript stability of *CCR-LIKE* (*CCL*) and *SENESCENCE ASSOCIATED GENE 1* (*SEN1*) are regulated by a downstream element (DST) in their 3'UTRs which is recognised for mRNA degradation pathway (Lidder et al., 2005). The study of microRNAs (miRNAs) has revealed the function of miRNAs in mRNA degradation and translational repression (Jung et al., 2007).

In addition to circadian clock, hormones are also known to affect a wide range of biological process including those regulated by circadian clock. Therefore, it is possible that circadian clock regulates biological processes partly through regulating hormone levels and response. Consistent with this, levels of ethylene,

cytokinins, and auxin are under circadian clock control (Davis, 2009), and a circadian gating mechanism is found to play a role in regulating sensitivity of plant in response to auxin (Covington and Harmer, 2007).

Another possible output pathway involves intracellular levels of Ca^{2+} which acts as a second messenger in many signals transduction pathways such as stomata closure. The cytosolic Ca^{2+} level in Arabidopsis was found to oscillate with a circadian rhythm which persists in constant light (Dodda et al., 2004). Additionally, the rhythm of Ca^{2+} level can be entrained by different photoperiods (Love et al., 2004). There is also evidence showing that Ca^{2+} is involved in circadian regulation of stomatal opening, leaf movement and photoperiodism (Webb, 2003).

In short, circadian output pathways are still a largely unexplored area and further advances in the understanding of output mechanisms is necessary.

1.4. Flowering and circadian clock genes in other species

As already described, flowering regulatory pathways in Arabidopsis have been well-documented and key genes involved are found to be conserved between species especially components of circadian clock are ubiquitous among species . This suggests common mechanism might exist and evolved to cope with different flowering requirement in different species. Circadian clock and flowering genes are thought to generate specific signals in response to different environmental or endogenous cues. These signals are then integrated through floral pathway integrator genes to induce the expression of floral meristem identity genes in the shoot apex meristem in order to trigger flower initiation at the precise time and in the right condition. This has opened up an exciting area in the study of flowering especially for agronomically important cereal crops such as cool-season/temperate (wheat, barley, and soybean) and warm

season cereals (rice and maize) in order to understand the natural variation of flowering and hence develop strategies to maximise the production.

In barley, the recessive mutant allele of *PPD-H1* was found to cause late flowering in many spring-sown barley varieties due to the reduced photoperiod response in SD which will eventually increase biomass and yields of barley. *PPD-H1* was later found to encode for a homolog of Arabidopsis *PRR7* and is found to affect photoperiod response in barley (Turner et al., 2005). Polymorphism of this locus also correlates with geographical distribution of barley. Furthermore study of *PPH-H1* haplotype in wild and cultivated barley also identified it could be important locus for domestication of barley (Jones et al., 2008). Besides photoperiod pathway, vernalisation plays an important role in the flowering regulatory pathways of temperate cereals especially in regulating different flowering response in winter or spring varieties. Wheat is another important temperate cereal crop. Different alleles of the three major genes for vernalisation, *VRN1*, *VRN2*, and *VRN3*, in wheat and barley were found to be associated with natural variation in vernalisation requirement and cold tolerance. *VRN1* and *VRN3* have been identified as homologs of Arabidopsis *AP1* and *FT* respectively whereas *VRN2* encodes for *ZCCT* gene including CCT domain which is present in protein involved in photoperiod and circadian clock such as CO, TOC1 and PRRs (Yan et al., 2003; Yan et al., 2004; Trevaskis et al., 2006; Yan et al., 2006). In soybean, flowering time has been used in classical breeding by farmers for years but the genetic pathways are not yet well characterised. Eight loci (E1-E7 and DJ) were found to be responsible for flowering time control in soybean (Cober et al., 1996) but the molecular identities have not yet been identified. However, the soybean genes involved in circadian clock including the core oscillator components *GmLCL1*, *GmLCL2* (*AtCCA1*/*AtLHY* orthologs) and *GmTOC1* (*AtTOC1* ortholog) have been

isolated recently suggesting the existence of conserved clock components (Quecini et al., 2007; Liu et al., 2009).

In warm-season cereals, the flowering regulatory pathways has been well characterised in short-day plant, rice. The genes involved in the circadian clock and flowering are well conserved between rice and Arabidopsis including photoreceptor genes, *PHY* and *CRY* (Izawa et al., 2003), key oscillator genes *TOC1* and *CCA1* (Izawa et al., 2002), *PRR* gene family (Murakami et al., 2003; Murakami et al., 2005), *ZTL*, *FKF1*, *LUX*/*PCL1* (Izawa et al., 2003; Murakami et al., 2007) and *GI* (Hayama et al., 2002). However, no orthologs of *LHY*, *ELF3* and *ELF4* are found in rice (Izawa et al., 2003; Hayama and Coupland, 2004). *CO* and *FT* orthologs are also found in rice which are *HEADING DATE1* (*Hd1*) (Yano et al., 2000) and *HEADING DATE3a* (*Hd3a*) (Tamaki et al., 2007) respectively which was discovered as flowering time quantitative trait loci (QTL) in rice. However, *CO* was found to inhibit *FT* expression in rice to confer the SD habit of rice. In another warm-season cereal, maize, 19 QTL for flowering time were found to be associated with Arabidopsis and rice genes involved in flowering regulatory pathways (Chardon et al., 2004). Among them, one of the major QTL, *VEGETATIVE TO GENERATIVE TRANSITION 1* (*VGT1*) was cloned recently and found to encode for an *APETALA-2* like gene. A strong relationship between polymorphism at *VGT1* QTL and flowering time was found in 395 maize inbred lines and is likely to attribute to maize altilatitudinal distribution (Ducrocq et al., 2008).

Besides cereal crops, the information gained from Arabidopsis has given major insights into the studies of other important species such as *Brassica* (Osborn et al., 1997; Axelsson et al., 2001), strawberry (*Fragaria vesca*) (Mouhu et al., 2009), Lemnas (Miwa et al., 2006), Pharbitis (*Pharbitis nil*) (Liu et al., 2001a) and pea (Hecht et al., 2005). Obviously, flowering regulatory pathways have been a subject of

scientific interest in several different species. From model species Arabidopsis to agronomically important crops, the genetic components seem to be conserved. This eased the study and comparison of flowering regulatory pathways in different species.

1.5. Flowering regulatory pathways in *Pisum sativum*

The study of genetic control of flowering in garden pea (*Pisum sativum*) has begun since Mendel and as such similar to Arabidopsis, the garden pea is an annual, vernalisation-responsive, and facultative LD plants. Early study of flowering in pea back in 1970s by Murfet and his colleagues was mainly focused on four major loci responsible for natural variation on flowering time which are *STERILE NODE* (*SN*), *LATE FLOWERING* (*LF*), *HIGH RESPONSE* (*HR*), and *EARLY INITIATING* (*E*) (Murfet, 1971c; Murfet, 1971a, 1973). Of these, *SN* and *HR* are believed to be involved in the photoperiod pathway. The research continued by mutants derived from radiation or EMS (ethylmethane sulphonate) mutagenesis in Europe including early-flowering mutants which carry recessive alleles at the *DIE NEUTRALIS* (*DNE*) (King and Murfet, 1985), *PHOTOPERIOD* (*PPD*) (Arumingtyas and Murfet, 1994; Taylor and Murfet, 1996) and *LV* (Weller et al., 1995) locus, late-flowering mutants which carry recessive alleles at *FAR-RED UNRESPONSIVE* (*FUN1*) (Weller et al., 1997a) and *GIGAS* (*GI*) (Beveridge and Murfet, 1996) locus and also non-flowering mutants which carry recessive alleles at *VEGETATIVE1* (*VEG1*) (Reid and Murfet, 1984) and *VEGETATIVE2* (*VEG2*) (Murfet, 1992) loci.

Throughout the 1970s to 1990s, a series of physiological and grafting experiments were interpreted to suggest a role for a graft-transmissible floral inhibitor in pea flowering pathway (Figure 1.5, (Weller et al., 1997b)). The concept of floral inhibitor was first suggested by Barber and Paton when they tested grafting between

early and late varieties in pea and believed the late varieties are late as they produce inhibitor that is not present in early varieties (Paton and Barber, 1955). The works of Barber were inherited by his student, Ian Murfet who proposed that production of this floral inhibitor depends on *SN*, *DNE*, and *PPD* genes because the early-flowering phenotype of mutants of these loci can be partially delayed by conditional grafting onto a wild-type stock (Murfet and Reid, 1973; King and Murfet, 1985; Arumingtyas and Murfet, 1994). The *HR* and *E* genes were suggested to modify the production of this floral inhibitor at different tissue types (Murfet, 1971b; Reid, 1979a) whereas *LF* can affect the sensitivity of shoot apex to this floral inhibitor (Murfet, 1992). Characterization of *fun1* and *lv* mutants demonstrated their photomorphogenesis defects to different quality of light and thus identified them as phytochrome-deficient mutant of *PHYA* and *PHYB* respectively. Grafting experiment also suggested *FUN1* and *LV* might somehow be involved in the regulation of floral inhibitor production (Weller et al., 1995; Weller et al., 1997a). On the other hand, *GIGAS* was proposed to regulate production of a floral stimulus since the late-flowering of *gigas* scions can be promoted by grafting onto a wild-type stock (Taylor and Murfet, 1994; Beveridge and Murfet, 1996). The *veg1* and *veg2* non-flowering mutant was discovered to block the transduction of the floral stimulus but have no effect on the floral inhibitor (Reid and Murfet, 1984; Murfet, 1992).

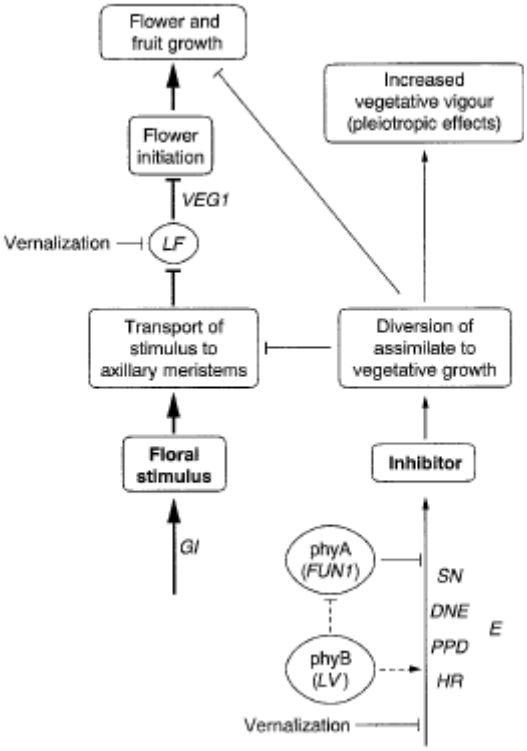

Figure 1.5 An early model of photoperiodic regulation of flowering in pea. Taken from (Weller et al., 1997b). Arrows represent a promoting effect whereas perpendicular lines represent a repressive effect. The full names of the genes/loci are included in the text.

Over the last two decades, works on flowering in Arabidopsis have advanced in the molecular era. The genetic flowering pathways of Arabidopsis as discussed in the previous sections have given insights into the conservation of molecular basis of flowering regulatory pathways between species. Therefore, a new project for understanding pea flowering pathway commenced in University of Tasmania in 2002. The project involved isolation of pea flowering gene homologs and new flowering mutants. Together with the older work done in pea, we hope to understand the molecular basis of pea flowering pathways and extend the existing flowering model by physiological and genetic approaches.

This project have successfully isolated numerous EMS-induced flowering mutants including six new late-flowering mutants (*late bloomer 1* to *6*), and additional mutant alleles for *SN* and *PPD* loci (Weller, 2007; Weller et al., 2009). On the other hand, the advance in molecular techniques and tools has allowed isolation and identification of pea homologues of Arabidopsis flowering genes. This is achieved by using the widely accessible of genomic sequence and expressed sequence tag (EST) of medicago and the high degree of synteny between medicago and pea genomes (Zhu et al., 2005; Aubert et al., 2006). Most of the genes involved in photoperiod pathways are found in pea with some alterations such as some genes are found to be duplicated and some gene families are found to be bigger in pea than in Arabidopsis (Hecht et al., 2005). By using comparative mapping and candidate gene approach based on the Arabidopsis model, the molecular identities of several mutant loci have been ascertained including *LF* as *TFL1c* (Foucher et al., 2003), *FUN1* as *PHYA* (Weller et al., 2004), *LV* as *PHYB* (Weller et al., 1995), and *LATE1* as *GIGIANTEA* (Hecht et al., 2007). However, the molecular identities of key photoperiod response loci, *SN*, *DNE*, *PPD* and *HR*, have not yet resolved.

Furthermore, new perspectives on florigen has gained from the Arabidopsis flowering model as FT has been showed as an important and well-conserved mobile floral stimulus in the photoperiodic control of flowering. Therefore, it becomes increasingly difficult to reconcile previous pea models with those in Arabidopsis. The old model about floral inhibitor was revisited and ruled out by the promotion of flowering of wild-type scions when grafted onto early-flowering mutant leafy stocks and vice versa. Therefore, the early experiments showing delayed flowering of early-flowering mutant scions when grafted onto wild-type stocks (Murfet and Reid, 1973) are probably due the epicotyl-epicotyl grafting system where there is no fully

expanded mature leaves in which the *FT* is expressed. At the same time, *CO* and *FT* orthologous genes in pea have been isolated based on medicago sequence data. Therefore, it is possible that the *CO* and *FT* mechanism on regulation of flowering in response to photoperiod is conserved in pea and *SN*/ *DNE*/ *PPD/HR* might play a role in the regulation of *CO* and *FT* expression.

The pea *SN*, *DNE*, *PPD* and *HR* loci are believed to play a role in regulating photoperiod responsiveness and inhibiting the production of the graft-transmissible florigen in pea. Comparison with Arabidopsis model suggests that *SN*, *DNE*, or *PPD* could be components of the circadian clock. (Figure 1.6).

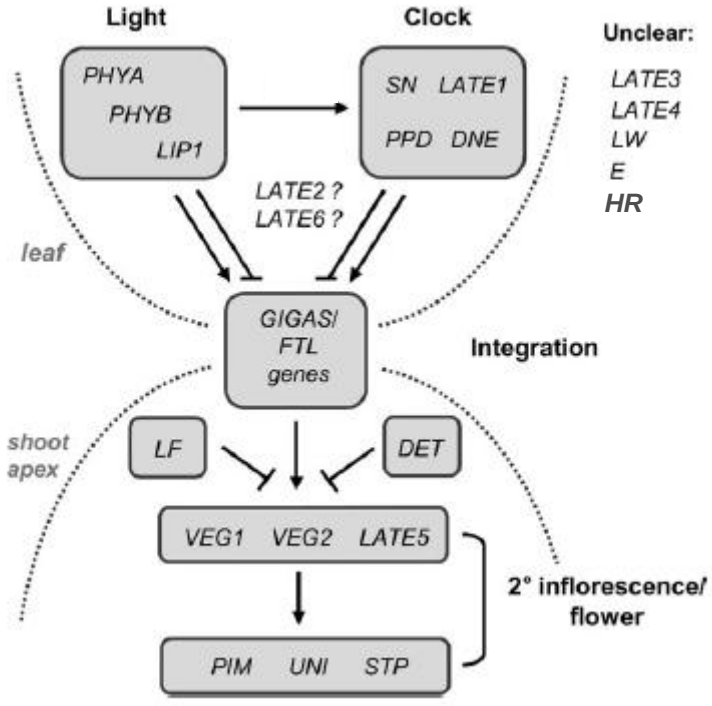

Figure 1.6 The current model on photoperiodic regulation of flowering in pea. Taken from (Weller et al., 2009). Arrows represent a promoting effect whereas perpendicular lines represent a repressive effect. The full names of the genes/loci are included in the text.

1.6. Aims

In a preliminary experiment on diurnal expression rhythms of *sn*, *dne* and *ppd* mutants, diurnal transcript rhythms of *ELF4* and another clock-regulated output gene *CHLOROPHYLL-A-BINDING PROTEIN 9* (*CAB9*) were disrupted in all three early mutants (Jones, 2004). This clearly places *SN*, *DNE*, and *PPD* in the circadian clock of the photoperiod pathways of flowering. Work in this thesis follows up this preliminary observation, with the overall aim to better define the circadian defects in these mutants, to identify if possible the molecular nature of *SN*, *DNE*, *PPD* and *HR* loci and to better define the roles of circadian clock in the photoperiodic control of flowering. To do this, this thesis is focused on three inter-related approaches: (1) isolating, mapping, and functional analysis of circadian clock genes in pea; (2) detailed physiological studies and genetics analysis on mutants (3) candidate gene evaluation for each locus. Together, this project will improve the understanding of physiological and molecular aspects of photoperiodic control of flowering time in legumes.

Chapter 2 General materials and methods

This chapter describes the general materials and methods used in this research project including bioinformatics, physiological, and molecular approaches. Detailed materials and methods used in specific studies will be described in individual chapters.

2.1. Plant materials

A wide range of different mutants and mapping parents are included in this study. A brief summary of the lines used is given in Table 2.1.

2.2. Plant growth conditions and general husbandry

All seeds were directly sown in a 1:1(v/v) mixture of dolerite chips and grade 3 vermiculite topped with 3cm of sterilised peat/sand potting mixture. In general, 140mm pots were used but in some cases, pot sizes varied in different experiments according to the purpose and the space available in growth cabinets. Plants were supplied with nutrient solution once weekly and watered on a regular basis. All plants were grown in growth cabinets or in the phytotron at the University of Tasmania, School of Plant Science. Controlled-environment growth cabinets were used for experiments in which accurate temperature or photoperiod controls were needed. Growth cabinets were maintained at a temperature of 20 °C and white light provided by cool-white fluorescent tubes (L40 W/20S cool white; Osram Germany) at an irradiance of 120 to 140μmol m^{-2} s^{-1} unless otherwise specified. Plants grown in the phytotron were exposed to a base photoperiod of natural light in conjunction with darkness or extended lighting to provide different photoperiods. Standard phytotron SD conditions consisted of an 8-h photoperiod of natural light, which was extended

for 8h to give a 16-h LD with white light from fluorescent tubes (L40 W/20S cool white, Osram Germany) at an irradiance of 10µmol m^{-2} s^{-1}. Monochromatic red (R), blue (B), far-red (FR) light (15µmol m^{-2} s^{-1}) was obtained from light-emitting diode arrays (Nichia NSPB510S WF3 Super Blue diodes, Shinkoh Electronics KL450-730GDDH [FR] and KL450-660GDDH [R] diodes). Spectral scans for all artificial light sources used can be viewed at http://www.utas.edu.au/glasshouse.gh_facilities.html.

2.3. Scoring of phenotypic traits

Flowering time was recorded as the node of first flower initiation (NFI) by counting the first scale leaf as node 1. The duration of the flowering phase was measured as the number of reproductive nodes produced (RN = TN – NFI +1) where TN is total number of nodes formed (both vegetative and reproductive) at senescence. Lateral branching was quantified as the ratio of total lateral branch length (TBL) to total plant height (TPH) at a specified age. Internode length was measured as the length between two specified nodes *a* and *b* (L*a*-*b*); e.g. L1-9 is the internode length between node 1 and node 9. Leaf area was estimated as the product of the length and width of a single leaflet from a specified leaf, or by direct measurement using a Java-based image processing software from National Institute of Health, Image J (http://rsbweb.nih.gov/ij/).

Table 2.1 The details of lines used in this study. The genetic WT background, description, and reference of individual lines are included.

Lines	Wild type background	Description	Reference
sn-1 (L59)	unknown	early-flowering under short-day (SD), reduced photoperiod responsiveness	Barber (1959) Murfet et al. (1971a)
Borek	Borek	wild-type plant (*le-1* dwarf)	Arumingtyas and Murfet (1994)
sn-2	Borek	early-flowering under short-day (SD), reduced photoperiod responsiveness	Arumingtyas and Murfet (1994)
ppd-1	Borek	early-flowering under SD, reduced photoperiod responsiveness	Arumingtyas and Murfet (1994) ;
ppd-2	Borek	early-flowering under SD, reduced photoperiod responsiveness	Taylor and Murfet (1996)
NGB 5839	Torsdag	wild-type plant (Torsdag *le-3*)	Lester et al. (1997)
sn-3	NGB5839	early-flowering under SD, reduced photoperiod responsiveness	Jones (2004) ; Weller et al. (unpubl.)
sn-4	NGB5839	early-flowering under SD, reduced photoperiod responsiveness	Hecht et al. (2007)
ppd-3	NGB5839	early-flowering under SD, reduced photoperiod responsiveness	Jones (2004) ; Weller et al. (unpubl.)
dne-1	NGB5839	early-flowering under SD, reduced photoperiod responsiveness; dne originally in Torsdag (LE) but re-selected in 5839 (*le*) background	King and Murfet (1985)
late1-1	NGB5839	late-flowering under long-day (LD)	Hecht et al. (2007)
late1-2	NGB5839	late-flowering under long-day (LD)	Hecht et al. (2007)
late2	NGB5839	late-flowering under long-day (LD)	Weller et al. (unpubl.)
Torsdag	Torsdag	Mapping parent	Loridon et al (2005)
Terese	Terese	Mapping parent	Loridon et al (2005)
Champagne	Champagne	Mapping parent	Loridon et al (2005)
WL771	WL1771	Mapping parent (*LE* tall)	Taylor and Murfet (1993)
JI1794	JI1794	Mapping parent	Weeden et al (1998)
Slow	Slow	Mapping parent	Weeden et al (1998)
JI281	JI281	Mapping parent	Hall et al (1997)
JI399	JI399	Mapping parent	Hall et al (1997)

2.4. Grafting

Plants used for stocks were grown for 18 d from sowing and had five to six fully expanded leaves at the time of grafting. Stock plants were decapitated above the uppermost fully expanded leaf, and a longitudinal slit was cut down the center of the stem to receive the scion. Seedlings used as scions were grown for 6 to 7 d after sowing, at which point they were just emerging through the soil. These seedlings were decapitated at the epicotyl approximately 1 cm above the cotyledonary node. A graft wedge was prepared from the cut end of the scion and inserted into the stock. The graft was secured by a small piece of silicon tubing, and pots were then enclosed in plastic bottles for 1 to 2 weeks to maintain high humidity during establishment of the graft union. Lateral shoots arising from the scion and stock were excised regularly.

2.5. Bioinformatics and genetics analysis

Sequences of Arabidopsis circadian-related clock genes obtained from Genebank were used to identify homologs in Medicago and other species using tBLASTx searches of the National Center for Biotechnology Information database (http://www.ncbi.nlm.gov), Medicago genomic database at the J. Craig Venter Institute (formerly TIGR, http://www.jcvi.org/cgi-bin/Medicago/index.cgi), and the Medicago EST database (http://compbio.dfci.harvard.edu). In some cases, to identify Medicago gene-based markers in pea, tBLASTx searches were performed against the Medicago genomic database at the J. Craig Venter Institute. The map positions of relevant genes were obtained by using Medicago Genome Browser (http://gbrowse.jcvi.org/cgibin/gbrowse/Medicago_imgag/).

Protein and nucleotide alignments were performed with ClustalX (Thompson et al., 1997) and adjusted manually where necessary using GENEDOC (Nicholas et al. 1997;

http://www.psc.edu/biomed/genedoc). Distance and parsimony-based methods were determined for phylogenetic analyses in PAUP* 4.0b10 (http://paup.csit.fsu.edu) using the alignments generated.

2.6. Primers

Degenerate primers for isolation of pea genes were designed using the CODEHOP strategy (Rose et al 1998) on conserved domains identified from protein sequence alignments using the BLOCK MAKER application (http://blocks.fhcrc.org/blockmkr/make_blocks.html). Selected primers were manually optimised by reference to the input legume sequences. Medicago-specific primers were designed using Primer3 (http://frodo.wi.mit.edu/primer3) based on Medicago sequences to target conserved regions in pea. The details of primer sequences are given in Appendix 1.

2.7. Gene isolation

2.7.1. DNA extraction

Genomic DNA was isolated from individual plants using a modified CTAB protocol. Harvested tissue was frozen in liquid nitrogen and ground to a fine powder in a mill mixer by adding tungsten carbide bead to each tube. 500µL of extraction buffer (100mM Tris-HCL pH8, 1.4M NaCl, 20mM EDTA, 2% w/v CTAB, 20mM 2-β-mercaptoethanol) was added into each tube prior to incubation at 60°C for 15 min. 500µL of Chloroform:Isoamylic alcohol (24:1) was then added to the tubes, and the contents were mixed by gentle inversion. The samples were centrifuged at 14000 rpm for 1 min and the upper aqueous phase was transferred to new tubes and again extracted. 1mL of precipitation buffer (50mM Tris-HCL pH8, 10mM EDTA, 1% w/v

CTAB) was added after the second extraction. The contents of the tube were mixed gently and allowed to rest at room temperature for 10-15 min until a thread-like precipitate was formed. The precipitate was collected by centrifugation (10min, 14000rpm) and dissolved in 300µL of 1.5M NaCl containing 1µL RNase A (25mg/mL). The solution was incubated at 50°C for 15min or until the pellet was fully dissolved. DNA was precipitated by adding 600µL of 100% ethanol and was collected by centrifugation (10min, 14000rmp). After centrifugation, the pellet was washed in 70% ethanol, air-dried and resuspended in 50µL of sterilised water.

2.7.2. DNA Quantification

DNA concentration was determined using Picogreen dsDNA quantification reagent (Molecular Probes, http://www.invitrogen.com/site/us/en/home/brands/Molecular-Probes.html) in a Picofluor fluorometer (Promega, formerly Turner Biosystems http://www.luminometer.com/instruments/fluorometer-for-RNA-DNA-proteins.php) or NanoDrop 8000 (Thermo Scientific, http://www.thermoscientific.com/wps/portal/ts/).

2.7.3. Polymerase Chain Reaction (PCR)

All PCR reactions were performed in 50 µL, which included 5µL of DNA template and 45µL of master mix. The master mix was prepared according to Table 2.2 and scaled up to the required number of reactions.

PCR was carried out in a thermal cycler with heated lid as follows: an initial template denaturation step at 94˚C for 5min, followed by 35 cycles of 94˚C for 1 min (denaturation of DNA into single strands), T_m (annealing temperature) for 1 min (annealing of primer), and 72˚C for 1 minute per 1000 base pairs of DNA being amplified (extension of newly synthesised strands). Reactions were concluded by

heating at 72˚C for 5min and then held at 10˚C. The T_m varied according to the length and composition of the primers used and the extension temperature varied according to the specific polymerase used. PCR products were analysed on agarose gels by electrophoresis, and purified using the Promega Wizard SV Gel and PCR Clean-Up System (Promega, http://www.promega.au) with the microcentrifuge protocol.

2.7.4. Cloning

Purified PCR products were ligated into a pGEM-T plasmid vector using the Promega pGEM-T Easy Vector System (Promega, http://www.promega.au) using the 10µL protocol. 5µL of the ligation was transformed into competent *E.coli* cells (50µL) by electroporation at 1.2kV. 400µL of Luria Broth (LB, $10gL^{-1}$ NaCl, $5gL^{-1}$ Bacto Yeast extract, $10gL^{-1}$ Bacto Tryptone, pH7.5) was added to each transformation to recover the bacteria and tubes were shaken at 37˚C for 1 h. Each transformation reaction was then spread across two LB agar plates (225µL per plate) containing 100µg/mL ampicillin and $1\mu LmL^{-1}$ 4% X-gal (5-bromo-4-indolyl-beta-D-galactopyranoside), and cultured at 37˚C overnight. White colonies were selected and screened for the presence of appropriate insert by colony PCR.

2.7.5. Colony PCR

Ten to twenty colonies were individually picked up with toothpicks, placed in 5µL of sterile water and denatured at 95˚C for 5 min. A 20µL aliquot of PCR master mix (Table 2.4) was added to each tube. PCR was carried out in a thermal cycler and analysed on agarose gels by electrophoresis as for normal PCR.

2.7.6. Plasmid DNA extraction

Single colony were cultured overnight in a shaking incubator at 37˚C in 5mL of

Terrific Broth (12g/L Bacto tryptone, 24gL^{-1} Bacto yeast extract, 4mLL^{-1} glycerol, 25mLL^{-1} KHPO) containing 100µg/mL ampicilin. Plasmids were extracted from the culture using Promega Wizard Plus SV Mini-prep DNA Purification System with the centrifugation protocol (Promega, http://www.promega.au).

2.7.7. Rapid Amplification of cDNA Ends (RACE) PCR

RACE-PCR was performed using the BD SMART RACE cDNA amplification kit (Clontech, http://www.clontech.com/) following the manufacturer's protocol. Gene-specific primers (GSPs) and nested GSPs (NGSPs) (Appendix 1) were designed for the 5'and 3'RACE reactions according to recommended guidelines (23-28 nucleotides, 50-70% GC, and T_m greater than 60˚C). First-strand cDNA was synthesised from total RNA using a modified lock-docking oligo (dT) primer, the SMART II A oligonucleotide and BD Powerscript Reverse Transcriptase. 5'- and 3'-RACE were performed on the cDNA synthesised using the different gene-specific primers. All PCR reactions were optimized for use with Advantage 2 Polymerase Mix (Clontech, http://www.clontech.com/).

2.7.8. Genome walking

Genome walking was performed using the Genome Walker universal kit (Clontech, http://www.clontech.com/) following the manufacturer's protocol. Genomic libraries were created by digesting genomic DNA with different restriction enzymes that leave blunt ends (such as DraI, EcoRV, and HpaI) and ligated to GenomeWalker adaptors. Gene-specific primers (GSPs) were designed as mentioned previously. Genome walking was performed on the genomic libraries using GSPs and adaptor primers (Appendix 1). All PCR reactions were optimized for use with Advantage 2 Polymerase Mix (Clontech, http://www.clontech.com/).

2.7.9. Sequencing

Purified PCR fragments and plasmids were sequenced at the Australian Genome Research Facility (AGRF, University of Queensland, Australia) or Macrogen (Tokyo University of Agriculture, Japan). Sequencing results were aligned and analysed using Sequencher 4.0 (Genecodes, http://www.genecodes.com/).

2.8. Gene expression

2.8.1. RNA extraction

Harvested tissue was frozen in liquid nitrogen and homogenised either using a mortar and pestle or by carbide beads and mill mixer. Total RNA was extracted using the Promega SV Total RNA isolation system according to the manufacturer's instructions (Promega, http://www.promega.au).

2.8.2. Quantification

RNA concentration was determined using Ribogreen RNA quantification reagent (Molecular Probes, http://www.invitrogen.com/site/us/en/home/brands/Molecular-Probes.html) in a Picofluor fluorometer (Promega, formerly Turner Biosystems http://www.luminometer.com/instruments/fluorometer-for-RNA-DNA-proteins.php) or NanoDrop 8000 (Thermo Scientific, http://www.thermoscientific.com/wps/portal/ts/).

2.8.3. Reverse transcription

First strand cDNA was synthesised from equal amount (1µg) of total RNA using the Epicentre MMLV high performance reverse transcriptase system (Epicentre, http://www.epibio.com/). RNA was first incubated with sterile water at 65˚C for 5min to denature any secondary structure. A master mix was prepared (Table 2.4) and a 7µL

aliquot was added to each tube. A negative control without reverse transcriptase (RT-) was included for each sample to check for the presence of genomic DNA contamination in the RNA sample. Reverse transcription was performed at 37˚C for 1 h with a final incubation at 72˚C for 10min to denature the enzyme. For use in real-time quantitative PCR (RT-qPCR), the synthesised cDNA was diluted five-fold with RNase-free water.

2.8.4. Real-time quantitative PCR (RT-PCR)

Real-time PCR reactions using SYBR green chemistry (Quantace Sensimix, Bioline, http://bioline.gene-quantification.info/) were set up with a CAS-1200N robotic liquid handling system (Qiagen, formerly Corbett Research, http://www.qiagen.com/) and run for 50 cycles in a Rotor-Gene RG3000 (Qiagen, formerly Corbett Research, http://www.qiagen.com/). Each reaction contains 2 µL of first-strand cDNA , 5.4µL Sensimix plus, 0.3µL forward primer and 0.3µL reverse primer. Two technical replicates were performed for each sample. Relative transcript levels for a target genes were all evaluated against an *ACTIN* reference gene (Foo et al., 2005) using nonequal amplification efficiencies (E) and deviation of threshold cycle (ΔCT) according to the following equation (Pfaffl, 2001):

$$\text{Relative transcript level} = (E_{target})^{\Delta CT\,(refrence\,-\,target)} * 100\%$$

All data shown represent the mean ± SE of two to three biological replicates, with each biological replicate consisting of pooled material from two plants.

Table 2.2 Reagent required for a 50 µL normal PCR reaction.

Reagent	For 1 reaction (50µL)
DNA template (added separately)	5µL
PCR buffer (5x)	10µL
$MgCl_2$	2 µL
dNTPs (10mM)	1µL
Forward primer (10µM)	1µL
Reverse primer (10µM)	1µL
DNA polymerase	0.2µL
Sterile water	29.8 µL

Table 2.3 Reagents required for a 25 µL colony PCR reaction.

Reagent	For 1 reaction (20µL)
PCR buffer (5x)	5µL
$MgCl_2$	1 µL
dNTPs	0.5µL
Forward primer (10µM)	0.5µL
Reverse primer (10µM)	0.5µL
DNA polymerase	0.1µL
Sterile water	12.4µL

Table 2.4 Reagents required for a 20µL reverse transcription reaction.

Reagent	RT+	RT-
RNA + Sterile water (added separately)	13µL	13µL
Epicentre RT buffer (10x)	2µL	2µL
DTT	2µL	2µL
dNTPs	1µL	1µL
Oligo-dT primer	1µL	1µL
ScriptGuard RNase inhibitor	1µL	1µL
Reverse transcriptase (RT)	1µL	- (1µL of water added)

2.9. Molecular markers, genotyping, and mapping

2.9.1. Mapping

Untranslated region and intron sequences were obtained by PCR on genomic DNA from parents of three different recombinant inbred line (RIL) populations JI281xJI399, (Hall et al, 1997), Terese x Champagne (Loridon et.al. 2005, Aubert et.al. 2006) and, JI1794 x Slow (Weeden et al 1998) (Table 2.1 and Table 3.3). Suitable polymorphisms were converted to cleaved-amplified polymorphic sequence (CAPs) or degenerate cleaved-amplified polymorphic sequence (dCAPs) markers and scored in corresponding recombinant inbred line populations. Mapping of markers in Terese x Champagne and JI1794 x Slow RIL populations was conducted in collaboration with Benedict Wenden and Catherine Rameau (INRA Versailles, France) and Norm Weeden (Montana State University, USA) respectively. For mapping of flowering loci, individual mutant mapping populations (*sn-4* x Terese, *ppd-3* x Terese, JI1794 *x ppd-3*, and *late2* x Terese) were also generated. The genetic distance between molecular markers was estimated from segregation data using Joinmap 3.0 software (van Ooijen, 2006). Primers used for mapping are listed in Appendix 1.

2.9.2. Genotyping

Coding region sequences were obtained by PCR on cDNA from wild-type and specified mutants. Identified mutations were converted into CAPs or dCAPs markers and scored in the relevant segregating population in order to confirm the cosegregation of the mutation with mutant phenotype or to follow segregation during backcrossing or selection.

Chapter 3 Isolation and characterization of circadian clock-related genes in pea

3.1. Introduction

As discussed in Chapter 1, the flowering pathway has been intensively studied in the model plant species, *Arabidopsis thaliana*, and this has provided clear evidence for the importance of the circadian clock in the photoperiodic flowering response. Circadian clocks are thought to be ubiquitous in higher plants and to play an important role in the photoperiod pathway of flowering time regulation. As a central component in the photoperiod pathway, circadian clock synchronises environmental cues (input) with endogenous rhythms (circadian rhythms), allowing plants to flower at the right time (output). This information gained from Arabidopsis have given major insights into the studies of other important species such as rice (*Oryza sativa*) (Yano et al., 2000; Murakami et al., 2003; Tamaki et al., 2007), Lemnas (Miwa et al., 2006) and pea (Hecht et al., 2005). Comparative biology between species suggests that a common mechanism might exist and evolved to cope with different flowering requirement in different species.

The legumes are a major plant group that contains many species of agronomic importance, including the grain legumes pea, lentil, chickpea, and the forage crops lucerne and clover. Among legumes, the genetic control of flowering has been long studied in model species, garden pea (*Pisum sativum*). Many flowering mutants including photoreceptor mutants, inflorescence mutants, and photoperiod response mutants have been characterised, in pea , as described in Chapter 1. Based on phenotypes and preliminary analyses of gene expression in *sn*, *dne*, *ppd* mutants, *SN*,

DNE, and *PPD* are clearly needed for normal response to photoperiod and may potentially affect the circadian clock. This is also potentially true for the *HR* locus. Numerous flowering gene homologs, including circadian clock-related genes were recently identified and mapped in pea (Hecht et al., 2005) based on information from the *Medicago truncatula* genome (release version 1.0).

Medicago truncatula is a clover-like small legume plant which was subjected to genome sequencing project since 2003 and the genome has been released for public access with annotations and chromosome locations. Predicted coding sequences and proteins sequences are searchable and downloadable. Comparative genome analysis between Medicago and pea has revealed high degree of synteny between Medicago and pea genomes (Choi et al., 2004; Kalo et al., 2004; Zhu et al., 2005). Consensus map between Medicago and pea generated using common marker existed in both species (Aubert et al., 2006) allows us to locate and isolate pea homologous genes based on genome sequences and map position of Medicago genes. In addition to this, the map positions of Medicago genes can be used to infer to map positions of their pea orthologs and suggest possible candidate genes around mutant loci or rule out genes that are not within region of interest.

Since the initial study by Hecht et. al. (2005), sequencing of Medicago genome and EST collection has progressed steadily and the most current genome assembly available for this study was version Mt 3.0 (J. Craig Venter Institute JCVI, formerly TIGR, http://jcvi.org/cgi-bin/ Medicago/index.cgi). In view of the improvements since the previous study of Hecht et a. (2005) it was of interest to rescreen the database for genes with a potential role in flowering and the circadian clock.

3.1.1. Aims

We initially adopted a candidate gene approach in an attempt to identify the *SN*, *DNE*, *PPD* and *HR* loci at the molecular level. This approach involved the isolation of pea homologs of genes with a known role in circadian clock function in other species, primarily Arabidopsis. The range of potential candidates was then narrowed by (a) using positional information to exclude candidates not mapping near mutant loci and (b) carrying out more detailed phenotypic characterization of mutants to identify the most functionally similar genes in Arabidopsis.

The main aim of the work presented in this chapter was therefore to extend the previous work of Hecht et. al. (2005) by identifying, isolating, and mapping additional putative circadian-clock related genes in pea. This included extending and/or mapping previously-isolated sequences related to *ELF3*, *ELF4*, *TOC1*, and two *LHY*/*CCA1*-like *MYB* sequences (*MYB1* and *MYB2*) (Hecht et al., 2005) and also attempting to isolate sequence for pea homologs of new genes in Arabidopsis circadian clock system identified since 2005. The second aim of the study was to conduct a preliminary characterization of these genes including phylogenetic analysis, gene structure comparison, and transcriptional regulation.

3.2. Materials and methods

3.2.1. Gene expression experiments

For the diurnal expression experiments, all plants were grown for 3 weeks from sowing at 20°C in growth cabinets under either LD (16-h photoperiod) or SD (8-h photoperiod). Harvested material consisted of single leaflet from the uppermost fully expanded leaf from two plants. Samples were harvested at 4h intervals, with 3 replicates per time point. Samples were harvested and processed by V. Hecht and K.

Claire. Several real-time PCR runs were done with assistance of V. Hecht.

3.3. Results

3.3.1. Identification of circadian clock-related genes in Medicago

Partial sequence of several circadian clock-related genes was previously isolated in pea (*ELF3*, *ELF4*, *TOC1*, *MYB1* and *MYB2*) ((Hecht et al., 2005); C. Lai, unpublished data) and several but not all were mapped. This represented most of the known Arabidopsis clock genes at that time but many more have subsequently been identified, including *LUX*, *TIC*, *RFI2*, *TEJ*, *FIONA1*, *XCT* and members of the *PRR* and *CDF* families (Matsushika et al., 2000; Makino et al., 2002; Panda et al., 2002; Hall et al., 2003; Hazen et al., 2005; Imaizumi et al., 2005; Chen and Ni, 2006b; Kim et al., 2008; Martin-Tryon and Harmer, 2008).

As an initial step, we performed a tBLASTx search for each Arabidopsis clock gene against the Medicago genome at the J. Craig Venter Institute (JCVI, http://www.jcvi.org/cgi-bin/Medicago/index.cgi) and the Medicago EST database (http://compbio.dfci.harvard.edu) and compiled a list of Medicago genomic sequences and ESTs which are homologous to Arabidopsis circadian clock genes (Table 3.1). EST contigs corresponding to genomic sequences were identified by BLASTn search against the Medicago genome database but some EST contigs were distinct from genomic sequences. Most of the known Arabidopsis clock genes are represented in Medicago databases, with some genes represented by a single sequence (eg. *ELF3*, *ELF4*, *TIC*) and others genes present as a gene family (eg. *MYB*, *PRR*, and *CDF*). In some cases, particularly for multiple genes in a gene family, Medicago sequences were "reciprocally" BLASTed back to the Arabidopsis genome database at The Arabidopsis Information Resource (TAIR, http://www.arabidopsis.org/index.jsp) to confirm that

the Medicago sequence identified were indeed most similar to the original Arabidopsis query sequence, and did not simply represent more distant homologs.

Furthermore, the map positions of Medicago sequence were obtained to suggest likely positional candidate genes for the mutant loci. In most cases, the map positions of the Medicago BAC sequences were available through the JCVI website (http://gbrowse.jcvi.org/cgi-bin/gbrowse/ Medicago_imgag/), both as a position on the genetic map and location on the physical map (pseudomolecule). Physical map positions are clearly provisional, as the pseudomolecule still incorporates many gaps where contigs have not yet been physically connected. However in many cases this position can be used to identify the likely location of the pea ortholog.

Table 3.1. Summary of Medicago genomic sequences and corresponding expressed sequence tags (ESTs) with homology to genes of circadian clock from Arabidopsis. The order of Bac is based on the return of top hit of Medicago BLAST result. Physical map position for genomic sequence of Medicago is indicated besides the Bac number.

Gene	Arabidopsi	Medicago					Type of protein	Reference
	Locus id	Name	Bac	Genecall	Physical	Corresponding ESTs		
ELF3	AT2G25930	*ELF3*	CU468275	Medtr3g140450	LG3-36.3	TC125285	Nuclear protein	McWatters et al. 2000
ELF4	AT2G40080	*ELF4a*	CT967317	Medtr3g093640	LG3-22.3	TC126609	Nuclear protein	Doyle et al. 2002
GI	AT1G22770	*GI*	AC148397	Medtr1g124650	LG1-27.2	TC115027	Nuclear protein	Park et al. 1999
TIC	AT3G22380	*TIC*	AC137838	Medtr1g132680	LG1-29.7	TC113764	Nuclear proten	Hall et al. 2003
LUX/PCL	AT3G46640	*LUXa*	AC202498	Medtr4g084460	LG4-17.8	TC134711	MYB related GARP protein	Hazen et al. 2005
			AC202347	Medtr4g084700	LG4-17.9	TC134711		
		LUXb	AC183371	Medtr7g105990	LG7-24.4	TC129203		
RFI2	AT2G47700	*RFI2*	AC144541	Medtr7g138550	LG7-32.9	TC135404	RING-domain zinc finger protein	Chen and NI 2006a,2006b
TEJ	AT2G31870	*TEJ*	AC122162	Medtr3g028610	LG3-7.4	-	poly-(ADP-ribose) glycohydrolase (PARG)	Panda et al. 2002
FIONA1	AT2G21070	-	No good match	-		BE247932	Nuclear protein	Kim et al. 2008
XCT	AT2G21150	*XCT*	AC140035	Medtr4g157300	LG4-39.2	TC128471	Nuclear protein	Martin-Tryon et al. 2008
LHY	AT1G01060	*MYB1*	AC150443	Medtr7g146200	LG7-34.9	TC114048	MYB related transcription facotr	Alabadi et al. 2001, 2002
		MYB2	AC126787	Medtr5g084860	LG5-32.3	TC117367		
		MYB3	AC150443	Medtr7g146190	LG7-34.9	TC136357		
		MYB4	AC137985	Medtr3g086700	LG3-20.4	-		
CCA1	AT2G46830	*MYB2*	AC126787	Medtr5g084860	LG5-32.3	TC117367	MYB related transcription facotr	Wang et al. 1997
		MYB3	AC150443	Medtr7g146190	LG7-34.9	TC136357		
		MYB4	AC137985	Medtr3g086700	LG3-20.4	-		
		MYB1	AC150443	Medtr7g146200	LG7-34.9	TC114048		
TOC1	AT5G61380	-	No good match	-		TC131807	Pseudo response regulator	Somers et al. 1998b
						TC122078		Strayer et al. 2000
PRR9	AT2G46790	*PRRa*	CR940305	Medtr3g122650	LG3-30.5	TC134196	Pseudo response regulator	Matsushika et al. 2000
		PRRb	AC149306	Medtr4g079920	LG4-16.2	TC116619, TC134985		Makino et al. 2002
		PRRc	AC150443	Medtr7g146130	LG7-34.9	TC124290		
						TC124074		

						TC120462		
PRR7	AT5G02810	*PRRa*	CR940305	Medtr3g122650	LG3-30.5	TC134196	Pseudo response regulator	Matsushika et al. 2000
		PRRb	AC149306	Medtr4g079920	LG4-16.2	TC116619, TC134985		Makino et al. 2002
		PRRc	AC150443	Medtr7g146130	LG7-34.9	TC124290		
						TC124074		
						TC120462		
PRR5	AT5G24470	*PRRa*	CR940305	Medtr3g122650	LG3-30.5	TC134196	Pseudo response regulator	Matsushika et al. 2000
		PRRb	AC149306	Medtr4g079920	LG4-16.2	TC116619, TC134985		Makino et al. 2002
		PRRc	AC150443	Medtr7g146130	LG7-34.9	TC124290		
						TC124074		
						TC120462		
PRR3	AT5G60100	*PRRa*	CR940305	Medtr3g122650	LG3-30.5	TC134196	Pseudo response regulator	Matsushika et al. 2000
		PRRb	AC149306	Medtr4g079920	LG4-16.2	TC116619, TC134985		Makino et al. 2002
		PRRc	AC150443	Medtr7g146130	LG7-34.9	TC124290		
						TC124074		
						TC120462		
CDF1	AT5G62430	*CDF1*	CT025840	Medtr5g044650	LG5-18.6	-	DOF transcription factor	Imaizumi et al. 2005
						TC95604		
						TC96008		
						BE999782		
CDF2	AT5G39660	*CDF2a*	AC166744	Medtr6g012960	LG6-25.9	-	DOF transcription factor	Imaizumi et al. 2005
		CDF2b	AC140025	Medtr7g010180	LG7-2.9	-		
						TC95604		
						TC96008		
						BE999782		
CDF3	AT3G47500	*CDF3*	AC202576	Medtr4g111370	LG4-25.5	-	DOF transcription factor	Imaizumi et al. 2005
						TC95604		
						TC96008		
						BE999782		

3.3.2. Isolation of circadian clock-related genes from pea

Degenerate primers or Medicago-specific primers (Appendix 1) were designed based on information from Table 3.1 and using the method outlined in Chapter 2 to target conserved regions of specific flowering genes (Section 2.6). Figure 3.1 shows an example from the isolation of the *LUX* gene. Primer pairs were designed on conserved regions of the Medicago LUX protein and used directly for PCR on pea, leading to successful amplification of the pea ortholog. The amino acids sequences targeted by the primers are identical in both species, and the pea nucleotide sequences differed in only a single position. Using this approach, fragments of a few putative pea homologs of several Arabidopsis clock-associated genes were identified in Medicago and partial sequences isolated from pea (*PsPRR37*, *PsPRR59*, *PsTIC*, and *PsLUX*). These newly isolated fragments were extended along with other partial sequences previously isolated by Hecht et. al. (2005) (*PsMYB2*, *PsELF3*, *PsELF4*, and *PsTOC1*) using RACE-PCR and/or genome walking approaches (Section 2.77 and 2.78). In summary, *PsMYB1* and *PsGI* were previously isolated in full length (Hecht et al., 2007), *PsELF3* and *PsELF4* were extended to full length in this study, *PsPRR37* and *PsLUX* were fully isolated from scratch. In addition, partial sequence of *PsMYB2* (71%), *PsPRR59* (82%), *PsTOC* (10%), and *PsTIC* (19%) were isolated from scratch and/or extended.

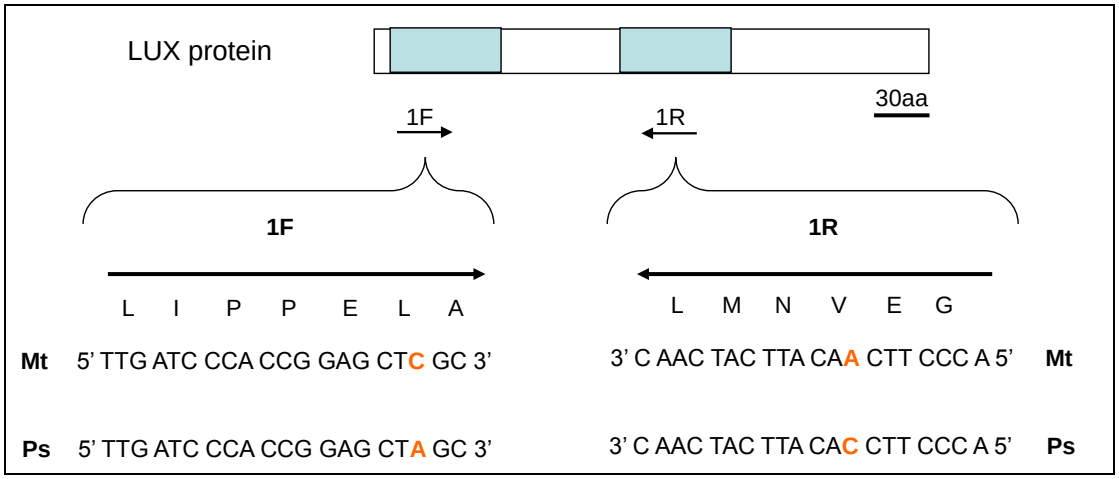

Figure 3.1 Medicago-specific primers to target conserved regions of *LUX* gene. The regions highlighted in blue are conserved region in LUX protein. The sequences of forward (1F) and reverse (1R) primers in Medicago are highly similar to pea sequence. The differences in primers are highlighted in orange colour.

Table 3.2 summarises isolated circadian clock-related genes in pea and shows the percentage of identity at the amino acid level with the corresponding Arabidopsis and Medicago genes. Most of the homologous pairs are pretty well conserved at the amino acid level but interestingly the %[a] identity for full length sequence range from 33% to 75% between Arabidopsis and pea genes. On the other hand, %[a] identity for full length sequence between Medicago and pea are more even (75% to 86%). The low %[a] identity between *AtCCA1* and *PsMYB2* (21%) does suggest *PsMYB2* is unlikely to be ortholog of *AtCCA1* gene and reciprocal BLAST (tBLASTx) back to Arabidopsis genome did not come back as top hit for either *CCA1* or *LHY* sequences.

Table 3.2. Summary of pea orthologous circadian clock-related genes to Arabidopsis. %[a] Identity percentage based on isolated sequence at amino acid level when compared to either Arabidopsis or Medicago; (FL) full length cDNA; Previous study, o = Hecht et.al. 2005, c = V. Hecht and C. Lai, unpublished

Arabidopsis		Medicago		Pea					
Gene	**locus id**	**Gene**	**Genecall**	**Gene**	**Previous study**	**This study**	**Accession**	**% [a] (At)**	**% [a] (Mt)**
LHY	AT1G01060	*MtMYB1*	Medtr7g146200	*PsMYB1*	FL[o]	-	AY826730	42%	78%
CCA1	AT2G46830	*MtMYB2*	Medtr5g084860	*PsMYB2*	11%[o]	71%	AY826731	21%	82%
ELF3	AT2G25930	*MtELF3*	Medtr3g140450	*PsELF3*	60%[c]	FL	AY830925	33%	82%
ELF4	AT2G40080	*MtELF4a*	Medtr3g093640	*PsELF4*	44%[o]	FL	AY830926	45%	86%
GI	AT1G22770	*MtGI*	Medtr1g124650	*PsGI*	FL[o]	-	EF185297	75%	75%
TOC1	AT5G61380	-	-	*PsTOC1*	9%[o]	10%	AY930927	90%	88%
PRR7	AT5G02810	*MtPRRb*	Medtr4g079920	*PsPRR37*	-	FL	FJ609177	36%	79%
PRR5	AT5G24470	*MtPRRa*	Medtr3g122650	*PsPRR59*	-	82%	FJ609180	37%	87%
TIC	AT3G22380	*MtTIC*	Medtr1g132680	*PsTIC*	-	19%		47%	91%
LUX	AT3G46640	*MtLUX*	Medtr4g084460	*PsLUX*	-	FL		44%	82%

3.3.3. Characterizations of pea orthologs of circadian clock-related genes

For some genes, particularly those in gene families, it was difficult to determine the relationship between the Medicago BLAST hits and the Arabidopsis genes. Therefore, in order to further characterise the isolated clock-related genes and to compare them to the corresponding Arabidopsis and Medicago genes, phylogenetic analysis was performed based on amino acid sequences from different species including Arabidopsis, Medicago, and pea. In addition, a comparison of gene structure was made between Arabidopsis, Medicago and pea, and patterns of transcription regulation under diurnal cycles (LD and SD) were also carried out for each gene.

3.3.3.1. ELF3

In Arabidopsis, *ELF3* is a 2085bp gene containing 4 exons and 3 introns and encodes for a 695aa nuclear protein (McWatters et al., 2000; Liu et al., 2001b)A phylogenic tree constructed from ELF3-related sequences consists of two major clades, monocot and dicot, with Arabidopsis and *Lemna* falling outside of these two groups (Figure 3.2A). The single Medicago ELF3-like sequence (MtELF3) clusters with other dicot ELF3-related sequences (Figure 3.2A). Partial cDNA of *PsELF3* (60%) was obtained in previous study by using degenerate primers which also include sequence of intron2 (V. Hecht and C. Lai and, unpublished data). In this study, a full length cDNA was isolated from this partial sequence by 5' and 3' RACE-PCR on previously isolated sequence and also the full length gDNA including previous intron and two newly amplified introns (intron 1 and 3) (Figure 3.2B).

PsELF3 and MtELF3 cluster together with GmELF3 and form a small legume clade (Figure 3.2A). Figure 3.2B shows that the gene structure of *AtELF3, MtELF3,* and *PsELF3* are very similar with three introns embedded within four exons. They have similar length for coding sequences (approximately 2000bp) and 3 introns in conserved locations. *ELF3* transcript in Arabidopsis does not show a very distinct diurnal rhythm like other clock-regulated genes. Bimodal peaks (a morning and night peak) were found in transcript rhythms of *ELF3* in LD and SD in two separate studies in Arabidopsis (Hicks et al., 2001; Yu et al., 2008). The expression patterns of *PsELF3* are found to be not rhythmic in SD but with possible low bimodal peaks (ZT12 and ZT20; ZT36 and ZT44) in LD (Figure 3.2C) in LD. The transcript level of *PsELF3* in SD is three-fold higher than in LD (Figure 3.2C).

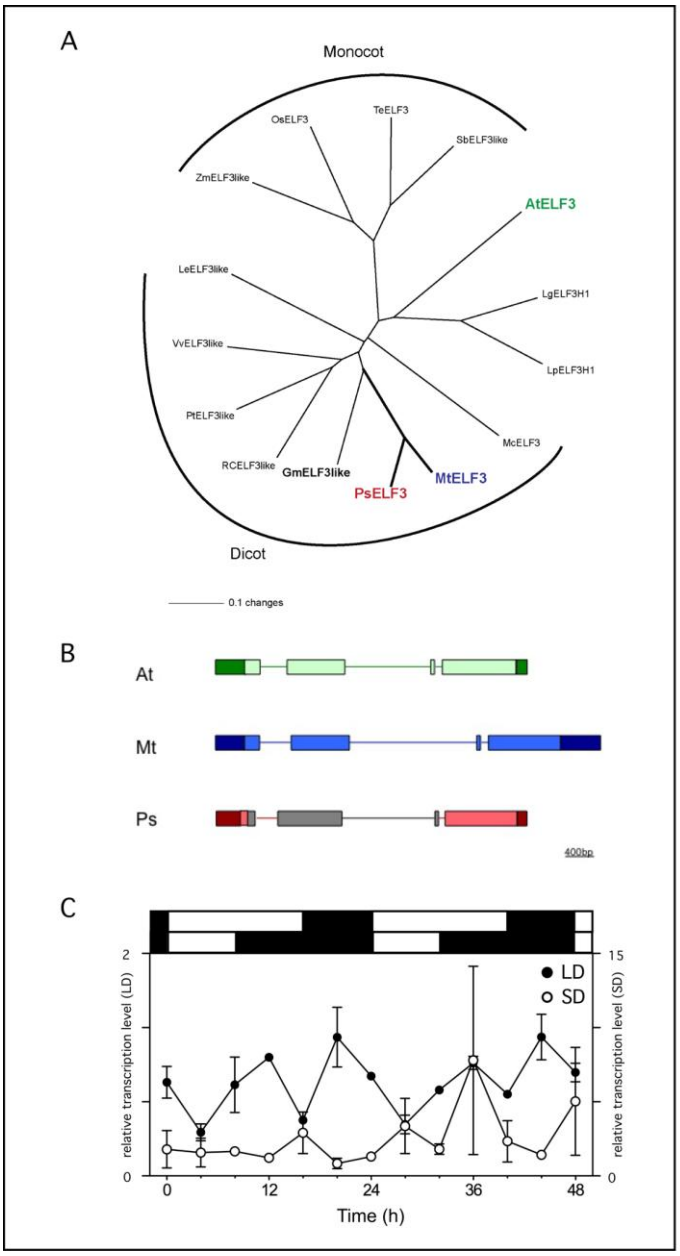

Figure 3.2 Identification and characterization of the *ELF3* orthologs in pea.
(A) Phylogenic tree of ELF3-related proteins. Braches with bootstrap value less than 50% have been collapsed. *Arabidopsis thaliana* (At) ELF3 NP_180164, *Glycine max* (Gm) ELF3like ACU18593, *Lycopersicon esculentum* (Le) ELF3like AK321534, *Lemna gibba* (Lg) ELF3H1 BAD97872, *Lemna paucicostata* (Lp) ELF3H1 BAD97868, *Mesembryanthemum crystallinum* (Mc) ELF3 AAQ73529, *Medicago truncatula* (Mt) ELF3 Medtr3g140450, *Oryza sativa* (Os) ELF3 NP_001056770, *Pisum sativum* (Ps) ELF3 AY830925, *Populus trichocarpa* (Pt) ELF3like XP_002309522, *Ricinus communis* (Rc) ELF3like EEF45821, *Sorghum bicolour* (Sb) ELF3like XP_002440379, *Triticum aestivum* (Te) ELF3 ABL11477, *Vitis vinifera* (Vv) ELF3like XP_002278577, *Zea mays* (Zm) ELF3like ACN34402 (B) A schematic diagram of Arabidopsis (At), Medicago (Mt), and pea (Ps) *ELF3* genomic sequence showing exons as shaded boxes and intron as straight line. The coding sequence (light color) and untranslated regions (dark color). Coloured region in pea sequence indicate sequence isolated in this study. (C) Diurnal rhythms of *ELF3* transcript in wild-type seedlings grown for 21 d under LD (16h L: 8h D; black symbols) or SD (8h L: 16h D; white symbols) and harvested every 4h over the next 48h. Tissue harvests consisted of the entire shoot apex above and including the uppermost expanded leaf. Data are mean SE for n=2 biological replicates, each consisting of pooled material from two plants.

3.3.3.2. *ELF4*

The *ELF4* gene in Arabidopsis has no intron and encodes for a 111 amino acid nuclear protein that is not homologous to any protein of known function (Doyle et al., 2002; Khanna et al., 2003). Phylogenetic analysis shows that ELF4 proteins fall into two major groups, which are designated as ELF4 and ELF4-like, on the basis of the Arabidopsis sequences they include (Khanna et al., 2003) (Figure 3.3A). However, Arabidopsis ELF4-like1 (AtELF4L1), Chlamydomonas (CrELF4), and moss ELF4 (PppELF4), sit outside of these two groups. MtELF4a falls in the clade of apparent ELF4 orthologs whereas three other Medicago *ELF4*-like genes cluster with Arabidopsis *ELF4*-like genes (MtELF4b to MtELF4d) in another clade. The short length of these proteins and their high amino acid similarity mean that none of Medicago *ELF4*-like sequences can be identified unambiguously with any of the Arabidopsis genes.

Previously, a partial pea sequence *ELF4* (44%) was isolated by degenerate-primer PCR and genome walking. This sequence included approximate 200bp of the coding sequence (3' end with the stop codon), the 3' UTR, and part of the adjacent gene (*Cyclophilin*) (Hecht et al., 2005). In this study, I used 5' RACE-PCR to amplify the 5' end of *ELF4* cDNA including the start codon and part of the 5'UTR (Figure 3.3B). Pea-specific primers were then designed to obtain full length *ELF4* cDNA and gDNA. As in Arabidopsis and Medicago, *PsELF4* has no introns (Figure 3.3B). Figure 3.2C also shows that *PsELF4* has a strong diurnal expression rhythm with characterization similar to *AtELF4* (Doyle et al., 2002), peaking in the evening at ZT12 in SD and ZT14 in LD.

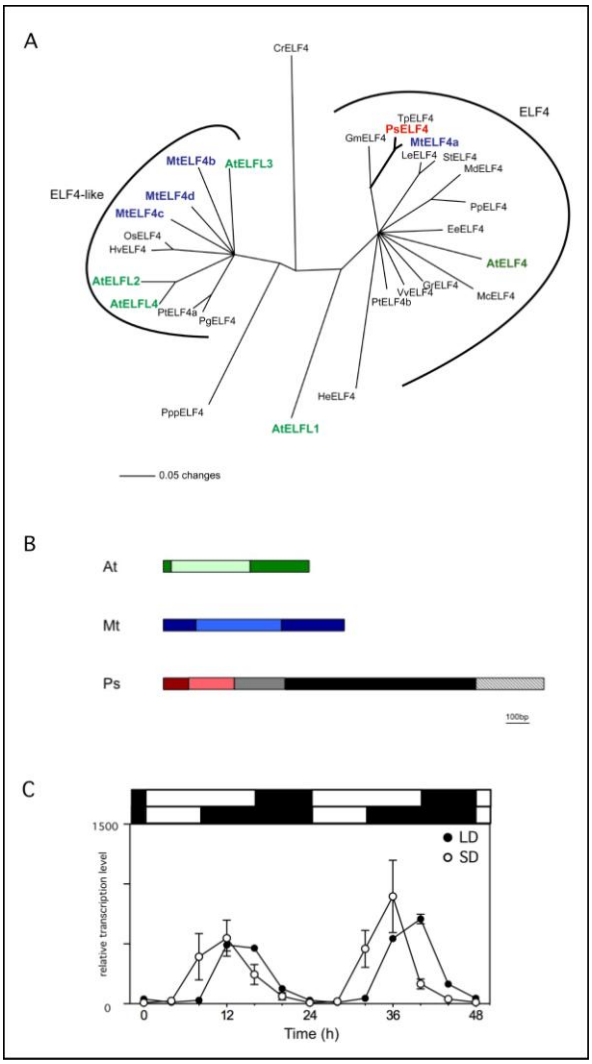

Figure 3.3 Identification and characterization of the *ELF4* orthologs in pea.
(A) Phylogenic tree of ELF4-related proteins. Braches with bootstrap value less than 50% have been collapsed. *Arabidopsis thaliana* (At) ELF4 NP_565922, AtELFL1 NP_180556, AtELFL2 AAL85042, AtELFL3 NP_565334, AtELFL4 NP_564024, *Chlamydomonas reinhardtii* (Cr) ELFL XP_001689467, *Euphorbia esula* (Ee) ELF4 DV136166, *Helianthus exilis* (He) ELF4 EE656495, *Glycine max* (Gm) ELF4 TC219480, *Gossypium raimondii* (Gr) ELF4 CO082442, *Hordeum vulgare* (Hv) ELFL BM376395, *Lycopersicon esculentum* (Le) ELF4 AAW22881, *Malus domestica* (Md) ELF4 DT042515, *Medicago truncatula* (Mt) MtELF4a AC145219_10, MtELFLb AC160841_2, MtELFLc TC103336, MtELFLd AJ501135, *Mesembryanthemum crystallinum* (Mc) ELF4 AAQ73526, *Oryza sativa* (Os) ELFL AAD27669, *Physcomitrella patens* (Ppp) ELFL EDQ60473, *Picea glauca* (Pg) ELFL EX380933, *Pinus taeda* (Pta) ELFL DR057888, *Pisum sativum* (Ps) ELF4 AY830924, *Populus trichocarpa* (Ptb) ELF4 TC65251, *Prunus persica* (Pp) AM288129, *Solanum tuberosum* (St) TC161315, *Trifolium pratense* (Tp) ELF4 BB912607, *Vitis vinifera* (Vv) CAO41364 (B) A schematic diagram of Arabidopsis (At), Medicago (Mt), and pea (Ps) *ELF4* genomic sequence showing exons as shaded boxes and intron as straight line. The coding sequence (light color) and untranslated regions (dark color). Coloured regions in pea sequence indicate sequence isolated in this study while black regions and shaded region (partial sequence of the following Cyclophilin gene) are sequences isolated from previous study of Hecht et.al. 2005 (C) Diurnal rhythms of *ELF4* transcript in wild-type seedlings grown for 21 d under LD (16h L: 8h D; black symbols) or SD (8h L: 16h D; white symbols) and harvested every 4h over the next 48h. Tissue harvests consisted of the entire shoot apex above and including the uppermost expanded leaf. Data are mean SE for n=3 biological replicates, each consisting of pooled material from two plants.

3.3.3.3. MYB1 and MYB2

Arabidopsis *CCA1* and *LHY* are related genes in Arabidopsis which encode transcription factors with a single MYB domain and play a partially redundant role in the core clock mechanism(Alabadi et al., 2002; Mizoguchi et al., 2002; Lu et al., 2009). The genomic sequence of *LHY* consists of 7 exons and 6 introns whereas *CCA1* has 4 exons and 3 introns (Wang et al., 1997; Wang and Tobin, 1998; Green and Tobin, 1999). BLAST searches of the Medicago genomic database identified four distinct Medicago genomic sequences with significant homology to *CCA1*/*LHY*, (*MtMYB1*-*MtMYB4*; Table 3.1) whereas two sequences were previously isolated in pea (*PsMYB1* and *PsMYB2*; Table 3.2). Initially, partial genomic sequences of *PsMYB1* (28%) and *PsMYB2* (11%) isolated with degenerate primers were obtained from Fabrice Foucher in the Rameau lab at INRA Versailles, France (Hecht et al., 2005). Full length *PsMYB1* cDNA and gDNA sequences were subsequently isolated using genome walking and RACE-PCR before the start of this project (V. Hecht, unpublished data). In this study, the partial sequence of *PsMYB2* was extended from 11% to 71% of full-length by 5' and 3' RACE-PCR (Table 3.2). Low amino acid identity with LHY/CCA1 (34%/21%) and failure to return either genes as top hit in blast of Arabidopsis protein database raised doubt about the identity of *PsMYB2* as a true *LHY*/*CCA1* gene.

Figure 3.4A show a phylogenic tree for proteins related to CCA1/LHY. In order to clarify the identity of *PsMYB2*, two other Arabidopsis *MYB* genes most similar to *CCA1*/*LHY* (At3g10113 and At1g18330) have been included as outgroups. Figure 3.4A confirm that *PsMYB1* and *PsMYB2* are orthologs of Medicago *MtMYB1* (Medtr7g146200) and *MtMYB2* (Medtr5g084860) respectively. The phylogenetic

analysis indicates that sequences are not clearly resolved in the larger group containing MYB1, group and the relative similarity of genes in this group to LHY and CCA1 is not clearly determined. This is the case for *PsMYB1*, which although clearly located in LHY/CCA1 group, cannot be identified with either gene. This is also the case for homologs identified in rice, Sorghum, maize, and tomato. Moreover, although soybean, Populus, and Lemna have two sequences included, these are not clearly identified as Arabidopsis CCA1 or LHY. On the other hand, MYB2 clearly falls outside of the other CCA1/LHY homologs and form an individual clade (CCA1/LHY-like) with the two other Medicago genomic sequences (MtMYB3 and MtMYB4) and two "CCA1" sequences from moss (*Physcomitrella patens*).

Comparisons of gene structure show that *PsMYB1* and *MtMYB1* are very similar in structure but somewhat more similar to Arabidopsis *CCA1* than *LHY*. Like both legume M1 genes, Arabidopsis *CCA1* has 4 exons and 3 introns (Figure 3.4B).

Figure 3.4C shows that like the Arabidopsis *LHY*/*CCAl* genes (Alabadi et al., 2002), *PsMYB1* is a morning-phased gene (Figure 3.4C), peaking before dawn (ZT20-24 in SD, ZT28 in LD) as (Fowler et al., 1999). In contrast, *PsMYB2* is expressed in the evening (ZT16 in SD, ZT20-24 in LD) and its transcript level in LD is very low compared to the SD level.

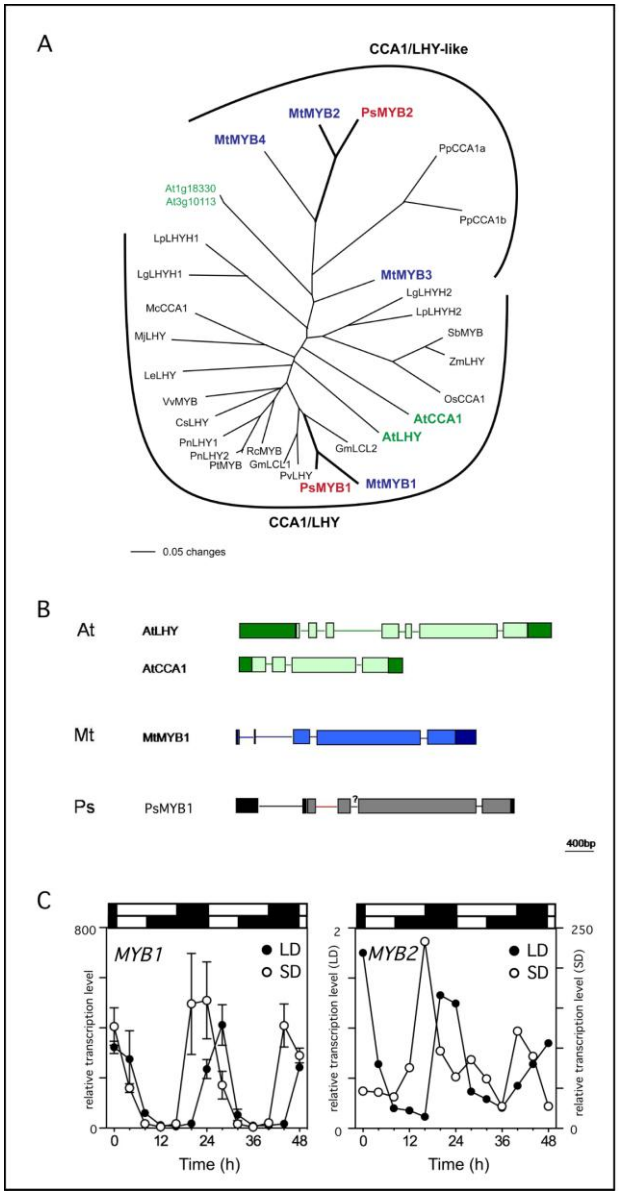

Figure 3.4 Identification and characterization of the *CCA1/LHY* orthologs in pea.
(A) Phylogenic tree of *CCA1/LHY*-related proteins. Braches with bootstrap value less than 50% have been collapsed. *Arabidopsis thaliana* (At) CCA1 NP_850460, LHY NP_171614, At3g10113 NP_683543, At1g18330 NP_101691, *Castanea sativa* (Cs) LHY AAU20773, *Glycine max* (Gm) LCL1 ABW87008, LCL2 ABW87009, *Lycopersicon esculentum* (Le) LHY BT012912, *Lemna gibba* (Lg) LHYH1 BAD97870, LHYH2 BAD97871 , *Lemna paucicostata* (Lp) LHYH1 BAD97866, LHYH2 BAD97867 , *Mesembryanthemum crystallinum* (Mc) CCA1 AAQ73524 , *Mirabilis jalapa* (Mj) LHY ACL81163, *Medicago truncatula* (Mt) MtMYB1 Medtr7g146200, MtMBY2 Medtr5g084860, MtMYB3 Medtr7g146190, MtMYB4 Medtr3g086700, *Oryza sativa* (Os) CCA1 NP_001061032, *Populus nigra* (Pn) PnLHY1 BAH09382, PnLHY2 BAH09383, *Physcomitrella patens* (Pp) CCA1a BAI39991, CCA1b BAI39992, *Pisum sativum* (Ps) MYB1 AY826730, MYB2 AY826731, *Populus trichocarpa* (Pt) MYB XP_002320238, *Phaseolus vulgaris* (Pv) LHY CAD12767, *Ricinus communis* (Rc) MYB XP_002515093, *Sorghum bicolour* (Sb) MYB XP_002443890, *Vitis vinifera* (Vv) MYB XP_002267720, *Zea mays* (Zm) LHY NP_001147482 (B) A schematic diagram of Arabidopsis (At), Medicago (Mt), and pea (Ps) *MYB1* genomic sequence showing exons as shaded boxes and intron as straight line. The coding sequence (light color) and untranslated regions (dark color). Coloured region in pea sequence indicate sequence isolated in this study. The (?) is intron 3 that has been determined using specific primers but not yet sequenced in pea **(continued on next page)**

Figure 3.4 (continued) (C) Diurnal rhythms of *MYB1/MYB2* transcript in wild-type seedlings grown for 21 d under LD (16h L: 8h D; black symbols) or SD (8h L: 16h D; white symbols) and harvested every 4h over the next 48h. Tissue harvests consisted of the entire shoot apex above and including the uppermost expanded leaf. Data are mean SE for n=3 biological replicates (n=1 for *MYB2*), each consisting of pooled material from two plants.

3.3.3.4. TOC1

The Arabidopsis core clock gene *TOC1* is also known as *PREUDO-RESPONSE REGULATOR 1* (*PRR1*). The *PRR* gene family in Arabidopsis has 5 members (*APRR1*, *APRR3*, *APRR5*, *APRR7*, and *APRR9*) defined by two conserved domains (PR and CCT domains). Following mutant studies of *TOC1* (Somers et al., 1998b; Strayer et al., 2000; Alabadi et al., 2001), all 5 genes are subsequently shown to participate in clock regulation (Matsushika et al., 2000). However, there is no good match of *TOC1* sequence in Medicago genomic database whereas two partial C-terminal Medicago EST sequences were found to be similar to Arabidopsis TOC1 sequence (Table 3.1). In phylogenetic analysis, these two EST sequences (MtTC131807, MtTC122078) are clearly fall in one clade with TOC1 sequences of other species and together shown to be closer to Arabidopsis *TOC1* rather than other *PRR* genes in Arabidopsis (Figure 3.5A).

In pea, *TOC1* was the first *PRR* gene that was isolated including a small piece of exon 6 (156bp) (Figure 3.5B) which encodes the CCT domain that is highly similar to Arabidopsis *TOC1* (Hecht et al., 2005). Several approaches were used in the present study to extend the existing *TOC1* sequence. However, neither RACE-PCR nor genome walking was successful. The alternative approach using Medicago sequence-specific primers designed on TC131807 sequences (the closest Medicago sequence to *PsTOC1*) resulted in isolation of a small fragment (288bp) spanning an intron. This sequence is highly similar to Arabidopsis intron4 and the flanking exon4

and exon5 sequences (Figure 3.5B). The PsTOC1 also clusters with the two Medicago EST sequences and TOC1 from other species in the phylogenic tree (Figure 3.5A).

Despite uncertainties about nature of legume TOC1 sequences, the expression rhythm of *PsTOC1* was found to be similar to *AtTOC1* (Makino et al., 2002). It is expressed around dusk in either SD (ZT8 and ZT32) or LD (ZT12 and ZT36) or (Figure 3.5C).

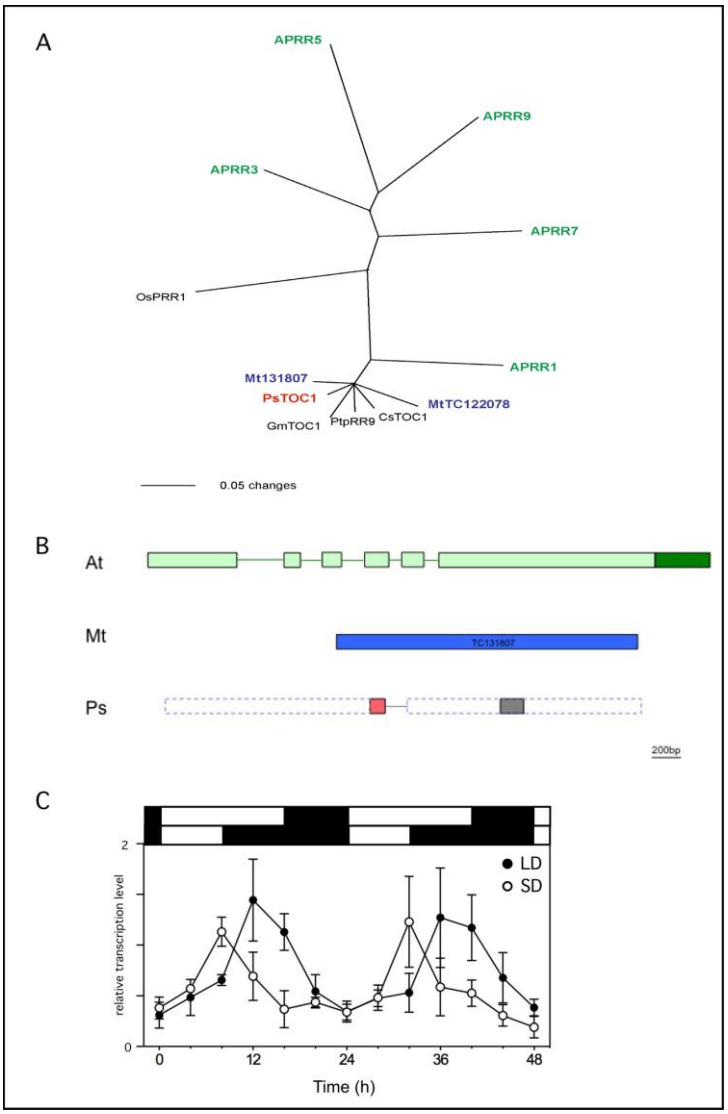

Figure 3.5 Identification and characterization of the *TOC1* orthologs in pea.
(A) Phylogenic tree of TOC1-related proteins derived from trimmed sequences to match known pea TOC1 sequence. Braches with bootstrap value less than 50% have been collapsed. *Arabidopsis thaliana* (At) APRR1 NP_200946, APRR3 NP_568919, APRR5 NP_568446, APRR7 NP_568107, APRR9 NP_973703, *Castanea sativa* (Cs) TOC1 AAU20772, *Glycine max* (Gm) TOC1 ABW87010, *Medicago truncatula* (Mt) TC131807 (partial C-terminal sequence), TC122078 (partial C-terminal sequence), *Oryza sativa* (Os) PRR1 BAD38854, *Pisum sativum* (Ps) TOC1 AY930927, *Populus trichocarpa* (Pt) pRR9 XP_002330130 **(continued on next page)**

Figure 3.5 (continued) (B) A schematic diagram of Arabidopsis (At), Medicago (Mt), and pea (Ps) (B) *TOC1* genomic sequence showing exons as shaded boxes and intron as straight line. The coding sequence (light color) and untranslated regions (dark color). Coloured region in pea sequence indicate sequence isolated in this study. (C) Diurnal rhythms of *TOC1* transcript in wild-type seedings grown for 21 d under LD (16h L:8h D; black symbols) or SD (8h L:16h D; white symbols) and harvested every 4h over the next 48h. Tissue harvests consisted of the entire shoot apex above and including the uppermost expanded leaf. Data are mean SE for n=3 biological replicates, each consisting of pooled material from two plants.

3.3.3.5. PRR37 and PRR59

Phylogenetic analysis based on PR and CCT domain protein sequences shows that PRR proteins fall into three distinct clades which can be designated as PRR1, PRR37, and PRR59 based on the Arabidopsis genes they include (Figure 3.6A). However, clear orthologs of individual Arabidopsis *PRR* genes are not present as indicated by rice and Lemna which have two distinct sequences in each of PRR37 and PRR59 clades. BLAST searches of Medicago databases identified three distinct genomic sequences (MtPRRa, MtPRRb, and MtPRRc), and two EST sequences (TC124074 and TC120462) (Table 3.1). These Medicago sequences fall into distinct groups of PRR phylogenic tree. MtPRRa and MtPRRc fall within the PRR59 clade, and MtPRRb and one of the EST contigs (TC124074) belong to PRR37 clade. Another EST (TC120462) is basal to both PRR59 and PRR37 groups.

To isolate other pea *PRR* genes, degenerate primers were designed to target the two conserved domains (PR and CCT domains) and two distinct fragments of PR domain were amplified. These two fragments were extended in both directions by RACE-PCR, to obtain one full length sequence and one partial sequence (82%). The two pea sequences belong to PRR37 and PRR59 clades, respectively, and they were designated as *PsPRR37* and *PsPRR59* (Figure 3.6). Moreover, they are apparent

orthologs of *MtPRRb* (Medtr4g079920) and *MtPRRa* (Medtr3g122650) respectively based on the phylogenetic analysis (Figure 3.6A).

Figure 3.6B shows the gene structure comparison of *PRR* genes (except *TOC1*) in Arabidopsis, Medicago and pea, including 4 Arabidopsis genes, 3 Medicago genes, and two pea genes. The comparison did not further resolve the identities of either *PsPRR37* or *PsPRR59* as the gene structures are similar even among four of the Arabidopsis genes. Moreover, only three introns have been identified so far in *PsPRR37* and more introns could be possible as full length genomic sequence has not yet been isolated. *PsPRR59*, on the other hand, was partially isolated (82% of the full length cDNA) with only 18% of the 5' region to be isolated. Interestingly, the second *PRR59*-like sequence in Medicago, *MtPRRc* has gene structure similar to Arabidopsis *PRR9*, indicating it is likely to have extra members of *PRR* gene family that have not yet been isolated in pea (Figure 3.6B).

In Arabidopsis, *PRR* gene family members are expressed after dawn in a sequential order of *PRR9*, *PRR7*, *PRR5*, *PRR3*, and *PRR1* (*TOC1*) (Matsushika et al., 2000). Diurnal rhythms of *PRR37* and *PRR59* (Figure 3.6C) are expressed after dawn and slightly affected by photoperiod, similar to those of Arabidopsis. *PsPRR37* expression peaks at ZT4-8 in SD and ZT8-12 in LD whereas *PsPRR59* is expressed subsequently at ZT8 in SD and ZT12 in LD. *PRR* genes in Arabidopsis are highly conserved especially at PR and CCT domains, it is therefore hard to conclude which pea gene corresponds to which Arabidopsis *PRR* gene. The results of *PRR37* and *PRR59* isolation have been published recently (Liew et al., 2009a) (Appendix 2).

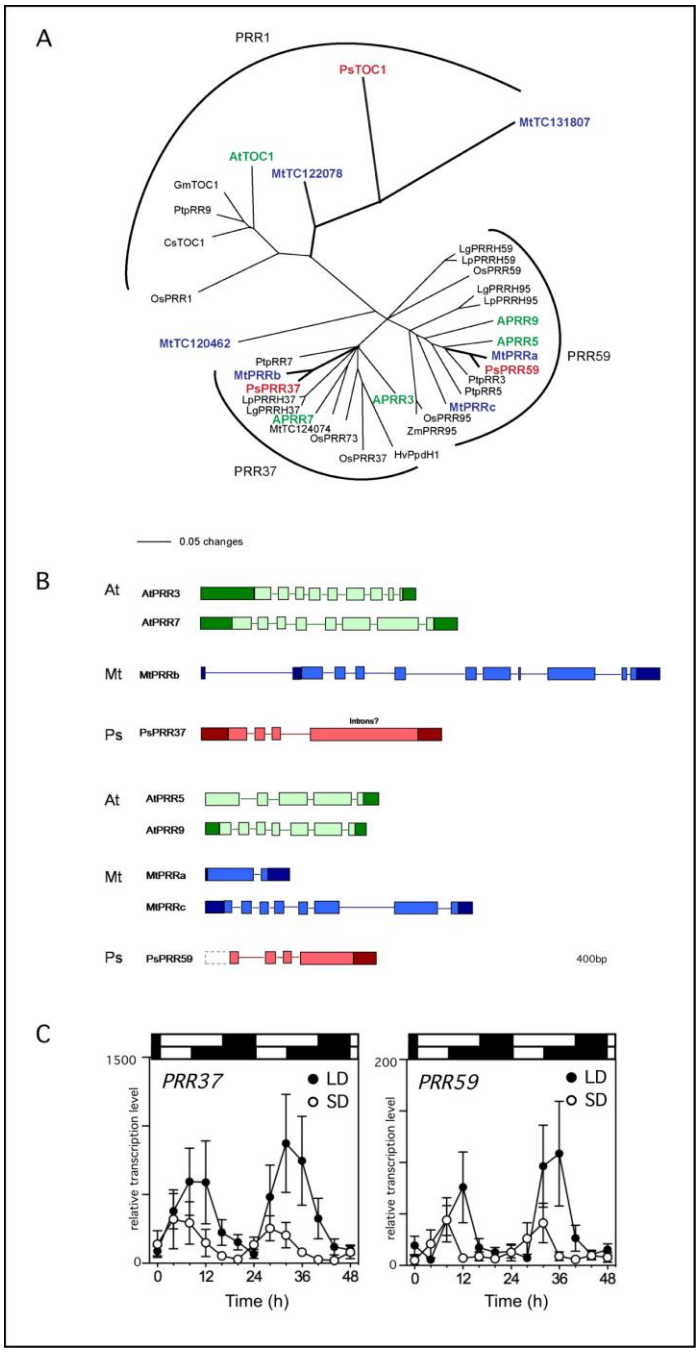

Figure 3.6 Identification and characterization of the *PRRs* orthologs in pea.
(A) Phylogenic tree of PRR-relatedproteins. Braches with bootstrap value less than 50% have been collapsed. *Arabidopsis thaliana* (At) TOC1 NP_200946, APRR3 NP_568919, APRR5 NP_568446, APRR7 NP_568107, APRR9 NP_973703, *Castanea sativa* (Cs) TOC1 AAU20772, *Glycine max* (Gm) TOC1 ABW87010, *Hordeum vulgare* (Hv) PpdH1 AAY17586, *Lemna gibba* (Lg) PRRH95 BAE72702, PRRH59 BAE72701, PRRH37 BAE72700, *Lemna paucicostata* (Lp) PRRH95 BAE72699, PRRH59 BAE72698, PRRH37 BAE72697, *Medicago truncatula* (Mt) Medtr3g122650, Medtr7g146130, Medtr4g079920, TC124074, TC120462 (partial N-terminal sequence), TC131807 (partial C-terminal sequence), TC122078 (partial C-terminal sequence), *Oryza sativa* (Os) PRR1 BAD38854, PRR95 BAD38857, PRR59 BAD38858, PRR73 BAD38856, PRR37 BAD38855, *Pisum sativum* (Ps) TOC1 AY930927, PRR37 ACU42263, PRR59 ACU42265, *Populus trichocarpa* (Pt) pRR3 XP_002321349, pRR5 XP_002320232, pRR7 XP_002311223, pRR9 XP_002330130, *Zea mays* (Zm) PRR95 NP_001151536 **(continued on next page)**

Figure 3.6 (continued) (B) A schematic diagram of Arabidopsis (At), Medicago (Mt), and pea (Ps) *PRR37* and *PRR59* genomic sequence showing exons as shaded boxes and intron as straight line. The coding sequence (light color) and untranslated regions (dark color). Coloured region in pea sequence indicate sequence isolated in this study. (C) Diurnal rhythms of *PRR37/PRR59* transcript in wild-type seedings grown for 21 d under LD (16h L:8h D; black symbols) or SD (8h L:16h D; white symbols) and harvested every 4h over the next 48h. Tissue harvests consisted of the entire shoot apex above and including the uppermost expanded leaf. Data are mean SE for n=3 biological replicates, each consisting of pooled material from two plants.

3.3.3.6. LUX

In Arabidopsis, *LUX* was identified independently by two research groups (Hazen et al., 2005; Onai and Ishiura, 2005) and is also referred to as *PCL1* (Onai and Ishiura, 2005). LUX belongs to a GARP protein family which includes type-B response regulator that functions as transcription factor in plants. The LUX protein also contains a MYB domain and nuclear localisation signal. The phylogenetic analysis of LUX protein sequence (Figure 3.7A) across different species shows that *LUX* is present as a single copy gene except in Arabidopsis where two other sequences (At5G59570 and AT2G40970) were found to be similar to AtLUX at the protein level. One of them has already been described as *AtPCLL* (At5G59570) and forms a clade with *AtLUX* (Onai and Ishiura, 2005). Two Medicago sequences were also identified with one of them (*MtLUXa*; Medtr4g084460) clustering in the LUX clade and another (*MtLUXb*; Medtr7g105990) forming a separate clade with the other Arabidopsis sequence At2G40970 (Figure 3.7A).

In present study, the pea ortholog of *LUX* was isolated initially using specific primers designed on Medicago ortholog sequences (Figure 3.1). The first attempt isolated a 400bp sequence near the 5' end of the gene. The full length sequence of *PsLUX* was subsequently amplified using 5' and 3'-end RACE-PCR. *PsLUX* is clearly an ortholog of *MtLUXa*, and clusters with *LUX* genes from other species. The gene structures of *LUX* in the three species are highly similar in the coding sequence

with an intron in the 3'UTR (Figure 3.7B). In Arabidopsis, *LUX* is expressed around the same time as *TOC1* (Hazen et al., 2005; Onai and Ishiura, 2005) and this is also found to be true in pea (Figure 3.7C). *PsLUX* is expressed in the evening before the transition to night in either SD (ZT8 and ZT32) or LD (ZT12 and ZT36).

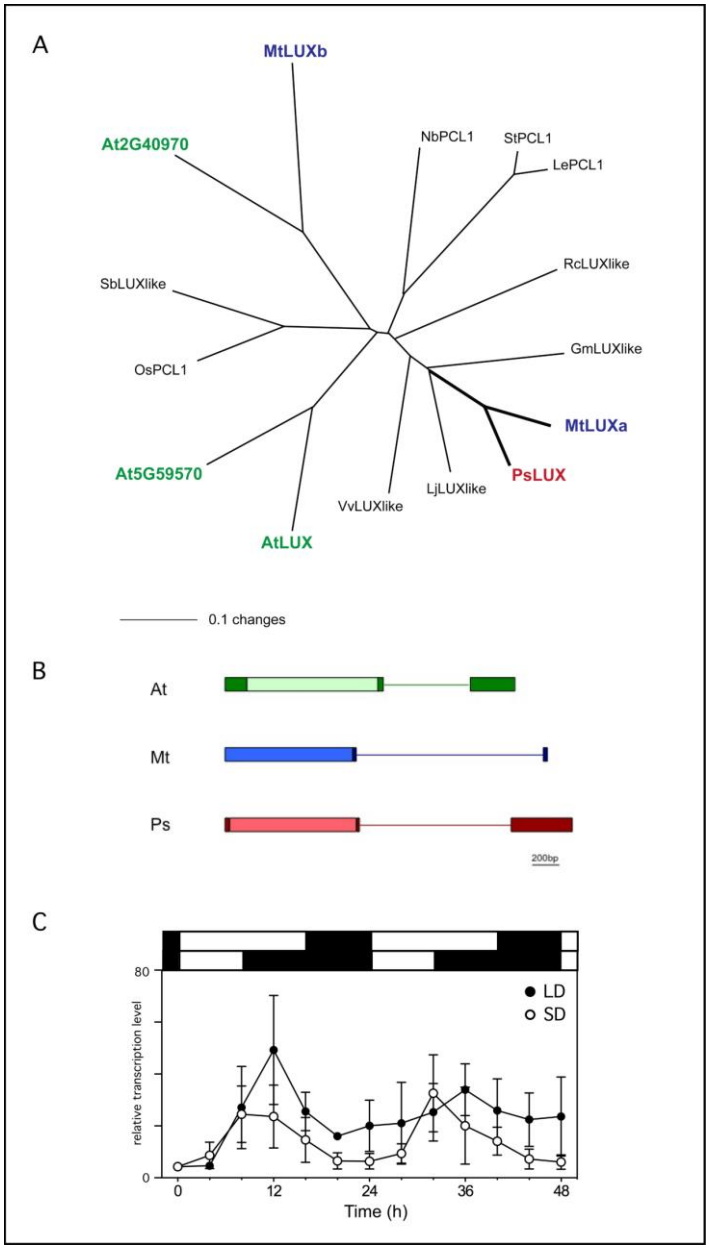

Figure 3.7 Identification and characterization of the *LUX* orthologs in pea.
(A) Phylogenic tree of LUX-related proteins. Braches with bootstrap value less than 50% have been collapsed. *Arabidopsis thaliana* (At) LUX NP_001030823, AT5G9570 ABG48421, AT2G40970 AAM14927, *Glycine max* (Gm) GmLUXlike AK245871, *Lotus japonicus* (Lj) LjLUXlike AK337516, *Medicago truncatula* (Mt) MtLUXa Medtr4g084460, MtLUXb Medtr7g105990, *Nicotiana benthamiana* (Nb) NbPCL1 AB219069, *Oryza sativa* (Os) OsPCL1 AB206578, *Ricinus communis* (Rc) RcLUXlike Xm_002520488, *Solanum tuberosum* (St) StPCL1 AB219071 *Sorghum bicolar* (Sb) LUXlike Xm_002459132, *Vitis vinifera* (Vv) VvLUXlike Xm_002283123 **(continued on next page)**

Figure 3.7 (continued) (B) A schematic diagram of Arabidopsis (At), Medicago (Mt), and pea (Ps) *LUX* genomic sequence showing exons as shaded boxes and intron as straight line. The coding sequence (light color) and untranslated regions (dark color). Coloured region in pea sequence indicate sequence isolated in this study. (C) Diurnal rhythms of *LUX* transcript in wild-type seedings grown for 21 d under LD (16h L:8h D; black symbols) or SD (8h L:16h D; white symbols) and harvested every 4h over the next 48h. Tissue harvests consisted of the entire shoot apex above and including the uppermost expanded leaf. Data are mean SE for n=3 biological replicates, each consisting of pooled material from two plants.

3.3.3.7. TIC

TIC (*TIME FOR COFFEE*) in Arabidopsis is a large gene with 5.3kb cDNA and 11 introns in the gDNA sequence that encodes a 1550aa nuclear protein (Hall et al., 2003). Mutations in TIC gene known to affect *LHY* expression level and light gating of *CAB* gene expression (Hall et al., 2003; Ding et al., 2007) suggesting role in light input. An apparent single Medicago ortholog of *TIC* was identified when Arabidopsis *TIC* sequence was used to blast against Medicago genomic and EST databases (Table 3.1). Partial gDNA sequences of *TIC* were then isolated in pea using degenerate primers. These sequences included a 1239bp region from exon2 to exon5 and partial sequence (267bp) of exon12 (Figure 3.8). Figure 3.8 shows a diagram of *PsTIC* and its Medicago ortholog genomic sequences. Based on these limited comparison, gene structures are well conserved between Medicago and Arabidopsis and structure of pea 5' fragment is also well conserved.

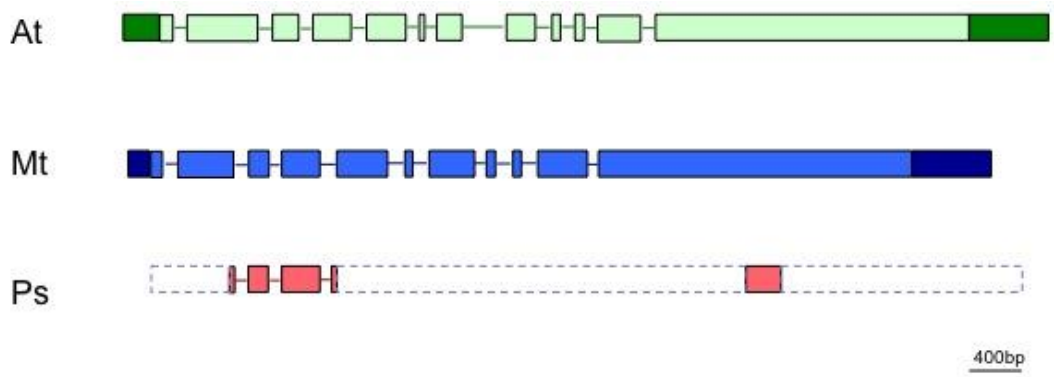

Figure 3.8 A schematic diagram of Arabidopsis (At) AT3G22380, Medicago (Mt) Medtr1g132680, and pea (Ps) *TIC* genomic sequence showing exons as shaded boxes and intron as straight line. The coding sequence (light color) and untranslated regions (dark color). Coloured region in pea sequence indicate sequence isolated in this study.

3.3.4. Mapping of circadian clock related genes in pea

In order to identify whether any of the nine pea clock-related gene isolated could be possible candidate genes for *DNE*, *SN*, *PPD*, and *HR*, it was necessary to determine their map positions. Synteny between Medicago and pea was supported in previous mapping of pea flowering-related genes (Hecht et al., 2005), which included two clock-related genes, *GI* and *MYB2*. *GI* was mapped on the bottom half of Ps LGII near the flowering locus *LATE1* which suggested a possible candidate gene relationship, and *LATE1* was subsequently identified as the pea ortholog of Arabidopsis *GI* (Hecht et al., 2005; Hecht et al., 2007). On the other hand, *MYB2* was mapped by Fabrice Foucher in JI281 x JI399 RIL population on top of Ps LGI (F. Foucher, unpublished data), a position that ruled it out as a candidate for any mutant loci in pea.

Several populations of recombinant inbred lines (RILs) are widely used for genetic mapping in pea (Table 3.3). These range from narrow cross between cultivars, Torsdag x Terese (Laucou et al., 1998; Loridon et al., 2005) to wider cross between cultivar and putative ancestral line Slow x JI1794 (*P. elatius* var humile) (Weeden et al., 1998), also including two moderately divergent RILs, JI281 x JI399 (Ellis et al., 1992; Hall et al., 1997) and Terese x Champagne (Aubert et al., 2006). These populations have been scored comprehensively with different type of markers, including Restriction Fragment Length Polymorphism (RFLP) and Randomly Amplified Polymorphic DNA (RAPD) markers. The resulting maps have been integrated through sharing of common (in particular gene-based) markers, making these RILs convenient for mapping of pea genes. In contrast, for mapping of pea loci, it was necessary to generate crosses of mutants. Three narrow F_2 populations were generated including *sn-4* x Terese, *ppd-3* x Terese, and *late2* x Terese (J. Weller,

unpublished data). They are not only useful for mapping of mutant loci, gene-based markers from Torsdag x Terese RILs can be scored in these populations as our mutants are in Torsdag (NGB5839) background. However although phenotypes can be easily scored in these population, it is sometime hard to locate polymorphism to be converted into suitable markers due to the similarity between Torsdag and Terese. For this purpose, wider crosses, JI1794 x NGB5839 (*hr*) and JI1794 x *ppd-3* were also generated to have a rough estimation of linkage distance.

Table 3.3. Summary of mapping populations used in this study.

Population name	Size	Type	Nature	Reference
JI281 x JI399	72	F8 RILs	landrace x cultivated (cv. Cennia)	Ellis et.al. 1992; Hall et.al. 1997
JI1794 x Slow	51	F10 RILs	wild (P. humile) x primitive	Weeden et.al. 1998
Terese x Champagne	164	F8 RILs	cultivated (spring x winter)	Loridon et.al. 2005; Aubert et.al. 2006
Torsdag x Terese	139	F7 RILs	cultivated (spring x spring)	Laucau et. al. 1998
sn-4 x Terese	80	F2	-	-
ppd-3 x Terese	92	F2	-	-
late2 x Terese	80	F2	-	-
JI1794 x NGB5839	92	F2	-	-
JI1794 x *ppd-3*	73	F2	-	-

In general, our mapping strategy is to isolate the sequences of introns as it is most likely to locate polymorphism between mapping parent lines (Section 2.9). Appropriate polymorphisms were converted to CAPs or dCAPs marker for mapping (Appendix 1). Using this approach, we manage to determine the approximate map positions of six out of the remaining eight circadian genes (Figure 3.9). These are shown both in context of actual map for that mapping population and on a comparative map integrate pea and Medicago physical map locations. *TIC* was mapped in JI281 x JI399 in the lower part of Ps LGII, is approximately 20cM below GI (Figure 3.9A). Three circadian genes, *ELF3*, *PRR59*, and *ELF4*, were mapped on

Ps LGIII in three different mapping populations (Figure 3.9B). *ELF3* was mapped approximate 2cM away from morphological marker *M* (seed coat marbling) in Terese x Champagne. *PRR59* was mapped in JI1794 x SLOW population near *UNI* and very close to a STS marker, *MnSOD* (N. Weeden, unpublished data). *ELF4* was mapped in the JI281 x JI399 population, between two RAPD markers *F15/9-* (2cM) and *A9/2- -* (5cM). *MYB1* and *PRR37* are both mapped in JI281 x JI399 population. *MYB1* is mapped on top of Ps LGV between GdcL and Ag/1+ markers (Figure 3.9C). *PRR37* was mapped near the bottom of Ps LGVII between Tps1/84+ and E3/6 - - markers (Figure 3.9D).

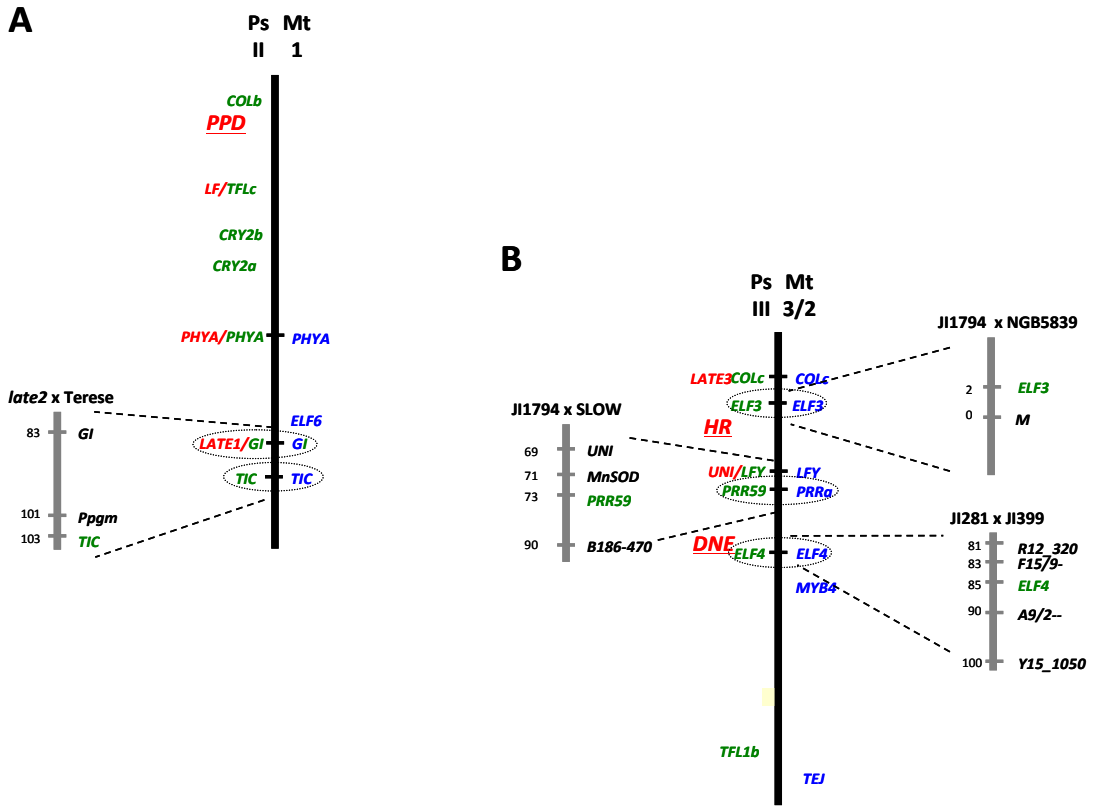

Figure 3.9 A schematic diagram of approximate map locations of circadian genes in pea and Medicago. (A) Ps LGII and Mt Chromosome 1 (B) Ps LGIII and Mt Chromosome 3/2. **(continued on next page)**

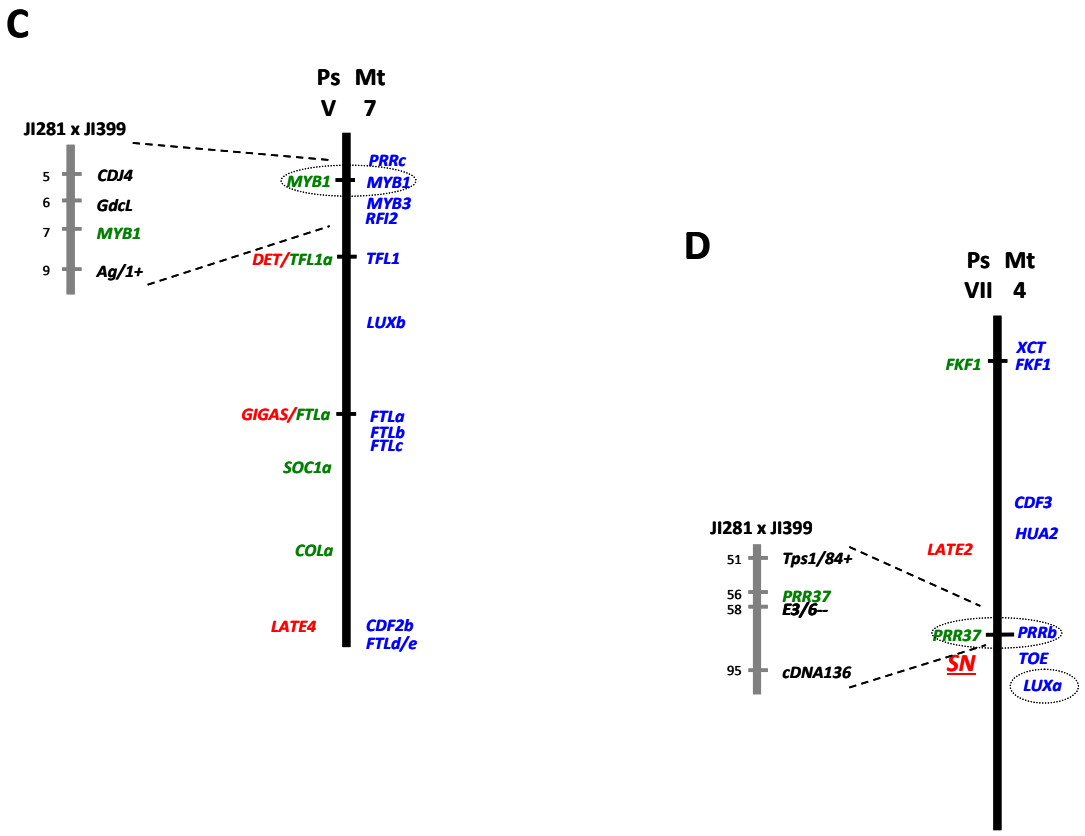

Figure 3.9 (continued) (C) Ps LGV and Mt Chromosome 7 (D) Ps LGVII and Mt Chromosome 4. This diagram represents the syntenic relationship between pea and Medicago (dark vertical line) and detailed linkage map in pea (grey vertical line) in relevant mapping population (JI281 x JI399; (Hall et al., 1997) and JI1794 x Slow (Weeden et al., 1998), Terese x Champagne (Aubert et al., 2006), Torsdag x Terese (Laucou et al., 1998), late2 x Terese and 5839 x JI1794 (J. Weller et. al., unpublished). The thick vertical lines correspond to pea linkage groups and corresponding Medicago chromosomes as indicated on top of each line. The homologous chromosomes are normalized in length, the map positions are relative for each linkage group/chromosome and each species. All pea (Ps) mutants loci (red) and genes (green) are indicated on the left whereas Medicago (Mt) genes (blue) are on the right. Orthologous genes in two species are joined by a horizontal line. Circadian clock related genes studied in this chapter are highlighted in circles. The approximate distance between genes is indicated on the left side of pea linkage maps.

Map positions for these six genes correspond well to the position of their Medicago orthologs, further emphasizing the useful nature of the pea and Medicago synteny. Unfortunately for *TOC1* and *LUX*, no polymorphism suitable for marker design was identified within the available sequence. For *LUX*, the map position of Medicago homolog (*MtLUXa*) suggests a likely location for *PsLUX* at the bottom of pea LGVII (Medicago Chromosome 4) (Figure 3.9D). However for *TOC1*, there is no clue about the likely map position as no good match of *TOC1* Medicago genomic

sequence was found. The map positions of several Medicago genes (*RFI2*, *TEJ*, *XCT*, *MYB3*, *MYB4*, *PRRc*, and *CDFs*) also indicate the possible map position for their pea orthologs that we have not yet isolated in pea (Figure 3.9).

As the map position of *DNE*, *SN*, *PPD* and *HR* loci have been determined previously and roughly located on a pea consensus map (Weeden et al., 1998) and a comparative pea/Medicago map (Hecht et al., 2005). As shown in Figure 3.9, the pea map positions of *MYB1*, *MYB2*, and *TIC* and inferred map position from Medicago of *RFI2*, *TEJ*, *XCT*, *MYB3*, *MYB4*, *PRRc*, and *CDFs* rule out any of these genes as candidates for the *DNE*, *SN*, *PPD* and *HR* loci. On the other hand, *HR* and *DNE* are mapped on Ps LGIII which is syntenic to Medicago chromosome 3/2. Interestingly, *ELF3*, *PRR59*, and *ELF4* are all mapped on Medicago Chromosome 3 with *ELF4* and *PRR59* mapped close to *DNE*, *ELF3* close to *HR*, suggesting these genes as potential candidates for the *DNE* and *HR* loci. *SN* locus is located in Ps LGVII in the general region in which *PsLUX* and *PsPRR37* have also been mapped. This again suggests these genes as candidates for *SN*. However, none of the circadian clock genes are located near the *PPD* locus at the top of Ps LGII (corresponds to Medicago Chromosome 1).

3.4. Discussion

3.4.1. Pea circadian clock gene orthologs are amplified using information collected from Medicago database

As described in Chapter 1, intensive genetic studies have been carried out in Arabidopsis to create a model for circadian clock system with regard to regulation of flowering time. This intriguing area of study has been extended to other important

model species such as rice, soybean, and wheat (Laurie and Devos, 2002; Izawa et al., 2003; Quecini et al., 2007).

This study initially extended previous work of Hecht et.al. (2005) to identify homologs of circadian clock genes in Medicago and to isolate and map orthologous sequences in pea. This study confirms that all of the main circadian clock components of Arabidopsis are represented in the Medicago genome (Table 3.1). In general those genes that are single copy in Arabidopsis, including *ELF3*, *ELF4*, *GI*, *TIC*, *LUX*, *RFI2*, *TEJ* and *XCT* are also appear to be single copy gene in Medicago. On the other hand, gene families such as *PRRs* and *CDF* are represented by multiple Medicago sequences and the evolutionary relationship of legume and Arabidopsis genes are not always clear. For example, the paralogous core clock genes *LHY* and *CCA1*, only one clear Medicago sequence was identified. However, comparison suggests it cannot be unambiguously determined as ortholog of either *LHY* or *CCA1* (Figure 3.4A). It is notable that only one *LHY* sequence is found in many other species such as rice and maize. Even two sequences are found in Lemna, Populus, and soybean, they share the same similarity to both Arabidopsis *CCA1* and *LHY*. This suggests gene expansion or deletion might occur to this gene family during species evolution. It is possibly due to the similar and redundant molecular functions of Arabidopsis *CCA1* and *LHY*. Although no clear Medicago genomic sequence was found for *TOC1* and *FIONA1*, ESTs for these genes were identified supporting presence of these genes in Medicago as Medicago genome sequencing project has not yet finalised (Table 3.1). The majority of Medicago genomic sequences have been allocated with map positions, allowing the map position of pea genes to be inferred from their orthologs in Medicago due to the synteny relationship established between pea and Medicago (Choi et al., 2004; Kalo et al., 2004; Aubert et al., 2006). Thus, our preliminary in silico survey of circadian clock-related

gene orthologs in Medicago not only provides useful information for isolation of clock genes in pea, but also allows initial identification of candidate genes based on close synteny between Medicago and pea.

Second step is to isolate pea sequences. Among a number of approaches used within our group such as library screening, genome walking, and degenerate primer, we found direct use of primers designed on Medicago sequences to be most efficient and effective. Four pea circadian orthologs (*PsPRR37, PsPRR59, PsTIC,* and *PsLUX*) were isolated from scratch while four previously amplified genes (*PsMYB2*, *PsELF3*, *PsELF4*, and *PsTOC1*) were extended using either degenerate primers or Medicago-specific primers (Table 3.2). As expected we found in all cases, phylogenetic analysis support the orthologous relationship between pea and Medicago where pea and Medicago orthologs always grouped in the same clade. This finding is also supported by a high degree of similarities between pea and Medicago for both amino acid identity and gene structure. (Figure 3.2 to 3.8)

Taken together, these results present a positive outlook for the use of Medicago as a 'bridging species' for rapid isolation and preliminary mapping of sequences in pea. However, we need to bear in mind that Medicago genome annotation is not always accurate due both to the ongoing progress of the Medicago genome sequencing project and possible genome rearrangement between species.

3.4.2. Arabidopsis circadian clock genes are conserved in pea

Full length or partial sequences of ten genes that proposed to play a role in the circadian clock in Arabidopsis have now been isolated in pea (Table 3.2). They are *PsMYB1* and *PsGI* that were previously isolated in full length (Hecht et al., 2007) and genes including *PsELF3, PsELF4, PsMYB2, PsTOC1, PsPRR37, PsPRR59, PsLUX*

and *PsTIC* were isolated or extended in this study. While the similarity at the level of amino acid identity and gene structure between pea and Arabidopsis varies somewhat for each gene, most pea genes showed diurnal expression patterns similar to their Arabidopsis homologs suggesting they may function in a similar way. As in Arabidopsis, expression rhythms of circadian clock genes in pea responded differentially to LD and SD photoperiods, consistent with the general idea that circadian clock functions in the response to photoperiod.

According to current understanding of the Arabidopsis clock mechanism, the two main gene families are *CCA1*/*LHY* and *PRR*, and representatives of both families were found in pea. As described in the model of Arabidopsis circadian clock, TOC1 and LHY/CCA1 reciprocally regulate each other and form a transcriptional-translational feedback loop which is a main component of the core oscillator (Alabadi et al., 2001). In pea, *PsTOC1* expressed after dusk while *PsMYB1* expressed before dawn which is the opposite phase of *PsTOC1*. This is essentially the same expression pattern in Arabidopsis and implies the same loop may exist in pea.

The family of *PRR* consists of three members in pea: *PsPRR37*, *PsPRR59*, and *PsTOC1*. These three sequences are highly similar in the PR and CCT domains, the rationale for the gene nomenclature is based on the Arabidopsis gene included in the same clade in the phylogenic tree. It is notable that both of Lemna and rice have sequences that are in *PRR59* and *PRR37* clade respectively and designated as *PRR59*, *PRR95*, *PRR37*, and *PRR73*. Like *PRR37* and *PRR59* found in pea, they resemble either *APRR3* and *APRR7* or *APRR5* and *APRR9*. The expression patterns of *PRR* genes were found to be similar to Arabidopsis *PRR* genes. They are expressed in a sequential order of *PsPRR37*, *PsPRR59*, and *PsTOC1* in pea. The BLAST search results against

Medicago genome database also suggest one or more genes (*MtPRRc* and two EST sequences) remained to be isolated in the *PRR* gene family (Table 3.1).

Of the ten circadian clock-related genes now known in pea, similarity in amino acid sequence, gene structure, and diurnal expression profile with Arabidopsis is well established. All key Arabidopsis clock genes are present in pea, supporting the proposal that a common molecular framework may exists in different species in the circadian clock regulation. It is therefore interesting to examine how the circadian clock function adapted in pea to regulate different flowering habits. This will obviously require isolation of mutants which can be done either by reverse genetics or expected to be followed by forward genetics via the studies of putative clock mutants in pea (*dne*, *sn*, *ppd* and *hr* mutants). Besides identification of mutant loci, comparison of circadian rhythms of clock gene expression and flowering initiation control between wild-type plant and the mutants will help us to explore the phenotypes of these mutants and the genetics interactions of the mutant loci. These phenotypic effects of *dne*, *sn*, *ppd*, and *hr* mutants on flowering and circadian rhythms will also suggest potential candidate genes by comparison to known Arabidopsis clock mutants. These will be elucidated and discussed in the following chapters.

3.4.3. Potential candidate gene relationship suggested by comparative mapping

As expected, map positions of pea genes corresponded nicely to predicted Medicago positions and further support the well-documented synteny between Medicago and pea. The results ruled out *MYB1*, *MYB2*, and *TIC* as candidate gene of any of the known mutant loci. This mapping exercise also added several new anchors to the pea and Medicago comparative map, and underlines the close synteny between them (Figure 3.9). Furthermore, the map positions of *SN*, *PPD*, *DNE* and *HR* loci have

already been determined (Weeden et al., 1998; Hecht et al., 2005). Mapping data of these new putative circadian clock genes in pea have suggested or ruled out candidate gene relationship with the putative circadian-related loci. These include potential candidate gene relationships between *DNE* and *PRR59*/*ELF4*, between *SN* and *PRR37*/*LUX*, and also between *HR* and *ELF3*. The possible candidate gene relationships will be further examined in the following chapters with integration of precise mapping using newly developed molecular markers based on Medicago genome information.

Even though there are no possible candidate gene identified for *PPD* mutant locus, further progress can nevertheless be made by refining the map position using information from Medicago genome. In the case that *PPD* is a novel gene that is not represented in Arabidopsis, refining map position of *PPD* may allow identification by classical positional cloning. However, for this purpose, a larger population is required. The first step in this strategy could involve identification of single copy loci around the syntenic region in Medicago where *PPD* is mapped and mapping of the corresponding genes in pea. However, also possible that other candidate gene may appear in the region as further improvements to Medicago genome and physical map are made.

Chapter 4 Characterization of the flowering locus *DIE NEUTRALIS* (*DNE*)

4.1. Introduction

Following initial analysis of naturally-occurring variation for flowering time, the locus *DIE NEUTRALIS*, *DNE* was the first pea flowering locus defined in studies of induced mutants (King and Murfet, 1985). The single known mutant at this locus, *dne-1* has an early, day-neutral flowering phenotype similar to that of the naturally-occurring *sn* mutant (Murfet, 1971c) suggesting *DNE* might play an important role on photoperiod control in pea. Like *SN*, *DNE* has been reported to influence other traits such as number of reproductive nodes, seed yield, and the balance of vegetative and reproductive growth (King and Murfet, 1985). Previous comparison between *dne* and *sn* mutants suggested *dne-1* allele could be a leaky allele as *DNE* is less effective than *SN* in the regulation of all these traits (King and Murfet, 1985). The map position of *DNE* locus was estimated to be in the middle of pea linkage group III and near locus *ST* (King and Murfet, 1985).

As mentioned in Chapter 1, early studies of flowering in pea proposed the concept of floral inhibitor to explain the early-flowering, day neutral phenotype typified by the *sn* mutant (Murfet and Reid, 1973). This was based on grafting studies, showing that flowering of these early mutants promote early flowering of wild-type scions whereas the early-flowering phenotypes of mutant scions are delayed when grafted onto a wild-type stocks. Therefore, *DNE*, together with *SN* and *PPD* were proposed to be complementary genes that are required for production of this graft-transmissible floral inhibitor in pea (Murfet and Reid, 1973; King and Murfet,

1985; Arumingtyas and Murfet, 1994). More recently a different grafting approach using pea leafy stocks with the *late1* mutant has led to the development of an alternative interpretation involving a mobile stimulus (Weller, 2005; Hecht et al., 2007; Weller, 2007). Furthermore, *FT* is now well-established in Arabidopsis as a mobile stimulus for flowering (Corbesier et al., 2007; Jaeger and Wigge, 2007). These contradictory findings of floral inhibitor in pea to Arabidopsis *FT* will be re-visited in this chapter using *dne* mutants.

The aim of this study was to characterise in detail the functions of *DNE* in regulation of flowering and the circadian clock and to investigate the molecular identity of *DNE* through a positional candidate gene approach. In other systems, particularly Arabidopsis, clock mutants are characterised by defective diurnal and circadian rhythms of gene expression, impaired de-etiolation, and mis-expression of downstream flowering genes. In this chapter, the characteristics of clock mutants will be examined in *dne* mutant to learn more about the functions of *DNE*. As *LATE1* has been showed to be ortholog of Arabidopsis *GI* which is known to be involved in circadian clock in Arabidopsis (Hecht et al., 2007), it is of interest to examine *DNE* and *LATE1* interaction in pea circadian clock, control of flowering and photoperiod responsiveness. In addition to this, candidate gene relationships established for *DNE* in Chapter 3 will be examined in this chapter, and possibly identify the molecular nature of *DNE* locus by positional approach.

4.2. Materials and methods

4.2.1. Gene expression experiments

For the diurnal expression experiments, all plants were grown for 3 weeks from sowing at 20°C in growth cabinets under either LD (16-h photoperiod) or SD

(8-h photoperiod). Harvested material consisted of entire shoot apex above and including the uppermost expanded leaf from two plants. Samples were harvested at 4h intervals, with up to 3 replicates per time point. Samples were harvested and processed by V. Hecht and K. Claire. Several real-time PCR runs were done with assistance of V. Hecht.

For circadian expression experiments, all plants were grown in growth cabinets under a light/dark cycle (12L: 12D) at 20°C for 3 weeks before transfer to continuous white light at 25μmol m^{-2} s^{-1} (LL) or continuous darkness at ZT36 (DD). Harvested material consisted of a single leaflet from the uppermost fully expanded leaf from two plants. Samples were harvested at 3h intervals, with 2 to 3 replicates per time point.

For developmental timecourse experiment, plants were grown in growth cabinets under SD condition (8L: 16D) at 20°C. Leaf and apical bud samples were harvested separately from each plant at 2-day interval from day 7 to day 56 for WT (day 35 for *dne* mutant). Samples were harvested at the same time during the day for each time point approximately 4 hours after light on. Leaf material consisted of single leaflet from the uppermost fully expanded leaf from two plants. Apical bud material consisted of dissected apical buds from two plants to 2-mm in length. 3 replicates were harvested per time point. Samples were harvested by V. Hecht and processed with the help of V. Hecht and R. Stephen. Several real-time PCR runs were done with assistance of V. Hecht and R. Stephen.

For the continuous light (CL) expression experiment, all plants were grown in the growth cabinets in darkness for 7 days until germination occur before transfer to continuous white light at 25μmol m^{-2} s^{-1} for 2 weeks. Both of the leaflets from the uppermost fully expanded leaf from single plant were harvested at 4h intervals for a

24h period, with 3 replicates per time point.

4.2.2. Real-time analysis

Due to lack of convenient marker for detecting circadian rhythms in pea, quantitative real-time PCR was employed as an approach to investigate circadian clock gene expression in pea. Statistical analysis (Fast Fourier Transform Non-Linear Least Square, FFT-NLLS) used to accessing periodicity in Arabidopsis relies on several cycles of data. Due to limitation of two cycles in pea, meaningful statistical test are not able to be performed and conclusion are limited to visual assessment. Different experiments were carried out at widely spaced interval, so expression level might vary between experiments.

4.2.3. Complementation studies

The Arabidopsis *elf4-1* mutation in the Ws background has been previously described (Doyle et al., 2002). Full-length cDNA for *ELF4* were generated by PCR from NGB5839 and *dne-1* mutant, and from Arabidopsis accession Ws, using primers listed in Appendix 1. The cDNA fragments were recombine into the binary vector pB2GW7 (Invitrogen, http://www.invitrogen.com/) using Gateway cloning (Karimi et al., 2002) and confirmed by sequencing. To measure hypocotyls length, seeds were surface sterilized and plated on $4gL^{-1}$ Murashige and Skoog without sucrose and $8gL^{-1}$ agar. Plates were stored at 4ºC in the dark for 48h and transferred into growth chambers with appropriate light regimes. The transformations were done in collaboration with R. Laurie, University of Otago, New Zealand.

4.3. Results

Most of the result in this chapter was already published recently in The Plant Cell (Liew et al., 2009b). Therefore, this chapter is presented as a mixture of published results together with results from a few novel experiments and additional results of published experiments.

4.3.1. The dne mutant shows early, photoperiod-insensitive flowering

The *DNE* locus is known from a single mutant allele, *dne-1*, which was isolated in the cv. Torsdag genetic background (King and Murfet, 1985). The *dne* mutant flowers early in SD and shows other traits characteristic of a WT plant grown in LD, including reduced branching, rapid termination of apical growth after flowering, and rapid senescence (Figure 4.1). The *dne* mutant thus appears to show constitutive activation of a LD developmental program and is essentially unresponsive to photoperiod differences. This is true regardless of the genotype at the *LE* locus, which governs the synthesis of the active gibberellins, GA_1 (Lester et al., 1997). Under LD, the *dne* mutant does typically flower slightly earlier than WT, but WT and *dne* are otherwise similar in phenotype (King and Murfet, 1985).

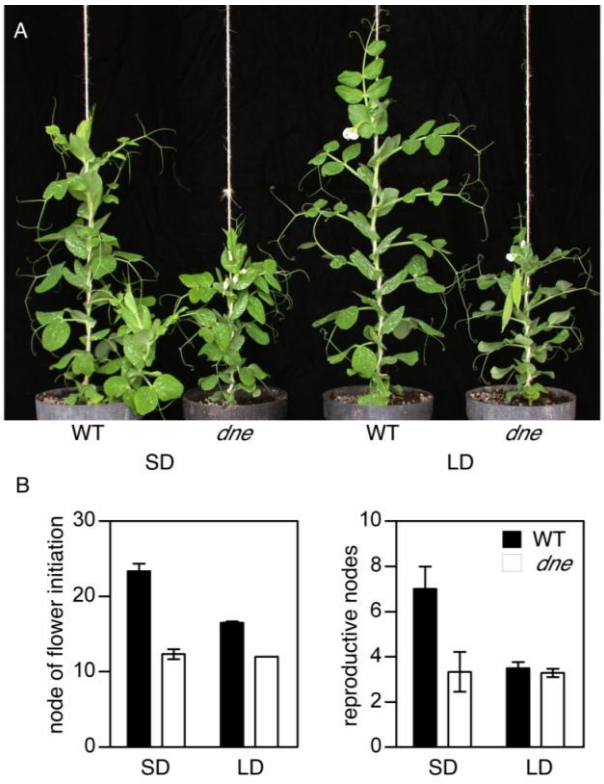

Figure 4.1 The *dne-1* mutant is early flowering and photoperiod-insensitive. (A) Representative of 8-week-old wild-type line NGB5839 and *dne-1* isogenic mutant plants. (B) Node of flower initiation (left) and final number of reproductive nodes (right). Data are mean ± SE for n = 8 plants. All plants were grown in the phytotron under standard SD or LD conditions.

4.3.2. The dne mutant shows altered rhythms of gene expression under light/dark cycles

The early-flowering phenotype of the *dne* mutant is similar to that of Arabidopsis circadian clock mutants *elf3*, *elf4*, *lux* and the *cca1 lhy* double mutant (Hicks et al., 1996; Doyle et al., 2002; Mizoguchi et al., 2002; Hazen et al., 2005), and we therefore considered that *dne* might have a defect in rhythmic expression of clock gene homologs. The pea circadian genes *MYB1*, *MYB2*, *TOC1*, *PRR37*, *PRR59*, *ELF3*, *ELF4*, *LUX*, and *GI* were shown to have LD and SD expression rhythms (Chapter 3) that are similar to Arabidopsis and LD expression rhythms of *MYB1*, *TOC1*, *ELF4*, and *GI* were shown to be altered in a *late1* mutant (Hecht et al., 2007).

Figure 4.2 shows that *dne* had no clear effect on expression of *MYB1* under either SD or LD, nor on *TOC1* under LD (Figure 4.2A, 4.2B). However, under SD, the expression rhythm of *TOC1* in WT showed a relatively sharp peak at dusk (ZT8) and dropped significantly by ZT12, whereas in the *dne* mutant, *TOC1* expression continued into the night, remaining high at ZT12 (Figure 4.2A), suggesting a small phase delay. *ELF4* expression in WT under SD showed a sharp peak early in the night (ZT12), whereas in the *dne* mutant, the peak occurred at dusk (ZT8) (Figure 4.2A). The earlier rise of *ELF4* expression during the day and the earlier drop during the night are consistent with a phase advance in *dne*. Under LD, the shape of the WT *ELF4* rhythm differed from SD, with a broader peak from ZT12 to ZT16 (Figure 4.2B). In LD the *ELF4* rhythm in *dne* peaked late in the day (ZT12), and also showed a small phase advance relative to WT. The *dne* mutation also affected *LATE1* expression under both SD and LD (Figure 4.2A, 4.2B). There was no clear indication of a phase shift under either photoperiod, but *LATE1* transcript levels were higher in *dne* than in WT throughout the night, similar to the effect of the *sn* mutant on *LATE1* (Hecht et al., 2007). Expression of the *PRR37* and *PRR59* were apparently unaffected by *dne* (Figure 4.2A, 4.2B). Expression of *ELF3* and *MYB2* was examined on single replicate of *dne* mutant. The *ELF3* expression is not rhythmic in either LD and SD in *dne* mutant as in WT (Figure 4.2A, 4.2B) but *dne* has increased *ELF3* transcript level in LD (Figure 4.2B). *MYB2* expression was slightly shifted in *dne* mutant under SD (Figure 4.2A) and highly expressed in *dne* mutant under LD (Figure 4.2B). However, the results of *ELF3* and *MYB2* expression in *dne* are based on one replicate, replications are needed to certain the level of expression. In summary, the *dne* mutant affects the diurnal expression of *TOC1, ELF4, LATE1*, *ELF3*, and *MYB2* under SD and/or LD but had no apparent effect on *MYB1*, *PRR37* or *PRR59* expression.

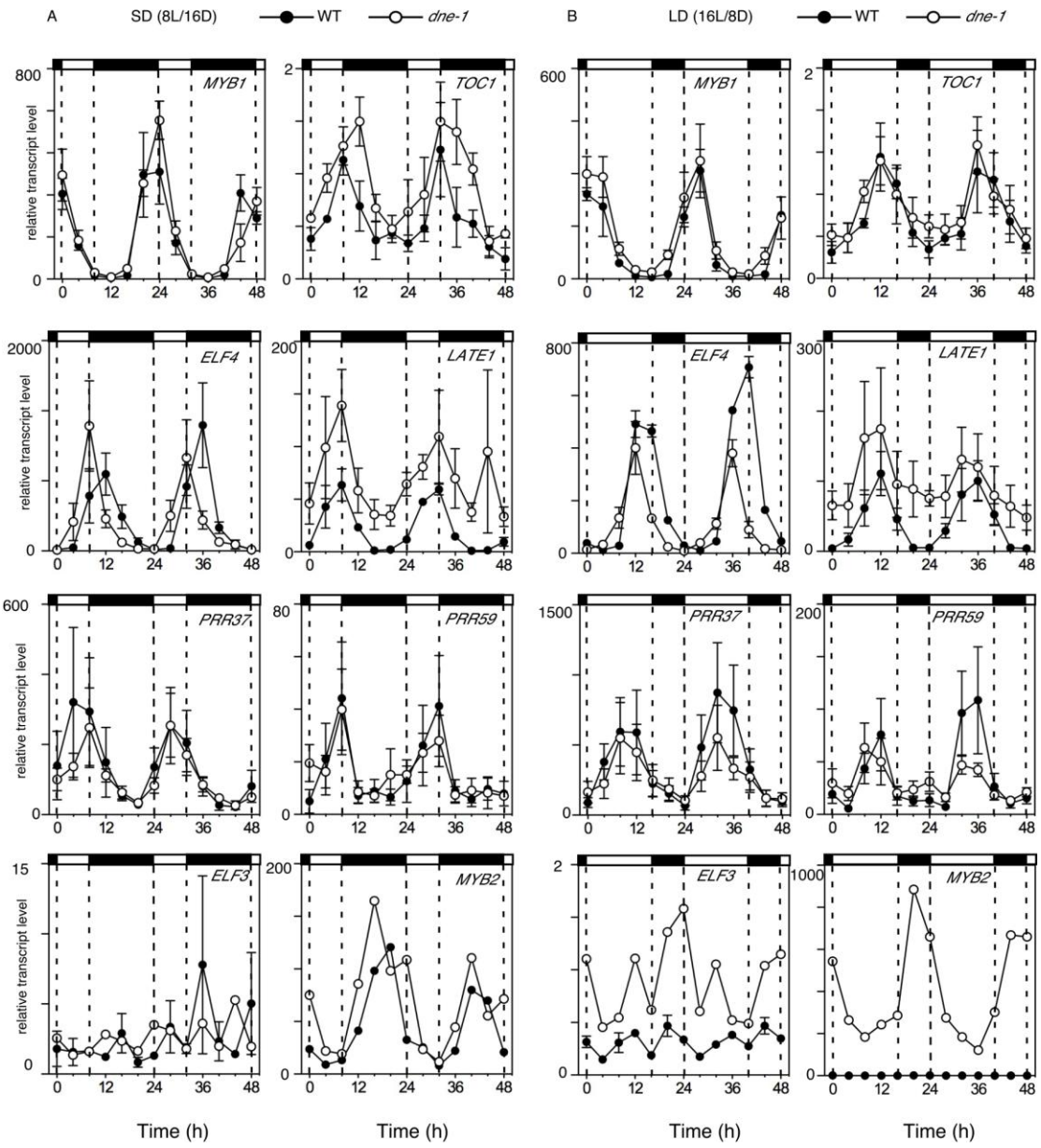

Figure 4.2 *DNE* affects diurnal rhythms of clock gene homologs under light/dark cycles.
(A) SD conditions (8-h photoperiod).
(B) LD conditions (16-h photoperiod).
All plants were grown for 21 d from sowing at 20°C before harvesting commenced. Data are mean ± SE for n = 3 biological replicates except *ELF3* (*dne-1*) and *MYB2* (both WT and *dne-1*), each consisting of pooled material from two plants. Day and night periods are indicated by open and closed bars, respectively, above the graph.

4.3.3. DNE affects rhythms of clock gene expression in constant light

We were next interested to examine whether *DNE* might affect circadian rhythms. The circadian clock has not been directly examined in pea, but in Arabidopsis, most circadian analyses have been performed under constant white light (LL), and robust rhythms for leaf movement and gene expression generally persist over several circadian cycles. We initially found that the strong expression rhythms seen for *MYB1*, *TOC1*, *LATE1* and *ELF4* in WT pea seedlings under diurnal cycles were significantly damped during the first subjective night after transfer to LL of moderate irradiance, resulting in lower peak levels for *MYB1* and *ELF4*, and higher trough levels for *TOC1* and *LATE1* (Supplemental Figure 2, (Liew et al., 2009b)). However under LL of lower irradiance, clear rhythmic expression was maintained for all four genes through at least one circadian cycle (Figure 4.3). For *ELF4*, the rhythm was maintained for at least 48h with a strong amplitude similar to the LD rhythm whereas rhythms for *MYB1*, *LATE1* and *TOC1* showed some damping by the second circadian cycle, towards trough levels for *MYB1* and intermediate levels for *TOC1* and *LATE1* (Figure 4.3). Although rhythms were only followed for two full circadian cycles, all four genes gave some indication of a shorter period, with peaks 18h apart for *ELF4*, and 21h apart for *MBY1* and *TOC1*.

We also examined the effect of the *dne* mutation in the same experiment (Figure 4.3). The *dne* mutant had subtle effects, including an apparent small phase advance of *TOC1* and *LATE1* expression in the second circadian cycle, suggestive of a shorter period. Interestingly, there is also a suggestion that the phase difference for *ELF4* expression between WT and *dne* under light/dark cycles may diminish after transfer to LL.

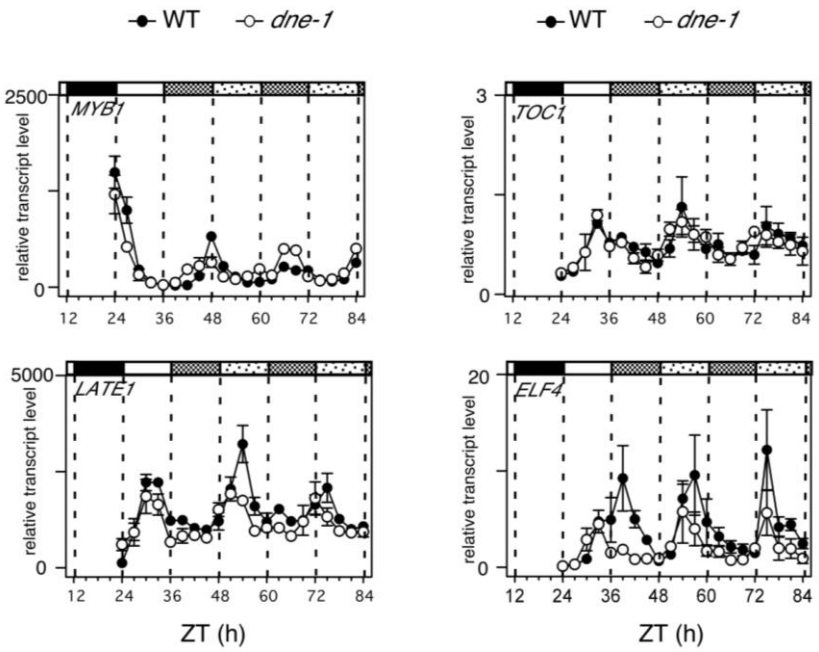

Figure 4.3 *DNE* and *LATE1* affect circadian rhythms of clock gene homologs in LL.
Plants were grown in growth cabinets under a light/dark cycle (12L:12D) at 20°C for 21 days before transfer to continuous white light at 25 µmolm-2s-1. Data are mean ± SE for n=2 biological replicates, each consisting of pooled material from two plants.
(A) Expression of clock genes in WT and *dne*
Zeitgeber time (ZT) refers to the time since lights-on of the last full entraining cycle.

4.3.4. DNE also affects rhythms of clock gene expression in constant darkness

Rhythmic expression of clock genes also persisted after transfer of WT plants from entraining conditions to constant darkness (DD), but differed from LL in several respects (Figure 4.4). The strongest rhythm in DD was seen for *MYB1* expression, which, as in LL, showed only moderate damping over the two circadian cycles (Figure 4.4). In contrast to LL, the *ELF4* rhythm was strongly damped in DD, although still clearly rhythmic. Both *ELF4* and *MYB1* rhythms showed periods of close to 24h. *TOC1* expression under DD, was not clearly rhythmic and in contrast to LL, damped to a low rather than intermediate level, appearing to lose the induction during the subjective day, instead of the repression phase during the subjective night in LL (Figure 4.3). Finally, the rhythm of *LATE1* under DD was very similar to LL both in amplitude and apparent period shortening.

In the *dne* mutant, *MYB1* expression continued to cycle in DD, but with an apparently shorter period, with peaks at ZT45 and ZT60 compared to ZT48 and ZT69 in the WT. No clear effect of *dne* on *TOC1*, *ELF4* or *LATE1* expression was detected (Figure 4.4).

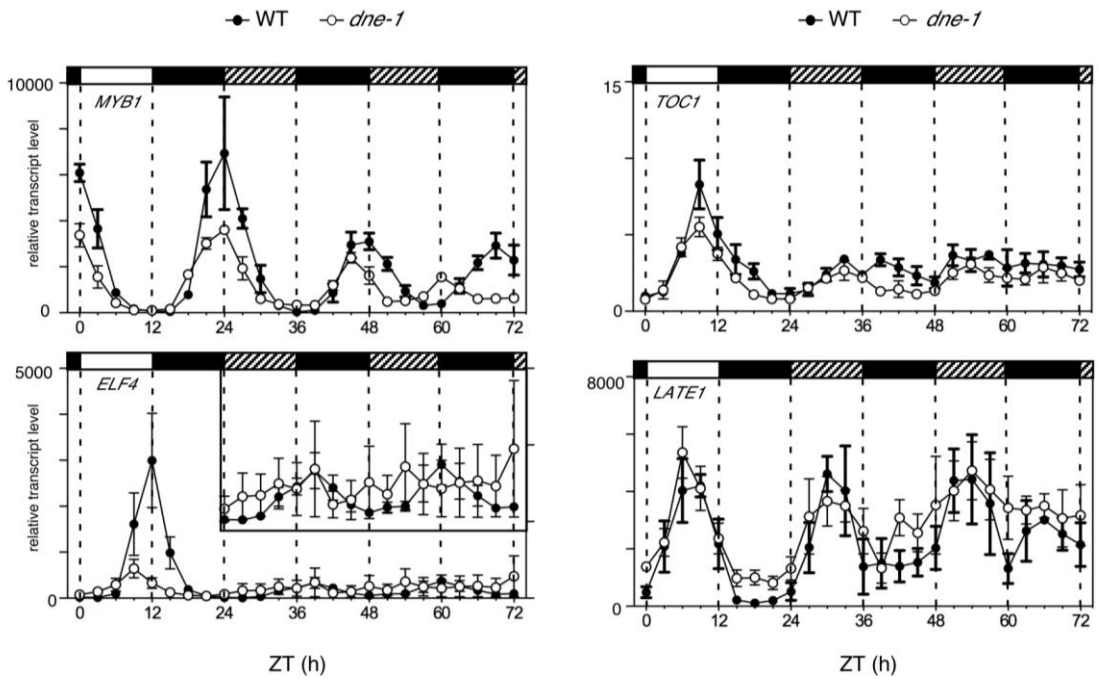

Figure 4.4 *DNE* affect circadian rhythms of clock gene homologs in DD. Plants were grown in growth cabinets under a light/dark cycle (12L:12D) at 20°C for 3 weeks before transfer to continuous darkness. Data are mean± SE for n = 2 to 3 biological replicates, each consisting of pooled material from two plants. Zeitgeber time (ZT) refers to the time since lights-on of the last full entraining cycle. Bars above the graph refer to periods of light (open bars) or darkness (closed or hatched bars). The hatched bars indicate the periods of subjective day during the period of continuous darkness.

4.3.5. DNE is the likely pea ortholog of Arabidopsis ELF4

The results from expression analyses demonstrate that the *dne* mutant affects the rhythmic expression of clock genes, and we therefore investigated whether any homologs of known clock-related genes were located in the *DNE* genomic region. As shown in Chapter 3, *PRR59,* and *ELF4* are located around the approximate region of where *DNE* is mapped previously. However, *PsPRR59* is mapped close to *UNI* (4cM) which *UNI* has been mapped previously in Torsdag x Terese RILs with a distance likely to be greater than 40cM from *DNE* locus (Laucou et al., 1998). On the other hand, *PsELF4* is mapped close to marker R12_320 in JI281 x JI399 RIL, previously shown to be closely linked to *DNE* (Rameau et al., 1998) (Figure 4.5A) confirming the conserved genomic location of these genes in pea and Medicago. Sequencing of *PsELF4* from *dne-1* revealed a mutation predicted to replace glutamine 64 (CAG) with a stop codon (TAG) (Figure 4.5B), which co-segregated perfectly with the early-flowering phenotype in over 500 progeny from segregating families. This shows that *DNE* is tightly linked to the *ELF4* gene at a distance of less than 0.2 cM.

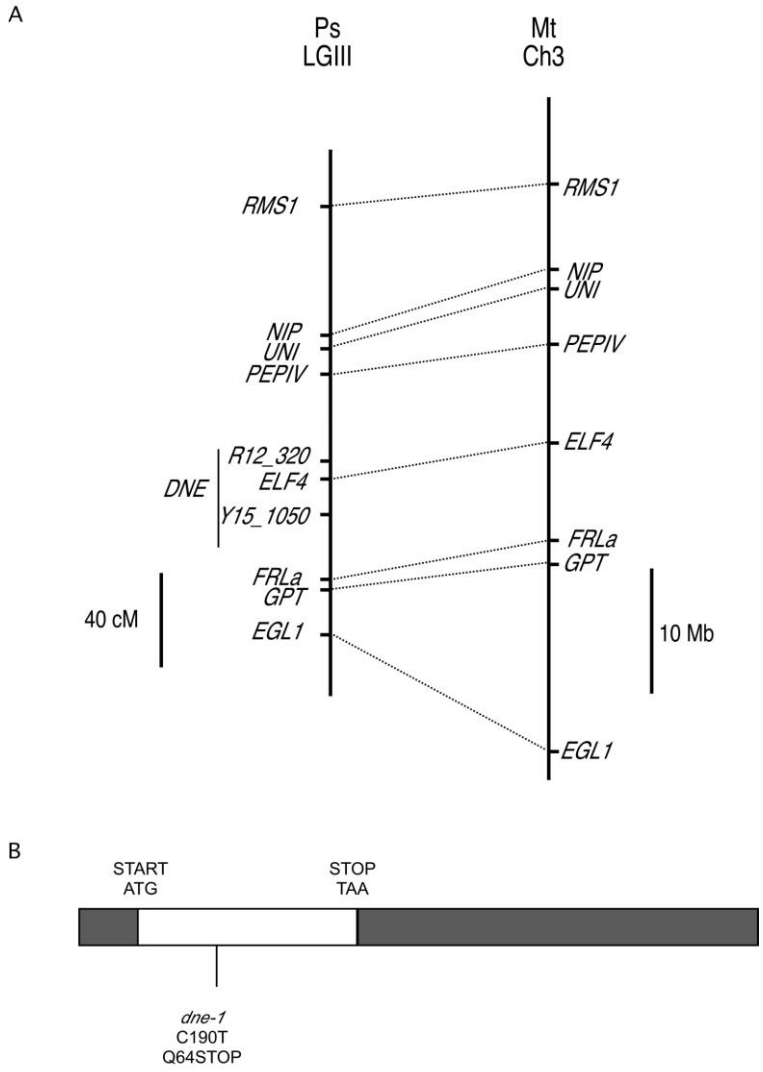

Figure 4.5 *DNE* is ortholog of Arabidopsis *ELF4*.
(A) Comparative map between linkage group III in pea and Chromosome 3 in Medicago. Orthologous genes are joined together by dashed line.
(B) Diagram of the *DNE* cDNA showing the location and nature of mutations in *dne-1*.

Alignment of ELF4 sequences revealed a highly-conserved central domain, but little sequence similarity in the short C- and N-terminal extensions (Figure 4.6A). As the truncated ELF4 protein in the *dne* mutant would lack most of the conserved central domain it is likely to be largely functionally inactive, and we tested this by complementation in Arabidopsis. Arabidopsis *elf4* mutants are unable to sense daylength and flower early under both LD and SD, with elongated hypocotyls and petioles (Doyle et al., 2002; McWatters et al., 2007). Figures 4.6B to 4.6E show that *PsELF4* expressed under the control of the 35S promoter complemented the Arabidopsis *elf4-1* mutation under both LD and SD, strongly delaying flowering in a manner similar to *35S:AtELF4*. In contrast, over-expression of *PsELF4* carrying the *dne-1* mutation had much less of an effect than *WT PsELF4* under both photoperiods despite comparable expression levels (Supplemental Figure 5, (Liew et al., 2009b)), and plants continued to produce elongated petioles, suggesting *PsELF4* activity had been mostly eliminated by the *dne-1* mutation. Under SDs, however, flowering time was significantly later than *elf4-1* suggesting some residual function of the truncated *dne-1* protein (Figure 4.6B). Nevertheless, the strong impairment of PsELF4 function caused by this mutation and the tight cosegregation of the *dne* mutant phenotype with the mutation strongly supports a conclusion that *DNE* is *PsELF4*.

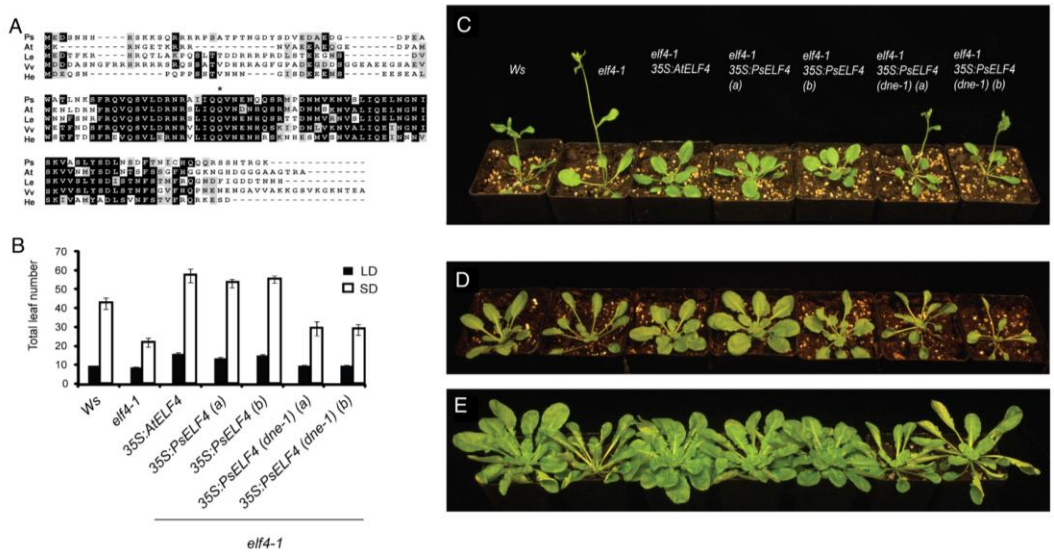

Figure 4.6 *DNE* can complement function of Arabidopsis *ELF4*.

(A) Alignment of ELF4 protein sequences. Conserved amino acids are shaded in black and the location of the Q64 residue altered by the dne-1 mutation is indicated by an asterisk. Ps, *Pisum sativum*; At, *Arabidopsis thaliana*; Le, *Lycopersicon esculentum*; Vv, *Vitis vinifera*; He, *Helianthus exilis*.

(B) to (E) Complementation of the Arabidopsis *elf4* mutant. All plants were grown in growth cabinets at 20°C, in either LD (16h) or SD (8h) conditions. (a) and (b) represent two independent transformants.

(B) Total leaf number at flowering of Arabidopsis plants in LD and SD. Data are mean ± SE for n=3.

(C) Representative plants grown in LD. Flower induction has occurred in *elf4-1* and *elf4-1* expressing mutated PsELF4 (*dne-1*), whereas other plants have not yet flowered.

(D) Representative plants grown in SD, showing elongated petioles in *elf4-1* and *elf4-1* expressing mutated PsELF4 (*dne-1*), whereas other plants have normal petiole length.

(E) Representative plants grown in SD, showing flower induction in *elf4-1* and *elf4-1* complemented with mutated PsELF4 (*dne-1*), whereas other plants have not yet flowered.

4.3.6. Genetic and physiological interaction of DNE and LATE1 in the control of flowering and clock gene expression

As both *DNE/PsELF4* and *LATE1/PsGI* appear to have a primary influence on the circadian clock, it seemed possible that both genes might affect flowering through the same pathway, and to test this we constructed a *dne late1* double mutant. Figure 4.7A shows that, under LD, the *dne late1* mutant is similar in overall appearance to the *late1* single mutant, with delayed senescence, increased branching, and an increased number of reproductive nodes compared to WT. Despite these similarities, the double mutant initiated the formation of its first flower at a much lower node than in the single *late1* mutant (Figure 4.7B). Interestingly however, the growth of flowers at the first few reproductive nodes of *dne late1* plants was arrested at an early stage (Figure 4.7A, inset) and fully-developed, open flowers were not produced until approximately the node at which flowering commenced in the *late1* single mutant (Figure 4.7A). The *dne* mutation was thus clearly able to promote the initiation of flowering in the absence of *LATE1*, but *LATE1* clearly influenced the subsequent development of these early-initiated flower primordia, and was epistatic to *DNE* in other respects.

Previous studies suggested that *LATE1* is necessary for the production of a mobile stimulus of flowering in LD (Hecht et al., 2007), and the *LATE1-DNE* interaction raised the possibility that *DNE* might act, in part, through the same mobile signal. Figure 4.7C shows that under SD, *dne* graft stocks possessing 3 or 4 true foliage leaves strongly promoted flowering of WT scions relative to WT-on-WT self-grafts. In contrast, flowering of *dne* scions grafted to WT stocks was not significantly delayed compared to *dne* self-grafts (P=0.74). This implies that the

early-flowering of the *dne* mutant in SD is associated with increased production of a mobile stimulus, rather than reduced production of an inhibitor as previously suggested (King and Murfet, 1985). Moreover, in *dne late1* double mutant stocks, the ability of *dne* to promote flowering of WT scions was completely blocked by the *late1* mutation (Figure 4.7C). This suggests that *LATE1* not only controls a mobile flowering signal in LD, but also acts downstream of *DNE* in the regulation of a similar signal in SD.

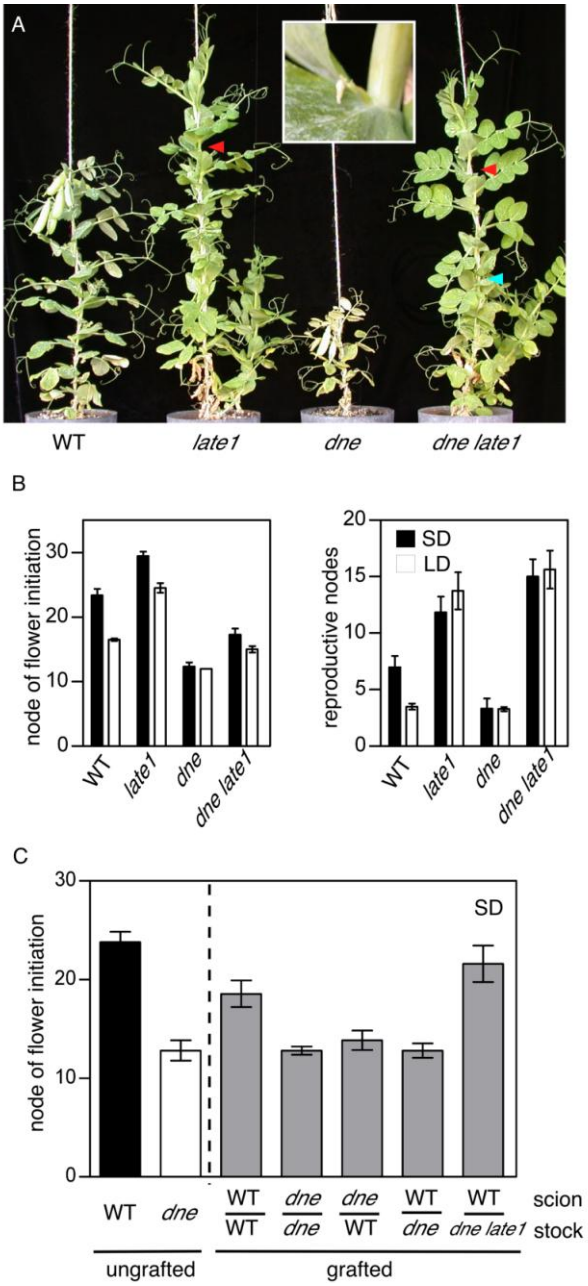

Figure 4.7 Interaction of *LATE1* and *DNE* in the control of flowering

(A) Representative eight-week-old plants grown under LD. Inset shows the first initiated flower primordium in the *dne late1* mutant, which is also indicated by the blue arrowhead in the main panel. The red arrowheads indicate the node of first open flower in *late1* and *dne late1*.

(B) Node of flower initiation (left) and final number of reproductive nodes (right). Data are mean ± SE for n=6-8 plants

(C) Node of flower initiation in ungrafted controls, self-grafts, and reciprocal grafts between WT, dne, and dne late1. Data are mean ± SE for n=12 plants.

All plants were grown in the phytotron under standard SD or LD conditions.

Since circadian rhythms are damped under LL, it is difficult to compare the effect of mutants on transcript level of circadian clock genes. We designed a novel experiment which plants are grown in the darkness at constant temperature for 7 days before transfer to continuous light for 2 weeks. This means plants are not subjected to clock entrainment before exposure to continuous light and steady-state level of expression rather than rhythmic expression might be obtained. The results on wild-type plants show that this is indeed the case. The transcript level of *MYB1*, *TOC1*, *ELF4*, and *LATE1* did not show rhythmic expression patterns (Figure 4.8A) as already seen in diurnal (LD or SD; Figure 4.2) or circadian cycles (LL; Figure 4.3 or DD; Figure 4.4). Instead, the relative expression level did not fluctuate much in all clock genes examined. This suggests steady-state level of expression might be present if plants are not exposed to entraining condition since germination.

This result might allow us to investigate the direct effect of *DNE* or/and *LATE1* on the level of clock gene expression. We repeated the same experiment by including *dne*, *late1*, and *dne late1* mutants (Figure 4.8B). Interestingly, the *dne late1* double mutants show the lowest transcript levels of *MYB1*, *TOC1*, *ELF4*, and *LATE1* among the four genotypes. The *dne* mutants have more or less the similar level of expression as the wild-type plants except the *ELF4* expression is slightly lower in *dne* mutant when compared to wild-type. On the other hand, the *late1* mutants have similar level of *TOC1* and *ELF4* transcripts as wild-type but *MYB1* and *LATE1* transcript level were damped as low as the *dne late1* mutants. However, no significance can be attached to any variation or patterns without further replications.

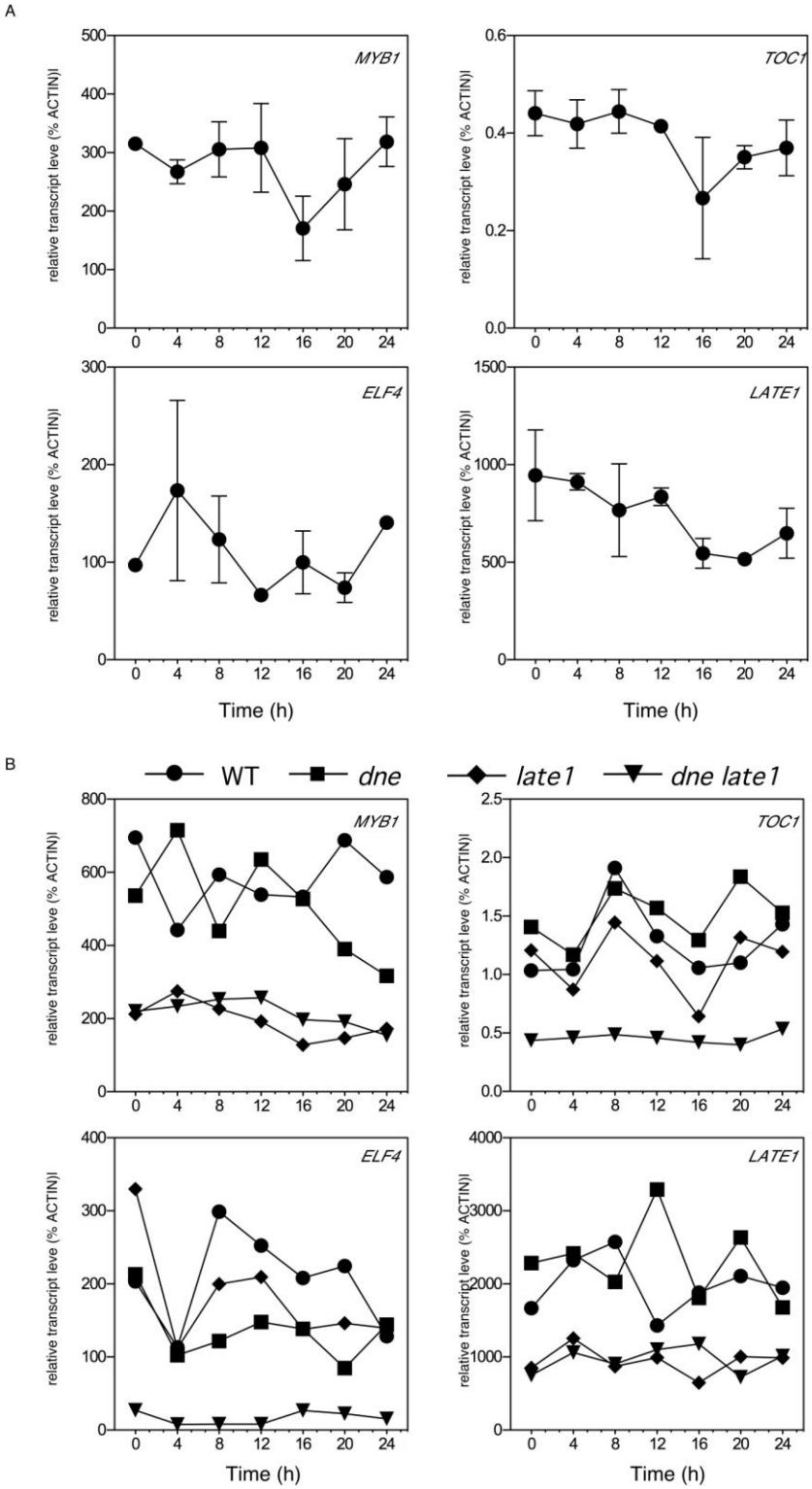

Figure 4.8 Circadian clock genes expression under continuous light without entrainment. Plants are grown in darkness for 7 days until germination occur before transfer to continuous light at 25 $\mu molm^{-2}s^{-1}$ for 2 weeks.
(A) Expression of clock genes in WT plants. Data are mean ± SE for n = 3 biological replicates, each consisting of pooled material from two plants.
(B) Expression of clock genes in WT, *dne*, *late1*, and *dne late1* plants. Data are single biological replicates which consist of pooled material from two plants.

4.3.7. Effects of DNE on CO and FT expression

In Arabidopsis, one of the main ways the circadian clock influences flowering is through control of the expression rhythm of the *CO* gene which in turn regulate *FT* expression. Pea and Medicago both possess a single group Ia *CO*-like gene (*COLa*) that is orthologous to the *CO*/*COL1*/*COL2* clade in Arabidopsis and shares the diurnal expression pattern of *COL1* and *COL2* but not *CO* (Hecht *et al.* 2007, Macknight laboratory, unpublished data). In a previous study, we showed that although *late1* affected the diurnal regulation of several clock-related genes and impaired the induction of the *FT* homolog *PsFTb2* (formerly *PsFTL*), there was no clear effect of *late1* on the expression rhythm of *COLa* (Hecht et al., 2007). One possible explanation is *PsCOLa* might not be the functional ortholog of *AtCO*. In addition to *COLa*, there are three other *CO*-like sequences found in medicago (*MtCOLb* to *MtCOLd*) but they do not group in *CO*/*COL1*/*COL2* clade and fall within *COL3* to *COL5* clade (Hecht et al., 2005). The ortholog of *MtCOLb* have been isolated in pea, designated as *PsCOLb*. Figure 4.9 shows that there was also no significant difference in the expression rhythm of either *COLa* or *COLb* under SD between WT and *dne*. Furthermore, *COLb* expression pattern is different from Arabidopsis CO as well.

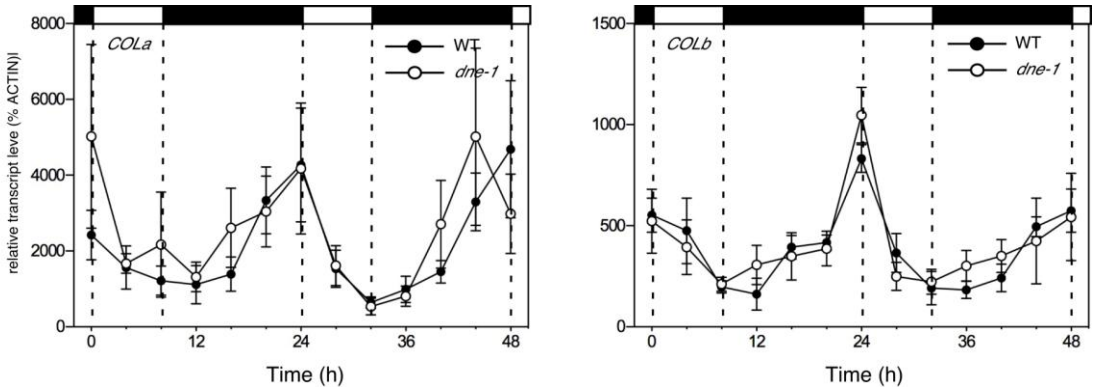

Figure 4.9 *DNE* affects diurnal rhythms of *CO* homologs under SD conditions (8-h photoperiod). All plants were grown for 21 d from sowing at 20°C before harvesting commenced. Data are mean ± SE for n = 3 biological replicates, each consisting of pooled material from two plants. Day and night periods are indicated by open and closed bars, respectively, above the graph.

We also examined whether the *dne* mutation might also affect expression of *FT*-like gene in pea. Previous surveys on medicago genome have identified five *FT*-like sequences (*MtFTa1* to *MtFTb2*) (Hecht et al., 2005; Liew et al., 2009b). Recently, a comprehensive paper about *FT* homolog in pea has been published (Hecht et al., 2011). In addition to previously reported *PsFTb2* (formerly *PsFTL*, ortholog of *MtFTLe*), four additional *FT*-like genes have been isolated in pea (*PsFTa1*, *PsFTa2*, *PsFTc*, *PsFTb1*). Phylogenetic analysis shows that the Medicago and pea genes are orthologous except *MtFTb1* and *MtFTb2* are so similar to each other that we cannot distinguish the pea genes, *PsFTb1* and *PsFTb2*, to either of them. This complex *FT*-like gene family in pea is associated with complex expression patterns as well. *FTa1* and *FTa2* are expressed in leaf and apex whereas *FTc* is only expressed in apex; *FTb1* and *FTb2* are only expressed in leaf (Hecht et al., 2011).

Under SD condition, *dne* mutant flowers approximate 10 nodes earlier than WT plants. We therefore expect to see increased transcript level of inflorescence genes such as *PIM* (pea ortholog of Arabidopsis *AP1*) associate with the early-flowering phenotype of *dne* mutants. The *PIM* expression was induced by week

3 in the *dne* mutant which is approximately 4 weeks earlier than the WT plant in SD (Figure 4.10). This is strongly correlated with the flowering nodes of *dne* and WT plants. Additionally, the *dne* mutant showed higher transcript level of *FTa1*, *FTa2*, *FTb1*, and *FTb2* in leaves and of *FTa1*, *FTa2*, and *FTc* in shoot apices (Figure 4.10). The expressions of *FT* started to rise since week 2 in the leaves and slightly delayed in the apex (week2 to 3) which is before *PIM* is induced. Overall in the *dne* mutant, the timing of increased expressions of *FT* genes is associated with elevated *PIM* expression started by week 3 (day 21). On the other hand, all the *FT* gene expressions in the WT stayed low and only induced at the end of the experiment (day 56) (Figure 4.10).

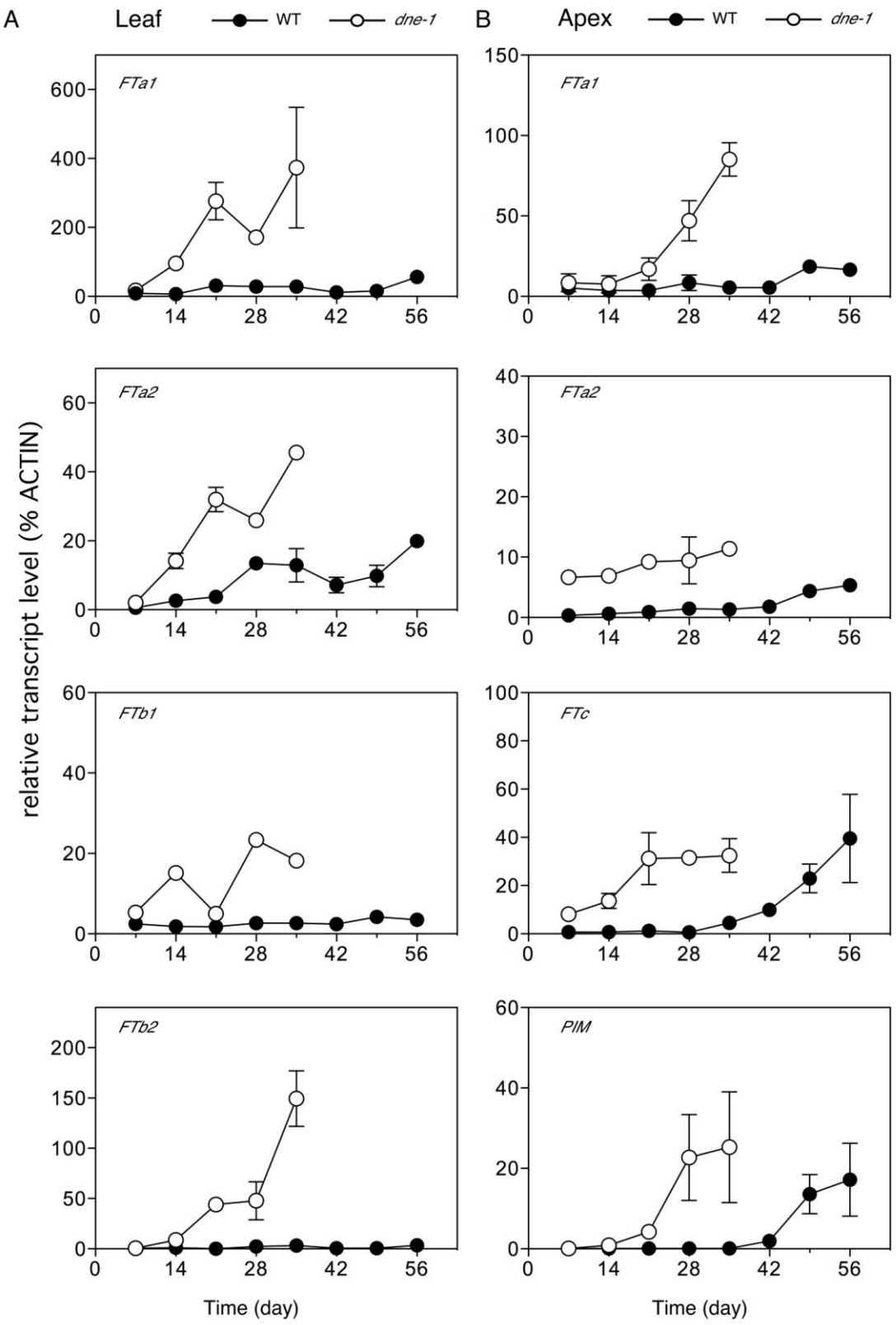

Figure 4.10 Pea *FT-like* and *PIM* gene expression in (A) uppermost leaf (B) shoot apex of *dne-1* and WT plants grown under SD (8h-photoperiod). All plants were grown at 20°C and harvesting commenced at day 8 up to day 35 for dne-1 and day 56 for WT. Data are mean ± SE for n=2 or 3 biological replicates, each consist of pooled material from two plants. Taken from Hecht et.al., 2011.

4.3.8. DNE also regulates stem elongation

In addition to effects on flowering, the circadian clock regulates other traits including rhythmic regulation of hypocotyl elongation and leaf expansion (Dowson-Day and Millar, 1999). Examples include the long-hypocotyl phenotypes of *lhy* (Mizoguchi et al., 2002), *elf3* (Zagotta et al., 1996) and *lux* (Hazen et al., 2005) mutants and short-hypocotyl phenotype of *ztl* (Somers et al., 2000) and *fkf1* (Nelson et al., 2000). As Arabidopsis *ELF4* is also proposed to function in phyB-mediated de-etiolation and shows long hypocotyls in *elf4* mutant (Khanna et al., 2003), we also examined de-etiolation in the *dne* mutant seedlings after 14 d from sowing under continuous light or darkness in growth cabinets at 20°C. Mutant *dne* seedlings were indistinguishable from WT in both darkness and white light but showed shorter internodes under red, blue and far-red, with the proportionately strongest effect seen under blue (Figure 4.11A). This is in clear contrast to the elongated hypocotyl phenotype seen in the *elf4* mutant (Khanna et al., 2003). In contrast, *dne* mutant and WT did not differ in leaf expansion in darkness or under any light condition.

We also examined whether *PsELF4* could complement the hypocotyl elongation phenotype of the Arabidopsis *elf4* mutant. Figure 4.11B shows that over-expression of *PsELF4* in the Arabidopsis *elf4-1* mutant resulted in shortened hypocotyls that were comparable in length to WT (*Ws*). No change in hypocotyl length was observed in seedlings over-expressing the *dne-1* mutant ELF4 protein, supporting the conclusion from the flowering time experiment (Figure 4.6) that the *dne-1* mutation severely impairs PsELF4 protein function. This result also suggests that the difference in elongation phenotype of the *dne* and *elf4* mutants is due to a species-specific context for DNE/ELF4 protein function, rather than being inherent to the two proteins.

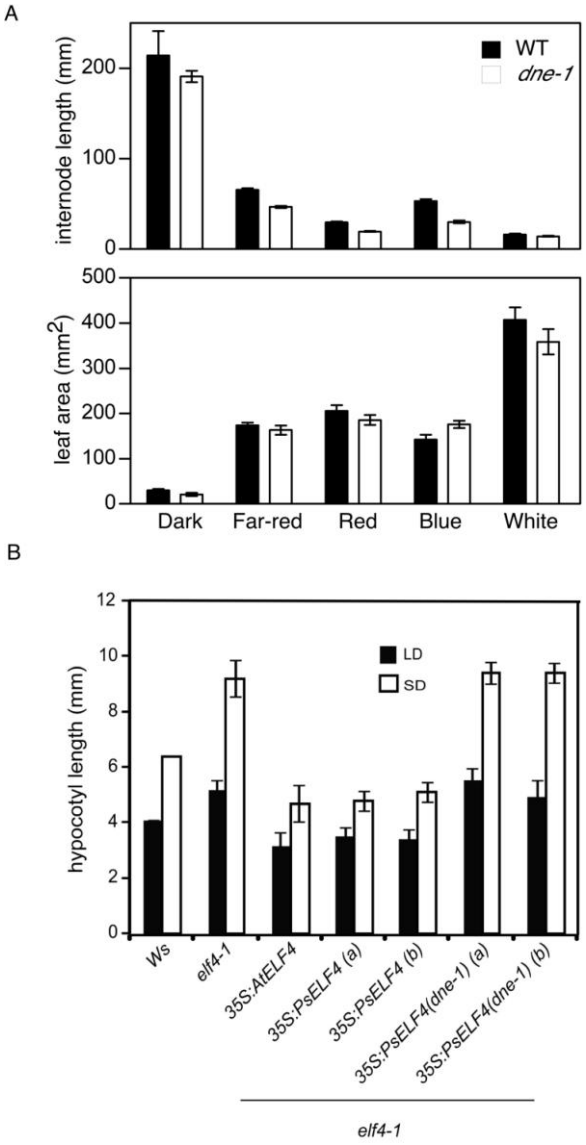

Figure 4.11 Effects of *DNE* on stem elongation
(A) Effect of the *dne* mutation on spectral sensitivity for de-etiolation responses.
(B) Hypocotyl length of Arabidopsis plants, showing elongated hypocotyl in *elf4-1* and *elf4-1* complemented with mutated *PsELF4* (*dne-1*), compared to normal hypocotyl lengths in wild-type plants and in elf4-1 mutant plants complemented with wild-type *PsELF4* (*DNE*).
All plants were grown in growth cabinets under continuous far-red, red or blue light at 15 µmolm-2s-1 (A) or white light at 100 µmolm-2s-1 (A, B). Data are mean ± SE for n=8-12 (A) or n=12-20 (B) Details on the light levels of the white and LED treatments can be found in Section 2.2.

4.4. Discussions

Early studies of photoperiod-responsive flowering in pea centered on the physiological and genetic analysis of three loci necessary for inhibition of flowering under non-inductive SD photoperiods; *SN*, *DNE*, and *PPD* (Murfet, 1971a; King and Murfet, 1985; Taylor and Murfet, 1996). More recent studies have identified genes necessary for promotion of flowering under inductive LD photoperiods, including *PHYA* (Weller et al., 2004) and *LATE1*, the ortholog of Arabidopsis *GI* (Hecht et al., 2007), but the primary physiological role and molecular nature of the *SN*, *DNE* and *PPD* loci has remained unclear. Here we show that *DNE* is necessary for the normal rhythmic regulation of circadian clock genes, and identify *DNE* as the pea ortholog of Arabidopsis *ELF4*.

ELF4 is thought to be a core component Arabidopsis circadian clock and functions in the *CCA1*/*LHY-TOC1* feedback loop of the central oscillator. *ELF4* also plays a role in the entrainment of the clock, functioning as part of the light input pathway. Despite these important roles, little is known about the function of *ELF4*-like genes outside of Arabidopsis, and true orthologs of *ELF4* may not exist in monocots (Khanna et al., 2003; Murakami et al., 2007). The identification of *DNE* thus provides the first opportunity to examine the function of this gene in another species.

4.4.1. Rhythmic expression of pea clock genes

Diurnal expression rhythms described here for *LHY*, *TOC1*, *ELF4*, and *LATE1* are consistent with a previous report (Hecht et al., 2007) and are similar to those of the corresponding Arabidopsis genes (Fowler et al., 1999; Matsushika et al., 2000; Doyle et al., 2002; Mizoguchi et al., 2002) with peak expression of *LHY* in the

morning and peak expression of *TOC1*, *ELF4* and *LATE1* in the evening. Clearly rhythmic expression is also seen for pea genes under low irradiance LL, but these rhythms are strongly damped at higher irradiances (Supplemental Figure 2, (Liew et al., 2009b)). A direct comparison with Arabidopsis data is difficult due to poor reporting of growth conditions in many published studies, but it is clear that strong rhythms do persist for all four genes under LL irradiances above 60 µmol $m^{-2}s^{-1}$ (e.g. (Park et al., 1999; Alabadi et al., 2001; Doyle et al., 2002; Mizoguchi et al., 2002; Hazen et al., 2005). In addition, even under low-irradiance LL, pea genes show signs of damping by the second circadian cycle. These apparent differences deserve further study, but in general do suggest that pea and Arabidopsis differ in their regulation by light.

In Arabidopsis, selective impairment of circadian rhythms under LL is reported for mutants in *ELF3*, *TIC* and *FHY3*; genes which are all thought to have a role in input of light signals to the clock (Hicks et al., 1996; McWatters et al., 2000; Covington et al., 2001; Hall et al., 2003; Allen et al., 2006). One explanation for the suppressed rhythmicity seen for several pea genes under higher irradiances of LL could be that our standard wild-type line NGB5839 is a natural mutant with reduced function of one of these genes, or in another gene needed for light input to the clock. In future this could presumably be evaluated using standard release-from-light and phase-response assays. It will also be important to determine whether this unusual circadian phenotype is common to other cultivars, or indeed to the entire species. In this respect it is notable that most garden pea cultivars (including NGB5839) and many spring-sown field pea cultivars carry recessive alleles at the *HIGH RESPONSE* (*HR*) locus (Murfet, 1973; Lejeune-Hénaut et al., 1999; Lejeune-Hénaut et al., 2008), which confer earlier flowering under SD and a reduction in the flowering response to

photoperiod. The light input mutants *elf3* and *tic* are also early-flowering in short days (Zagotta et al., 1996; Hall et al., 2003), and it will therefore be of interest to test if the weaker LL rhythms we observe reflect loss of *HR* function.

In addition to the unexpected damping or loss of rhythms under LL, we also observed differences in the expression rhythms of pea clock genes in DD in comparison to their Arabidopsis counterparts. The patterns of *ELF4* and *TOC1* expression in DD are similar in pea and Arabidopsis, with both rhythms damping rapidly to trough and median levels, respectively (Strayer et al., 2000; Doyle et al., 2002), and rhythmic *GI*/*LATE1* expression persists in both species ((Park et al., 1999), Figure 4.4). However, the persistence of rhythmic *MYB1* expression in DD (Figure 4.4) differs from expression patterns of *CCA1* and *AtLHY*, which both damp rapidly to near trough levels (Wang and Tobin, 1998), and the residual low amplitude rhythm we observed for pea *ELF4* is not apparent in the Arabidopsis data (Doyle et al., 2002). In addition, whereas in Arabidopsis the period of expression for several clock genes in DD is generally longer than 24h (Halaban, 1968; Hicks et al., 1996; Wang and Tobin, 1998), the rhythms of *MYB1* and *LATE1* expression rhythms under DD appeared significantly shorter than 24h.

In summary, despite the fundamental importance of the circadian clock, significant differences in the expression of clock genes are evident between Arabidopsis and pea. This suggests that the function of clock components and mechanisms for clock entrainment may differ between plant species. Interestingly, a similar conclusion has been drawn from work in another legume, *Phaseolus* (Kaldis and Prombona, 2006).

4.4.2. Roles of DNE in diurnal and circadian rhythms

To assess the effect of the *dne* mutation on the pea circadian clock, we analysed the expression of pea clock genes under both LL and DD. We found that in contrast to Arabidopsis *elf4* mutations, which severely impair rhythmic expression of *LHY*, *CCA1*, *TOC1* and *ELF4* under LL (Doyle et al., 2002; McWatters et al., 2007), *dne* has only relatively minor effects on phase of *TOC1*, *LATE1* and *ELF4* in *LL*, and all four genes cycle with amplitude similar to wild-type. In DD, the *dne* mutation also causes a reduction in amplitude and a phase advance in the *DNE* rhythm and an apparent period shortening of the *LHY* rhythm in DD. Less is known about the effects of Arabidopsis *elf4* in DD except that, as in LL, it severely impairs the *CCA1* expression rhythm (Doyle et al., 2002). Overall, these results suggest that *DNE* may have a more subtle role in clock regulation than Arabidopsis *ELF4*, or that there may be a greater degree of redundancy within the family of *ELF4*-like genes in pea, or that there may be some residual DNE activity in the *dne-1* mutant, as suggested from the Arabidopsis complementation experiments. However, regardless of which of these explanations may be true, it is evident that a strong effect of the *dne-1* mutation on photoperiodic flowering is associated with only relatively minor effects on circadian rhythms of clock gene expression.

Under LD cycles Arabidopsis *elf4* had no effect on *CCA1* expression, while under SD the *CCA1* rhythm in *elf4* showed a reduced ability to anticipate dawn and an increased sensitivity to light immediately after dawn (McWatters et al., 2007). In contrast, the *MYB1* rhythm was not significantly affected by *dne* under SD or LD, and we found no clear evidence for impaired anticipation of dawn in *dne*, although this could in part reflect the lower resolution of our measurements and in future should be examined in more detail. It will also be interesting to examine whether *DNE*, like

Arabidopsis *ELF4* for *LHY*, has a role in the light induction of *MYB1*, and in the gating of light signals to the clock. It is notable that in SD the *dne* mutation causes a phase delay in *TOC1* expression but a phase advance in expression of *DNE* itself, despite both genes being expressed in the evening. This is difficult to reconcile with a primary effect of *DNE* on the core clock mechanism and may instead reflect a role in light input. Such a role may also be suggested by the fact that the timing of peak *TOC1* expression is less sensitive to photoperiod in *dne* than in WT.

Other comparisons also suggest that *DNE* does not have a simple interaction with the putative core clock components *LHY* and *TOC1*. For example, in DD, where *dne* clearly affected the *LHY* rhythm, it had little effect on expression of the evening genes *TOC1* and *LATE1* (Figure 4.4), but under SD cycles, where the rhythm of *LHY* was not affected, *dne* did affect both *TOC1* and *LATE1* (Figure 4.2A). This could imply either that *dne* mutation may independently affect light signalling to *LHY* and *TOC1* and/or that it may affect the coupling of *LHY* and *TOC1* expression. In Arabidopsis, most analyses of the core clock mechanism have been conducted in constant light, where coupling of antiphased *CCA1*/*LHY* and *TOC1* expression rhythms are normally observed. However, it has been shown in de-etiolating Arabidopsis seedlings that *ELF4* can act independently of *TOC1* to regulate *CCA1*/*LHY* expression, and that rhythmic *TOC1* expression does not completely depend on the regulation of *CCA1*/*LHY* (Kikis et al., 2005). The presence of an additional factor "X" necessary for the coupling of the *TOC1-GI* loop to *CCA1*/*LHY* has been predicted from computational modeling, and *ELF4* has been proposed as one candidate for X (Locke et al., 2006; Ueda, 2006; Zeilinger et al., 2006). Given the complexity of the circadian clock, more detailed comparisons between pea and Arabidopsis will require application of similar modelling approaches in both species.

4.4.3. Coupling of DNE and LATE1 to flowering output pathways

Previous models for flowering in pea proposed that *dne* mutation blocks production of a mobile inhibitor of flowering in SD (King and Murfet, 1985), a suggestion difficult to reconcile with current understanding of photoperiodic flowering in Arabidopsis, where the primary target of clock regulation (FT) acts as a mobile stimulus (Turck et al., 2008). However, we show here that in grafts with leafy donor tissue, the major effect of *DNE* in SD is to inhibit a graft-transmissible flowering stimulus (Figure 4.7C), and that increased ability of the *dne* mutant to promote flowering across a graft union is associated with elevated expression of the *FT*-like gene *FTb2* (Liew et al., 2009b). The correlation between flowering time, effect on a mobile stimulus and *FTb2* (formerly *FTL*) expression is also seen for the late-flowering photoperiod response mutant *late1* under LD (Hecht et al., 2007).

Together, these results are superficially similar to those from Arabidopsis showing that the induction of *FT* expression is necessary for the LD response, and that *ELF4* and *GI* act in opposite ways to regulate expression of *FT* (Suarez-Lopez et al., 2001; Doyle et al., 2002). In Arabidopsis, this regulation occurs at least in part through *CO* (Doyle et al., 2002; Mizoguchi et al., 2005). However, as reported previously for the *late1* mutant (Hecht et al., 2007), *dne* also had no effect on the *COLa* and *COLb* expression rhythm under conditions where its flowering phenotype is strongest (Figure 4.9A). It is possible that other *COL* genes may have assumed the function of Arabidopsis *CO*, and this can now be addressed using reverse genetics (Hecht et al., 2007; Dalmais et al., 2008; Tadege et al., 2008).

We also used a *dne late1* double mutant to examine the interaction between *DNE* and *LATE1* in control of flowering. The comparable interaction in Arabidopsis between *ELF4* and *GI* has yet to be described. In most respects *late1* and *dne* show a

straight-forward interaction in which *late1* is epistatic to *dne*, with respect to overall phenotype in both short and long days (Figure 4.7A, B) and graft-transmissible effects on flowering in SD (Figure 4.7C), suggesting that *LATE1* is necessary for *DNE* effects on both a mobile flowering stimulus and on general photoperiod responsiveness. However, a more complex interaction between *dne* and *late1* in the control of flower initiation is suggested by the early flower initiation of flower primordia in the *dne late1* double mutant. This distinct phenotype of the *dne late1* double suggests that *dne* can affect flowering independently of *late1*, a conclusion that is superficially contradictory to the observation that *late1* completely blocked the effect of *dne* on flowering in graft stocks (Figure 4.7C). However, these two experiments differ in that the intact *dne late1* plants carried the *dne* and *late1* mutations in all tissues, whereas the grafted plants carried the mutations in the graft stock only, which might mean that the overall effect of the *dne* mutation was less in these plants. Alternatively, the difference could reflect the existence of a heterogenous mobile flowering signal and differential effects of *dne* and *late1* on components of such a signal.

One possible interpretation for these results is that the role of *FT* in pea may not be carried out by *FTb2* alone but by one or more additional *FT*-like genes. In Arabidopsis, the *FT* family has two members, *FT* and *TSF*, which have similar regulatory characteristics and functions (Yamaguchi et al., 2005), but several recent studies have shown that the *FT* family in other species is expanded relative to Arabidopsis, with individual members showing distinct patterns of regulation with respect to daylength, seasonal and tissue specificity (Izawa et al., 2002; Faure et al., 2007; Igasaki et al., 2008; Hou and Yang, 2009) and interactions with different downstream partners (Li et al., 2008). This was recently showed to be the same case in pea where the *FT* gene family consists of five genes, *PsFTa1*, *PsFTa2*, *PsFTc*,

PsFTb1, and *PsFTb2* and each of them showed distinct expression patterns (Hecht et al., 2011). *PsFTa1* and *PsFTa2* are expressed in both leaf and apex. *PsFTc* is specifically expressed in shoot apex whereas *PsFTb2* is only expressed in leaf. *PsFTb1*, on the other hand, is weakly expressed in both tissue types.

The early-flowering phenotype of the *dne* mutant is strongly associated with elevated level of *PIM* expression which is associated with early induction of all five *FT*-like genes in pea. Opposite results are also found in the late-flowering *late1* mutant which *FT* genes expressions are delayed (Hecht et al., 2011). It is therefore be interesting to examine if the novel phenotype of the *dne late1* double mutant is due to differential (spatial or temporal) expression of *FT*-like genes. That would imply the existence of at least two pea *FT*-like genes are important for photoperiodic control of flowering; one associated with general photoperiod responsiveness, and one with a narrower role in initiation of flowering. This hypothesis is consistent to the research on *gigas*/*FTa1* mutant that *FTa1* and *FTb2* regulate two distinct mobile floral stimuli which might regulate flowering independently through different mechanisms (Hecht et al., 2011). Therefore, it will be of interest to determine how these *FT* genes are differentially regulated by *DNE* and *LATE1* in the *dne late1* mutant under different conditions.

Chapter 5 Characterization of the flowering locus *STERILE NODES* (*SN*)

5.1. Introduction

5.1.1. Pea sn mutant

The *STERILE NODES* (*SN*) locus was first identified in early studies of naturally-occurring variation for flowering in pea. Homozygous recessive alleles of *SN* were found in many early flowering and day neutral varieties of commercial pea such as Massey and Alaska (Barber, 1959). Detailed genetic studies on the *SN* locus using artificial short-day environments established that *sn* mutant has an early-flowering, daylength insensitive phenotype. Lines carrying dominant *SN* also show an increased response to photoperiod and vernalisation, primarily due to a strong delay of flowering under SD. *SN* lines also show a slower rate of leaf formation and a small reduction in internode length under SD, whereas recessive alleles reduce these responses due to strong promotion of flowering in SD (Barber, 1959). Dominant *HR* alleles act together with dominant *SN* to further delay flowering in SD and increase the photoperiod response (Murfet, 1971a, 1973). Subsequent studies documented pleiotropic effects of the *SN* locus on seed growth, fruit set, senescence, and outgrowth of basal laterals (Reid, 1979b, 1980; Ross and Murfet, 1985; Murfet, 1988; Kelly and Spanswick, 1997).

Naturally-occurring recessive forms of *SN* are widespread in cultivated pea germplasm and it is thus unclear how many actual alleles are present. The simplest initial assumption is that there may only be a single recessive allele. This provisionally referred to here as *sn-1*. Three additional induced mutant alleles have been identified in subsequent induced mutagenesis; *sn-2* (from radiation mutagenesis in cv. Borek

background) (Arumingtyas and Murfet, 1994) and *sn-3* and *sn-4* (from EMS mutagenesis in NGB5839 (cv. Torsdag) background) ((Jones, 2004), J. Weller et. al. unpublished). *SN* is previously reported to show close linkage with the *Amy1* amylase locus (Weeden et al., 1988) and more recently was mapped between two isozyme loci *Aldolase* (*Aldo*) and *Galactosidase2* (*Gal2*) on the bottom half of pea linkage group VII (Murfet and Sherriff, 1996).

The similarity of *SN* and *DNE* was previously noted ((King and Murfet, 1985), Chapter 4), and in view of the fact that *DNE* has been identified as the pea ortholog of Arabidopsis circadian clock gene *ELF4* (Chapter 4), it seems likely that the complementary gene, *SN* could be a component of the circadian clock as well. Preliminary examination of expression rhythms for clock regulated genes *CAB9* and *ELF4* in the *sn-4* mutant supported this idea, showing that expression rhythms of both genes under SD shifted to an earlier phase in the *sn-4* mutant compared to WT (Jones, 2004).

The main aim of the work presented in this chapter was to identify and evaluate potential candidate genes for the *SN* locus, using both functional and positional information. As in the case of *DNE*, detailed characterization of physiological traits, expression rhythms, and genetic interaction will be investigated in *sn* mutants. Evaluation of the two candidate genes, *PRR37* and *LUX*, identified in Chapter 3 will also be carried out. Additionally, as *DNE* has been discovered to regulate expression of pea *FT*-like genes during development (Chapter 4), this chapter will also examine whether the same is true for *SN*.

5.2. Materials and methods

5.2.1. Gene expression experiments

For the diurnal expression experiments, all plants were grown for 3 weeks from sowing at 20°C in growth cabinets under either LD (16-h photoperiod) or SD (8-h photoperiod). Harvested material consisted of entire shoot apex above and including the uppermost expanded leaf from two plants. Samples were harvested at 4h intervals, with up to 3 replicates per time point. Samples were harvested and processed by V. Hecht and K. Claire. Several real-time PCR runs were done with assistance of V. Hecht.

For circadian expression experiments, all plants were grown in growth cabinets under a light/dark cycle (12L: 12D) at 20°C for 3 weeks before transfer to continuous darkness at ZT36 (DD). Harvested material consisted of a single leaflet from the uppermost fully expanded leaf from two plants. Samples were harvested at 3h intervals, with 2 to 3 replicates per time point.

For developmental time course experiment, plants were grown in growth cabinets under SD condition (8L: 16D) at 20°C. Leaf and apical bud samples were harvested separately from each plant at 2-day interval from day 8 to day 24. Samples were harvested at the same time during the day for each time point approximately 4 hours after light on. Leaf material consisted of single leaflet from the uppermost fully expanded leaf from two plants. Apical bud material consisted of dissected apical buds from two plants to 2-mm in length. 3 replicates were harvested per time point.

5.2.2. Generation of the mapping population of sn4 x Terese

An F_2 population of 80 plants was generated from a crossing between the *sn-4* mutant (in the NGB5839 background) and *cv.* Terese. Plants were grown under SD to allow maximal expression of phenotypic difference between *SN/-* and *sn* segregants.

The node of flower initiation (NFI) was scored for all plants. The early-flowering *sn* mutants were clearly distinguishable in the population (Figure 5.6), but in order to further distinguish homozygous WT from heterozygous F_2 plants, F_3 progenies from *SN/-* F_2 segregants were grown under same conditions. F_2 plants were designated as heterozygous if any early segregant appeared in the F_3, or if not, as homozygous WT if family size > 8 and as undetermined if family size < 8. Four categories were coded differentially in the Joinmap linkage map program according to the developers' instructions.

5.2.3. Genotyping using High Resolution Melting (HRM)

High Resolution Melt (HRM) analysis is a molecular technique for the detection of polymorphism in double-stranded DNA samples based on the temperature required for melting (separation) of two strands. HRM was used for genotyping of the *sn-4* mutation, using the CFX96 Real time PCR system (Bio-rad). and Precision Melt Analysis software (Bio-rad). Known *sn sn*, *SN sn* and *SN SN* genotypes were included as positive controls in all the runs.

5.3. Results

5.3.1. The sn mutant shows early, photoperiod-insensitive flowering

Previous studies have shown natural (*sn-1*) and induced (*sn-2*) mutant alleles confer early-flowering phenotypes. We also examined flowering in two new alleles, *sn-3* and *sn-4* which similar flowering phenotypes were found (Figure 5.1).

Detailed physiological characterization of the *sn* phenotype was carried out using *sn-4* mutant primarily because this mutant is on the same genetic background as the majority of other flowering mutants. Like *sn-1* (Murfet, 1971c; Murfet, 1982, 1992),

the *sn-4* mutant is photoperiod insensitive, flowering early regardless of photoperiod, and in SD, shows other traits characteristic of a wild-type plant grown in LD such as rapid termination of flowering after a few reproductive nodes and rapid senescence (Figure 5.2).

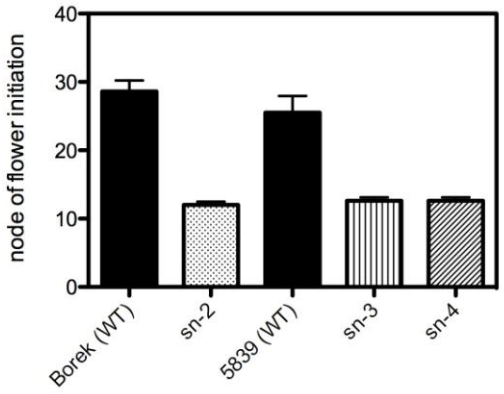

Figure 5.1 The early flowering phenotypes in *sn* alleles. All plants were grown in the growth cabinet under SD (8L: 16D) and node of flower initiation was measured. Data are mean ± SE for n=10 plants.

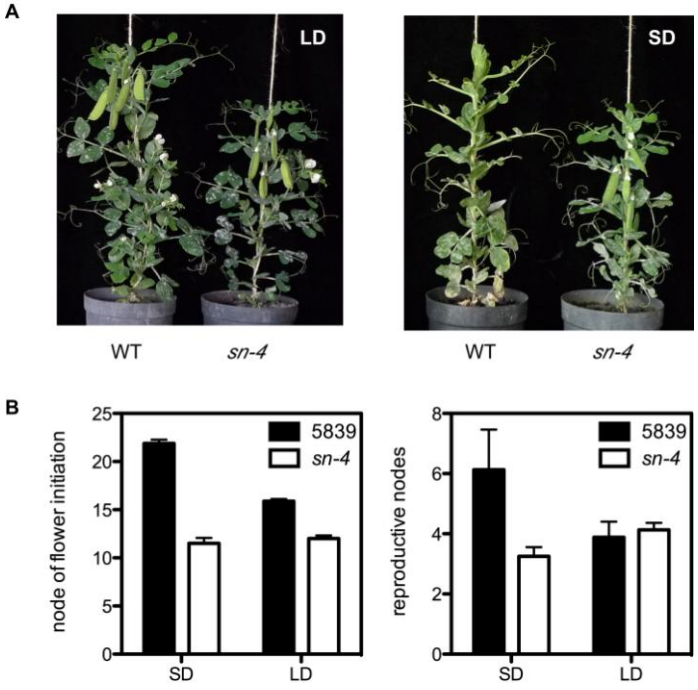

Figure 5.2 The *sn-4* mutant is early flowering and photoperiod-insensitive. (A) Representative of 8-week-old wild-type line NGB5839 and *sn-4* isogenic mutant plants. (B) Node of flower initiation (left) and final number of reproductive nodes (right). Data are mean ± SE for n = 8 plants.
All plants were grown in the phytotron under standard SD or LD conditions.

5.3.2. SN affect seedling photomorphogenesis

In Arabidopsis the circadian clock plays a central role in controlling responses to light and photoperiod, and loss of circadian-related gene function may be manifested in seedlings as photomorphogenic defects. Photomorphogenic responses including stem elongation and leaf expansion were therefore examined in *sn* mutants seedlings. The *sn-2* and *sn-4* mutants (in Borek and NGB5839 backgrounds respectively) were included in this analysis as a control for potential background-specific effects. Seedlings of *sn-2* mutants have slightly shorter internode in white light ($P = 0.017$) and slightly longer internode in darkness than the WT (Borek) ($P = 0.002$) (Figure 5.3A, left). In contrast, *sn-4* mutants did not differ from WT (NGB5839) in internode length in white light ($P = 0.89$) whereas the mutants have slightly longer internodes in darkness than the WT (NGB5839) ($P = 0.001$) (Figure 5.3A, right). However, the mutant seedlings of both *sn-2* and *sn-4* showed shorter internodes under red, far-red, and blue light ($P < 0.001$) (Figure 5.3A). This shorter internode phenotype is more obvious in NGB5839 genetic background and also under blue light. In general, photomorphogenic defects are reflected in opposite effects on elongation and leaf expansion. Consistent with this, the *sn-2* mutants had a larger leaf area than WT under any light conditions (Figure 5.3B, left). However, there was no significant effect of *sn-4* on leaf area except a slight increase under blue light ($P = 0.022$) (Figure 5.3B, right). In short, the results are slightly different when comparing *sn* mutants from two genetic backgrounds. However, compared to WT, the *sn* mutant seedlings in both backgrounds showed largest difference in internode length and leaf area under blue light.

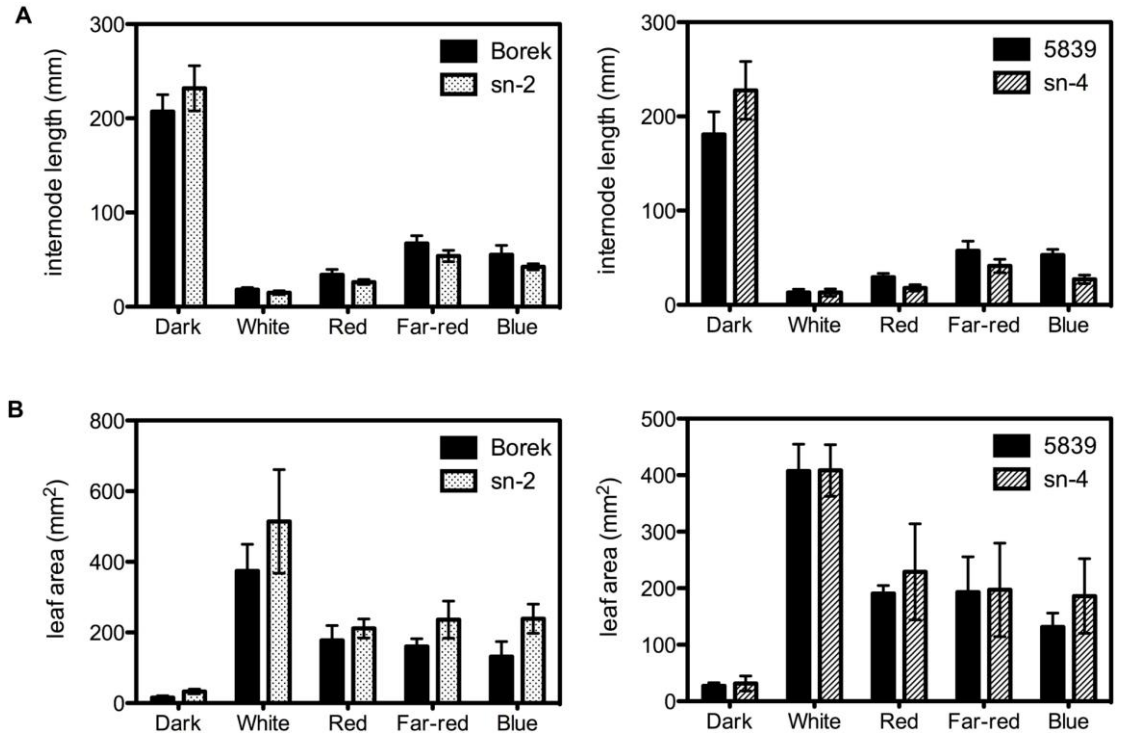

Figure 5.3 Effect of *SN* in stem elongation and leaf expansion. (A) Effect of the *sn* mutation on spectral sensitivity for deetiolation responses. Internode elongation was quantified as the length between nodes 1 and 3 (B) Leaf area was estimated as the product of the length and width of a single leaflet from leaf 3. Seedlings were grown for 14 d from sowing under continuous light or darkness. Data are mean ± SE for n = 12 plants. Details on the light levels of the white and LED treatments can be found in Section 2.2.

5.3.3. The sn mutant shows altered expression rhythms of circadian clock gene homologs under light/dark cycles

As both flowering and de-etiolation are both well known as clock-regulated pathways and are affected in *sn* mutants, we considered that *SN*, like *DNE* (Chapter 4) might have a primary effect on circadian clock system. This hypothesis is also consistent with a preliminary finding that the *sn-4* mutant showed altered diurnal rhythms of *ELF4* and *CAB9* expression (Jones, 2004). The effect of *SN* on the circadian clock was therefore examined in more detail by examining diurnal expression rhythms for a number of pea circadian clock gene homologs in the *sn-4* mutant.

As previously shown in Chapter 3, pea genes *MYB1*, *MYB2*, *TOC1*, *ELF4*, *LATE1*, *PRR37*, *PRR59*, and *ELF3* have diurnal expression rhythms similar to their Arabidopsis counterparts, with clear rhythmic expression found for all genes except *ELF3*. In the case of the *dne* mutant, rhythms of gene expression were altered but the effect was quite subtle in comparison to effects of the orthologous Arabidopsis mutant *elf4*. The *sn-4* mutant was included in the same experiment, using the same conditions and WT control plants. Similarly, some differences in these diurnal rhythms of clock gene expression were observed in the *sn* mutant when compared to WT (Figure 5.4).

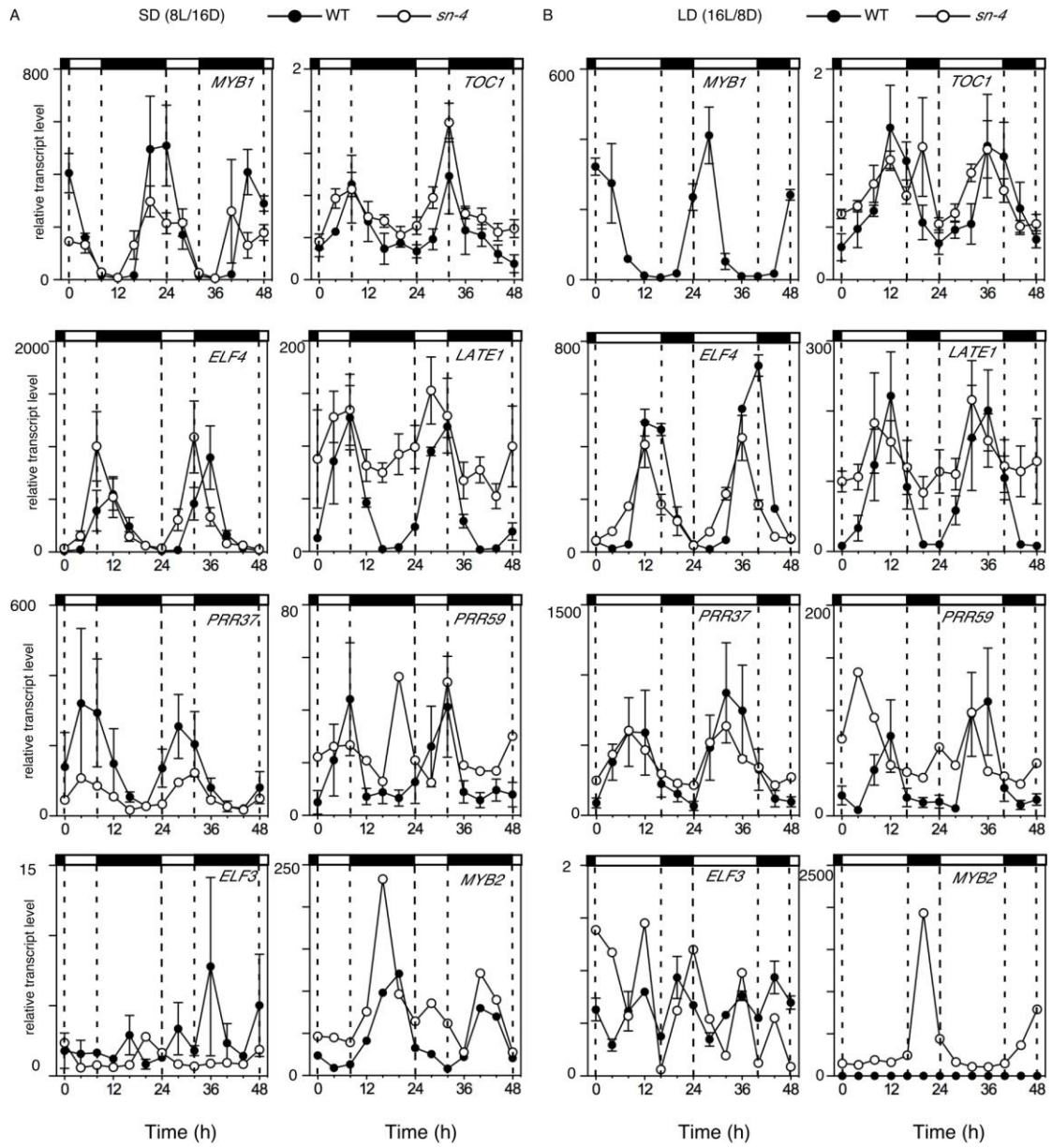

Figure 5.4 *SN* affects diurnal rhythms of clock gene homologs under light/dark cycles.
(A) SD conditions (8-h photoperiod).
(B) LD conditions (16-h photoperiod).
All plants were grown for 21 d from sowing at 20°C before harvesting commenced. Data are mean ± SE for n = 3 biological replicates except *PRR37*, *PRR59*, *ELF3* and *MYB2*, each consisting of pooled material from two plants. Day and night periods are indicated by open and closed bars, respectively, above the graph. *MYB1* expression in *sn* mutant under LD was not included due to technical issues.

We examined rhythms under both LD and SD, but since the strongest phenotypic expression of *sn* is in SD, it is of greater interest to consider the effect of *SN* in SD first. Figure 5.4A shows that transcript level of *MYB1* of *sn* in SD is higher at ZT16 and ZT40 and lower at ZT20 and ZT44 when compared to WT indicating a broader peak of *MYB1* expression rhythm in the *sn* mutant. There is a suggestion that the expression of *TOC1* is slightly higher in *sn* mutant in SD. The *ELF4* expression rhythm in *sn* mutant under SD reached a similar peak level, but peaks were shifted approximately 4h earlier than WT, from ZT12 to ZT8. The expression of *LATE1*/GIGANTEA in *sn-4* under SD appeared to had much higher trough level (ie night, up to 70 fold higher at ZT16) and peak 2-4h earlier in the day (ZT4 and ZT28). Peak (daytime) expression of *PRR37* in *sn-4* was significantly reduced whereas trough levels were similar to WT (ZT16-20 and ZT40-44). The expression rhythm of *PRR59* was somewhat obscured in *sn-4* due to an aberrant peak at ZT20. However, as only one replicate was examined, this cannot be determined as real or technical problem. Other replicates need to be examined before any definitive conclusion can be drawn. As shown in Chapter 3, the diurnal expression rhythm of *PsELF3* is not very clear in the NGB5839 background nor indeed, in Arabidopsis. Overall *ELF3* expression was unclear in the *sn* mutant as well. The expression of *MYB2* in *sn* mutant is higher at most of the time points especially during day-time, but again, the result for *ELF3* and *MYB2* should be confirmed by further replication.

Under LD, effect of *sn* on *TOC1*, *ELF4*, *LATE1*, and *PRR59* diurnal rhythms were similar to those seen under SD (Figure 5.4B). However, a smaller phase advance was suggested for *ELF4* (approximate 2h compared to 4h in SD). In contrast to SD, *PRR37* expression in *sn* had similar peak level to WT but slightly higher trough level at ZT0, ZT24, and ZT48. No clear rhythm for *ELF3* was seen in either *sn* or WT. Lastly,

MYB2 was much more highly expressed in *sn* than WT in LD, or compared to *sn* in SD.

In summary, the *sn* mutant affects the diurnal expression rhythms of all the circadian clock gene homologs examined under both LD and SD conditions with possible exception of *PRR37* in LD. The results of *PRR37*, *PRR59*, *ELF3*, and *MYB2* will need to be confirmed in the other two replicates.

5.3.4. SN affect rhythms of clock gene expression in constant darkness

A critical property of circadian rhythms is their persistence in the absence of external cues, so we next examined circadian rhythms in *sn-4*. In Arabidopsis, circadian rhythms are commonly examined under constant light (LL) but in pea, circadian clock genes show weaker and/or damped expression rhythms under these conditions (Chapter 4). We therefore restricted our examination to follow the expression rhythms of clock genes in *sn-4* after transfer from entraining conditions to constant dark (DD).

As shown in Chapter 4, *MYB1* expression in WT persists under DD condition with an approximately 24h period but with reduced amplitude. In the *sn* mutant, *MYB1* expression is slightly decreased in DD and shows a shorter period, with successive peaks occurring at ZT42 and ZT60 compared to ZT45 and ZT69 in WT. The *TOC1* and *ELF4* expression rhythms in the WT are damped low in DD relative to the entraining cycle (approximate 75% and 87% respectively). The *sn* mutant slightly reduced the expression level of both genes during peak phase under DD, but with clearer peaks than WT for TOC1 (at ZT30 and ZT54) and a early peak of approximate 3-6h in *ELF4* (from ZT39 to ZT33/36 and from ZT60 to ZT54). The elevated trough expression of *LATE1* seen in *sn* mutant under diurnal cycles was also seen in DD. Despite an increased variability in the DD cycles (that might caused by technical issue) making successive circadian peaks more ambiguous for other genes, the *LATE1* expression peaks early at

approximately at ZT30 and ZT48 in *sn* mutant when compared with ZT33 and ZT54 in wild type (Figure 5.5).

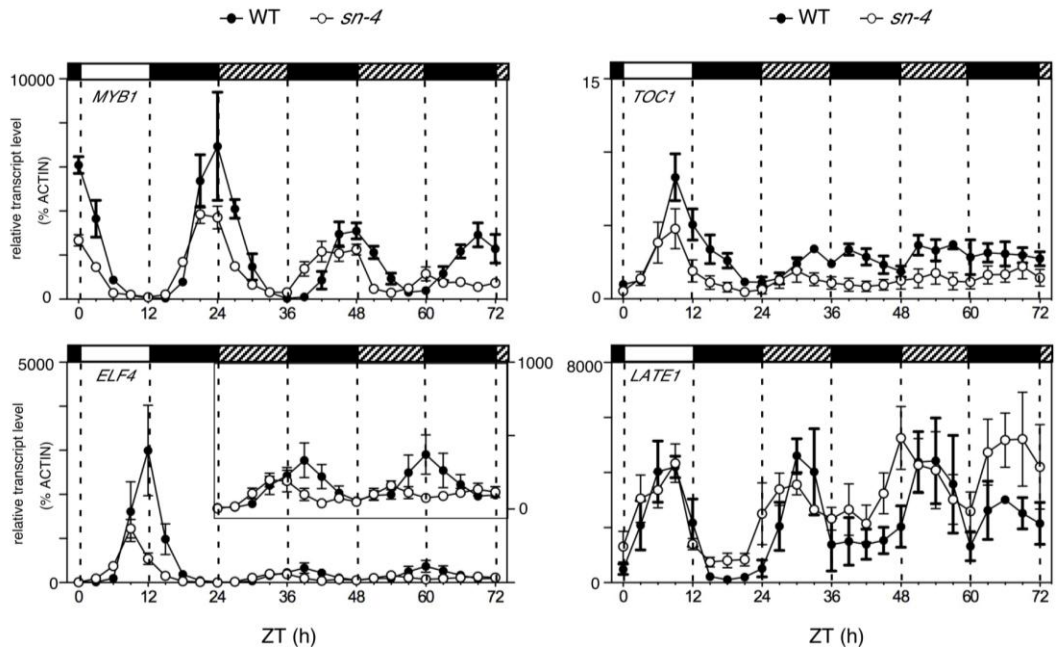

Figure 5.5 *SN* affect circadian rhythms of clock gene homologs in DD. Plants were grown in growth cabinets under a light/dark cycle (12L:12D) at 20°C for 3 weeks before transfer to continuous darkness. Data are mean± SE for n = 2 to 3 biological replicates, each consisting of pooled material from two plants. Zeitgeber time (ZT) refers to the time since lights-on of the last full entraining cycle. Bars above the graph refer to periods of light (open bars) or darkness (closed or hatched bars). The hatched bars indicate the periods of subjective day during the period of continuous darkness.

5.3.5. Comparative mapping provides a refined map position for SN

The *sn* mutation not only affects clock-regulated traits such as flowering and stem elongation but also the diurnal and circadian rhythms of clock genes, further strengthening the hypothesis that *SN* might correspond to a circadian clock gene. I next attempted to narrow down the range of potential circadian clock candidate genes by using genome information from Medicago and a comparative mapping approach.

Initial reports suggested *SN* was linked to amylase locus (*Amy1*) (Weeden et al., 1988) and *SN* was subsequently located between two isozyme loci *Aldo* and *Gal2* (Murfet and Sherriff, 1996) close to a RAPD marker A17_1700 (Laucou et al., 1998) at

the bottom of the chromosome VII of pea. To further define the map position of *SN* locus and locate it on a comparative pea and Medicago map, a new F_2 mapping population was generated from a cross between *sn-4* (Torsdag) and Terese. Figure 5.6 shows the node of flower initiation (NFI) in the F_2 population grown under SD segregated in an approximate 1: 3 ratio (21 early: 59 late), indicating that mutant segregants could be clearly distinguished.

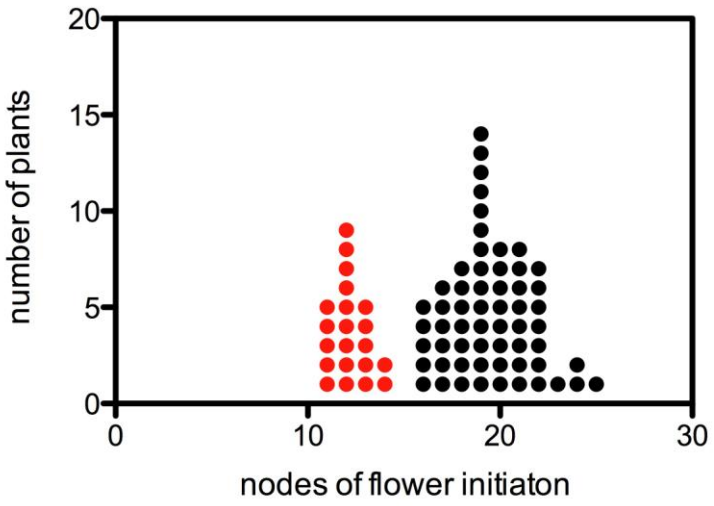

Figure 5.6 Segregation of node of flower initiation (NFI) in the F_2 population of *sn-4* (Torsdag) x Terese under SD. The early segregants (red symbols): late segregants (black symbols) ratio is approximate 1:3.

As mentioned in Chapter 3, LG VII of pea is syntenic with Chromosome 4 in Medicago (Choi et al., 2004; Kalo et al., 2004), producing a basis for improving the *SN* map position by (1) designing new markers and (2) locating possible positional candidate genes. First of all, BLAST searches were done against Medicago genome database to locate putative Medicago homologs of all the existing markers including isozyme markers previously used in *SN* mapping (Weeden et al., 1988; Murfet and Sherriff, 1996) and gene-based markers from Torsdag x Terese RILs (Aubert et al., 2006). Although clear Medicago orthologs could not be determined for *Amy1* and *Gal2*

sequences, other putative Medicago orthologs of existing gene-based markers (around region of *SN*) in Torsdag x Terese mapping population including *Acetisom, Aldo, Sym29, Clpser, Sod9*, and *Pip2* (Aubert et al., 2006) were identified from the BLAST searches (Table 5.1) and confirmed to be in the syntenic region of Medicago Chromosome 4. Based on the information provided in the Medicago Genome build Mt 3.0, the region (from *Acetisom* to *Sod9*) is estimated to be around 10Mb but contains several gaps where adjacent BAC contigs are not yet joined. By mapping these markers relative to *SN* locus, *SN* was found to be located between *Clpser* and *Pip2*. Due to the lack of markers to further refine map position for *SN*, the information from Medicago physical map was used as a basis for the design of additional markers. This involved identifying both additional flowering-related genes and single copy genes from each BAC contig within the 10Mb region in Medicago Chromosome 4. Using this approach, several genes were identified and targeted for further isolation including *Hua2*, *Pcfs4, Vrn1, Fpa, U131248, Lux, Ivdh, Toe1*, *PRR37, Phot2*, and *1voc* (Table 5.1, highlighted in colour). Amongst them, *LUX* and *PRR37* were already isolated in pea as circadian gene homologs and suggested to be potential candidates for *SN* (Chapter 3). A few others are genes involved in flowering, light response or circadian clock not yet isolated in pea; including *HUA2* (Chen and Meyerowitz, 1999; Doyle et al., 2005; Wang et al., 2007), *PCFS4* (Xing et al., 2008), *TOE1* (Aukerman and Sakai, 2003), and *PHOT* (Kinoshita et al., 2001).

Table 5.1 The relevant flowering genes on Medicago Chromosome 4 based on Mt 3.0 genome build. Data included bac accession, gene calls, and physical map position. New possible markers for *SN* mapping are highlighted in colour. The gene have not yet been isolated in pea are highlighted in green and clock gene have been isolated in Chapter 3 are highlighted in red. The approximate location of *SN* locus is indicated as region within the dashed lines.

Gene	Bac accession	genecall	map position (mbp)
ACETISOM	AC135231	4g109610	24.6
HUA2	AC146777	4g101070	21.7
PCFS4	AC121235	4g098610	21.3
ALDO	AC174316	4g097260	20.8
SYM29	AC121244	4g096400	20.3
CLPSER	AC225505	4g095340	19.8
VRN1	AC137825	4g092810	19.5
FPA	AC225496	4g092490	19.3
U131248	AC131248	4g089720	18.8
LUX	AC202498	4g084460	17.8
PIP2	AC229715	4g081730	17.2
IVDH	AC152176	4g080840	16.7
TOE1	AC145164	4g080040	16.3
PRR37	AC149306	4g079920	16.2
PHOT2	AC148218	4g079760	16.1
1VOC	AC202518	4g078800	15.5
SOD9	AC126007	4g076170	15.1

In order to refine the comparative map around *SN* region, the sequences of the additional markers (Table 5.1, highlighted in green) were blasted back to Arabidopsis genome database to identify the Arabidopsis homologs and the conserved regions between Arabidopsis and Medicago sequences. Putative intron-spanning primers were then designed on the Medicago sequences to maximize the chance of discovering polymorphism. Primers used to amplify pea sequences and where polymorphism identified between mapping parents (Table 3.3), markers were designed following the procedure outlined in Section 2.9 and Section 3.2.4.

Markers developed using this approach are summarised in Appendix 1. They included four markers (*Hua2*, *Toe*, *U131248*, and *Phot1b*) in Torsdag x Terese that allowed direct linkage analysis relative to *SN* locus in the F_2 mapping population of *sn-4*

(Torsdag) x Terese. For other genes, suitable polymorphisms were not identified between these parents, but polymorphisms in other populations were used to obtain an approximate chromosomal location. The *Ivdh* and *Prr37* genes were thus mapped in JI281 x JI399 and the *Pcfs4* was mapped in JI1794 x Slow. In contrast, *Vrn1*, *Fpa*, *Lux*, and *1Voc* genes could not be mapped in any available population using the initial genomic fragments obtained.

Figure 5.7 shows a comparative map between pea and Medicago for the *SN* region that summarises the mapping results from two mapping populations in pea including both published and newly designed markers. The linkage results in pea are found to be consistent with the Medicago physical map in most cases with the exception that rearrangement was found for an interval containing *Sod9*, *Toe*, *Phot1b*, and *Pip2* markers. This could reflect an actual difference between two species but could also be explained by incorrect orientation of BAC contigs within the incomplete Medicago physical map in this region. In addition, for two markers (*Pcfs4* and *U131248*), the positions in pea are entirely inconsistent with the locations expected from position in Medicago, as neither of them is linked to the *SN* region. The position of *U131248* is not known but *Pcfs4* is mapped near the top of pea linkage group VI. This inconsistency could be due to small rearrangements between pea and Medicago but could also be explained if more than one ortholog of these two genes exists in the pea genome.

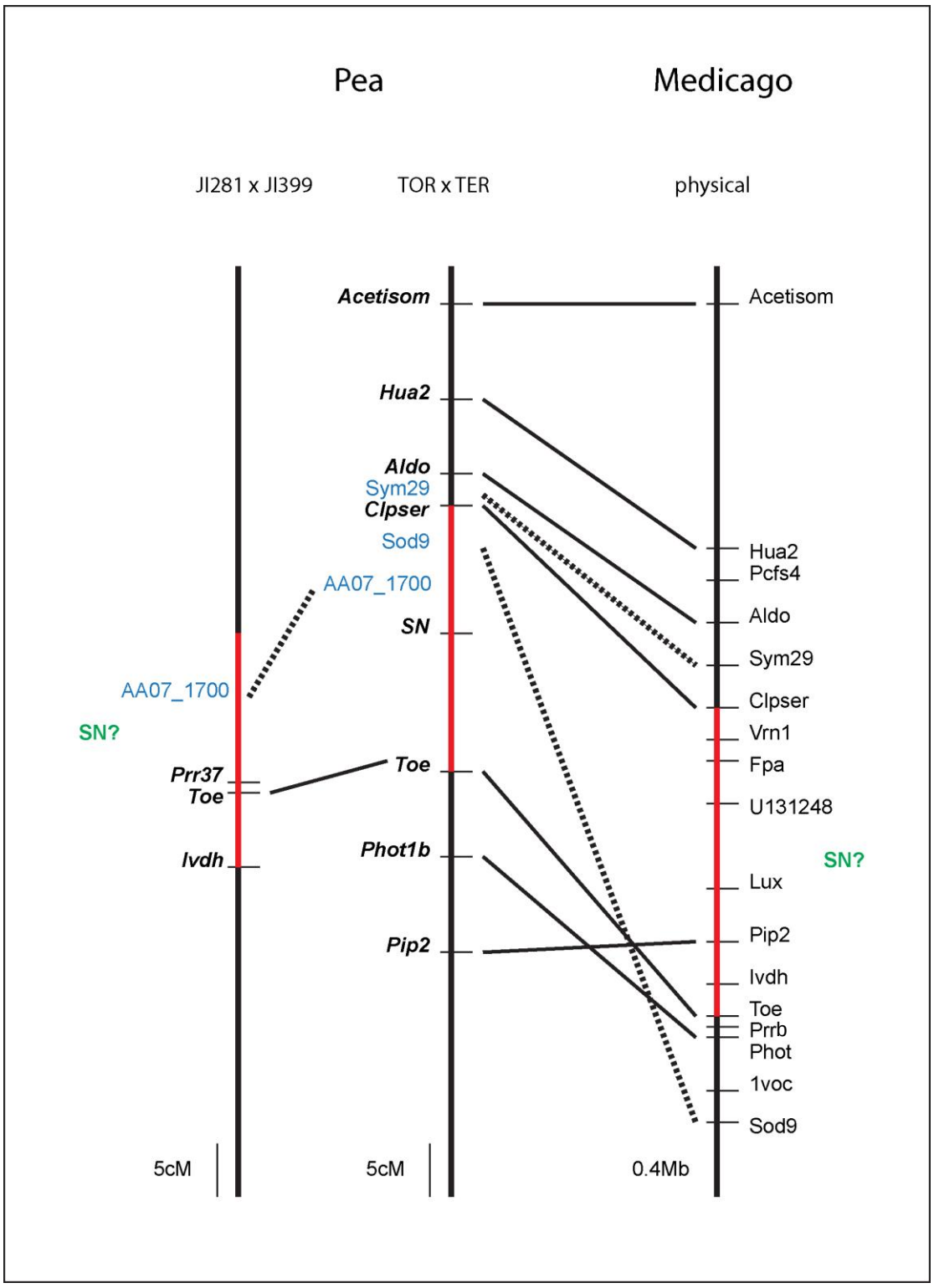

Figure 5.7 Comparative map between linkage group VII in pea and Chromosome 4 in Medicago based on Mt 3.0 genome build. Markers mapped in this study are indicated in bold and italics, markers that are published in previous study are highlighted in blue colour (Laucou et al., 1998; Aubert et al., 2006). Orthologous genes are joined together by solid lines (markers used in this study) or dashed line (previous markers). The regions in the map which is highlighted in red are the approximate region where *SN* is located.

By mapping molecular markers relative to *SN* in *sn-4* x Terese mapping population, the location of *SN* was narrowed to a region between *Clpser* and *Toe* which is correspond to approximate 3.5Mb in Medicago genome. The mapping results also ruled out *TOE*, *PHOT1b*, and *HUA2* as possible candidate genes for *SN* due to presence of recombinants between the two loci. The common marker *Toe* in the two mapping populations, together with two additional markers *Prr37* and *Ivdh* were mapped in JI281 x JI399 population next to the RAPD marker AA07_1700 which was previously mapped close to *SN* (Laucou et al., 1998). This result places *PRR37* next to *Toe* within the region where *SN* is located although the physical map of its Medicago ortholog, *MtPRRb* is in between *Toe* and *Phot* in Medicago. Surprisingly, no polymorphism was found for *LUX* even though it contains a relatively large intron (1109bp) in the 3'UTR (Figure 3.7). However, its Medicago ortholog is located between *Clpser* and *Toe* providing further support that it could be potential candidate gene for *SN*.

5.3.6. SN is the pea ortholog of Arabidopsis LUX

From the comparative mapping approach, *PRR37* and *LUX* were both suggested to be positional candidate genes for *SN* locus. In addition to the map positions, *PRR37* and *LUX* are both known to affect flowering and circadian rhythms in Arabidopsis (Matsushika et al., 2000; Onai and Ishiura, 2005). In Arabidopsis, *LUX* delays flowering (like *SN* in pea) (Hazen et al., 2005; Onai and Ishiura, 2005) whereas *PRR3* and *PRR7* promote flowering (Murakami et al., 2004; Matsushika et al., 2007) suggesting *LUX* is a more likely functional candidate for *SN*. Nevertheless, given uncertainty of mapping and functional comparisons, the entire coding region of both genes in *sn* mutants was therefore sequenced. Sequencing of entire coding region of *PsPRR37* in three induced *sn* mutants (*sn-2* to *sn-4*) did not identify any difference from

their isogenic WT line Borek (*sn-2*) and NGB5839 (*sn-3* and *sn-4*) respectively.

The full coding sequence of *LUX* was also determined from the four known *sn* mutants (*sn-1* to *sn-4*) and in the case of the *sn-2* to *sn-4* mutants, from their isogenic wild-type lines. Both *sn-1* and *sn-2* mutants were discovered to carry small deletions while a single base substitution was found in *sn-4* mutant. The deletion of 10bp (from nucleotides 364-373) in *sn-1* mutation is predicted to cause the addition of one nonsense amino acid after Arg-121 followed immediately by premature stop codon (Figure 5.8A). Although there is no clear WT for *sn-1* to compare with, the fact that this deletion was the only difference observed between *sn-1* and the two WT (NGB5839 and Borek) suggesting the deletion is probably the only significant change. A different deletion of 8bp was found in *sn-2*, causing a frameshift after Lys-108 and predicted to introduce a premature stop codon after 10 nonsense amino acids (Figure 5.8A). The single base substitution in *sn-4* mutant is predicted to replace Trp-15 (TGG) with a stop codon (TAG) thus eliminating most of the *LUX* coding sequence (Figure 5.8A). In the case of *sn-3*, the *LUX* cDNA sequence was found to be identical to WT (NGB5839) in the coding region and in the 500bp 3'UTR. It is still possible that mutation might exist in either the 5' UTR or the promoter region, and might possibly affect a functional element such as the evening element that is present in the promoter of the Arabidopsis *LUX* gene. This element is also present in *TOC1* and is believed to be bound by *CCA1*/*LHY* to regulate *TOC1* expression. Alignment of LUX amino acid sequences revealed a highly conserved GARP or MYB-DNA binding domain in the central region of the protein; a domain commonly found in plant transcription factors (Figure 5.8B). As showed in Figure 5.8A and B, all three *sn* mutations are predicted result in truncated proteins without the conserved GARP domain, and are therefore likely to result in loss of LUX protein function and thus suggesting *SN* is the likely ortholog of Arabidopsis *LUX*.

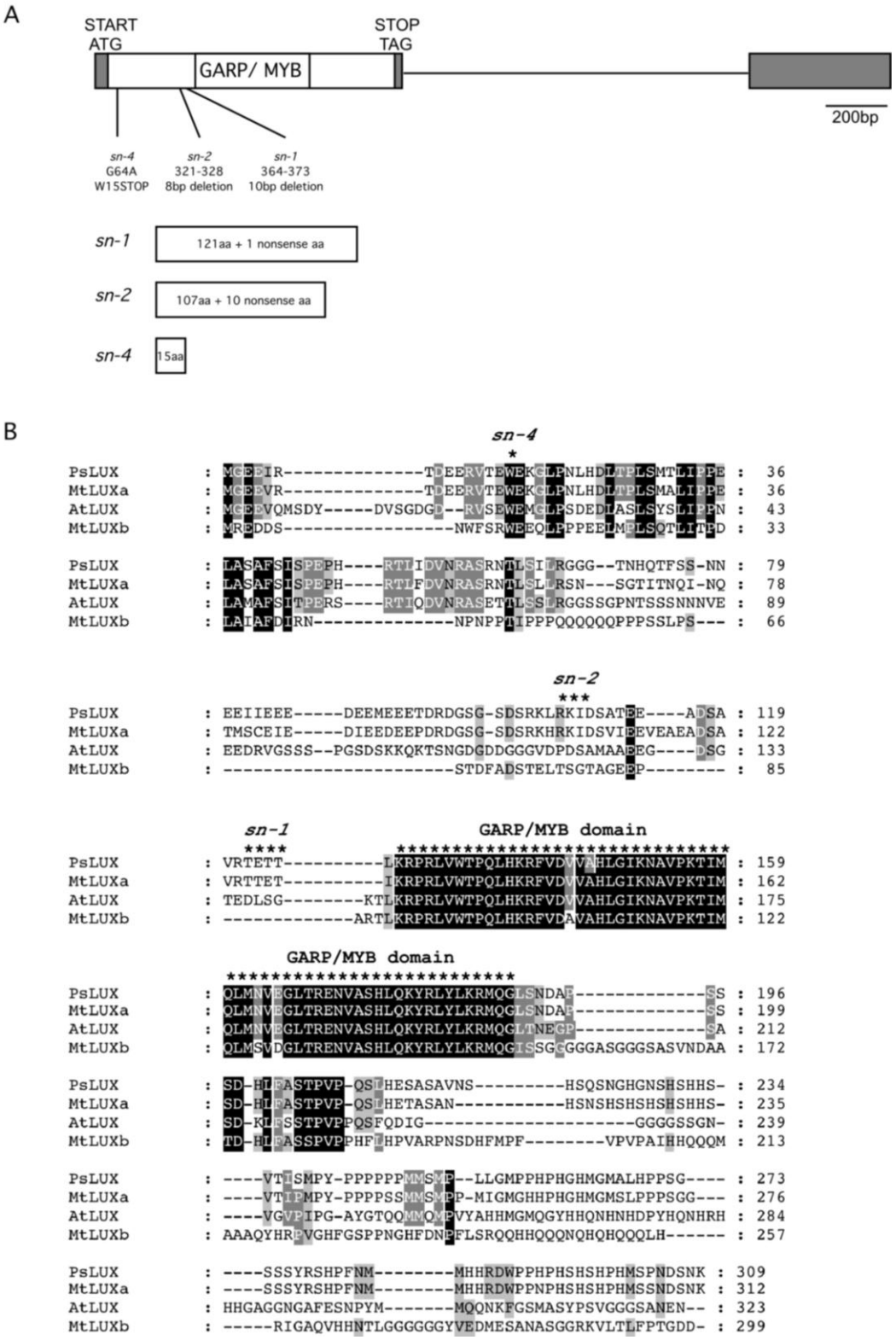

Figure 5.8 Molecular characterization of *SN* locus. (A) Diagram of the *SN* gDNA showing the location and nature of mutations in *sn-1*, *sn-2*, and *sn-4* mutants and also the predicted proteins of each mutation. Intron positions are marked by straight line. (B) Amino acid sequence alignment of LUX proteins in pea, Arabidopsis, and Medicago aligned by ClustalX. Genedoc was used to shade the residues in the following manner: dark =100%, gray =75%, light gray=50% and white <50% identity. All accessions number can be found in Figure 3.7.

In order to test co-segregation of the *LUX* mutation and *sn* phenotype, the *sn-4* mutation was genotyped in the existing *sn-4* x Terese mapping population. The *sn-4* mutation did not create a convenient CAPs or dCAPs marker so High Resolution Melt (HRM) analysis was used as an alternative. HRM analysis is a relatively new technique for the detection of polymorphism in double-stranded DNA samples based on the temperature required for separation of the two strands, and is a cost-effective method for detecting SNP in small-scale genotyping exercises. WT, artificial heterozygote and *sn-4* mutant samples were first tested and found to produce distinct melt curves differing by 0.2°C, with wild type at 84.6°C, heterozygote at 84.4°C, and *sn-4* mutant at 84.2°C (Figure 5.9). They were included in subsequent runs as positive controls and samples from the population were found to separate into distinct groups with the corresponding positive controls. Based on this analysis, the *sn* allele was found to segregate in approximate 1: 2: 1 ratio (18 WT: 41 Heterozygous: 21 mutants) in the *sn-4* x Terese mapping population and to co-segregate perfectly with the early-flowering phenotype (Figure 5.6).

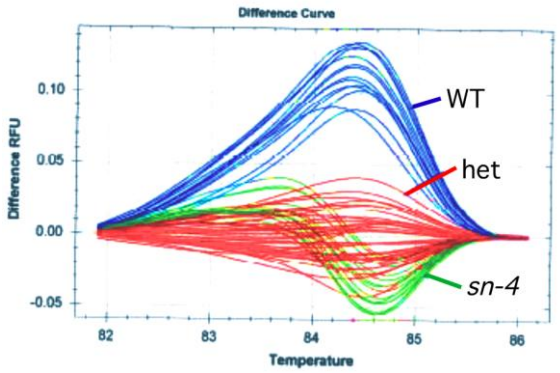

Figure 5.9 Melt curve of HRM analysis in the *sn-4* x Terese population. Samples are separated into distinct groups with the positive controls based on the melting temperature: WT (blue), heterozygous (red), *sn-4* (green).

5.3.7. SN regulation of the CO- and FT-like genes expression

In Arabidopsis, photoperiod or clock mutants were found to have altered level of *CO* and *FT* expression where late-flowering mutants always associated with reduction in *CO* and *FT* expression and early-flowering mutants have elevated *CO* and *FT* expression. However, as described elsewhere, *COLa*, the closest pea homolog to Arabidopsis *CO*, showed no difference in diurnal expression pattern in either the *late1* (late-flowering) (Hecht et al., 2007) or *dne* (early-flowering) mutants (Chapter 4). Figure 5.10 shows that there was also no significant difference in the expression of *COLa* between *sn-4* mutant and WT under SD conditions. The *COLb* gene, which is most similar to Arabidopsis *COL3* and *COL4* (Hecht et al., 2005; Hecht et al., 2007) also showed no significant difference in expression level between *sn-4* and WT. These results are similar to those found for the *dne* mutant (Figure 4.9).

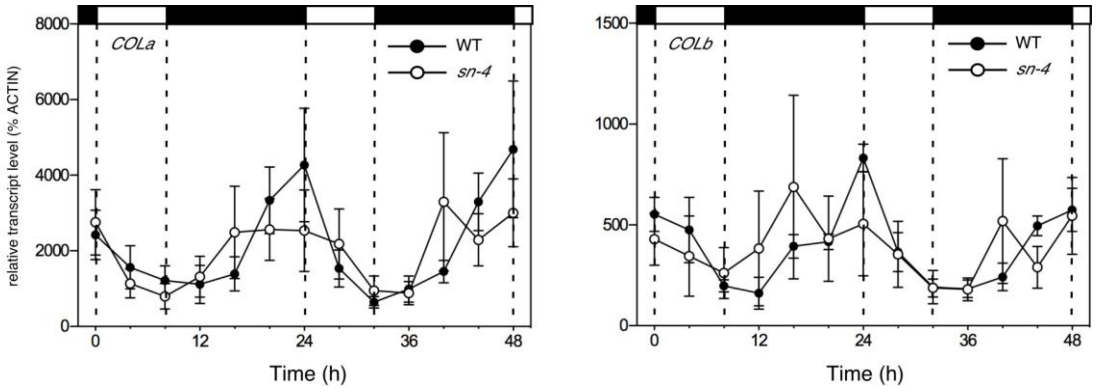

Figure 5.10 *SN* affects diurnal rhythms of *CO* homologs under SD conditions (8-h photoperiod). All plants were grown for 21 d from sowing at 20°C before harvesting commenced. Data are mean ± SE for n = 3 biological replicates, each consisting of pooled material from two plants. Day and night periods are indicated by open and closed bars, respectively, above the graph.

As discussed in Chapter 4, the *dne* mutant is a null mutant for *PsELF4*. The early-flowering phenotype of *dne* is reflected in early induction of the inflorescence identity gene, *PIM* (the pea ortholog of Arabidopsis *AP1*). This earlier expression of *PIM* appears to be associated with elevated expression of several pea *FT* orthologs. We also examined *FT* expression in the *sn-4* mutant which as shown above is a probable null mutant for *PsLUX*. Similar results are expected in *sn* mutant since the *sn* mutation cause early-flowering through the circadian clock as well. Figure 5.11A and 5.11B show the expression of pea *FT* orthologs in leaf and apex respectively of *sn-4* and WT. The appearance of flower buds in the *sn* mutant at day 24 is associated with high expression of *PIM* in the apex whereas *PIM* transcripts stay low in the wild-type plants which have not yet committed to flowering by day 24. This earlier induction of *PIM* in *sn* mutant is associated with dramatically elevated expression of *FTa1* and *FTa2* in both leaf and apex, *FTc* in apex, and *FTb2* in the leaf (Figure 5.11). Similar to *dne* mutant, the *FTb1* transcripts do not show any significant differences between *sn* mutants and wild-type plants. Nonetheless, all the results are based on single replicate, and a second replicate should be examined in order to confirm this conclusion.

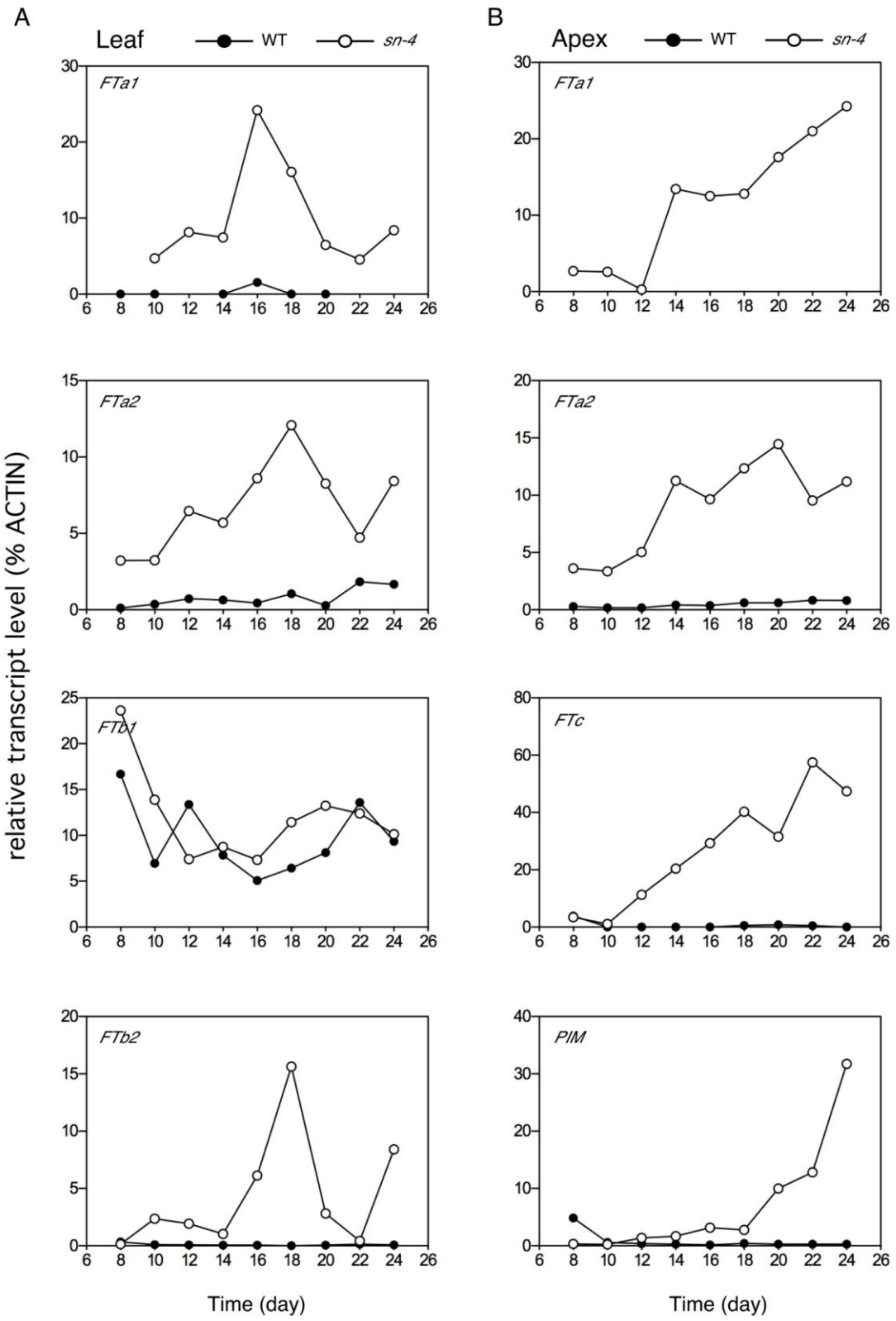

Figure 5.11 Pea *FT-like* and *PIM* gene expression in (A) uppermost leaf (B) shoot apex of *sn-4* and WT plants grown under SD (8h-photoperiod). All plants were grown at 20°C and harvesting commenced at day 8 up to day 24. Data are from 1 biological replicate which consist of pooled material from two plants. FTa1 expression in WT is hardly detected after 50 cycles and the CT (cycle threshold) cannot be determined in some samples as fluorescence did not cross the threshold.

5.3.8. Genetic and physiological interaction of SN, DNE and LATE1 in the control of flowering

As an initial step in understanding how the clock genes, *SN*, *DNE*, and *LATE1* might interact to regulate circadian clock function and flowering, generation of double and triple mutants was undertaken. In particular, in view of the relatively subtle clock defects found in *sn* and *dne* mutants compared to Arabidopsis *lux* and *elf4* mutants, it was of interest to test whether loss of both *SN* and *DNE* might have a stronger effect on either flowering phenotypes or clock gene expression rhythms.

5.3.8.1. *sn dne* double mutant

Since the *dne* and *sn* single mutant are highly similar in flowering phenotype and both single mutants already insensitive to photoperiod, it is difficult to identify double mutant based on phenotypic selection in F_2, particularly as double mutant studies were initiated before the molecular characterization of the *SN* locus.

As an alternative to laborious backcrossing approach, an alternative approach was attempted based on the observation that *sn* mutant appeared to have shorter internode length than *dne* mutant under blue light (Figure 4.11, Figure 5.3A) suggesting that it might be possible to use this characteristic as a selection tool for *sn*. To confirm the internode-length phenotype was a pleiotropic effect of *sn*, internode lengths were recorded on F_2 progeny of a cross between *sn-4* and NGB5839 after growth under blue light for 2 weeks before transfer to SD. Figure 5.12A shows that the shorter internode phenotype co-segregates with the early-flowering phenotype. In the F_2 generation of *sn-4* x *dne-1* cross, plants segregated for flowering time in an approximate 9 (27 late): 7 (17 early) ratio (χ^2=2.12, 0.1<P_{df}=1<0.25), and plants with short internode length in the early-flowering class (Figure 5.12B) were selected, theoretically enriching for

individuals recessive at *SN* locus. These plants were genotyped for *DNE* locus once a marker became available, and the seeds heterozygous plants were grown on to obtain *sn-4 dne-1* double mutant in the F_3 by again genotyping for *DNE* locus. As anticipated, the *sn-4 dne-1* double mutants have the same phenotype as the single mutants, flowering at around node 12 and producing only 2-4 reproductive nodes (Figure 5.12C).

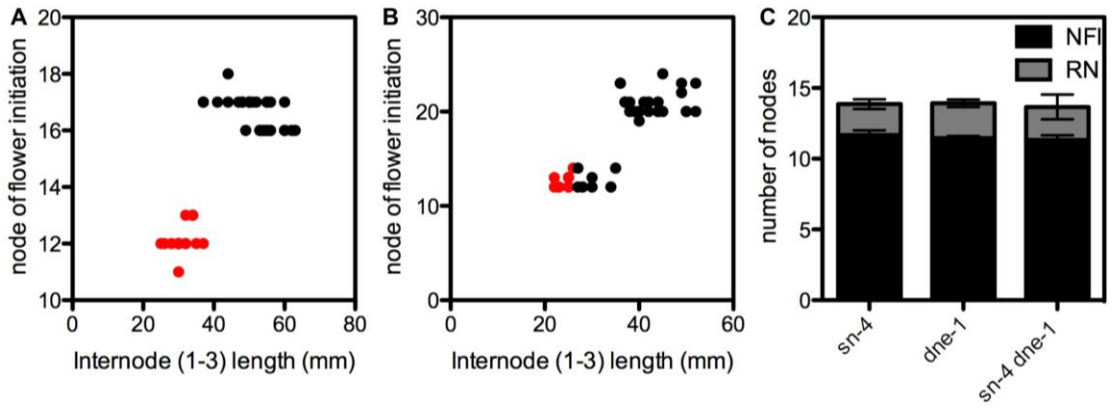

Figure 5.12 The selection of *sn-4 dne-1* double mutant. (A) Cosegregation of early-flowering with shorter internode length (red symbols) in *sn-4* x NGB5839 F_2 population under LD (B) The segregation of node of flowering and interrnode length in F_2 population of *sn-4* x *dne-1* under SD. The putative homozygous *sn* alleles are highlighted in red. (C) Node of flower initiation and number of reproduce nodes of putative *sn-4 dne-1* double mutants. Data are mean ± SE for n = 8 plants.

In addition to flowering phenotype, the diurnal expression of several pea clock gene orthologs was examined in the *sn-4 dne-1* double mutant under 12h SD (Figure 5.13). Due to time constraints, it was only possible to analyse one replicate, but no obvious additional difference was observed in the *sn-4 dne-1* double mutant when compared to either *sn-4* or *dne-1* single mutant. The subtle difference are the early-phased advance of *MYB1* expression and slightly reduced transcript level of *TOC1* in both of the *sn dne* double mutant and *sn* single mutant. Moreover, *ELF4* expression level is lower in *sn dne* double mutant and *dne* single mutant whereas the *GI* expression appeared to be higher at the trough for *sn*, *dne*, and *sn dne* mutants. The flowering and diurnal rhythms of *sn dne* double mutants thus suggest they might act through the same

pathway in regulation of circadian clock and photoperiodic control of flowering.

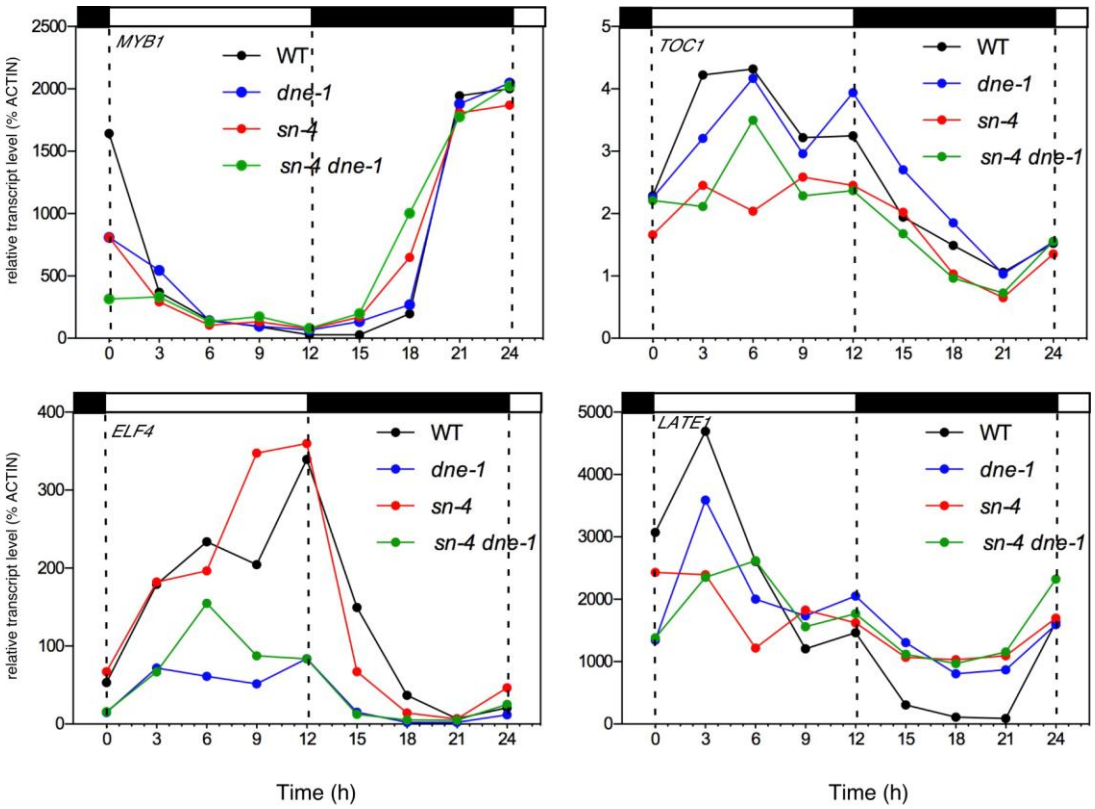

Figure 5.13 The *SN* and *DNE* affect diurnal rhythms of clock gene homologs under light/dark cycles (12L: 12D). All plants were grown for 21 d from sowing at 20°C before harvesting commenced. Data are mean ± SE for n = 1 biological replicates, each consisting of pooled material from two plants. Day and night periods are indicated by open and closed bars, respectively, above the graph.

5.3.8.2. *sn late1 double mutant*

In work described in the previous chapter showed a novel phenotype of *dne late1* which combined features of both monogenic mutants. Flower initiation in *dne late1* occurred as early as *dne* parent but over the next several nodes, flower buds did not develop and plant ultimately produced more reproductive nodes than *dne*, similar to *late1*. A similar phenotype appeared in F_2 of cross *sn-4* x *late1* (Figure 5.14A, B). Early-flowering segregants were grown on from the F_2 to select a pure family with the

novel double mutant phenotype in the F_3. The phenotype suggests *SN* interacts with *LATE1* similarly to *DNE* and therefore emphasises possibility that *DNE* and *SN* might function in the same pathway for flowering time regulation. As both single mutants shown to affect stem elongation, we also examined the interaction of *SN* and *LATE1* in a seedling light experiment. As previously shown (Figure5.3A), the *sn* mutant seedlings had shorter internodes than WT under red (R) or blue (B) lights. Figure 5.14C shows the internode lengths of WT, *late1* and *sn* single mutant, and also the *sn late1* double mutant after grown under R or B for 2 weeks. Under R, the double mutant shows an intermediate phenotype between the two single mutants, suggesting a likely additive effect of *SN* and *LATE1* under R. Under B, the short internode phenotype of *sn* mutant was completely reverted by *late1*, suggesting *LATE1* is largely epistatic to *SN* under B.

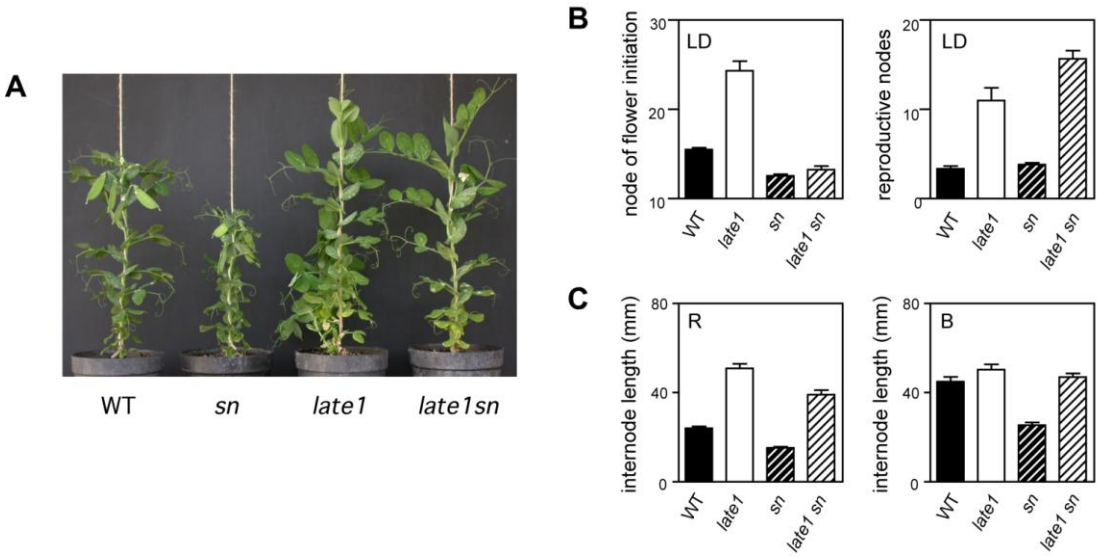

Figure 5.14 Interaction of *LATE1* and *SN* in control of flowering. (A) Representative 8-week-old plants grown under LD. (B) Interaction of *late1-1* and *sn-4* mutations in the control of initiation of flowering and the duration of the reproductive phase under LD conditions. Left, Node of flowering initiation; right, number of reproductive nodes. Plants were grown in the phytotron where they received an 8-h photoperiod of natural daylight extended for 16 h with white fluorescent light (10 mmol m^{-2} s^{-1}). (C) Interaction of *late1-1* and *sn-4* mutations in the control of internode elongation under monochromatic R (left) and B (right). For each data point, n = 8 to 12 and bars represent SE. (B) and (C) are taken from (Hecht et al., 2007)

5.3.8.3. *sn dne late1* triple mutant

As both *dne late1* and *sn late1* show similar flowering phenotypes and *sn dne* did not show additional difference for flowering and diurnal rhythms than either of the single mutant, we also constructed triple mutant, considering the possibility that an additive phenotype might be clearer in the later flowering background of *late1*. The *sn dne late1* triple mutant was generated from a cross of *sn-4 late1-1* and *dne-1 late1-1*. As expected, F_1 were all late flowering like *late1* single mutant. The F_2 showed clear segregation for NFI with bimodal distribution corresponding approximately to a ratio of 9 (26 late): 7 (22 early) although the segregation was not discrete (Figure 5.15A), again suggesting a complementary rather than an additive interaction between *SN* and *DNE* in control of flower initiation. All the early segregants (red symbol) were genotyped for *DNE*. The early segregants with heterozygous alleles at *DNE* locus would have genotype of *snsn DNEdne late1late1* in order to flower early. These plants were grown in the F_3 generation and the triple mutants selected by genotyping for homozygous recessive allele at *DNE* locus. Like *sn late*1 and *dne late 1* double mutants, the *sn dne late1* triple mutants flower early around node 12 to 14 and the first few flower buds never develop into real flowers (Figure 5.15B). In summary, *SN* and *DNE* are largely epistatic to *LATE1* in the regulation of flower initiation whereas *LATE1* acts independently of *SN* and *DNE* to regulate floral development.

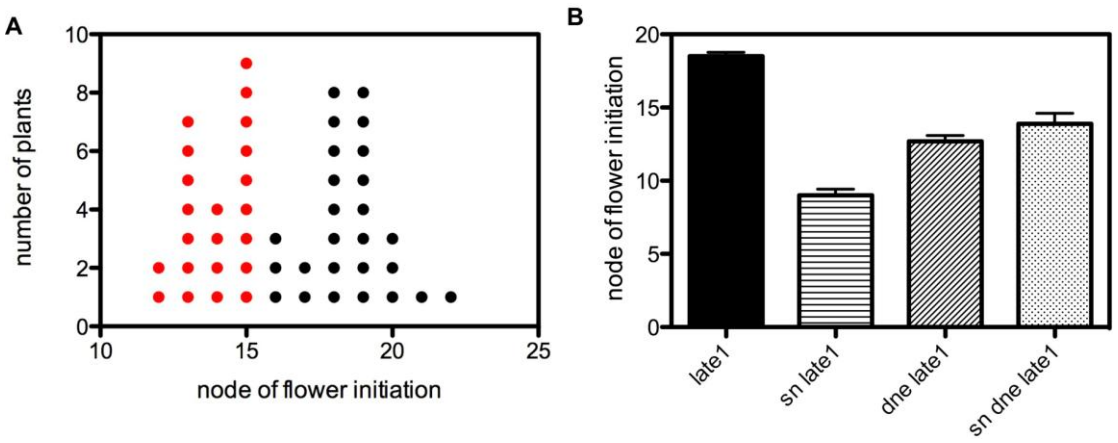

Figure 5.15 The selection of *sn-4 dne-1 late1-1* triple mutant (A) The F_2 generation of (*sn-4 x late1-1*) and (*dne-1 late1-1*) cross. The early (red symbols) and late flowering (black symbols) are in approximate 7: 9 ratio. (B) Node of flower initiation of *sn-4 dne-1 late1-1* triple mutant. Data are mean + SE for n = 8.

5.3.9. Genetic and physiological interaction of SN and HR in the control of flowering

Early studies showed that *sn* is epistatic to *HR* in regulation of flowering because recessive *sn* alleles cause early-flowering in pea regardless of the genotypes at *HR* (Murfet, 1971a, 1973). The fact that our standard WT, NGB5839 like many spring cultivars, carries recessive *hr* alleles (Chapter 7) meant that it has *SN hr* genotype. We re-examined this previous result by re-selecting the *sn-4* mutant (isolated in the NGB5939 *hr* background) onto an *HR* background. Figure 5.16 outlines the approach used to reselect the *sn-4* mutant in *HR* background by crossing *sn-4* mutant (*sn hr*) to *HR* from 5839 x *HR* BC3. In the F_2 of a cross between the *sn-4* mutant (*sn hr*) to an *HR SN* line, an approximate 9 (14 late): 3 (5 WT): 4 (6 early) ratio was seen for segregation of flowering time and the late segregants (*SN/-HR/-*) were selected to grow on for F_3. In F_3, families with early segregants are selected and these segregants thus had genotype of *sn/sn HR/hr* or *sn/sn HR/HR*. Homozygous *HR* plants were then identified using a molecular marker for *HR* (see Chapter 7) and grown on to obtain pure families for further experiments.

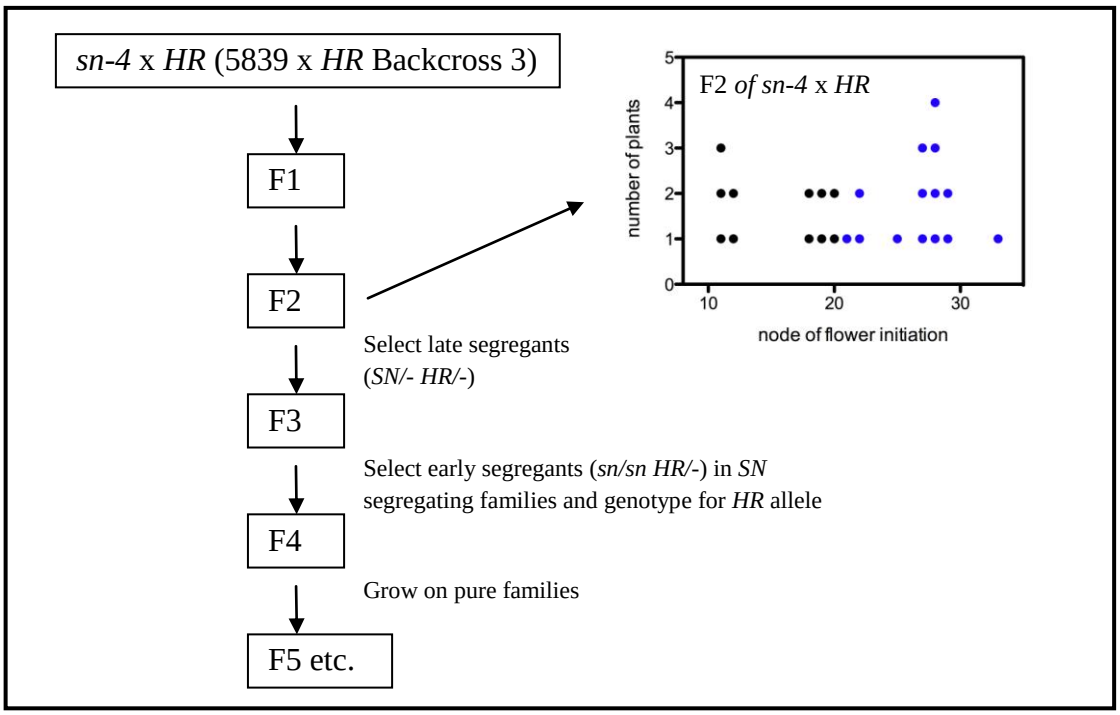

Figure 5.16 A flowchart outlining the re-selection of the *sn* mutant in the *HR* background by crossing *sn-4* mutant with *HR*. The histogram shows the node of flowering initiation segregation of F_2 generation of *sn-4* x *HR* (5839 x *HR* BC3) with late segregants highlighted in blue.

Figure 5.17 shows that plants with *sn HR* and *sn hr* genotypes flower earlier than their near-isogenic wild-type lines regardless of the photoperiod they are grown in (Figure 5.17B, left), consistent with the previous studies with *sn-1* mutant (Murfet, 1973). However when *SN* is dominant, introgression of *HR* alleles cause small delays in flowering node under both SD and LD (Figure 5.17B, left), differ from previous result where *HR* shows stronger delay in SD (30 nodes later) than LD (Reid and Murfet, 1977). In addition to node of flower initiation, *sn* mutation terminates the reproductive growth after 2-5 nodes regardless of *HR* genotypes and photoperiod conditions (Figure 5.15B, right). This is different from results from older studies indicating that *sn HR* plants tend to have prolonged reproductive growth compared to *sn hr* plants (Murfet, 1973). The introgression of *HR*, on the other hand, produce more reproductive nodes than *SN hr* in both SD and LD (Figure 5.17B, right), even *SN hr* produces more reproductive nodes

already in SD than in LD. The difference between this experiment and previous findings could be due to different genetic background or different light quality used for the day extension in LD conditions, as flowering in *HR* lines was previously shown to be affected by light quality of day extensions and night breaks (Reid and Murfet, 1977).

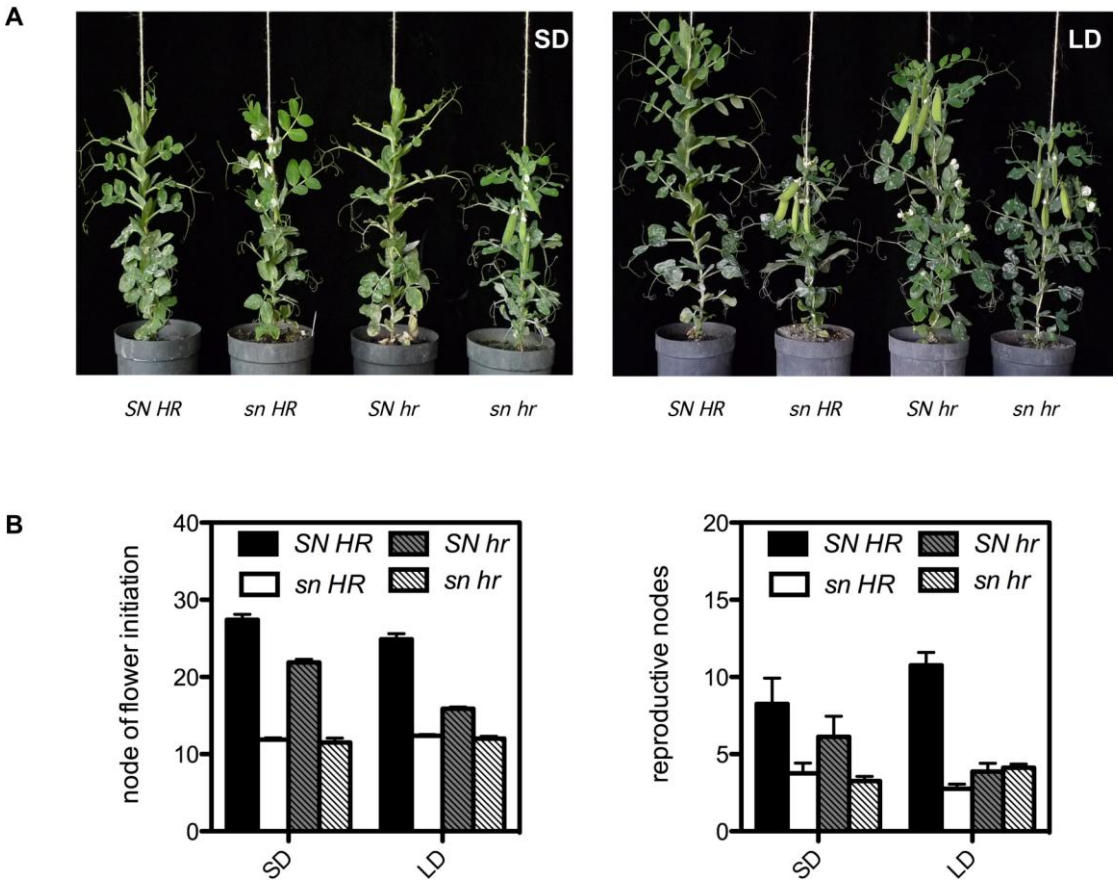

Figure 5.17 The *sn HR* mutant is early flowering and photoperiod-insensitive. (A) Representative of 8-week-old plants of *sn HR* and *sn hr* mutants and their isogenic wild-type *SN HR* and NGB5839 (*SN hr*). (B) Node of flower initiation (left) and final number of reproductive nodes (right). Data are mean ± SE for n = 8 plants. All plants were grown in the phytotron under standard SD or LD conditions.

5.4. Discussion

As one of the first pea photoperiod-responsive loci to be identified, physiological roles of *SN* have been extensively studied over a period of several decades.

The *SN* locus has been shown to influence graft-transmissible signals and was originally proposed to positively regulate a mobile floral inhibitor. However, more recent molecular characterizations of photoperiod loci in several species have showed that these loci are involved in circadian clock and influence on mobile stimulus production. In this chapter, *SN* has been identified to be the pea ortholog of Arabidopsis *LUX* gene and shown to be necessary for regulation of photomorphogenesis, diurnal and circadian rhythms, mobile flowering signals.

5.4.1. Comparative mapping and candidate gene approach in identifying SN as ortholog of Arabidopsis LUX

Among legumes genomes, synteny relationship is closest and best documented for Medicago and pea (Choi et al., 2004; Kalo et al., 2004; Aubert et al., 2006). This has provided an efficient mean for candidate gene isolation and evaluation in pea, as successfully demonstrated for *DNE* locus in Chapter 4.

In this chapter, a similar but more sophisticated approach was utilised to investigate the *SN* locus, in which a more detailed comparative map of Medicago and pea was generated. The genome sequencing project of *Medicago truncatula* has provided well-annotated information for developing of new gene-anchored markers, and we tested this approach by amplifying pea orthologs around the region where *SN* is located. These Medicago primers are more beneficial than degenerate primers in several ways as they are less expensive, more specific in PCR amplification, and more straightforward for optimisation of annealing temperature. However, the limitation of using Medicago primers for pea orthologs isolation is mainly the incomplete status of the Medicago physical map. The latest version (Mt 3.0 pseudomolecule) is not yet complete and there are several gaps between non-overlapping BAC contigs, creating

uncertainty about the position and orientation of some (particularly short) contigs. This could in some cases result in observed apparent differences in the genomic location of pea and Medicago orthologs. In this study, comparative mapping has refined the map in the region of *SN*. The order of pea markers in the linkage group appears to be quite consistent with the Medicago chromosome beside a few exceptions which might be due to the presence of gaps in adjacent BAC contigs in Medicago genome.

Moreover, the comparative map generated can be used as an aid in the selection of candidate genes for *SN* locus so that impossible candidate genes can be ruled out based on their Medicago map position without actually isolating the pea orthologs. Together with phenotypic similarity of loss-of-function mutants in Arabidopsis and pea, the mapping data suggested a positive candidate gene relationship between *LUX* and *SN*. Sequencing of *LUX* gene in *sn* mutants has verified *SN* as pea ortholog of Arabidopsis *LUX* gene and identified 3 different *sn* alleles (Figure 5.8). This suggests comparative mapping as a useful tool for candidate gene approach in mutant loci identification.

5.4.2. Roles of SN in the circadian clock

In this chapter, the circadian rhythms in the putative null *sn-4* mutant were only examined under DD because the rhythms in WT (NGB5839) were previously shown (Chapter 4) to be damped to a low level under LL. Overall, the *sn-4* mutation shows to have relatively subtle effects on both diurnal and circadian rhythms of pea clock orthologs, causing minor alteration to phase or amplitude (Figure 5.4 and 5.5). The subtle nature of the defects is similar to those found in the *elf4* (*dne-1*) mutant in pea (Chapter 4).

As we did not examine circadian rhythm of *sn* mutant under constant light

condition, direct comparison with Arabidopsis *lux* (*pcl*) mutant is difficult. Under LL, Arabidopsis *lux* mutant was found to have low, arrhythmic expression for *CCA1* and *LHY* expression and high, arrhythmic expression for *TOC1*, *ELF4*, *GI*, and its own expression (Onai and Ishiura, 2005). In pea *sn* mutant, higher *GI* gene expression diurnal and circadian rhythms in *sn* mutant are found to be consistent to what has been found in Arabidopsis *lux* mutant (Onai and Ishiura, 2005). However, low expression of *MYB1* (pea ortholog of *CCA1*/*LHY*) is found in *sn* mutant but the rhythm is still clear. For *TOC1* and *ELF4* expression, low expression of *TOC1* and *ELF4* were detected in *sn* mutant but the transcript level of *TOC1* and *ELF4* were found to be low even in the wild type. This makes it hard to compare with Arabidopsis. Furthermore, *PCL-ox* does not seem to affect *TOC1* and *ELF4* expression in Arabidopsis (Onai and Ishiura, 2005). Therefore, it is hard to draw a conclusion of *TOC1*/*ELF4* regulation by *LUX* as it might require other clock component. Likewise, as the ortholog of Arabidopsis *LUX* gene, mutation in *SN* locus does not cause arrhythmia of any clock genes identified so far under constant dark condition. This is different to what has been discovered in *lux* mutant. Therefore, the function of *LUX* gene might not be fully conserved between species. Another possible explanation is the *hr* mutation in the NGB5839 wild-type background blocks the effect of *LUX* on regulation of expression rhythms. It is therefore interesting to examine the circadian rhythm in dominant *HR* lines especially under constant light condition. Moreover, the *sn dne* double mutant, the putative *lux elf4* double mutant, does not show more severe effect on expression rhythms in SD when compare to either of the single mutant. This result is not expected as *LUX* and *ELF4* each seems to play an important role in the circadian clock. The *lux elf4* double mutant has not yet been described in Arabidopsis, and either single mutant alone has already caused more severe effect on SD diurnal expression rhythms. Additionally, the *sn dne*

double mutant could potentially be triple mutant as the NGB5839 (Torsdag) carries recessive *hr* alleles (Chapter 7).

5.4.3. Photomorphogenic effect of SN

To assess the effect of *sn* mutation on photomorphogenesis, the internode length and leaf area were measured in plants exposed to different monochromatic lights. The *sn* mutants have shorter internode length in all the monochromatic light conditions examined but not in darkness, indicating that *sn* mutants are hypersensitive to red, far-red, and blue lights during the seedlings de-etiolation process (Figure 5.3). These results are consistent in two of the mutant alleles with different wild-type background. In comparison with the shorter internode length in pea *sn* mutants, *lux* mutants have long hypocotyl under light/dark cycle but not under constant dark or light condition (Hazen et al., 2005). However, the regulation of *SN* on leaf expansion is unclear since different results are obtained from mutant alleles with different wild-type background. Other than that, the obvious difference in stem elongation and leaf expansion are observed in blue light. The effects of de-etiolation by *sn* mutation are totally blocked by *late1* mutation in blue monochromatic light where the *sn late1* mutant showed the exactly same phenotype on internode length as the *late1* single mutant. This implies *LATE1* is epistatic to *SN* in the de-etiolation pathway under blue light but there is no evidence to prove this regulation is directly acting through circadian clock or not. In *Arabidopsis*, circadian clock have been proposed to involve in "gating" of the light signal transduction pathway to regulate hypocotyls growth. When the gate is closed, the light signaling pathways are inhibited, even in the presence of light. This repression leads to the growth of hypocotyls. When the gate is open, the clock allows the light input signals, inhibiting hypocotyl elongation (Dowson-Day and Millar, 1999; Más,

2005). This implies *SN* and *LATE1* might involved in blue light perception or signalling pathways or even specifically involved in circadian gating of blue light.

5.4.4. Effect of SN in flowering output pathway and the interaction with DNE and LATE1

As discussed in the first chapter, *SN*, *DNE*, and *PPD* are proposed to involve in the production of floral inhibitor in pea. This hypothesis was ruled out by grafting experiments using leafy-stock (Chapter 4) and the discovery of *FT* as mobile stimulus in several species (Faure et al., 2007; Jaeger and Wigge, 2007; Igasaki et al., 2008; Hou and Yang, 2009; Wang et al., 2009; Kong et al., 2010). *FT* is known to be mainly regulated by photoperiod pathway through *CO* and *CO* expression is monitored by circadian clock. Correlation between early-flowering time and earlier induction of several *FT* orthologs in *sn* mutant has highlighted the fact that *SN* is involved in clock regulation of production of mobile stimulus in pea. It is possible that intermediate levels of these *FT* orthologs decide the flowering time in pea or they have different roles in flowering time regulation. However, as mentioned before, no effect on expression rhythms of the two closest pea homologs of *CO* were detected in either the early-flowering mutant (*dne*) (Chapter 4) or late-flowering mutant (*late1*) (Hecht et al., 2007). This is also the case in the early-flowering *sn* mutant (Figure 5.11), further emphasizing that *CO* function may not be directly comparable in pea. One possibility is that other more distantly-related CO-like genes may still have CO-like function or alternatively, some other unrelated gene may play the role of *CO* in *FT* induction. A third possibility is that *FT-like* genes in pea can be directly regulated by circadian clock through *CO* independent pathway such as *GI*-regulated miR172 is found to promote flowering by upregulating *FT* expression even in the absence of functional *CO* (Jung et

al., 2007).

In addition to the effect of *SN* alone, double and triple mutants were generated to examine the interaction between *SN* and *DNE*/*LATE1* in the control of flowering time. The *sn late1* double mutant is early-flowering with the first few flower buds never develop into real flower and increased reproductive nodes. The phenotype of *sn late1* double mutant is similar to *dne late1* double mutant in which *LATE1* is epistatic to *DNE* and *SN* in reproductive node production and responsiveness to light during seedling de-etiolation. However, the same early flower initiation was seen in the *sn late1* and *dne late1* double mutant as in the *sn* or *dne* single mutant but the first few flowers never develop into real flowers. This suggests that although *DNE* /*SN* and *LATE1* all act in circadian clock they might differentially regulate *FT*-like gene family members with different roles in the flowering process although. This scenario would be somewhat different from Arabidopsis where clock genes act together to regulate *FT*. On the other hand, the *sn dne* double mutant are identical to either of the single mutants in LD or SD photoperiods. Therefore, *SN* and *DNE* are likely to function in the same pathway to regulate flowering. The phenotype of the *sn dne late1* triple mutant is found to be similar to *sn late1* and *dne late1* double mutants. This further reinforces the idea that *SN* and *DNE* work in the same pathway in circadian clock to regulate flower initiation and *LATE1* acts epistatically to *SN* and *DNE* to control general photoperiod responsiveness. It will therefore be interesting to examine *FT*-like gene expression in the double and triple mutants in order to understand how *SN*, *DNE*, and *LATE1* can act together to regulate circadian clock gene expression and photomorphogenesis but act independently on flower initiation. In a practical approach, it is worthwhile to examine the distribution of *sn* alleles in commercial lines and natural population in order to examine its correlation with flowering time and other photoperiod responsiveness traits.

Chapter 6 Characterization of the flowering locus *PHOTOPERIOD* (*PPD*)

6.1. Introduction

Like the previously described *dne* and *sn* mutants, mutants at the *PHOTOPERIOD* (*PPD*) locus have an early-flowering, photoperiod insensitive phenotype. The similarity of these mutant phenotypes also implies that the normal photoperiod response in pea requires the presence of all three genes *SN*, *DNE*, and *PPD* which act together in a complementary manner. In light of the identification of *SN* and *DNE* as orthologs of Arabidopsis *LUX* and *ELF4* respectively, it is likely that *PPD* is also involved in the circadian clock. This is supported by preliminary data suggesting that diurnal rhythms of *CAB9* and *ELF4* expression are defective in a *ppd* mutant (Jones, 2004).

Two induced mutants (*ppd-1* and *ppd-2*) derived from cv. Borek by gamma radiation have been described previously (Arumingtyas and Murfet, 1994; Taylor and Murfet, 1996). A third mutant (*ppd-3*) was generated more recently in the NGB5839 genetic background by EMS mutagenesis, conveniently allowing comparison of all three mutants in same background. ((Jones, 2004), J. Weller, unpublished). While there is little different in phenotype between *sn*, *dne,* and *ppd* mutants, one distinct characteristic of the ppd mutants is their disturbed segregation. The segregation of *ppd-2* alleles was found to be disturbed in a segregating population in which the proportion of mutant segregates was 25% less than expected. Test crosses between heterozygous plants and either the male or female parent suggested there is a male

gametic selection against the *ppd-2* allele (Murfet and Taylor, 1999). This implies *PPD* might also affect pollen viability or growth.

PPD has been mapped to the top of pea linkage group II (LG II). Linkage was initially detected between *PPD* and *A* (anthocyanin production) (Arumingtyas and Murfet, 1994), and the map position of *PPD* was later refined to a region of LG II between a branching gene *RMS3* (*RAMOSUS 3*) and the isozyme locus *Aatp* (*aspartate aminotransferase*) (Murfet and Taylor, 1999).

The main aim of this chapter is to further characterise the *ppd* mutants and identify potential candidate genes for the *PPD* locus. Detailed characterization of *ppd* mutants will be carried out on flowering, diurnal expression rhythms, and circadian rhythms. Since no clear candidate flowering gene homolog was identified for *PPD* in the initial isolation and mapping of clock-related gene in Chapter 3, the map position of *PPD* was further investigated to refine the map position as an aid to future positional and candidate genes approaches.

6.2. Materials and methods

6.2.1. Gene expression experiments

For the diurnal expression experiments, all plants were grown for 3 weeks from sowing at 20°C in growth cabinets under either LD (16-h photoperiod) or SD (8-h photoperiod). Harvested material consisted of entire shoot apex and including uppermost expanded leaf from two plants. Samples were harvested at 4h intervals, with 3 replicates per time point. Samples were harvested and processed by V. Hecht and K. Claire. Several real-time PCR runs were done with assistance of V. Hecht.

For circadian expression experiments, all plants were grown in growth cabinets under a light/dark cycle (12L: 12D) at 20°C for 3 weeks before transfer to

continuous darkness at ZT36 (DD). Harvested material consisted of a single leaflet from the uppermost fully expanded leaf from two plants. Samples were harvested at 3h intervals, with 2 to 3 replicates per time point.

For developmental timecourse experiment, plants were grown in growth cabinets under SD condition (8L: 16D) at 20°C. Leaf and apical bud samples were harvested separately from each plant at 2-day interval from day 8 to day 24. Samples were harvested at the same time during the day for each time point approximately 4 hours after light on. Leaf material consisted of single leaflet from the uppermost fully expanded leaf from two plants. Apical bud material consisted of dissected apical buds from two plants to 2-mm in length. 3 replicates were harvested per time point.

6.2.2. Generation of the mapping population of ppd-3 x Terese

An F_2 population of 96 plants was generated by crossing the *ppd-3* mutant (in the NGB5839 background) to cv. Terese. Plants were grown under SD to allow maximal expression of phenotypic difference between *PPD/-* and *ppd* segregates. The node of flower initiation (NFI) was scored for all plants. The early-flowering *sn* mutants were clearly distinguishable in the population while the rest was categorised as late flowering. The segregation of NFI in this population can be found in Figure 6.3B.

6.3. Results

6.3.1. The ppd mutant shows early, photoperiod insensitive flowering

All three *ppd* mutants alleles result in early flowering in SD when compared to their isogenic wild-type (Figure 6.1). The *ppd-1* and *ppd-2* mutants are both approximately 15 nodes earlier than their isogenic Borek wild-type. The *ppd-1* was

found to flower 1 node later than *ppd-2* mutant (P<0.001, Figure 6.1). This result is consistent with a previous finding suggesting that *ppd-1* might be a leaky mutant (Arumingtyas and Murfet, 1994). On the other hand, *ppd-3* mutant flower 10 nodes earlier than its isogenic NGB5839 wild-type and 2 nodes later than the *ppd-1* and *ppd-2* mutants (Figure 6.1). This small difference in the proportional effect of *ppd-3* alleles might be due to the difference in genetic background.

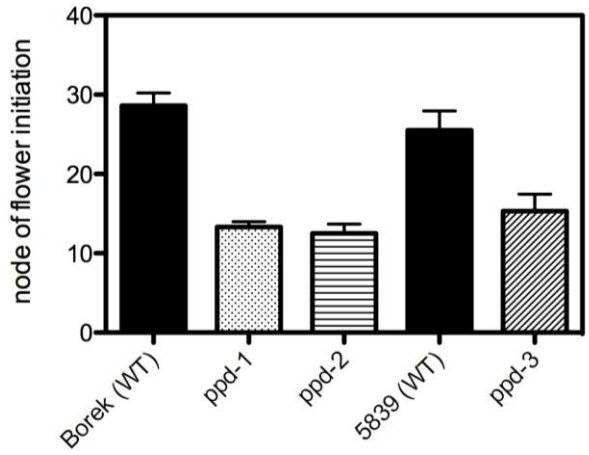

Figure 6.1 The early flowering phenotypes in *ppd* alleles. All plants were grown in the growth cabinet under SD (8L: 16D) and node of flower initiation was measured. Data are mean ± SE for n=10 plants.

Detailed physiological characterization of the *ppd* phenotype was carried out using *ppd-3* mutant as this is on the same genetic background as other flowering mutants. As showed in Figure 6.2, *ppd-3* mutant flowers earlier than the WT (NGB5839) regardless of the photoperiod conditions.

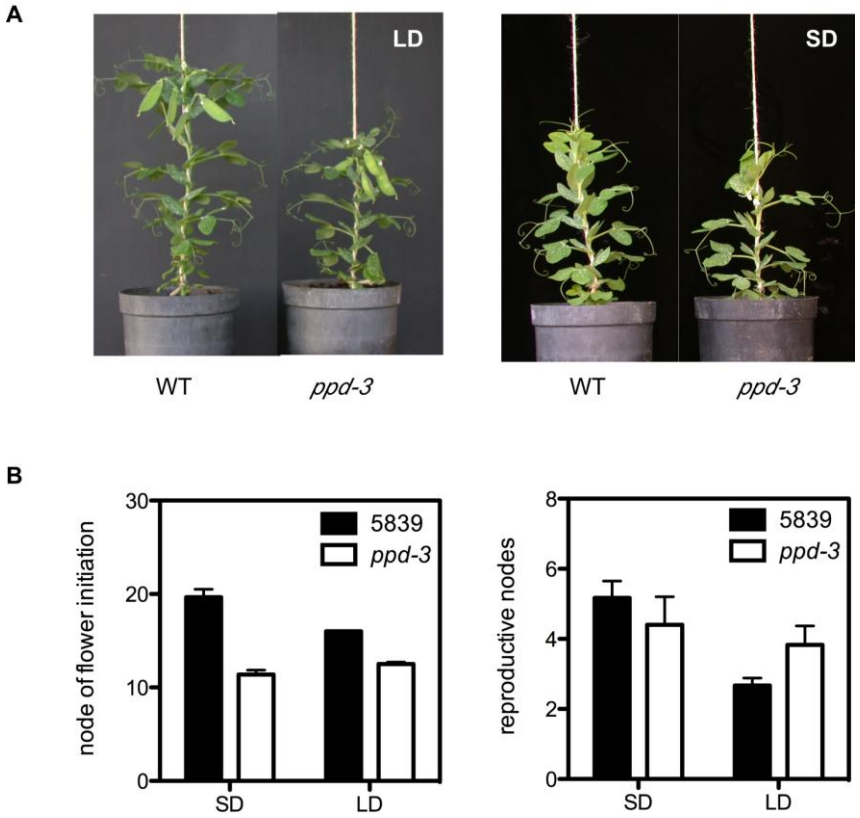

Figure 6.2 The *ppd-3* mutant is early flowering and photoperiod-insensitive. (A) Representative of 6-week-old wild-type line NGB5839 and *ppd-3* isogenic mutant plants. (B) Node of flower initiation (left) and final number of reproductive nodes (right). Data are mean ± SE for n = 8 plants. All plants were grown in the phytotron under standard SD or LD conditions.

In addition to flowering phenotype, the segregation of *ppd-3* was also examined in a *ppd-3* x 5839 and *ppd-3* x Terese population to see if the disturbed segregation of *ppd-2* alleles is also evident for *ppd-3*. In an F_3 progeny from heterozygous F_2 plants of *ppd-3* and 5839 cross, only 16 early-flowering *ppd-3* mutants appeared from of 80 F_3 plants, in a 1 (mutant):4 (WT) ratio (Figure 6.3A). Similarly, In an F_2 progeny of *ppd-3* and Terese, only 16 early-flowering *ppd-3* mutants out of 96 F_2 plants (1 (mutant):5 (WT) ratio) (Figure 6.3B). The segregation of *ppd-3* alleles in both populations are less than the expected 1:3 ratio of single gene segregation ($\chi^2 = 1.06$, $0.1<P_{df=1}<0.5$ for *ppd-3* x 5839 F_3; $\chi^2 = 3.55$, $0.05<P_{df=1}<0.1$ for *ppd-3* x Terese F_2).

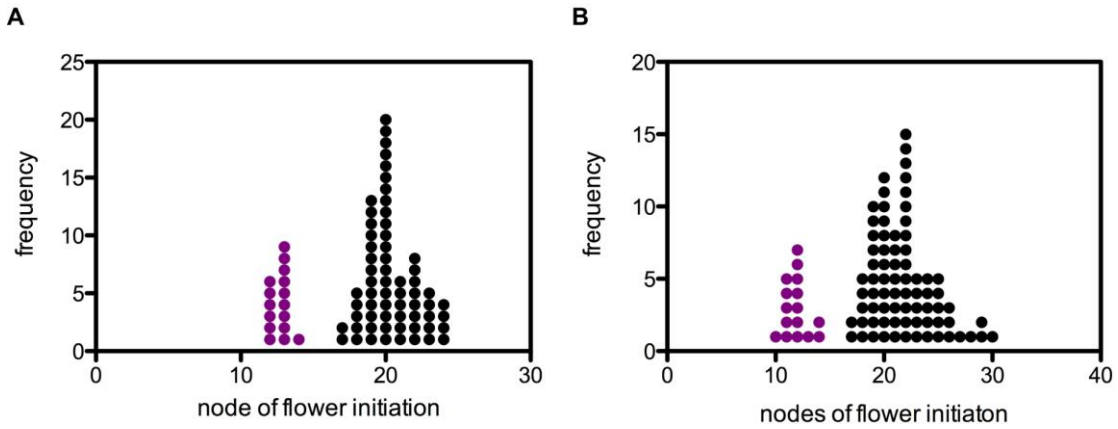

Figure 6.3 The segregation of *ppd-3* allele. (A) *ppd-3* x 5839 F_3 population (B) *ppd-3* x Terese F_2 population. All plants were grown under SD (8L: 16D) and node of flower initiation was measured. Early segregates (*ppd-3*) are highlighted in purple colour.

6.3.2. PPD affect seedling photomorphogenesis

As in the case of *dne* and *sn* mutants, effects of *PPD* on seedling de-etiolation were also examined in view of photomorphogenic phenotypes of some Arabidopsis clock mutants. In darkness, the *ppd-1* mutant did not differ in internode length from WT cv. Borek whereas *ppd-2* had shorter internodes (Figure 6.4A). In white light, both *ppd-1* ($P = 0.02$) and *ppd-2* ($P < 0.001$) have slightly shorter internode than wild-type (Figure 6.4A). This difference is more obvious when the seedlings are exposed to monochromatic red, far-red, and blue light. The *ppd-2* allele shows bigger differences than *ppd-1* allele in all conditions examined (Figure 6.4A). The *ppd-3* mutant was similar to *ppd-1* ,showing no difference in darkness but slightly shorter internodes under all light conditions except far-red light ($P = 0.45$) (Figure 6.4A). For leaf expansion, both *ppd-1* and *ppd-2* mutants had a larger leaf area in darkness and under all light conditions, except that no significant difference was found for *ppd-2* in white light ($P = 0.06$) (Figure 6.4B). However, in the case of *ppd-3*, the mutant had larger leaflets only under red light ($P = 0.018$) (Figure 6.4B).

In short, *PPD* affects de-etiolation and leaf expansion under all light conditions, but the effect seems to vary between the alleles possibly depending on

genetic background.

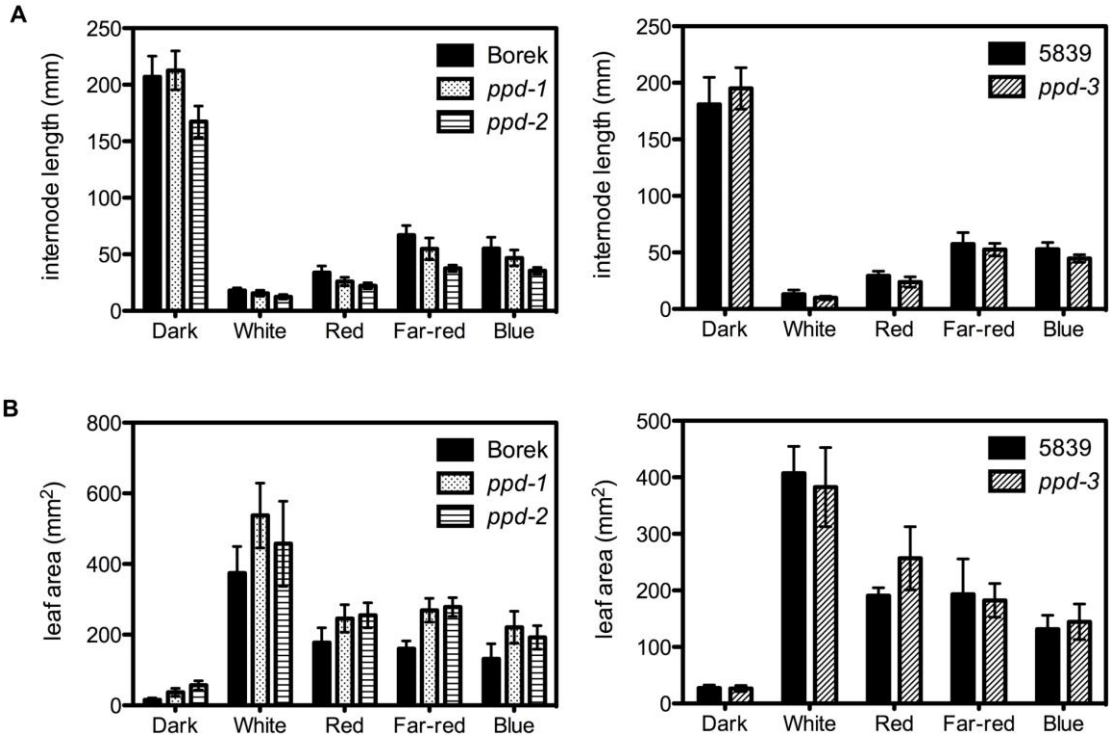

Figure 6.4 Effect of *PPD* in stem elongation and leaf expansion. (A) Effect of the *ppd* mutation on spectral sensitivity for deetiolation responses. Internode elongation was quantified as the length between nodes 1 and 3 (B) Leaf area was estimated as the product of the length and width of a single leaflet from leaf 3. Seedlings were grown for 14 d from sowing under continuous light or darkness. Data are mean ± SE for n = 12. Details on the light levels of the white and LED treatments can be found in Section 2.2.

6.3.3. The ppd-3 mutant shows altered expression rhythms of circadian clock gene homologs under light/dark cycles

Similar to *dne* and *sn* mutants, the effect of *ppd* on diurnal rhythms was also examined. The overall results of *ppd* mutant appear to be similar to *dne* and *sn* mutants for which only relatively small effects were found (Figure 6.5). Figure 6.5A and B show the diurnal rhythms of clock gene expression in *ppd-3* under SD and LD respectively. In SD, the diurnal expression rhythms of *LATE1*, *PRR37* and *PRR59* showed strongest differences between the *ppd-3* mutant and WT plants. The *LATE1* expression is elevated in the *ppd-3* mutant especially at the trough levels (ZT16-20 and ZT40-44). The *ppd* mutant has greatly reduced *PRR37* expression in SD during

day-time where the peak expression is observed. In the case of *PRR59* expression, *ppd-3* has relatively higher trough level during night time (ZT16-20 and ZT40-44). *TOC1* expression appears to be slightly higher in *ppd-3* mutant than WT at night (ZT16 and ZT40). For *ELF4* expression, a small phase advance was suggested for *ppd-3* mutant at ZT8 and ZT38 compared to ZT12 and ZT40 for WT. No clear difference in diurnal rhythms of *MYB1* and *MYB2* was found between *ppd-3* and WT under SD. The *ELF3* expression is again found to be arrhythmic in both WT and *ppd-3* mutant in SD.

In LD (Figure 6.5B), *LATE1* and *PRR59* transcripts in *ppd-3* mutant were again found to have higher trough level during night time (ZT16-24 and ZT40-48). A slightly higher expression level of *TOC1* in *ppd-3* mutant at ZT4-8 and ZT28-32 suggest a phase advance of *TOC1* expression rhythm under LD. Similarly, even though *ppd-3* has lower peak level of *ELF4* expression than WT, the relatively higher expression at ZT4-8 and ZT28-32 again suggest a possible phase advance of *ELF4* expression rhythms in *ppd-3* mutant. Intriguingly, a diurnal rhythm for *ELF3* transcript was found in *ppd* mutant in LD based on single replicate which peak around dawn (ZT24 and ZT48). The *ppd* mutation like *sn* mutant (Figure 5.4) also shows higher *MYB2* expression level in LD. However, no obvious difference was found for *PRR37* rhythms in LD between *ppd-3* and WT plants. More replications are needed for *PRRs*, *ELF3*, and *MYB2* expression before any conclusion is made.

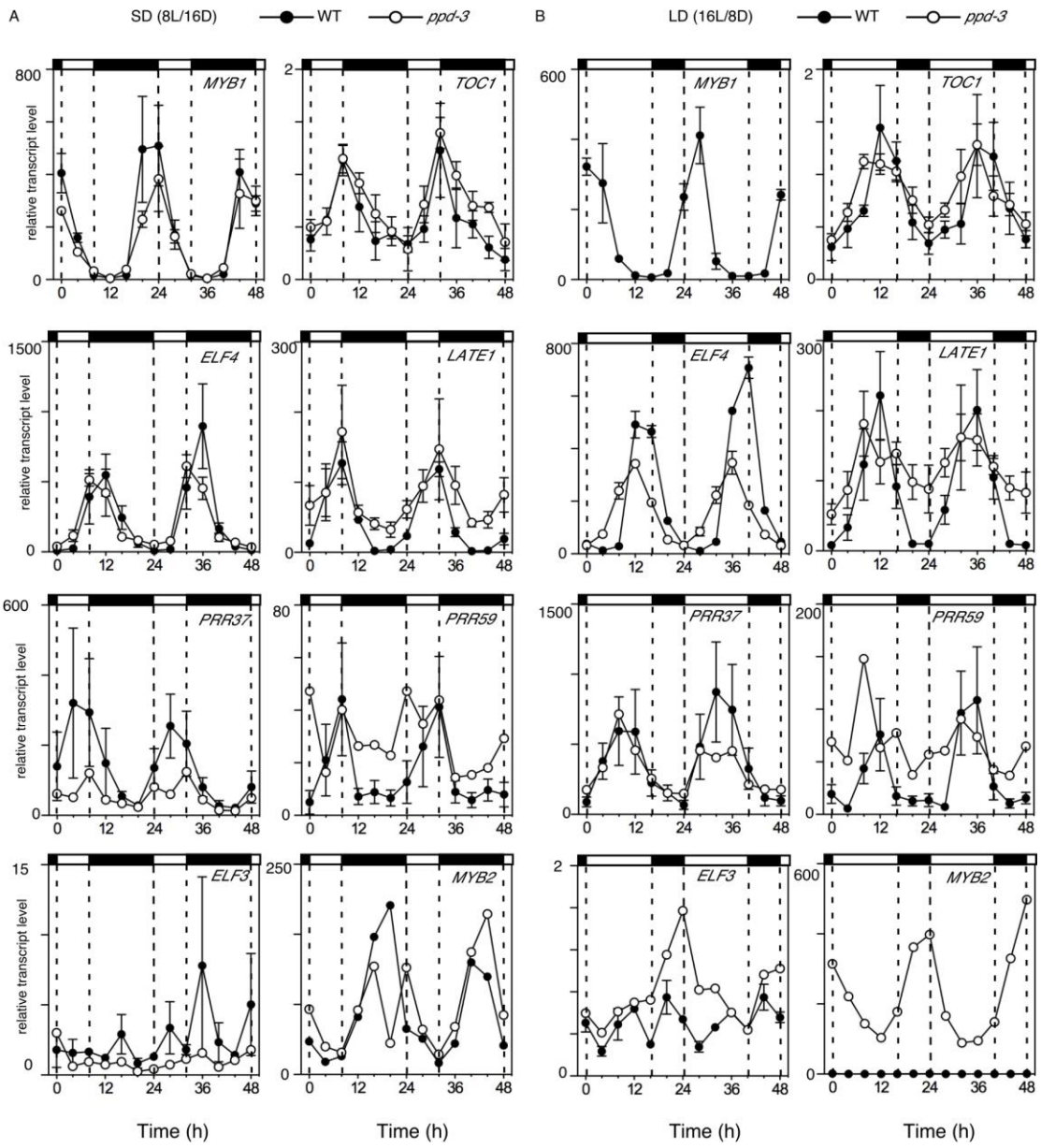

Figure 6.5 *PPD* affects diurnal rhythms of clock gene homologs under light/dark cycles.
(A) SD conditions (8-h photoperiod).
(B) LD conditions (16-h photoperiod).
All plants were grown for 21 d from sowing at 20°C before harvesting commenced. Data are mean ± SE for n = 3 biological replicates except *PRR37*, *PRR59*, *ELF3* and *MYB2*, each consisting of pooled material from two plants. Day and night periods are indicated by open and closed bars, respectively, above the graph. *MYB1* expression in *ppd* mutant under LD was not included due to technical issues.

6.3.4. PPD affects rhythms of clock gene expression in constant darkness

As *dne* and *sn* mutants, the effect of *ppd* mutation on the circadian rhythms of the four main clock genes, *MYB1*, *TOC1*, *ELF4*, and *LATE1*, was examined in DD (Figure 6.6). In the *ppd* mutant, a clear circadian rhythm of *MYB1* expression with slightly reduced amplitude of peaks was observed. The first circadian peak occurs after an interval of approximate 24h at ZT44, but the following cycle is shorter at around 16h with the second peak at ZT60 suggesting some degeneration of the rhythm in the mutant. Although the *ELF4* rhythm was much weaker, there was also the suggestion of a similar pattern, with the first peak at ZT33 as expected after a 24h interval but the second peak only 21h later at ZT54. The overall *TOC1* expression level was substantially lower in DD if compared with diurnal cycle but the *ppd-3* was found to have even lower expression rhythms of *TOC1* at most of the time points under both diurnal and DD conditions. This is different from what is observed under SD or LD where no clear difference on expression level of *TOC1* was found between *ppd-3* and WT. On the other hand, *LATE1* expression has a gradually elevated trough level in the WT under DD. The elevated trough expression of *LATE1* seen in *ppd* mutant under diurnal cycles (Figure 6.5) was also seen in DD. Despite the large error bars in DD, the *LATE1* expression rhythm seems to be lost in the *ppd-3* mutant after the first circadian cycle.

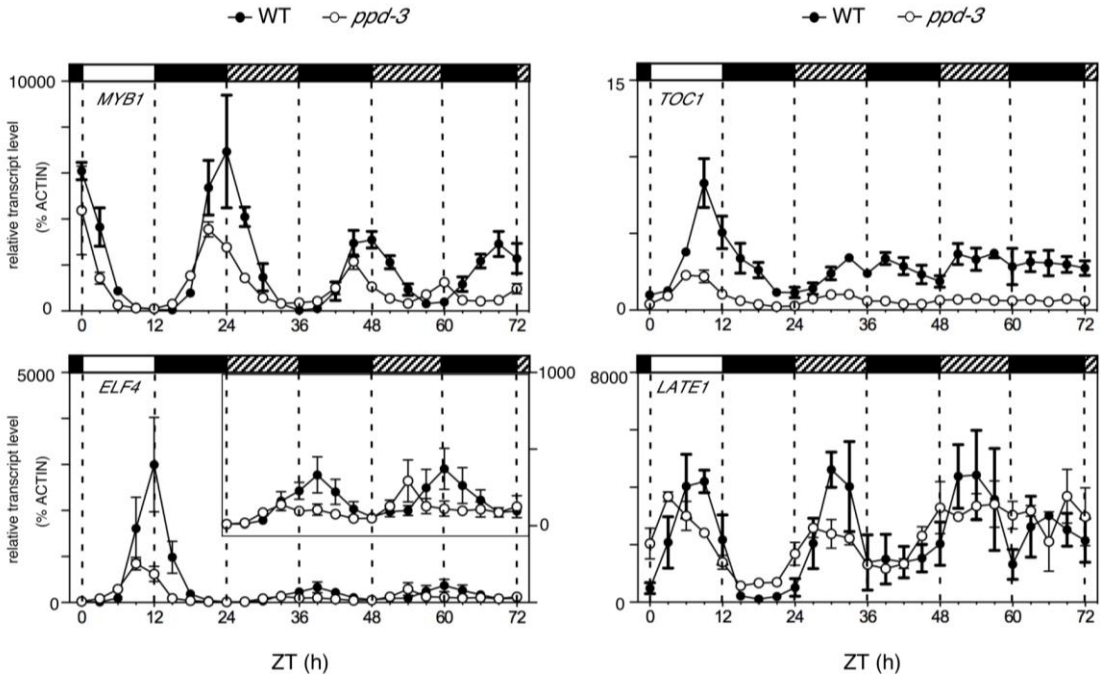

Figure 6.6 *PPD* affect circadian rhythms of clock gene homologs in DD. Plants were grown in growth cabinets under a light/dark cycle (12L:12D) at 20°C for 3 weeks before transfer to continuous darkness. Data are mean± SE for n = 2 to 3 biological replicates, each consisting of pooled material from two plants. Zeitgeber time (ZT) refers to the time since lights-on of the last full entraining cycle. Bars above the graph refer to periods of light (open bars) or darkness (closed or hatched bars). The hatched bars indicate the periods of subjective day during the period of continuous darkness.

6.3.5. Comparative mapping between pea and Medicago refine PPD map position

The effects of *ppd-3* on diurnal and circadian rhythms of clock gene expression and the similarity of flowering phenotype of *ppd* mutant to *dne* and *sn* mutants strongly suggest that *PPD* is involved in circadian clock system. However, none of the pea orthologs of known circadian genes from Arabidopsis was mapped near *PPD* ((Hecht et al., 2005), Chapter 3), suggesting *PPD* might be a novel gene that not represented in Arabidopsis. Therefore, the next step for identification of *PPD* involves refining the map position of *PPD* locus to narrow the range of candidates by positional information alone. A more precise map position of *PPD* locus can be also be useful for future mapping and linkage analysis of circadian genes and flowering

loci in other species.

PPD was previously mapped on top of pea LGII near physiological marker *A* and between the isozyme locus *Aatp* and branching locus *RMS3* (Arumingtyas and Murfet, 1994; Murfet and Taylor, 1999). The *A* gene was recently identified as a bHLH transcription factor (Hellens et al., 2010) enabling the identification of its Medicago ortholog, but no clear Medicago ortholog of Aatp could be identified. Therefore, the previous information from older literature cannot be easily related to the Medicago physical map. For this reason, the information from the published composite map based on gene-anchored markers (Aubert et al., 2006) was used as a starting point for *PPD* mapping. Table 6.1 shows the physical map position of known gene-anchored markers in pea and relevant flowering genes across the syntenic Medicago Chromosome 1.

Table 6.1 The relevant flowering genes across Medicago Chromosome 1 based on Mt 3.0 genome build. Data included bac accession, gene calls, and physical map position. Genes represented in the pea map of Aubert et.al. (2006) were highlighted in green.

Gene	Bac accession	genecall	map position (mbp)
PutTIP	AC202471	1g007370	0.4
PepTrans	AC157646	1g010210	1.6
GA3ox2	AC146722	1g013080	2.2
GID1	AC147471	1g013750	2.6
COLb	AC229735	1g016230	3.1
Thiolp	AC150207	1g023920	5.5
STH2	AC183777	1g028510	6.9
SPL14/16	AC140774	1g039740	9.2
CRY2a/2b	AC122171	1g042700	9.9
PHYA	AC148406	1g103220	21.4
SPL1	AC136840	1g105980	22.0
ELF6	AC144928	1g120550	26.0
GI	AC148397	1g124650	27.2
PM3/AGL6	AC148527	1g129880	29.1
TIC	AC137838	1g132680	29.7

These markers have been mapped in Terese x Torsdag mapping population. To enable the use of the same markers in mapping of *PPD*, an F_2 population was generated from a cross between *ppd-3* (Torsdag) and Terese. The early-flowering phenotype was scored as a marker for *PPD* and as mentioned above, the segregation ratio was somewhat distorted in this population (Figure 6.3B). A comparative map between pea Chromosome II and Medicago Chromosome 1 (Figure 6.7) was generated by using the linkage results generated in this study and integrating them with the published map of Aubert et.al. (2006).

This analysis places *PPD* between the *Thiolp* and *PepTrans* markers, which correspond to a genomic region on Medicago Chromosome 1 of around 4Mb according to the Mt3.0 Genome build (Table 6.1, Figure 6.7). This distance is again only approximate as the region includes numerous gaps where adjacent BAC contigs have not yet been joined. A *TIC* ortholog is the only circadian clock gene that appears in Medicago Chromosome 1 and information from earlier genome releases initially indicated a physical map position for this gene at the top of Medicago Chromosome 1. However, the pea ortholog was mapped at the bottom of pea LGII tightly linked to the *Ppgm* marker (Figure 3.9 and 6.7) suggesting a syntenic position for MtTIC at the bottom of chromosome 2. A revised position for *MtTIC* in Medicago Genome 3.0 is now consistent with our observed position for *PsTIC*

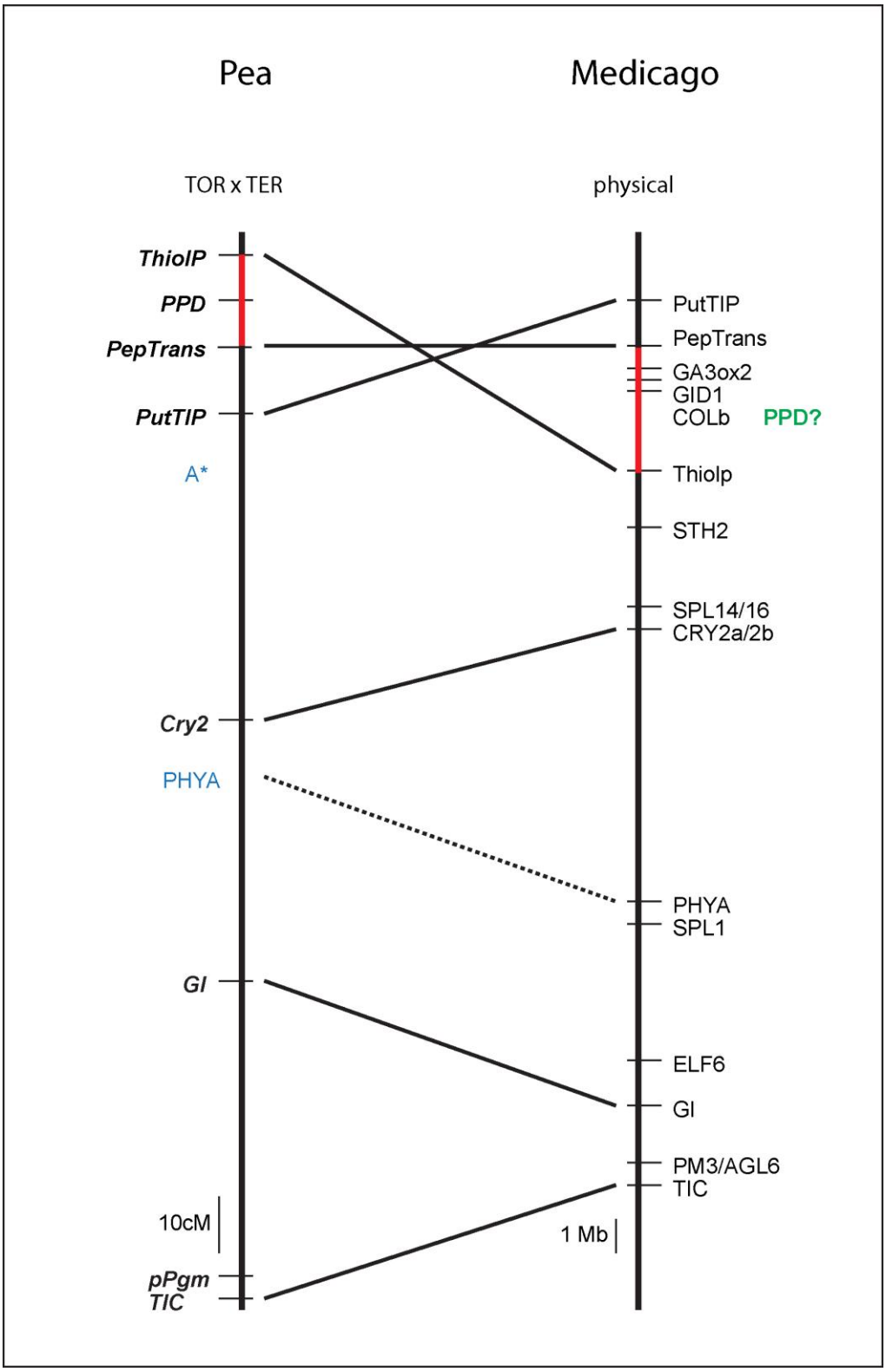

Figure 6.7 Comparative map between linkage group II in pea and Chromosome 1 in Medicago. Markers mapped in this study are indicated in bold and italics, markers that are published in previous composite map are highlighted in blue colour (Aubert et al., 2006). Morphological markers are marked by * symbol. Orthologous genes are joined together by solid lines (markers used in this study) or dashed line (previous markers). The regions in the map which is highlighted in red are the approximate region where *PPD* is located.

The only other obviously flowering-related gene towards the top of pea LGII is *COLb* which is indicated as *COLa* in Aubert's composite map in pea (Aubert et al., 2006)and its Medicago ortholog is also positioned between *Thiolp* and *PepTrans* orthologs on Medicago Chromosome 1 (Table 6.1, Figure 6.7). Full length cDNA and one intron of *PsCOLb* had already been isolated in our lab before the start of this study. No polymorphism was identified in the only intron between mapping parents of NGB5839 (Torsdag) and Terese so without further isolation of flanking sequence, *COLb* could not be mapped in *ppd-3* x Terese mapping population. Alternatively however, a dCAPs marker for *COLb* was identified between NGB5839 and JI1794 mapping parents. A mapping population of *ppd-3* x JI1794 (Chapter 3) was generated in order to test the cosegregation between *PPD* locus and *COLb* dCAPs marker. While the divergent nature of these parents meant that phenotypic segregation was somewhat complex, several segregants were clearly identified as early-flowering and day-neutral in the F_2 under SD and one of these clearly carried *COLb* alleles from the JI1794 parents suggesting recombination occur between *PPD* and *COLb*. This recombinant appears to rule out *COLb* as a candidate gene for *PPD* locus. However, future confirmation of this result in the *ppd-3* x Terese cross is clearly necessary, but may not be straight-forward as isolation of genomic sequence flanking *COLb* will be necessary.

6.3.6. PPD regulation on CO and FT expression

As in the case of *late1*, *dne*, and *sn* mutants, the diurnal expression rhythms of *COLa* and *COLb* genes were also examined in *ppd-3*, and similar to *dne* and *sn* (Chapter 4 and 5), no significant differences were apparent between *ppd-3* mutant and wild-type (Figure 6.8).

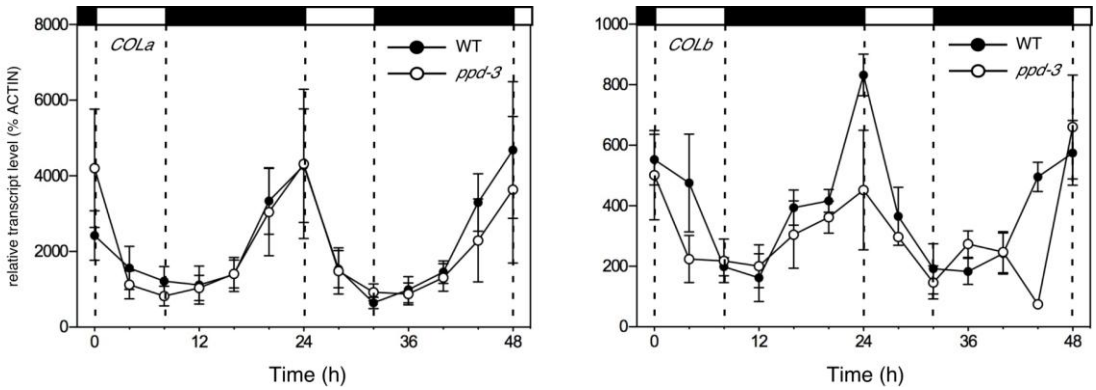

Figure 6.8 *PPD* affects diurnal rhythms of *CO* homologs under SD conditions (8-h photoperiod). All plants were grown for 21 d from sowing at 20°C before harvesting commenced. Data are mean ± SE for n = 3 biological replicates, each consisting of pooled material from two plants. Day and night periods are indicated by open and closed bars, respectively, above the graph.

Overall, the effect of *PPD* on *FT*-like gene expression was also generally similar to *dne* and *sn*. The *ppd-3* mutant used in this experiment flowered slight later than *dne* or *sn*, which is reflected in a delayed induction of *PIM*, which by day24 (Figure 6.9B) only started to increase and not yet reached high levels as seen for *dne* (Figure 4.10B) and *sn* (Figure 5.11B) mutants at this time point. Moreover, floral buds were not seen in *ppd-3* mutants by day24 whereas clear floral buds were observed in both *dne* and *sn* mutants. Nevertheless, substantially elevated level of *FTa1*, *FTa2*, *FTb2* in leaf and *FTa1*, *FTa2*, *FTc* in apex were found in *ppd-3* mutant relative to WT. In contrast, no significant difference was spotted on *FTb2* transcript level which is again similar to *dne* and *sn* mutants. These results of elevated *PIM* and *FT* genes are consistent with the early-flowering phenotype of *ppd-3* mutant.

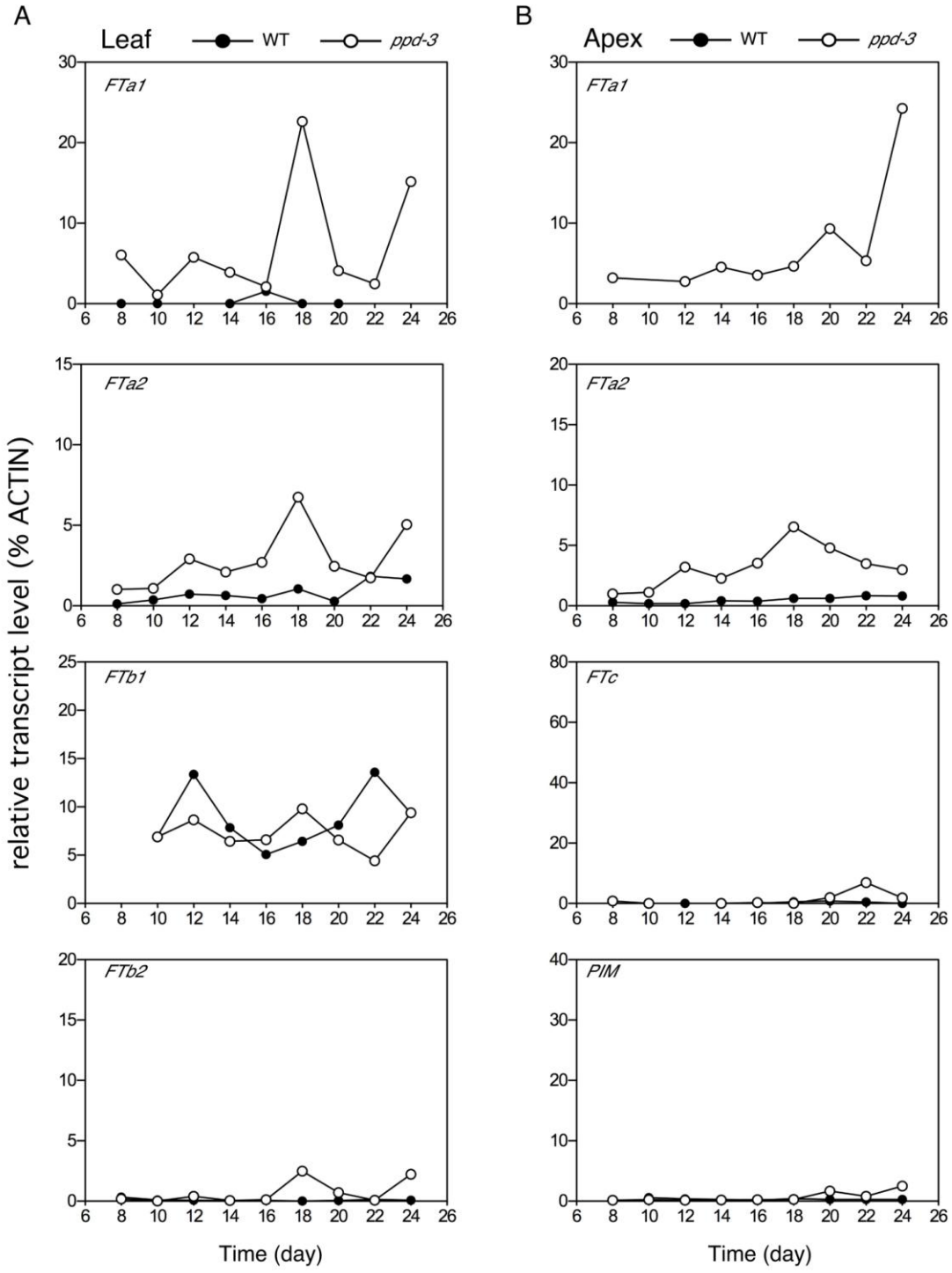

Figure 6.9 Pea *FT-like* and *PIM* gene expression in (A) uppermost leaf (B) shoot apex of *ppd-3* and WT plants grown under SD (8h-photoperiod). All plants were grown at 20°C and harvesting commenced at day 8 up to day 24. Data are from 1 biological replicate which consist of pooled material from two plants.

6.4. Discussion

In this chapter, *ppd* mutation has been identified to result in defective characteristics in flowering, photomorphogenesis, diurnal rhythms, and circadian rhythms of clock gene expression. In general, the defects in *ppd* mutant are similar to what have been found in *dne* and *sn* mutants. The phenotypes of *ppd* mutants suggest *PPD* locus is highly likely to be involved in the same pathway of *DNE* and *SN* which is the circadian clock system in pea. Unfortunately, comparative mapping of *PPD* locus did not identify any potential candidate genes that are involved in circadian clock. However, map position of *PPD* has been refined to be in between *ThiolP* and *PepTrans* which is located on top of pea LGII.

6.4.1. Physiological Role of PPD on flowering

The early-flowering phenotype of *ppd-3* is associated with early induction of *PIM* but the transcript level of *PIM* is 10-fold lower than what have been found in *dne-1* (Figure 4.10B) and *sn-4* mutants at the same timepoint (Figure 5.11B). This is likely to reflect the fact that *ppd-3* mutant flowers 2-3 nodes later than *dne-1* and *sn-4* mutants. Again similar to *dne* and *sn* mutants, expression of all the *FT*-like genes except *FTb1* are higher in *ppd-3* mutant than WT. However, if compared with *dne-1* and *sn-4* mutants, expression level of *FTa2* (2-fold), *FTc* (10-fold), and *FTb2* (10-fold) are substantially lower in *ppd-3* mutant which is consistent with lower level of *PIM* transcript level. This suggests one or more of these *FT*-like genes are responsible for the induction of inflorescence gene induction and hence initiation of flowering. In contrast, *ppd* mutation does not affect the diurnal rhythms of *COLa* and *COLb* expression in SD. In Arabidopsis, circadian clock mutants affect *CO*

transcript level in a way correlates to their flowering phenotypes such as Arabidopsis *elf3* and *elf4* mutants have increased *CO* expression associated with their early-flowering phenotype (Doyle et al., 2002; Kim et al., 2005). This emphasises the idea that the closest ortholog of Arabidopsis *CO*, *PsCOLa* does not share a similar function in the flowering pathway. However, there are 16 *COL* genes in Arabidopsis (Ledger et al., 2001; Cheng and Wang, 2005). Identification of other *CO-like* genes in pea is required before we ruled out conserved function of *CO* in pea flowering.

Besides slightly delay on flowering time of *ppd-3*, it shares the similar flowering phenotype (early-flowering and daylength insensitive) to both *ppd-1* and *ppd-2* alleles. However, the segregation of the early-flowering phenotype seems to be distorted in the *ppd-3* segregating population. There are less *ppd-3* mutants than expected according to single gene segregation (Figure 6.3). This result was found to be consistent with previous result of disturbed *ppd-2* segregation (Murfet and Taylor, 1999). However, in this case the distortion was seen in crosses made with the mutant as the maternal parent, and the reciprocal cross was not examined. This suggests that the *ppd-3* allele may also affect viability or receptivity of the egg in addition to the effect on paternal inheritance previously described for *ppd-2*. These effects could point to a specific role for *PPD* in clock regulated gamete viability or growth. More general effects of the clock on vegetative growth have been reported for the Arabidopsis *ztl* (long-period) and *toc1* (short-period) mutants which have decreased photosynthesis, growth, survival, and competitive advantage when exposed to normal 24h period (Dodd et al., 2005).

6.4.2. Roles of PPD on diurnal and circadian rhythms

The studies of diurnal and circadian expression rhythms of circadian clock gene orthologs in *ppd* mutant also suggest it may be involved in circadian clock regulation (Figure 6.5 and 6.6). Not surprisingly, the results were again similar to what have been discovered in *dne* and *sn* mutants which are small alterations on clock gene expression in both diurnal and circadian conditions. The strongest differences were observed in *ELF4*, *LATE1*, and *PRRs* diurnal rhythms where rhythm of *ELF4* was shifted earlier in LD, *PRR37* expression is reduced in SD, *PRR59* and *LATE1* expression were clamped high. The circadian rhythms of *MYB1* and *ELF4* persist in *ppd-3* mutant after 2 cycles in DD but the period length were found to be deviated from the normal 24h in the second cycle. On the other hand, large variations were found for *TOC1* and *LATE1* rhythms in DD but there are indications of alteration of level and loss rhythms in *ppd-3* mutants if compared with WT.

6.4.3. The map position of PPD locus was refined using comparative mapping

Comparative mapping have been a real success in identifying the molecular identities of both *DNE* and *SN* loci. Similar approach was utilised for *PPD* mapping. However, unlike *DNE* and *SN*, *PPD* have not yet been mapped using molecular markers. It is only known to be linked to morphological marker *A* and located in between classical markers *Aatp* and *RMS*. This study is the first attempt to locate *PPD* precisely using molecular markers. With the aid of the published pea composite map (Aubert et al., 2006), the existing molecular markers across pea LGII from Torsdag x Terere cross were employed to estimate the approximate position of *PPD* in the newly generated *ppd-3* x Terese cross. This approach managed to place *PPD* on top of pea LGII which is consistent with previous studies and further refine the map location to

be in the middle of *ThiolP* and *PepTrans*. Additionally, two possible candidate genes, *TIC* and *COLb* have been ruled out by linkage analysis with *PPD* locus and comparative mapping. However, isolation of more genomic sequence *PsCOLb* might allow us to map *PsCOLb* in *ppd-3* (Torsdag) and Terese population which will confirm this conclusion and further refine the map position of *PPD*. From our current knowledge on circadian clock genes in Arabidopsis, no circadian clock gene was mapped near *PPD*. However, map positions of *TOC1* and *FIONA1* have not yet been determined in pea nor have they been found in the Medicago genome (Chapter 3). Similar to *ppd* mutant, both of the Arabidopsis *toc1* (Somers et al., 1998b) and *fiona1* (Kim et al., 2008) mutants are early-flowering and affect rhythms of clock gene expression, and *TOC1* and *FIONA1* could therefore still be possible candidate gene for *PPD*.

Chapter 7 Characterization of the flowering locus *HIGH RESPONSE* (*HR*)

7.1. Introduction

The locus *HIGH RESPONSE*, *HR*, is one of four flowering loci (*SN*, *LF*, *E*, and *HR*) identified in early studies of naturally-occurring variation for flowering in pea (Murfet, 1973). *HR* acts together with the *SN* locus and dominant alleles at both loci confer the near-obligate LD requirement for flowering in pea. The recessive alleles at *HR* locus relax this requirement while recessive *sn* alleles eliminate it completely. The late flowering phenotype of *HR SN* genotype in SD is coupled with stronger response in flowering promotion to cool ambient temperature (11 – 14 °C) if compared with *hr SN* genotype (Murfet, 1973). In contrast, introgression of dominant *HR* allele into our standard WT in this study showed to delay flowering in both LD and SD to a similar extent (Chapter 5).

Linkage analysis previously placed *HR* on LGIII, tightly linked to the seed marbling gene *M* (Murfet, 1973). In addition, two QTL studies have located two major QTLs (quantitative trait locus) mapped to a position near *HR*. Firstly, a study of QTL involved in domestication progress using wild (JI1794) and cultivated crosses (Slow) has highlighted a locus for flowering time (assumed to be *HR*) located near branching gene *RMS1* and a major flowering QTL on LGIII which also is collocated with a QTL for root/shoot ratio (Weeden, 2007). Another QTL analysis by Lejeune et al. (2008) in a cross between a late-flowering winter cultivar (Champagne) and an early-flowering spring cultivar (Terese) crosses identified co-localisation of major QTL for winter frost tolerance and flowering

time in the region of *HR*, and these have also been assumed to be equivalent to the *HR* locus as originally defined(Lejeune-Hénaut et al., 2008). These studies not only improved map position of *HR* locus, but also suggest likely scenario for *HR* distribution. The primitive and winter cultivars (JI1794 and Champagne) of pea have near-obligate LD requirement to flower are likely to carry dominant *HR* allele where recessive allele at *HR* locus relax this requirement in cultivated and spring peas (Slow and Terese). In addition to this, these QTL studies also suggest either *HR* locus has pleiotropic effects on multiple pathways or multiple closely linked loci around *HR* could control these polymorphic traits.

It is hard to answer these questions without knowing the molecular identity of *HR*. Previously, Hecht et. al. (2005) have suggested *FRI* and *FLC* could be possible candidate gene for *HR* because like *hr*, the Arabidopsis *fri* or *flc* vernalisation mutants show strong delay of flowering in SD (Johanson et al., 2000; Caicedo et al., 2004). Although no *FLC* ortholog has been found in pea, orthologs of both *FRI* and *FRIGIDA-like a* (*FRLa*) are present in Medicago and pea. *PsFRI* is mapped in the region of *HR* and *PsFRLa* is also located on pea LGIII as well (Hecht et al., 2005). An alternative, *HR* might act like *SN*, *DNE*, and *PPD* loci in photoperiod pathway. *HR* only delays flowering in the presence of *SN* as *sn* mutants in *HR* and *hr* background are both early-flowering in LD and SD (Chapter 5). This suggests *SN* is epistatic to *HR* in flowering regulation. Results from early grafting studies indicate that floral inhibitor remains high in *HR* plants for a longer time if compared to *hr* plants. *HR* locus appears to mainly regulate floral inhibitor production in the leaves so that inhibitor production decline slowly in the presence of dominant *SN* (Reid, 1979a). These findings support *HR* may act in the same pathway of *SN* to regulate photoperiodic response and flowering regulation.

In previous chapters (Chapter 4), the circadian rhythms of several circadian regulated genes in pea are lost under LL condition but persist under DD condition in our standard wild-type line NGB5839. In Arabidopsis, strong circadian rhythms are seen under both conditions. It is notable that NGB5839 like most of the spring peas carry recessive alleles at the *HR* locus which make NGB5839 flower earlier in SD like *dne*, *sn*, and *ppd* mutants but still retain the photoperiod response. Therefore, it is intriguing to discover if it is the *hr* mutation in NGB5839 causes the conditional arrhythmia in LL condition. If it is the case, *HR* locus is likely to involve in circadian clock like the other photoperiod loci *SN*, *DNE*, and *PPD*.

Therefore, the aims of this chapter are to examine if *HR* functions in circadian clock of the photoperiod pathway and to identify the molecular nature of *HR*. This will allow us to investigate the distribution of *HR* alleles and its association with photoperiod responsiveness across wide range of pea varieties. It is also useful to work out what *HR* is in order to answer if *HR* a pleiotropic gene.

7.2. Materials and methods

7.2.1. Gene expression experiments

For the transfer experiment, all plants were grown in the growth cabinets under a light/dark cycle (12L: 12D) at 20°C for 3 weeks before transfer to continuous white light at 25μmol m^{-2} s^{-1} at ZT12 and back to continuous darkness at ZT36. Harvested material consisted of single leaflet from the uppermost fully expanded leaf from two plants. Samples were harvested at 4h intervals, with 3 replicates per time point.

For circadian expression experiments, all plants were grown in growth

cabinets under a light/dark cycle (12L: 12D) at 20°C for 3 weeks before transfer to continuous white light at 25μmol m^{-2} s^{-1} (LL) or continuous darkness at ZT36 (DD). Harvested material consisted of a single leaflet from the uppermost fully expanded leaf from two plants. Samples were harvested at 4h intervals, with 2 to 3 replicates per time point. Samples were harvested by V. Hecht and B. Wenden and processed with the help of B. Wenden. Several real-time PCR runs on the first replicate were done with assistance of B. Wenden.

7.2.2. Pisum germplasm collection study

Representative lines from JI Pisum Germplasm Collection were selected for preliminary analysis of *HR* allele distribution and its association with relevant phenotypes. The seeds was received from the Department of Primary Industries (DPI) Victoria and individual plants were grown in LD (16L: 8D) or SD (8L:16D). The leaf tissues of individual lines were harvested for DNA extraction and sequencing. The genealogical relationship among *ELF3* sequences of the selected germplasms were estimated in a haplotype network by TCS version 1.21 ((Clement et al., 2000), http://darwin.uvigo.es/software/tcs.html) using the statistical parsimony method (Templeton et al., 1992). The phenotypic characteristics were measured according to methods outlined in Section 2.3.

7.2.3. Frost tolerance study

Plants are grown in growth cabinets under SD (8L:16D) at 20°C day temperature and 20°C night temperature for 3 weeks for non-acclimated plants or 20°C day temperature and 20°C night temperature for 2 weeks and 10°C day temperature and 3°C night temperature for 1 week for acclimated plants. The uppermost fully expanded leaf was harvested and placed into plastic zip lock bags

and subjected to cold treatment (-2, -5, -7, or -10°C) for 3 hours. The damage of leaves following cold treatments was determined by leaf photochemical efficiency (ratio of variable to maximum fluorescence, Fv:Fm) measurement using a pulse-amplitude modulated fluorometer (PAM–2000, Walz, Effieltrich, Germany).

7.3. Results

7.3.1. Circadian rhythms restored in NGB5839 on transfer from constant light to constant dark

In Chapter 4, the circadian expression rhythms of several pea clock orthologous genes were shown to be repressed in the wild-type NGB5839 under constant light (LL) but to persist under constant dark (DD). In order to further examine this phenomenon, we performed another transfer experiment in which entrained plants were transferred back to DD after a single LL cycle to test whether arrhythmicity in LL is due to light-dependent repression of circadian rhythms under LL.

The results in Figure 7.1 show that the four genes examined showed damping in the initial LL cycle similar to that observed in previous LL experiment (Figure 4.3) and that subsequent transfer to DD resulted in restoration of rhythms typical of these conditions (Figure 4.4). Under LL, the rhythm of the morning gene (*MYB1*) was repressed at the peak of the expression whereas evening genes (*TOC1*, *ELF4*, and *LATE1*) are damped high in the trough phase. Nonetheless, *ELF4* expression level is also overall elevated by light if compared to DD. Therefore, the damped rhythm in NGB5839 in LL is due to light-dependent repression but not malfunction of circadian clock.

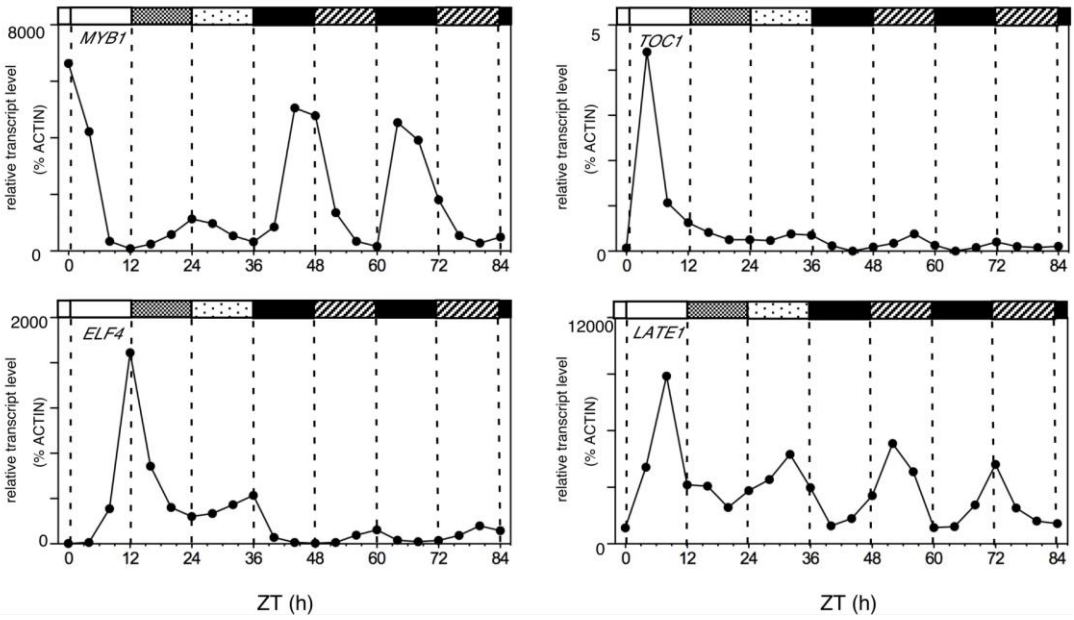

Figure 7.1 Constant dark restores circadian rhythms in NGB5839 under constant light. Plants were grown in growth cabinets under a light/dark cycle (12L:12D) at 20°C for 3 weeks before transfer to continuous light for 1 cycle and back to constant darkness. Data are single biological replicate which consisting of pooled material from two plants. Zeitgeber time (ZT) refers to the time since lights-on of the last full entraining cycle. Bars above the graph refer to periods of light (open or stippled bars) or darkness (closed or hatched bars). The heavy and light stippled bars indicate the periods of subjective night and subjective day respectively during the period of continuous light whereas the hatched bars indicate the periods of subjective day during the period of continuous darkness.

7.3.2. The HR locus affects rhythms of clock gene expression under constant conditions

Since loss of *HR* function in NGB5839 does not result in a complete non-functional circadian clock, it is possible that the effect of NGB5839 on circadian rhythms under LL reflects the masking or damping of rhythms by constant illumination when *HR* is absent. In order to test this hypothesis, we examined whether the introgression of *HR* to NGB5839 background restore circadian rhythms in LL similar to those found in DD. Figure 7.2A and Figure 7.2B showed the circadian rhythm of clock gene expression in *hr* (NGB5839) and its isogenic *HR* lines under DD and LL respectively. Under the entraining cycle, there were no distinct differences between *hr* and *HR* except a sharper peak was found in *HR* line for *LATE1* expression. In DD, there was no clear difference between circadian rhythms of *hr* and *HR* alleles except *hr* mutant showed to have much higher *GI* expression than *HR* line (Figure 7.2A). In LL, introgression of *HR* restores the expression rhythms of *MYB1*, *LATE1*, and *LUX* to be similar to those found in DD (Figure 7.2B). For *TOC1* expression, the rhythm in *HR* in LL was stronger than NGB5839 in DD suggesting a light independent component of *TOC1* regulation by *HR*. However, there is no clear difference of *ELF4* expression between *hr* and *HR* lines.

Overall this restoration of clock gene expression rhythms in LL by introgression of *HR* suggests that *HR* has a role in regulation of light input to circadian clock. These results may also explain why *dne* (Chapter 4), *sn* (Chapter 5), and *ppd* (Chapter 6) mutants only show subtle effect on diurnal and circadian rhythms as they are all effectively double mutants for clock components.

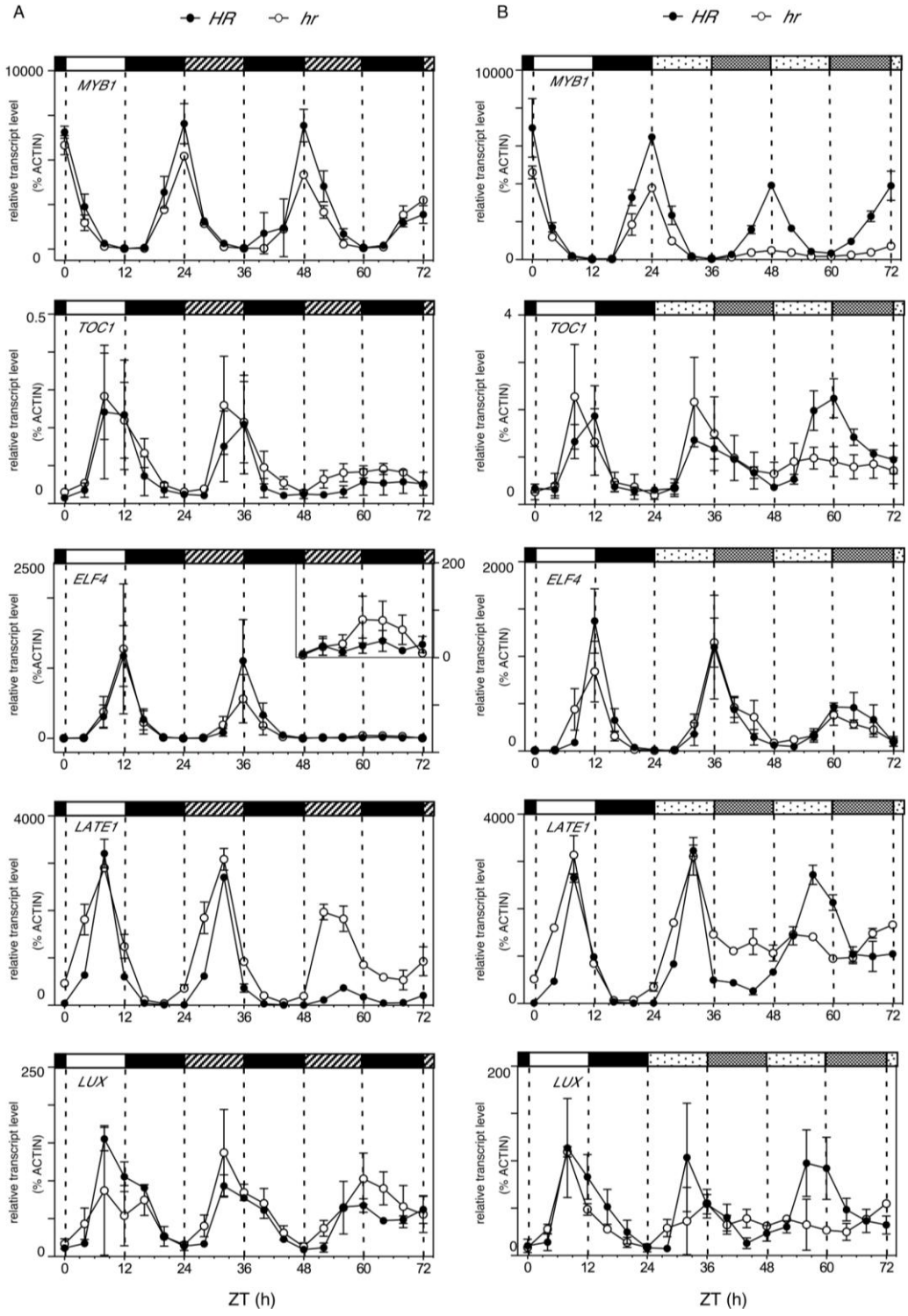

Figure 7.2 *HR* affects the circadian rhythm in constant light. Plants were grown in growth cabinets under a light/dark cycle (12L:12D) at 20°C for 3 weeks before transfer to (A) continuous dark or (B) continuous light. Data are mean± SE for n = 2 biological replicates, each consisting of pooled material from two plants. Zeitgeber time (ZT) refers to the time since lights-on of the last full entraining cycle. Bars above the graph refer to periods of light (open or stippled bars) or darkness (closed or hatched bars). The heavy and light stippled bars indicate the periods of subjective night and subjective day respectively during the period of continuous light whereas the hatched bars indicate the periods of subjective day during the period of continuous darkness.

7.3.3. Comparative mapping between pea and Medicago refine the HR map position

These results from expression experiments suggest that *HR* might have a role in regulating light input to circadian clock. In Arabidopsis, several genes are known to have a role in regulating light input to clock, including *ELF3* (Hicks et al., 1996; McWatters et al., 2000; Covington et al., 2001), *TIC* (Hall et al., 2003; Ding et al., 2007) and *FHY3* (Allen et al., 2006) and we considered that the corresponding pea genes might be candidates for *HR*.

Previous mapping studies showed that *HR* is located in the top half of LG III near the seed marbling gene *M* and branching gene *RMS1* (Murfet, 1973). The syntenic relationship between pea and Medicago is well-documented (Kalo et al., 2004) and comparative maps have been generated (Aubert et al., 2006). The top half of pea LG III where *HR* is located corresponds to the bottom half of Chromosome 3 of Medicago. Previous results from our lab suggested *FRI* and *FLC* could be possible candidate gene for *HR* (Hecht et al., 2005; Weller et al., 2009). Although no *FLC* homolog has been found in Medicago, homologs of both *FRI* and *FRIGIDA-like* (*FRL*) are present in Medicago (Hecht et al., 2005). The map position of *FRLa* in top half of Medicago Chromosome 3 rules it out as a candidate for *HR*, and the same is true for *TIC* which mapped at the bottom of pea LGII (Chapter 3). Although *FHY3* has not yet being isolated in pea, its homolog in Medicago was found to be mapped above *FRLa* at the top of Medicago Chromosome 3. On the other hand, *FRI* is located close to *HR* region suggest it could be potential candidate gene for *HR*. Nonetheless, *ELF3* homolog in Medicago is located at the bottom of Medicago Chromosome 3 and close to *FRI*. In summary, preliminary survey on the syntenic region on Medicago Chromosome

3 has suggested *FRI* and *ELF3* could be potential candidate gene for *HR* locus.

Our standard mapping cross of Torsdag x Terese is not relevant to *HR* mapping because both of the mapping parents are recessive at *HR* locus. In collaboration with the group of I Lejeune in France, we made use of a mapping population between Terese (*hr*) and Champagne (*HR*) specifically generated to investigate the *HR* locus. The common markers between these two populations were scored (V. Hecht and C. Rameau, unpublished data). By using information from the Medicago Genome (Mt 3.0) database, the flowering related genes across Medicago Chromosome 3 were identified (Table 7.1), and a comparative map between Medicago and two of the pea mapping population was generated (Figure 7.3).

Table 7.1 The relevant flowering genes across Medicago Chromosome 3 based on Mt3.0 genome build. Data included bac accession, gene calls, and physical map position.

Gene	Mt accession	physical map	map position (mbp)
FRI	CT010504	3g151640	40.2
LFY/UNI	AC139708	3g151360	40.1
ELF3	CU468275	3g140450	36.3
COLc	CU013524	3g138670	35.5
RMS1	CR956392	3g130620	33.2
PRR59	CR940305	3g122650	30.5
ELF4	AC145219	3g093640	22.3
FRLa	AC121232	3g077030	18.0
FHY3	CT030192	3g016350	3.2

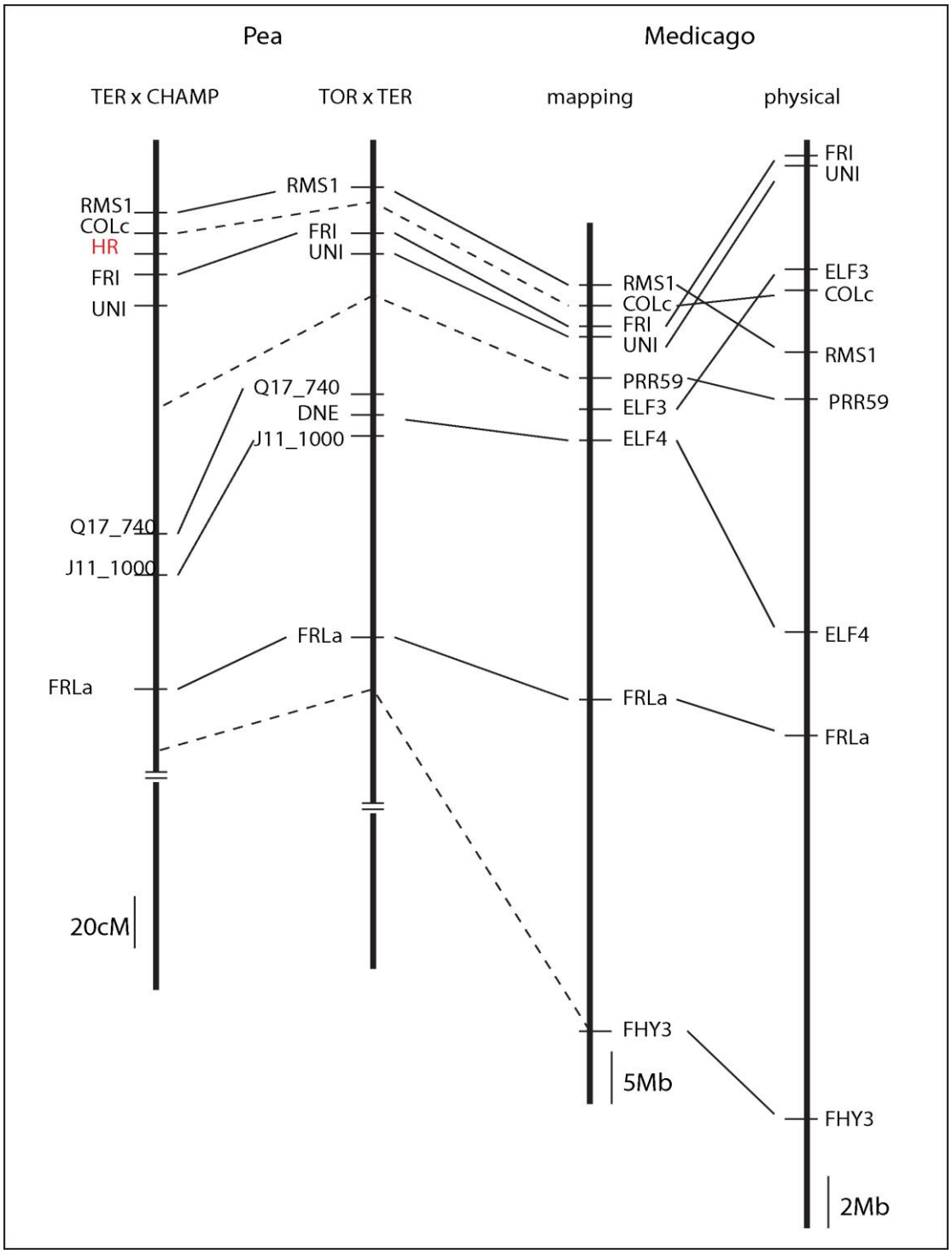

Figure 7.3 Comparative map between linkage group III in pea and Chromosome 3 in Medicago based on Mt3.0 genome build. Markers are mapped in previous studies (V. Hecht, unpublished data) or by collaborator in French (B. Weeden and C. Rameau, unpublished data). Orthologous genes are joined together by solid lines (markers present in both mapping populations) or dashed line (present in single mapping population).

The comparative map (Figure 7.3) shows that order of markers or genes are conserved across two pea mapping populations (Terese x Champagne and Terese x Torsdag) and between pea and Medicago including clock genes (*ELF3*, *PRR59*, and *ELF4*) that were isolated in Chapter 3 and mapped in other populations. However, some re-arrangement did occur between linkage data and physical mapping data of Medicago. Comparative mapping ruled out *FRI* as potential candidate gene for *HR* as recombinants were found in Terese x Champagne RIL population. Another *CO*-like homolog (*COLc*) was located in Medicago genome at the approximate position where *HR* is located. Its ortholog was isolated and mapped in Terese x Champagne RILs population in relative to *HR* locus (V. Hecht and B. Wenden, unpublished data). Again, like *FRI*, pea *COLc* was excluded as a candidate gene for *HR* because recombinants were found between *COLc* and *HR* in the Terese x Champagene RILs population. On the other hand, the map position of *ELF3* in Medicago is within the range of where *HR* is mapped. Mapping data from Chapter 3 placed *PsELF3* on top of pea LGIII and linked to morphological marker *M* in NGB5839 (Torsdag) x JI1794 F_2 mapping population. These results are consistent with the map position of *HR* as *HR* is tightly linked to *M* as well (Murfet, 1973). Unfortunately, we were unable to test candidate gene relationship between *ELF3* and *HR* by directly checking their co-segregation in mapping population of Terese and Champagne (where *HR* is mapped previously) since there is no polymorphism detected in introns of *ELF3* between the mapping parents. Regardless, map position of Medicago and pea *ELF3* ortholog supports it as a potential candidate gene for *HR* where the candidate gene range of *HR* is narrowed down in between *FRI* and *COLc* in both species by comparative mapping approach.

7.3.4. HR is the likely pea ortholog of Arabidopsis ELF3

Despite difficulty encountered with mapping *PsELF3* relative to *HR*, taken together, the phenotypes with characterization of *HR* and mapping relative to flowering-related genes strongly suggest it is highly likely that *ELF3* is a possible candidate gene for *HR*. Therefore, the *ELF3* sequence was examined directly. As outlined in Chapter 3, the *PsELF3* has been isolated in our standard wild-type NGB5839 before the start of this project (C. Lai and V. Hecht, unpublished data) and extended to full length in both cDNA and gDNA in current study. Careful annotation of this sequence revealed a frameshift mutation in exon 1 of *PsELF3* predicted to introduce a premature stop codon. A comparison of *ELF3* cDNA sequence in NGB5839 (*hr*) with the *HR* line WL1771 (Taylor and Murfet, 1993) revealed a normal full length ELF3 predicted in WL1771 (HR), but a single nucleotide insertion in *hr* before intron 1 which will resulting in the observed frameshift. This "6C" mutation is predicted to truncate ELF3 protein after 21 nonsense amino acid (Figure 7.4A).

The recessive *hr* allele in NGB5839 is a naturally occurring mutation and its origin is obscure. Therefore, to get a better idea of the origin and distribution of this mutation, we examined a number of different lines including primitive lines *P. abyssinicum*, *P. elatius*, and *P. fulvum* for the presence of *ELF3* "6C" mutation (Figure 7.4B). The preliminary sequencing results showed that primitive lines including *P. abyssinicum*, *P. elatius*, and *P. fulvum* carry the "5C" alleles. In addition to that, winter pea cultivars including a few lines (Champagne, AustrianWinter, and Winterberger) that is known to be *HR* alleles (Lejeune-Hénaut et al., 1999) carry the "5C" alleles while spring cultivars have "6C" alleles. Together, all these results show that *HR* is the pea ortholog of Arabidopsis *ELF3*

and it is mutated in our standard wild-type NGB5839. Furthermore, there is a hint that winter cultivars carry WT alleles while spring cultivars carry mutated alleles at *HR* locus.

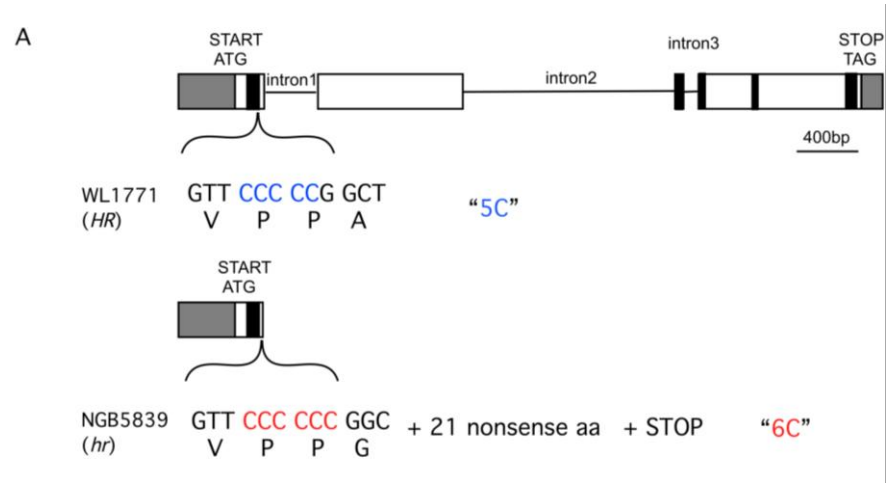

B

	Species	Sowing type	Lines	Sequences	Group
Wild	*P. abyssinicum*		JI2	GAACAATTCGGTTCCCCC-GGCTTCCTCGAGCCAG	3.1
	P. elatius		JI64	GAACAATTCGGTTCCCCC-GGCTTCCTCGAGTCAG	3.2
	P. elatius		JI1794	GAACAATTCGGTTCCCCC-GGCTTCCTCGAGCCAG	3.U
	P. fulvum		JI1796	GAACAATTCGGTTCCCCC-GGCTTCGTCGAGTCAG	3.6
Cultivated	*P. sativum*	Winter	Champagne	GAACAATTCGGTTCCCCC-GGCTTCCTCGAGCCAG	1.u
	P. sativum	Winter	WL1771	GAACAATTCGGTTCCCCC-GGCTTCCTCGAGCCAG	-
	P. sativum	Winter	AustrianWinter	GAACAATTCGGTTCCCCC-GGCTTCCTCGAGCCAG	1.6
	P. sativum	Winter	Winterberger	GAACAATTCGGTTCCCCC-GGGTTCCTCGAGCCAG	-
	P. sativum	-	JI281	GAACAATTCGGTTCCCCC-GGCTTCCTCGAGCCAG	U
	P. sativum	Spring	NGB5839	GAACAATTCGGTTCCCCCCGGCTTCCTCGAGCCAG	1.2
	P. sativum	Spring	Terese	GAACAATTCGGTTCCCCCCGGCTTCCTCGAGCCAG	1.U
	P. sativum	Spring	JI399	GAACAATTCGGTTCCCCCCGGCTTCCTCGAGCCAG	2.1
	P. sativum	Spring	Vitalis	GAACAATTCGGTTCCCCCCGGCTTCCTCGAGCCAG	1.U
	P. sativum	Spring	Cameor	GAACAATTCGGTTCCCCCCGGCTTCCTCGAGCCAG	-

Figure 7.4 Molecular characterization of *ELF3* locus.
(A) Diagram of the *ELF3* cDNA showing the location and nature of *hr* mutation in NGB5839 when compared to WL1771 (*HR*) and also the predicted protein. Intron positions are marked solid lines whereas regions highlighted in black are conserved amino acids sequence based on the phylogenetic analysis of ELF3-related proteins from Fig 3.2.
(B) Preliminary sequencing results within the insertion mutation site across selected pea varieties including wild and cultivated pea (winter or spring cultivars). "5C" haplotypes are highlighted in blue while "6C" haplotypes are highlighted in red. The subgroup classification of each line is listed according to Jing et.al. (2010).

7.3.5. Distribution of HR alleles and its correlation with photoperiod responsiveness

To examine in more detail the possible distribution of the *ELF3* "6C" mutation, a small representative set obtained from JI pisum collection was selected for the presence of *hr* mutation and its correlation with photoperiod responsiveness. Selection was guided by a recent report (Jing et al., 2010) characterized genetic diversity on more than 3000 lines in JI germplasm using 45 retrotransposon based insertion polymorphism (RBIP) markers. The structure analysis revealed three groups (Group 1 to 3) in the JI germplasm (Figure 7.5A). Group 1 and 2 are almost entirely cultivated lines including Champagne, AustrianWinter, NGB5839, Terese, JI399, and Vitalis cultivars whereas Group 3 is made up of a mixture of primitive lines (*P. abyssinicum* (subgroup 3.1), *P. elatius* (subgroup 3.2), and *P. fulvum* (subgroup 3.6) and landrace (Jing et al., 2010). Lines from Group 3 were selected for study because it might be where the origin of *Pisum* domestication events occurred. A single line was chosen from each of the subgroups 3.1, 3.2, and 3.6 and eight representative lines was selected for subgroups 3.3 to 3.5 for the study of distribution of *ELF3* "6C" mutation.

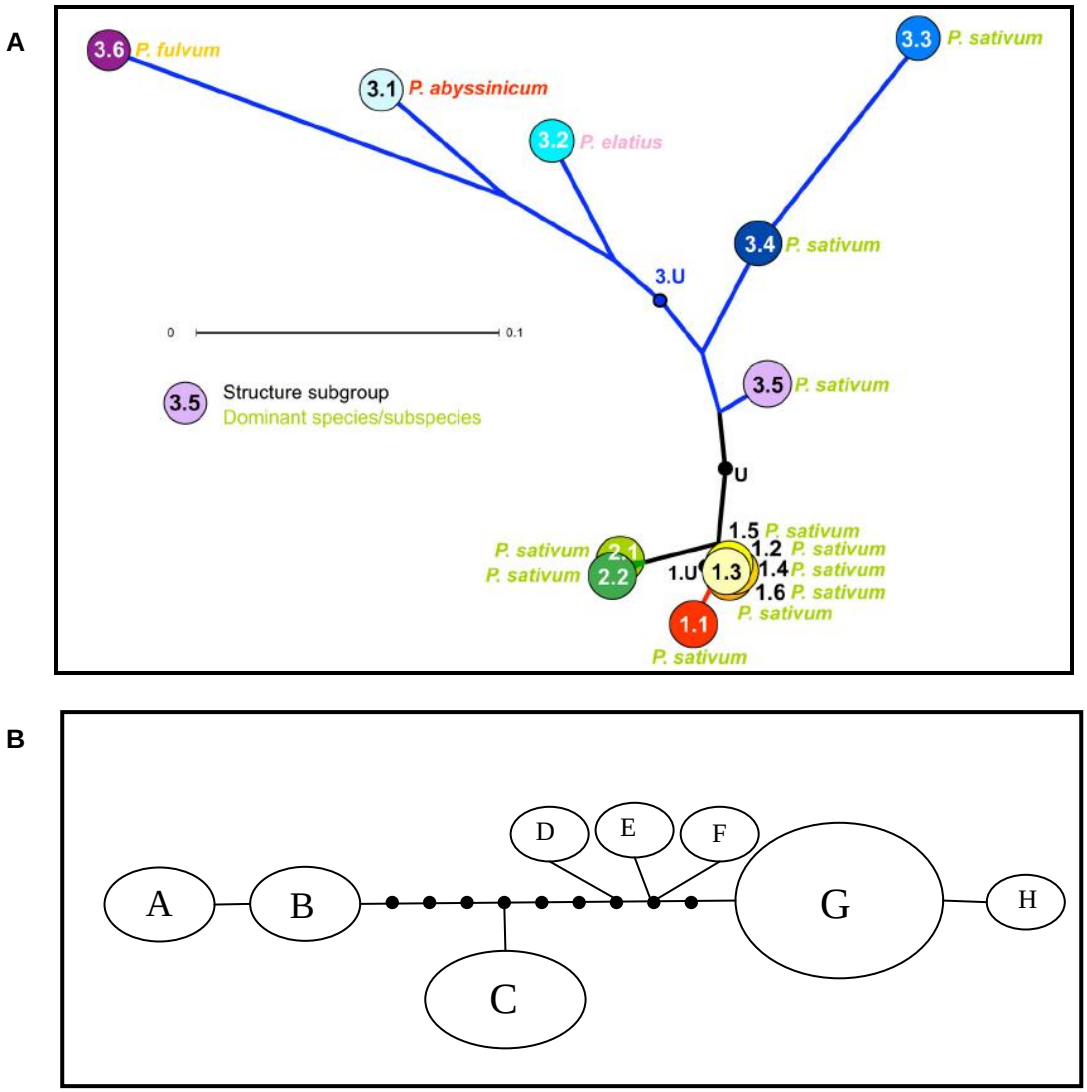

Haplotypes (frequency)	Nucleotide position (bp) from ATG											
	220	227	233	246	251	256	272	325	335	349	363-369	376
A (6)	C	C	C	T	C	-	A	G	A	G	A	T
B (6)	-	C	C	T	C	-	A	G	A	G	A	T
C (7)	-	C	C	T	C	-	A	A	G	A	GTTG	A
D (1)	-	C	C	A	T	G	A	G	G	G	GTTG	A
E (1)	-	G	T	A	T	G	A	G	G	A	GTTG	A
F (1)	-	G	T	A	T	G	G	G	G	G	GTTG	A
G (9)	-	C	T	A	T	G	A	G	G	G	GTTGTT	A
H (1)	-	G	T	A	T	G	A	G	G	G	GTTGTT	A

Figure 7.5 Distribution of *HR* mutation across Pisum germplasm collections. (A) Relationship among subgroups of Pisum germplasm defined by structure analysis (taken from Jing et.al. 2010) (B) Haplotype network estimated by statistical parsimony and a summary of polymorphism for each haplotype. Each of the 8 haplotypes is designated by letters and the areas of the ovals are approximately proportional to frequency. Each single line represents one polymorphism and small black circles represent missing haplotypes. Analysis is based on preliminary sequencing result of partial *ELF3* genomic DNA sequences (approximate 200bp).

Preliminary sequencing data around the "5C/6C" mutation including partial intron1 sequences (approximate 200bp in total) identified 8 distinct haplotypes (A-H) defined by 13 different polymorphisms (Figure 7.5B). Among them, only haplotype A includes the '6C' polymorphism and the rest (haplotype B to H) are all carrying '5C' alleles. Haplotype A includes NGB5839, Terese, JI399, JI1624, JI1629, and JI2712. JI2712 is from Subgroup 3.4 whereas JI1624 and JI1629 are from subgroup 3.5. Interestingly, haplotype B differs from haplotype A only at the site of '6C' mutation. It is present in two known *HR* lines (WL1771 and Champagne) and JI281 (group U) and 3 other lines from subgroup 3.4 (JI3459) and 3.5 (JI103 and JI1474). Haplotype C differs from haplotype A and B by 5 polymorphisms and is present in lines from subgroup 3.3 (JI1660, JI2702, JI3471) or 3.4 (JI1054, JI1510, JI1531, and JI5335). Haplotype D and E are each represent the single lines from subgroup 3.1 (JI1067, *P. abyssinicum*) and 3.6 (JI1633, *P. fulvum*) respectively. They differ from haplotype C by 4 to 5 polymorphisms. Haplotype F (JI1794, subgroup 3.U) appears to have only one difference to Haplotype E (JI1633, subgroup 3.6). Haplotype G is present in several lines from subgroup 3.3 (JI859, JI1190, JI1653, JI2709), 3.4 (JI106, JI1682), and 3.5 (JI2706, JI2711, and JI3470). Haplotype H has one extra polymorphism from Haplotyope G which represents single line JI858 from Subgroup 3.2 (*P. elatius*). Even in short *ELF3* sequences, the presence of same '6C' mutation from divergent lines suggest single origin of *ELF3* mutation. The difference of haplotype A and B is strongly based on different alleles on *HR* locus.

In parallel with *ELF3* sequencing, several photoperiod-responsive traits including flowering, branching, and leaf area were also scored for selected lines from Figure 7.5. Figure 7.6A shows that all of the lines flower in LD with node of

first flower initiation ranging from 15 to 25. However, in SD only 6 lines out of the 24 lines examined had flowered 3 months after sowing. This includes the 3 lines carrying the *ELF3* '6C' allele (JI2712, JI1624, and JI1629) and 3 lines from subgroup 3.5 (JI103, JI1474, and JI2711). The other lines showed obligate LD requirement for flowering.

Lines were also extremely variable in branching phenotype. Whereas most lines showed strong photoperiod response without branching in LD, some showed branching in LD which was enhanced by SD (Figure 7.6B). Interestingly however, three of the '6C' lines were distinguished by the fact that they showed no branching in either LD or SD.

Similar result was also found in leaf area (Figure 7.6C), the three lines with '6C' allele have no difference in leaf area between LD-grown and SD-grown plants. The rest of the lines showed larger leaf area in LD if compared to SD. All these results indicate that the '6C' mutation in *ELF3* is highly associated with relaxed LD requirement for flowering and reduced sensitivity of photoperiod responsiveness.

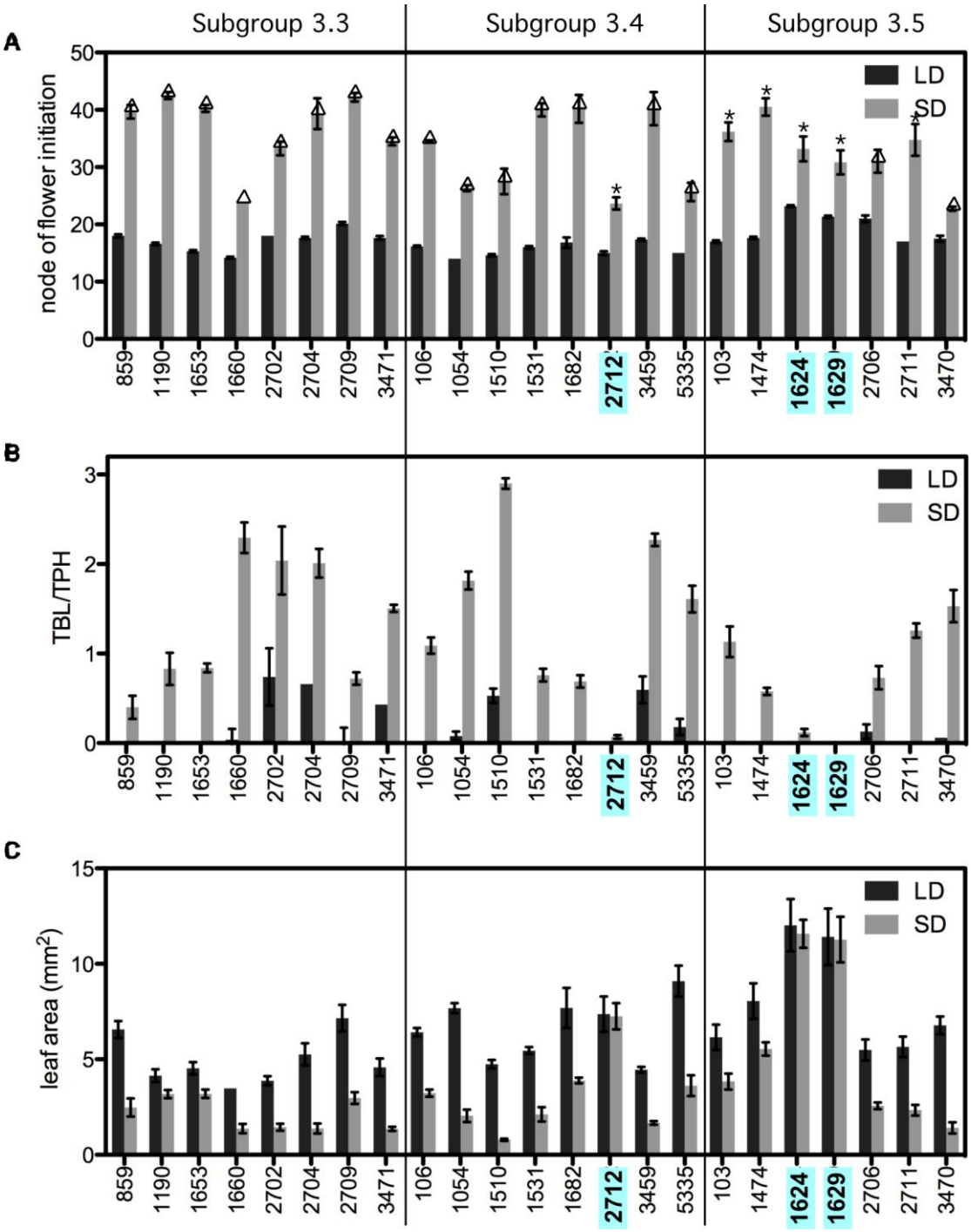

Figure 7.6 Association of *ELF3* mutation with photoperiod-responsive traits. (A) node of flower initiation (B) branching (Total Branch Length (TBL)/ Total Plant Height (TPH)) (C) leaf area. Plants with "6C" allele are highlighted in blue. Plants flower in SD are marked with * symbol whereas the others (Δ) are scored as total node number after 3 months from sowing. Data are mean ± SE for n = 3 to 6 plants.

7.3.6. The hr mutant shows early, photoperiod-dependent flowering

The observation that *HR* involved in circadian clock and photoperiod responsiveness encourages us to revisit its effect on flowering. As shown in Figure 7.7, NGB5839 which is the *hr* mutant flowers earlier than its isogenic wild-type (*HR*) in both SD and LD. However, *hr* mutant is still response to photoperiod as it flowers earlier when grown in LD than in SD. This photoperiod response to flowering is still present in *HR* lines but their flowering is delayed in both SD (8 nodes) and LD (10 nodes) (Figure 7.7B, left). As for reproductive node, *HR* lines produce more reproductive nodes than *hr* line in both LD and SD (Figure 7.7B, right). Intriguingly, the difference between *hr* and *HR* lines in SD is not as big as described in previous literature (Reid and Murfet, 1977) that *HR* should flowers around node 50 which is approximately 30 node later than *hr* mutant. The flowering node differences between present experiment and previous literature could be due to difference in genetic background or quality of light during the extension period in phytotron. Consistent with this, the flowering node of *HR* lines were previously showed to be highly affected by light quality and night break of different lights (Reid and Murfet, 1977). It will be interesting to examine the flowering phenotype in different light quality in the future. In short, *HR* appears to delay flowering and cause prolonged reproductive growth.

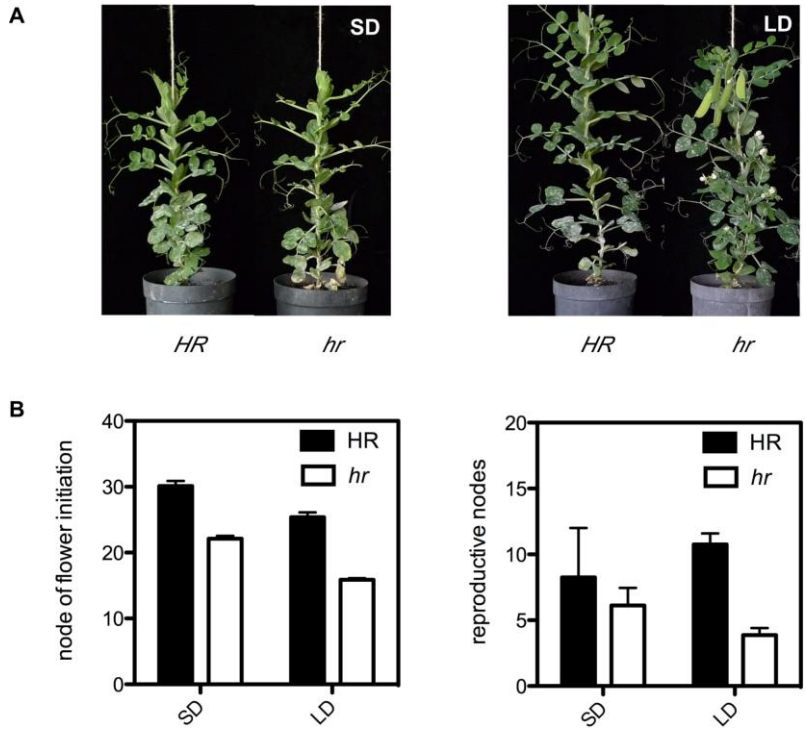

Figure 7.7 The *hr* mutant is early flowering and photoperiod-dependent. (A) Representative of 8-week-old of NGB5839 (*hr*) and its isogenic wild-type lines. (B) Node of flower initiation (left) and final number of reproductive nodes (right). Data are mean ± SE for n = 8 plants. All plants were grown in the phytotron under standard SD or LD conditions.

7.3.7. Effect of HR on CO and FT expression

In view of the effect of *HR* on flowering time, it is also of interest to examine its effect on expression of *CO*- and *FT*-like genes. Here the expressions rhythms of both diurnal and circadian of *CO* and *FT*-like genes are examined in *hr* and its isogenic line. This is also the first time the circadian regulation of these genes has been examined.

As described in previous chapters (Chapter 4-6), the closest homolog to Arabidopsis *CO*, *PsCOLa* showed a clear diurnal expression rhythm in WT peaking at dawn (ZT0 and ZT24), but showed no difference in the early mutants (*dne-1*, *sn-4*, *ppd-3*). Since we now know our standard WT (NGB5839) is carrying the *hr* mutation, a loss of function allele for *ELF3*, it is of interest to examine

COLa expression again in a line with functional *HR*. Figure 7.8 shows that the introgression of *HR* affects neither diurnal nor circadian rhythms of *COLa* expression when compared to *hr* line. Similar to *COLa*, *COLb* expression was previously showed to be rhythmic under diurnal cycle with peaks around dawn (ZT0 and ZT24) as well. As for *COLa*, no clear difference was spotted between early mutants (*dne-1*, *sn-4*, *ppd-3*) and their WT (Chapter 4-6). Here the diurnal rhythms of *COLb* in *hr* line are similar to what have been showed in previous chapters but rhythm of *COLb* in LL is abolished (Figure 7.8). However, *COLb* expression is always higher in *hr* if compared to *HR* lines in either diurnal or LL cycles.

In the *hr* (NGB5839) line, the clearest rhythm regulation was seen for *FTa2* which showed a peak around dusk at ZT8. *FTa1* and *FTb1* showed weak diurnal rhythms peak at ZT8 and ZT20 respectively while no clear rhythm was found for *FTb2* in *hr* line (Figure 7.8). In LL, weak rhythms were found for *FTa2* and *FTb1* in *hr* alleles whereas *FTa1* and *FTb2* rhythms are clearly not rhythmic (Figure 7.8). When compared to isogenic *HR* line, all the *FT*-like pea orthologs are expressed higher in *hr* except for *FTa1* which has similar level in both *hr* and *HR* lines. However, only expression rhythms of *FTa2* of *HR* line persist in LL for at least one cycle (Figure 7.8). In short, higher levels of *FT*-like genes expression are consistent with early flowering of *hr* mutant.

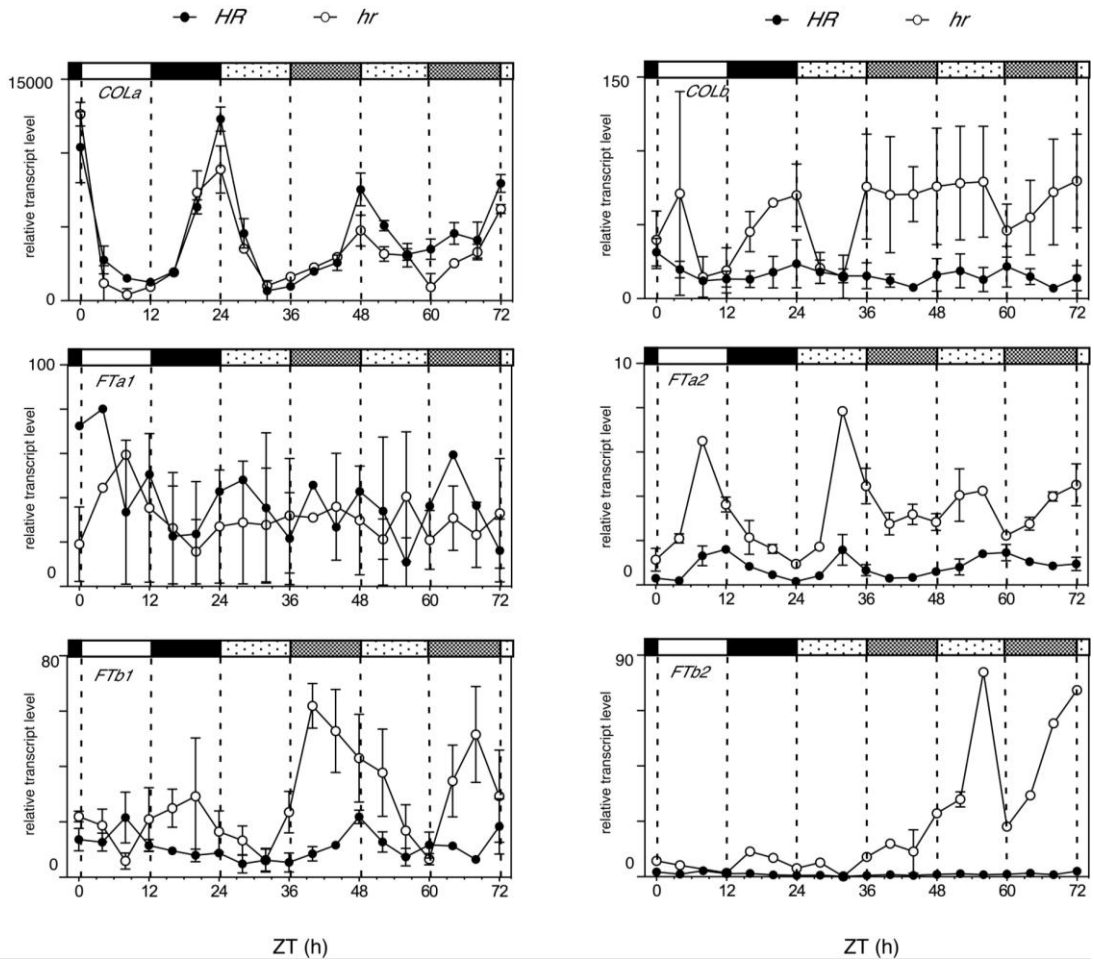

Figure 7.8 Effect of *HR* on *CO*- and *FT*-like gene expression. Plants were grown in growth cabinets under a light/dark cycle (12L:12D) at 20°C for 3 weeks before transfer to continuous light. Data are mean± SE for n = 2 biological replicates, each consisting of pooled material from two plants. Zeitgeber time (ZT) refers to the time since lights-on of the last full entraining cycle. Bars above the graph refer to periods of light (open or stippled bars). The heavy and light stippled bars indicate the periods of subjective night and subjective day respectively during the period of continuous light.

7.3.8. Effect of HR on cold tolerance

In addition to its effects on flowering and photoperiodism, *HR* locus has also been reported to colocalise with a major QTL for winter frost tolerance in field condition (Lejeune-Hénaut et al., 2008). As mentioned in the introduction of this chapter, this might reflect either a pleiotropic effect of *HR* or the involvement of closely linked genes. In the QTL study, winter frost damage of 164 F_8 RILs from Terese and Champagne cross were measured in the field in 11 different locations across 3 years timeframe based on assessment on the damage to the aerial part of the plants (Lejeune-Hénaut et al., 2008). One possibility is that *HR*/*ELF3* like *GI*, another clock gene in Arabidopsis, is involved in cold stress response and resulted in Arabidopsis *gi* mutant is less tolerant to cold and defected in cold acclimation (Cao et al., 2005). Therefore, it is of interest to examine if there is any difference on foliar frost tolerance response between lines of *hr* and *HR* genotypes. Besides NGB5839 (*hr*) and its isogenic line (*HR*), I also included Champagne in the preliminary study of effect of *HR* on cold tolerance as a reference to I. Lejeune- Hénaut's study. Frost tolerance was examined by leaf photochemical efficiency on leaflets from plants both with or without a preceding acclimation period of cold treatment. Leaf photochemical efficiency (Fv:Fm, ratio of variable to maximum fluorescence) was used as a measurement of plant photosynthesis performance with a healthy leaf expected to have a Fv:Fm of approximate 0.8 while damaged leaf should have lower Fv:Fm ratio.

Figure 7.9A shows the Fv:Fm value on plants exposed to normal temperature followed by cold treatment over a range of freezing temperature (-2°C to -10°C). At -2°C of cold treatment, no reduction in Fv:Fm was observed in any genotype. The Fv:Fm value started to decline at -5°C in all three genotypes. At

-7°C, the leaf of Champagne is totally damaged by the cold treatment. Similar result was observed at -10°C, but no difference was found between NGB5839 and its isogenic *HR* line. On the other hand, Figure 7.9B shows the Fv:Fm value on plants exposed to cold acclimation before subjected to cold treatment. In overall, cold acclimation increase the freezing tolerance of all genotypes examined. Severe damage was only observed at -10°C in plants exposed to cold acclimation where Champagne line was dramatically damaged while NGB5839 and *HR* have similar value of Fv:Fm across all the temperature.

In conclusion, there is no apparent association between *HR* genotype and cold tolerance in either treatment. We expected NGB5839 with *hr* allele to be more sensitive to freezing than a near-isogenic *HR* allele and cv. Champagne. In contrast, NGB5839 was found to be either similar or even more tolerant to cold than the other two genotypes in either treatment. This result suggest the major contribution of *HR* to frost tolerance might not occur at the level of foliar tolerance but might be through the delay in flowering time or other modification on growth habits but not on tissue level.

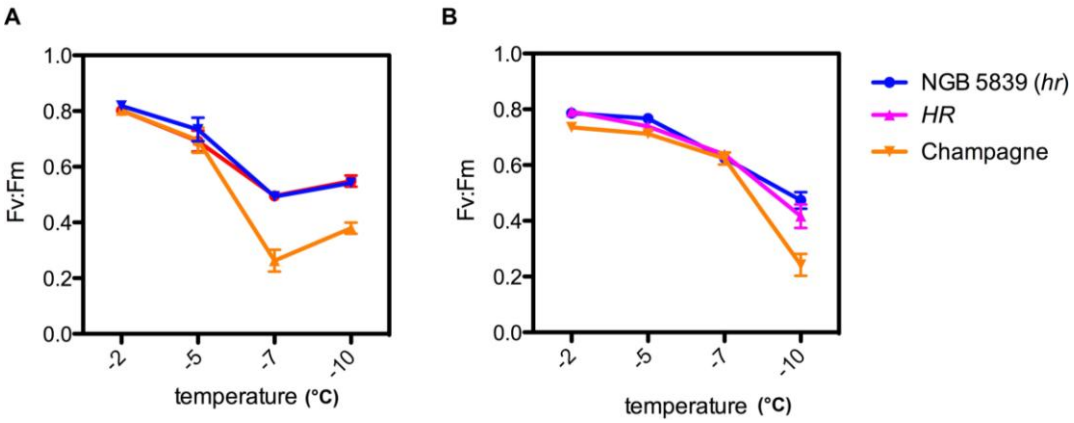

Figure 7.9 Effect of cold stress on leaf photochemical efficiencies (Fv:Fm) in different *HR* line. Plants are grown in growth cabinets under a light/dark cycle (8L:16D) at (A) 20°C day temperature and 20°C night temperature for 3 weeks (B) 20°C day temperature and 20°C night temperature for 2 weeks and 10°C day temperature and 3°C night temperature for 1 week before subjected to cold treatment (-2, -5, -7, or -10°C) for 3 hours. Data are mean ± SE for n = 6 plants. Fv = variable fluoresces; Fm = maximum fluoresces.

7.3.9. Effect of sn on circadian rhythms in HR background

The fact that NGB5839, like many spring cultivars, carries recessive *hr* means that all mutants generated in this background are essentially double mutants. This is particularly significant for our previous analyses of *dne-1*, *sn-4*, and *ppd-3* mutants as the full effect of these loci on rhythmic gene expression might be disturbed or masked by the presence of recessive *hr* alleles in NGB5839. As the *sn HR* genotype had already been selected (Chapter 5), we used this material to re-examine the effect of *SN* on a *HR* background. Due to time constraint, single replicate was examined but clear difference was found between *SN HR* and *sn HR* genotype. As previous experiment (Figure 7.2), *SN HR* shows diurnal and circadian rhythms in most of the clock genes in the single replicate examined except *ELF3* (Figure 7.10). Small differences with previous experiment were observed such as *LUX* expression showed strong first peak in diurnal cycle followed by weak circadian rhythm and an extra peak for *ELF4* transcript found at ZT21 suggesting replication is needed.

In *sn HR*, phase advances were found in *ELF4*, *LATE1*, *PRR37*, and *PRR59* under 12L: 12D diurnal condition (Figure 7.10). These results are consistent with diurnal rhythms of *sn* mutant in *hr* background in 16h SD condition (Figure 5.4). *MYB1* expression was slightly lower at peak level in *sn HR* mutant which again is similar to those found in *sn*-4 (*sn hr*) (Figure 5.4). In LL, the expression level of *MYB1*, *TOC1*, *ELF4* and *PRR37* were damped low in *sn HR* compared to *SN HR* (Figure 7.10). The single replicate in *SN HR* did not show a clear rhythm for *LATE1* and *PRR59* in LL making comparisons difficult, but a similar early-shifted broad first peak were observed in *sn HR* (Figure 7.10). It is also hard to compare the effect of *sn* mutation in *HR* background on *ELF3* and

LUX expression since the circadian rhythms of *ELF3* and *LUX* are unclear and need to be checked in other replicates. In contrast, the expression rhythm of *TOC1*, *ELF4*, *LATE1*, *PRR37*, and *PRR59* become arrhythmic in *sn* mutant after transfer to LL condition. The only exception is *MYB1* expression which stayed low but rhythmic in *sn* mutant (Figure 7.10).

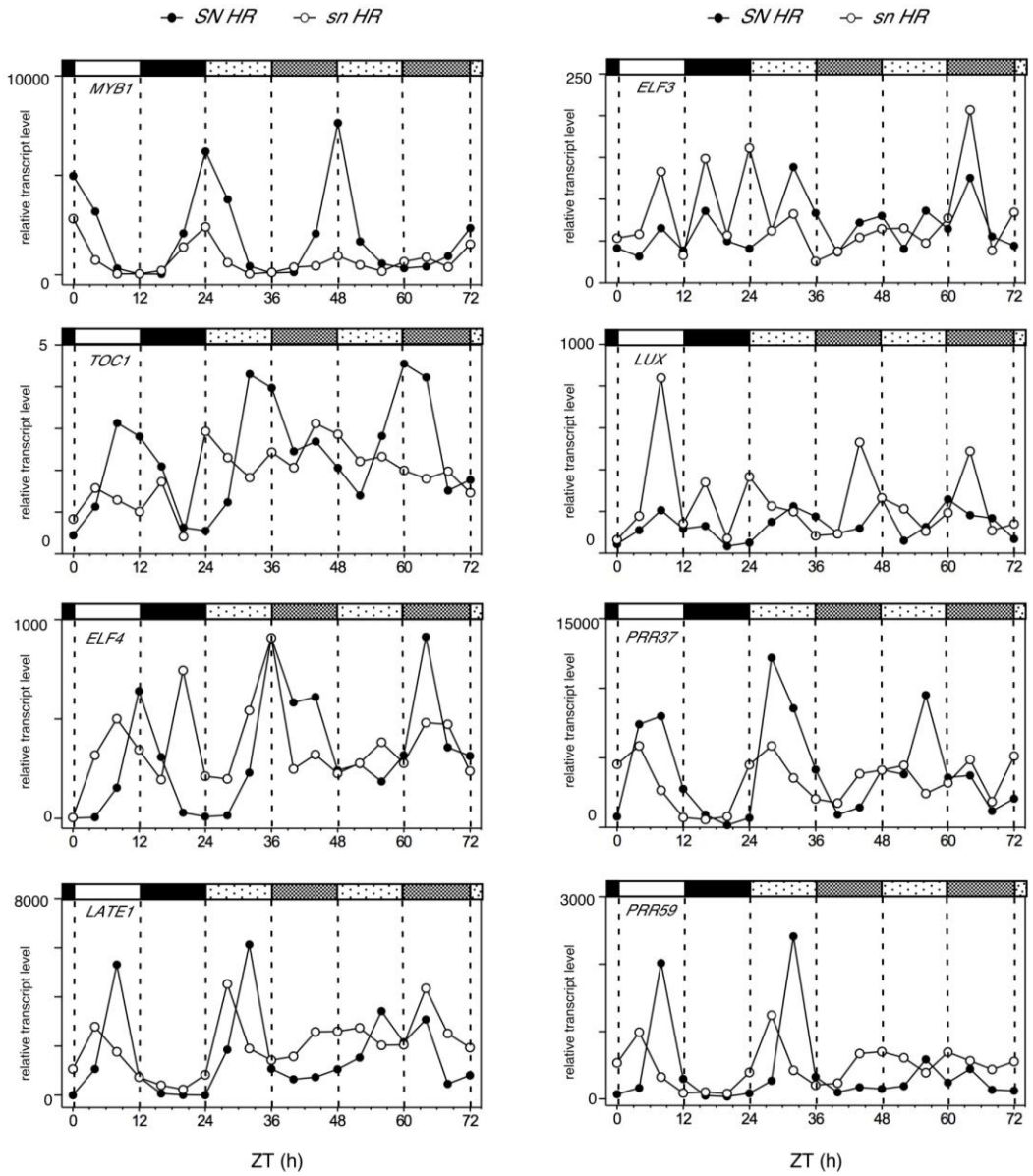

Figure 7.10 Effect of *SN* on clock gene expression in *HR* background. Plants were grown in growth cabinets under a light/dark cycle (12L:12D) at 20°C for 3 weeks before transfer to continuous light. Data is single biological replicate consisting of pooled material from two plants. Zeitgeber time (ZT) refers to the time since lights-on of the last full entraining cycle. Bars above the graph refer to periods of light (open or stippled bars). The heavy and light stippled bars indicate the periods of subjective night and subjective day respectively during the period of continuous light.

Expression of *FTa2* was also examined in *sn HR* since *FTa2* was the only *FT-like* gene showing clearly rhythmic expression under LL (Figure 7.8). As in the previous experiment, rhythms of *FTa2* of WT (*SN HR*) peaked in the evening (ZT8), and the *sn* mutant caused a phase shift of 4 hours earlier in entraining cycle and the first subjective day before the rhythms become arrhythmic and constitutively high under LL (Figure 7.11).

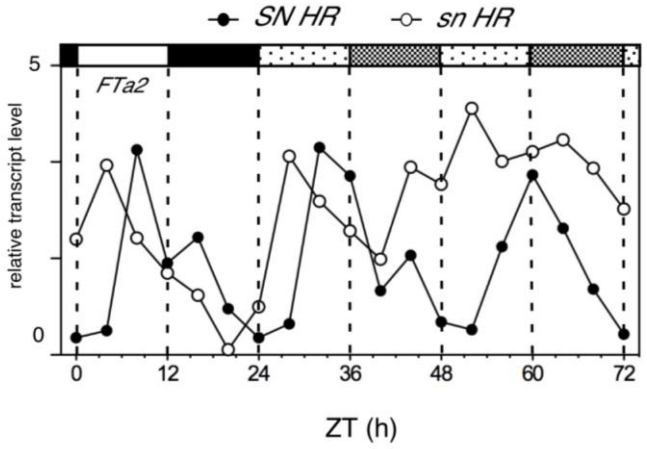

Figure 7.11 Effect of *SN* on *FTa2* expression in *HR* background. Plants were grown in growth cabinets under a light/dark cycle (12L:12D) at 20°C for 3 weeks before transfer to continuous light. Data is single biological replicate consisting of pooled material from two plants. Zeitgeber time (ZT) refers to the time since lights-on of the last full entraining cycle. Bars above the graph refer to periods of light (open or stippled bars). The heavy and light stippled bars indicate the periods of subjective night and subjective day respectively during the period of continuous light.

7.4. Discussions

This chapter sets out to investigate molecular basis for *HR* locus through physiological studies and positional candidate gene approach. Initially however, abnormally damped circadian rhythms in LL were found in our standard wild-type NGB5839. Introgression of a functional *HR* allele restores these circadian rhythms in LL back to normal. This suggests that the defective circadian rhythms and early SD flowering in NGB5839 might both be consequences of the recessive *hr* allele. Together with this phenotype of conditional arrhythmia in LL, comparative mapping has successfully identified candidate gene relationship between *ELF3* and *HR*. Broader investigation of *ELF3* sequence variation in range of pea germplasm supported identity of *HR* as *ELF3* and its association with photoperiod responsive traits including flowering, branching, and leaf expansion.

7.4.1. Roles of HR in circadian clock

The recessive *hr* allele in NGB5839 causes arrhythmic expression rhythms of *TOC1*, *LATE1*, and *LUX* in LL and maintained at a median level when compared to its isogenic *HR* line (Figure 4.3 and 7.2). These results are similar to those reported for Arabidopsis *elf3* mutants (Schaffer et al., 1998; Fowler et al., 1999; Alabadi et al., 2001; Hazen et al., 2005). *MYB1* (the closest pea homolog of Arabidopsis *LHY/CCA1*) has reduced circadian rhythms in *hr* mutant but the rhythm is sustained for at least 2 cycles under LL. This finding was exactly what has been found for *LHY* expression in *elf3* mutant (Schaffer et al., 1998). However, *HR* appears to have no significant effect to *ELF4* expression. This is different from what has been studied in Arabidopsis where *ELF4* expression was found to be elevated in the *elf3* mutant under constant red light (Kikis et al., 2005).

Nonetheless, unlike Arabidopsis *ELF3*, expression of *ELF3* ortholog in pea under LL is not rhythmic. Therefore it is hard to compare the effect of *hr* mutation on *ELF3* expression which is found to be self-regulated in Arabidopsis (Hicks et al., 2001). Despite the significant roles of *ELF3* on circadian rhythms under LL, little effect was seen in DD. The only exception is *LATE1*/*GIGANTEA* expression in DD which is highly expressed in *hr* when compared to its near-isogenic *HR* line. This result is also similar to what have been found in Arabidopsis where *GI* expression are all time higher in *elf3* mutant under LD, SD, and LL (Fowler et al., 1999).

The conditional arrhythmia under LL but not DD condition in NGB5839 (pea *elf3* mutant) suggests *PsELF3*/*HR*, similar to *AtELF3*, functions in regulation of light input to circadian clock (Covington et al., 2001). Based on Arabidopsis model, ELF3 might serve as an adaptor for COP1-mediated degradation of GI in the dark (Kim et al., 2005; Yu et al., 2008). However, GI level is maintained in the light where it interacts with ZTL to target light-dependent TOC1 protein degradation (Kim et al., 2007). TOC1 then regulates *LHY* expression through the core negative-feedback loop. Consistent with damped *LHY* expression, *TOC1* expression was arrhythmic at the median level in the *hr* mutant which peak at the opposite phase of *LHY* expression rhythms. Our results in the study of *HR* in pea are quite consistent with the Arabidopsis model where *HR* is required for controlling light input to circadian clock and regulating stability of *GI* which in turn affect *MYB1*, *TOC1*, and *LUX* expression. In addition to light-dependent function of *ELF3* on circadian clock, *elf3* mutant in Arabidopsis failed to maintain rhythmicity when entrained to thermocycle which eventually suggest *ELF3* might be important to ambient temperature response and temperature entrainment

(Thines and Harmon, 2010). This could be an interesting area for future study of *HR* in pea.

Since our standard wild-type is a mutant of *HR*, it is now understandable why we did not see clear rhythms under constant light condition. Furthermore the recessive *hr* allele in NGB5839 might have blocked the effect of *dne*, *sn*, and *ppd* mutants generated in this background due to the circadian nature of all these loci. In Chapter 5, *sn* mutant in *HR* background is similar in flowering phenotype to *sn hr* double mutant which imply *SN* is epistatic to *HR* in regulation of photoperiodic control of flowering time. Here, circadian rhythms under LL in *sn HR* mutant (Figure 7.10) were studied and compared to what have been published in Arabidopsis *lux* mutant (Hazen et al., 2005; Onai and Ishiura, 2005). In *sn HR*, the circadian rhythms of *MYB1* gene expression is rhythmic and damped low whereas *TOC1*, *ELF4*, *GI*, and *LUX* are arrhythmic but clamped at moderate level. This result is consistent to what have been found in *lux* mutant (Hazen et al., 2005; Onai and Ishiura, 2005). This suggest *SN*, like its Arabidopsis ortholog *LUX*, is necessary to promote *LHY* expression and inhibit *TOC1*, *ELF4*, *GI* and its own expression. Furthermore, we also noticed *PRR37* and *PRR59* expression rhythms are also arrhythmic and high in *sn HR* which have not yet examined in Arabidopsis *lux* mutant. The overall effect of *SN* on circadian rhythm is similar to its Arabidopsis ortholog which suggest the function of *SN* on circadian clock is conserved in these two species. As both of the *sn* and *hr* mutations is now known to cause arrhythmia under LL, it is therefore hard to separate the effect of *SN* and *HR* alone in LL or to study their interaction on regulation of circadian rhythm in LL. However in DD, it is clear that *sn* mutation does not intensify the arrhythmicity caused by recessive *hr* alleles but did show alteration to the phase

and/or period of the cycle (Figure 5.5 and Figure 7.2).

7.4.2. Pleiotropic effect of HR

The early, photoperiod-insensitive flowering initiation of *elf3* mutant is one of the characteristics which distinguished it from Arabidopsis phytochrome mutants which otherwise have similar effects on hypocotyl elongation (Zagotta et al., 1996). The pea *hr* mutation appears to confer only a reduction but not a complete loss of photoperiod response, where the *hr* mutant in SD flowers earlier than *HR* in SD but still later than *hr* in LD. In Arabidopsis, the early-flowering phenotype of *elf3* mutant was found to be associated with elevated diurnal *FT* rhythms in the inductive LD condition (Kim et al., 2005) with a peak around dusk at ZT16. In the pea *hr* line NGB5839, elevated level of several *FT*-like gene (*FTa2*, *FTb1*, and *FTb2*) expressions were found under diurnal (12h-SD) and circadian cycle (LL) (Figure 7.8) relative to a near-isogenic *HR* line. However, *FTa2* is the only *FT*-like gene which shows clear diurnal in SD and circadian rhythms in LL which also peak around dusk at ZT8 under SD and subjective day at ZT32 and ZT60 respectively (Figure 7.8 and 7.11). The *hr* mutation not only causes elevated *FTa2* diurnal and circadian expression but also results in arrhythmic *FTa2* circadian rhythms in LL. Similar result on *FTa2* expression was also found in *sn* mutant in *HR* background. This suggests both of *HR* and *SN*, pea ortholog of Arabidopsis *ELF3* and *LUX*, are required for regulation of circadian rhythm of *FTa2* expression. Besides pea and Arabidopsis, *FT* homologs have been isolated in several other species including rice (Izawa et al., 2002), soybean (Kong et al., 2010), barley (Faure et al., 2007), poplar (Hsu et al., 2006; Igasaki et al., 2008), morning glory (Hayama et al., 2007) and orchid (Hou and Yang, 2009). Despite

different growth habits of these species, diurnal and/or circadian rhythms have been found for these homologous genes. Soybean which is another member of legume family, has 10 *FT* members and two of them, *GmFTa3* and *GmFTc1*, were found to be up-regulated by the inductive SD (Kong). *GmFTa3* is the likely homolog of pea *PsFTa2* (Hecht et al., 2011) and *GmFTa3* showed diurnal rhythm peaking at ZT4 in a 12h SD cycle which is around the same time as *PsFTa2*. In additional to diurnal or circadian rhythms, the expression of *FT*-like genes throughout the development should be examined in the future between *hr* and *HR* genotypes in order to figure out which *FT*-like is likely to be associated with reproductive development.

Besides *FT*-like genes expression, we also examined *COL* gene expressions in *hr* mutant (Figure 7.8). However, similar to previous results on *dne*, *sn*, and *ppd* mutants, the closet homolog to Arabidopsis *CO* in pea, *COLa*, does not show any difference in expression between *hr* and *HR* genotypes (Hecht et al., 2005). Intriguingly, *COLb* expression is higher in *hr* mutant where there is no difference found in the other three early mutants. However, the phylogenetic analysis of *CO*-like genes in legume and Arabidopsis showed that *COLb* clusters with *AtCOL3* and *AtCOL4* which little is known about their function in Arabidopsis (Hecht et al., 2005). It is therefore hard to prove that *COLb* is functionally involved in the flowering in pea. Nonetheless, the elevated *COLb* transcript level might be associated with increase of *GI* expression in *hr* mutant as GI in Arabidopsis is known to form FKF1-GI complex which is responsible for the LD-specific peak of *CO* in the evening (Sawa et al., 2007). However, studies in Arabidopsis also suggest *ELF3* might negatively regulate *FT* expression through a CO-independent pathway by down-regulating *SVP*/*FLC* expression (Yoshida et al.,

2009). It is therefore be interesting to examine *SVP* mRNA and protein level in *hr* mutant.

In the germplasm study, 3 out of 24 lines are found to carry recessive *hr* allele ('6C' mutation) and all of them flower in SD while majority of the rest did not flower after 3 months from sowing (Figure 7.6). Nonetheless, there are 3 lines from Subgroup 3.5 without the *ELF3* '6C' alleles also initiate flower in SD as well. There are two possible explanations for this result. First of all, there might be *hr* mutant alleles other than the '6C' alleles present in these lines as only partial sequences were analysed here. For this reason, it is interesting to sequence full length *ELF3* and hunt for other possible alleles or use eco-tilling to look for novel *ELF3* alleles. The second explanation is these lines might be mutated at other naturally-occurring photoperiod-responsive locus such as *LF* which can also promote flowering in SD. Sequencing the *LF* gene will help resolve this question.

As pea is a long-day plant, it not only flowers later in SD than in LD, but often develops smaller leaf and more basal branching in SD. The distribution of recessive *hr* alleles ('6C' mutation) in pea germplasm is also found to be strongly correlated with these two photoperiod responsive traits, branching and leaf expansion (Figure 7.6). The strong association of branching and *ELF3* '6C' alleles could be due to genetic linkage of *ELF3* and *RMS1* or to a pleiotropic effect of *ELF3* on photoperiod control (Weeden, 2007). As shown in Figure 7.3, *RMS1* is mapped on top of pea LG III and very close to *ELF3*. Sequencing *RMS1* gene in these lines might help to answer this question. Moreover, no difference in leaf area was found for plants with '6C' alleles between LD and SD. A recent QTL study in Arabidopsis has identified *ELF3* as a major QTL for shade avoidance response where different natural alleles at *ELF3* locus result in different shade avoidance

response (Jimenez-Gomez et al., 2010). Again, the result of leaf expansion could be due to defect of *hr* mutant in shade avoidance response or effect of other closely linked loci.

In addition to photoperiod response, *HR* locus was also found to colocalise with one of the six major frost tolerance QTL in pea (Lejeune-Hénaut et al., 2008). The preliminary *ELF3* sequencing results also agree with this finding as *ELF3* '5C' WT alleles is limited to winter cultivars. However, cold tolerance experiment in this study showed there is no apparent association between *HR* genotype and tissue-level cold tolerance. NGB5839 with *hr* allele showed either similar damage or even more cold tolerance than its isogenic *HR* line (Figure 7.9). However, as the frost damage was only measured at leaf tissue, we cannot rule out the possibility that *HR* may somehow affect cold tolerance at the whole plant level. The other possible explanation could be that *HR* does not directly regulate the susceptibility of plant to cold but allows plants to escape winter frost by delaying flowering time or other modification of growth habits. In many other crops (cereals or brassicas), vernalization and photoperiod are regulated through separate pathways. Vernalization genes act to suppress *FT* expression while photoperiod genes promote *FT* expression. As mentioned in old literatures (Reid and Murfet, 1975; Murfet, 1977), photoperiod and vernalization seem to act competitively to regulate flowering time in pea and *SN* and *HR* are suggested to confer those responses.

Chapter 8 General Discussion

8.1. Concluding remarks

By using a 'positional candidate' gene approach, the molecular identities of three out of four loci (*DNE*, *SN*, *PPD*, and *HR*) in this thesis have been identified. *DNE*, *SN*, and *HR* are shown to be orthologs of Arabidopsis clock genes, *ELF4*, *LUX*, and *ELF3* respectively. This represents a major advance in molecular analysis of flowering control pathways in pea. It is also the first time that *ELF3* and *LUX* orthologs have been identified as major determinants of natural variation of flowering time in any species. The map position of *PPD* was also refined using molecular markers designed based on the genomic information from syntenic region on Medicago. The use of Medicago as a 'bridging species' is proved to be positive for gene isolation and comparative mapping in pea. The identifications of mutants have improved our understanding on circadian clock and photoperiodic control of flowering. As most of the pea circadian clock genes show similar diurnal and circadian expression rhythms to their Arabidopsis homologs, similar functions of these genes are suggested. This suggests components of circadian clock are likely to be highly conserved from one species to another species which enable us to use comparative genomics for clock gene isolation.

However insight into functional comparison of mutants with Arabidopsis mutants showed that mutation of *DNE* and *SN* did not cause a severe defect on diurnal and circadian expression rhythms despite the fact that strong flowering phenotypes were observed similar to those of their Arabidopsis homologs. Table 8.1 summarises the effects of *dne*, *sn* and *ppd* mutants on diurnal expression rhythms of clock-related genes in pea under LD and SD. The difference between pea and Arabidopsis can be

possibly explained by the presence of recessive allele of *HR* in our standard WT line (NGB5839) and demonstrated that *dne*, *sn* and *ppd* mutants are all effectively double mutants.

In addition to effect on circadian clock genes, several pea *FT*-like genes are elevated in *dne*, *sn* and *ppd* mutants and associated with flowering control which is different from Arabidopsis where single *FT*-like gene is mainly responsible for flowering regulation. Furthermore, no homolog of *CO* gene has been discovered in pea suggesting photoperiodic regulation on flowering time in pea might act through *CO*-independent pathway or other genes might replace the role of *CO* in pea. However, in addition to isolation of other putative *COL* members in pea, test needs to be carried out to completely rule out post-transcriptional or post-translational regulation of *FT* by *COLs*.

Table 8.1 Summary of diurnal expression rhythms of clock-related genes in pea in *dne-1*, *sn-4*, and *ppd-3* mutants when compared to WT (NGB5839) in LD and SD. This summary is based on Figure 4.2, Figure 5.4 and Figure 6.5.

Gene	*WT*		*dne-1*		*sn-4*		*ppd-3*	
	SD	**LD**	**SD**	**LD**	**SD**	**LD**	**SD**	**LD**
MYB1	peak at ZT20 -24	peak at ZT28	no effect	no effect	broader peak slightly lower	nd	no effect	nd
TOC1	peak at ZT8 & ZT32	peak at ZT12 & ZT36	phase delay 4h	no effect	slightly higher	slightly higher	slightly higher at night	phase advance 2-4h
ELF4	peak at ZT12 & ZT36	peak at ZT12-16 and ZT36-40	phase advance 4h	phase advance 2-4h	phase advance 4h	phase advance 2h	phase advance 2-4h	phase advance 2-4h lower peak
LATE1	peak at ZT8 & ZT32	peak at ZT12 & ZT36	higher trough	higher trough	higher trough shifted early 2-4h	higher trough shifted early 2-4h	higher trough	higher trough
PRR37	peak at ZT4-8 & ZT28-32	peak at ZT8-12 & ZT32-36	no effect	no effect	reduced peak	slightly higher trough	reduced peak	no effect
PRR59	peak at ZT8 & ZT32	peak at ZT12 & ZT36	no effect	no effect	obscured replication needed	obscured replication needed	higher trough	higher trough
ELF3	not rhythmic	bimodal peaks ZT12 & 20 and ZT36 & 44	not rhythmic	not rhythmic higher level	weak rhythm reduced level	not rhythmic	not rhythmic	Weak rhythm
MYB2	peak at ZT16	peak at ZT20-24 low level	slightly shifted	higher level	higher level	higher level	no effect	higher level

8.2. Improvement on techniques

In this study, quantitative real-time PCR was employed as an approach to investigate circadian clock genes expression. It is not necessary a high throughput, universal assay for clock function examination and also requires careful handlings in lab preparation and normalization calculation to minimise experiment variation. To get around this problem, firefly Luciferase (*LUC*) reporter gene assay has been used to monitor circadian rhythms in Arabidopsis and proved to be accurate in circadian phase determination (Millar et al., 1992; Millar et al., 1995). By using fusion of *LUC* with promoter of gene of interest, it is possible to track the bioluminescence rhythms of the target gene in transfected cells. It is therefore extremely useful and sensitive in circadian rhythms detection. Recently, a method using luciferase reporter gene coupled with artificial microRNA (amiRNA) allows rapid determination of gene function when the expression of amiRNA reduces the transcript level of gene of interest (Kim and Somers, 2010). This further enhances the investigation of circadian gene function *in vivo*. However, transfection or transformation is not practical and routine in pea if compared to other species, and it is doubtful whether this approach is feasible for routine analysis of circadian rhythms in pea.

In addition to luciferase-based assays, delayed fluorescence rhythms have recently been proved to be a simple and high throughput method to measure circadian rhythms in a few important crops and model plant species (Gould et al., 2009). Delayed fluorescence is a light emission from chlorophyll a in chloroplast after illumination and it basically utilize same imaging technique as luciferase assay to detect the illumination but without the requirement of transfection. Delayed fluorescence could be the next generation technology to measure circadian rhythms

especially in non-transformable plant species.

8.3. Future works

There are much still remains to be learnt about circadian clock and photoperiodic control of flowering. For the future, it is important to study the distribution and diversity of the naturally-occurring *SN* and *HR* alleles in detail and their correlation with photoperiodic control of flowering in *Pisum* germplasm. It is essential to generate single mutant of *DNE*, *SN*, and *PPD* in *HR* background in order to study the true effect of single locus and also to understand the genetic interaction between them in the absence of *hr* mutation.

Beside transcriptional regulation, post-transcriptional also plays an important role in circadian clock such as post-transcriptional regulation on CO protein level (Ishikawa et al., 2006; Jang et al., 2008). It is interesting to figure out if any of the clock mutants in pea has a defect on protein level of *CO*-like genes (*COLa* and *COLb*) using technique such as western blot in order to understand the role of *CO* in photoperiodic control of flowering in pea. Furthermore, protein-protein interaction is also involved in circadian clock regulation such as FKF1-GI in *CO* mRNA regulation (Sawa et al., 2007) and COP1-SPA1 in CO protein regulation (Ishikawa et al., 2006; Jang et al., 2008). Yeast two-hybrid technique could be a possible approach to target these questions.

In addition to *ELF3*, *ELF4*, and *LUX*, several other pea homologs of Arabidopsis clock genes have been isolated in this study but lack of pea mutant to specifically study their function in pea. It is therefore a potential area of research to utilize reverse genetics methods such as TILLING (targeting induced local lesion in genomes) (Dalmais et al., 2008; Triques et al., 2008) and VIGS (virus induced gene

silencing) (Baulcombe, 1999; Burch-Smith et al., 2004) to generate mutants of these genes.

8.4. Implication for other legumes

Despite many possible approaches could be used to advance our understanding on circadian clock in pea, pea is not an ideal model for clock study. However, molecular information which we learnt from pea could be useful for other species especially the closely-related legumes species in the Papilionoideae subfamily such as lentil, faba bean, chickpea and common bean (Figure 8.1). The synteny relationship between several important model and crop species including soybean, Lotus, Medicago, alfafa, chickpea, mugnbean, and pea has been established (Choi et al., 2004; Zhu et al., 2005; Gondo et al., 2007) which suggest it is highly likely to transfer genomic information between species. Furthermore, soybean, Lotus, and Medicago have been selected for genome sequencing projects and soybean complete genome was released in 2010 (Kim et al., 2010) while Medicago and Lotus are currently in the progress of completion. The availability of genomic information from these species together with genetics information from pea will aid the QTL identification and gene isolation in other legume species through comparative genome analysis and 'positional candidate' gene approach as outlined in this thesis.

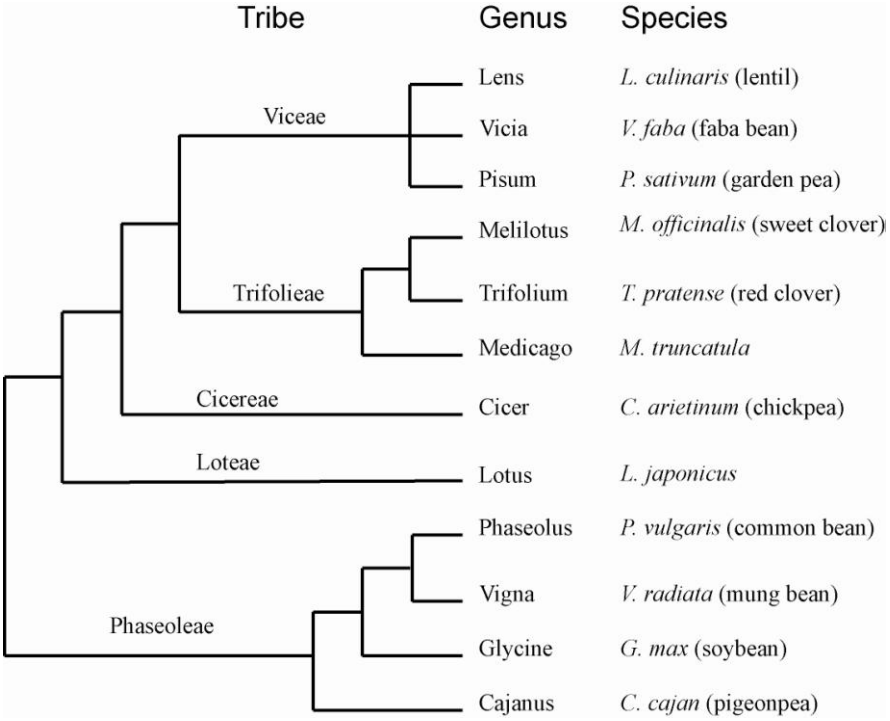

Figure 8.1 Dendogram of phylogenetic relationship of legume Papilionoideae subfamily. (Taken from Choi et. al. 2004)

In a linkage study of lentil, majority of pea and lentil genome are conserved where morphological and molecular markers are found to be co-linear in both species (Weeden et al., 1992). A major gene, *SN* is found to be responsible for early flowering of lentils from south Asia which carry recessive allele on this locus (Sarker et al., 1999). Furthermore, two major QTLs on LG4 and LG12 respectively are found to be responsible for earliness in flowering of lentil (Tullu et al., 2008). The lentil LG4 and LG5 is corresponding to pea LGVII where pea *SN* locus is located (Weeden et al., 1992). It is therefore possible to test if *SN*/*PsLUX* represent in lentil and involve in flowering regulation.

Faba bean is another species which is closely-related to pea but less study

was done on this species. A QTL study on agronomic important trait of Faba bean has identified two QTLs that regulate the character of flowers per inflorescence but failed to identify any QTL for determination of nodes with flower (Avila et al., 2005).

Compared to Faba bean, the genetic studies of flowering time in chickpea have started 20 years ago. Two major genes, *EFI* (Kumar and Rheenen, 2000) and *PPD* (Or et al., 1999), have been identified to cause bimodal distribution for time of flowering in chickpea. Recessive alleles on these two loci will result in early flowering and the latter one also resulted in weak photoperiod response when mutated. A join segregation analysis supported the finding that these two major genes explain the majority (>65%) of phenotypic variation of flowering time of chickpea (Anbessa et al., 2006). A QTL on LG4 was found to explain for 20% of phenotypic variation of days to flowering and linked to two QTLs for seed size and yield respectively (Cobos et al., 2007).

In common bean, nine QTLs have been discovered for days to flowering and maturity in a QTL study between cultivated and wild cross and two of them located at LGB9 explained 13-22% of the phenotypic variations (Blair et al., 2006). On another study on genes involved in photoperiodism of common bean, two major loci, *PPD* and *HR*, are found to confer sensitivity of photoperiod and degree of photoperiod responsiveness (Gu et al., 1998). There is a 15-20 days difference in flowering time between recessive and dominant alleles of *PPD* and dominant *HR* allele only delay the response in the presence of dominant *PPD* alleles (Gu et al., 1998). These phenotypic interactions are similar to what have been found in *SN*/*DNE*/*PPD* and *HR* pea loci. Flowering and photoperiodic genes have recently isolated in common bean using degenerate primers developed based on conserved motifs among Arabidopsis, soybean, peanut, Medicago, and/or lotus sequences (Kwak et al., 2008). As already

showed in this study, we have successfully isolate pea homologs using primers designed based on genomic information from Medicago and identified candidate genes for *DNE*, *SN*, and *HR*. As bean is more diverge from Medicago, soybean genomes could be more effective for gene isolation in common bean. Mapping and QTL studies were also done in other legumes species such as soybean (Cober et al., 1996; Quecini et al., 2007; Liu et al., 2009), lotus (Gondo et al., 2007), lupin (Phan et al., 2007; Boersma et al., 2008), and cowpea (Menéndez et al., 1997).

However although mapping and linkage analysis have been carried out in many of these legumes species, the existing maps or linkage groups cannot be linked to each other due to lack of common markers. In order to have a direct assessment on flowering or clock-related loci, flowering and clock genes from pea can be transferable and converted into gene-anchored markers for comparative mapping and linkage analysis in QTL or specific mapping population.

Knowledge of molecular and genetics of flowering or other important agronomic traits not only improve our basic understanding on the mechanism of plant physiology but also allow us to use the linkage maps and molecular markers for marker-assisted selection (MAS) and breeding. MAS will allow the screening of desired trait become more robust and time-efficient compared to visual identification. By using molecular marker for trait of interest, generation of new hybrid can be achieved at faster pace than conventional breeding as progress of introgression and backcrossing can be improved based on early and easy selection of indirect character. Moreover, the selection is more specific because introduction of unwanted gene might happen if using traditional breeding. The development of molecular markers and techniques will help to improve the selection of desired trait for particular farming environments and eventually improve the plant breeding and yield.

References

Abe, M., Kobayashi, Y., Yamamoto, S., Daimon, Y., Yamaguchi, A., Ikeda, Y., Ichinoki, H., Notaguchi, M., Goto, K., and Araki, T. (2005). FD, a bZIP protein mediating signals from the floral pathway Integrator FT at the shoot apex. Science **309,** 1052-1056.

Alabadi, D., Yanovsky, M.J., Mas, P., Harmer, S.L., and Kay, S.A. (2002). Critical role for CCA1 and LHY in maintaining circadian rhythmicity in *Arabidopsis*. Current Biology **12,** 757-761.

Alabadi, D., Oyama, T., Yanovsky, M.J., Harmon, F.G., Mas, P., and Kay, S.A. (2001). Reciprocal regulation between *TOC1* and *LHY/CCA1* within the *Arabidopsis* circadian clock. Science **293,** 880-883.

Allen, T., Koustenis, A., Theodorou, G., Somers, D.E., Kay, S.A., Whitelam, G.C., and Devlin, P.F. (2006). Arabidopsis FHY3 specifically gates phytochrome signaling to the circadian clock. The Plant Cell **18,** 2506-2516.

Anbessa, Y., Warkentin, T., Vandenberg, A., and Ball, R. (2006). Inheritance of time to flowering in chickpea in a short-season temperate environment. Journal of Heredity **97,** 55-61.

Arumingtyas, E.L., and Murfet, I.C. (1994). Flowering in Pisum: a further gene controlling response to photoperiod. Journal of Heredity **85,** 12-17.

Aubert, G., Morin, J., Jacquin, F., Loridon, K., Quillet, M.C., Petit, A., Rameau, C., Lejeune-He´naut, I., Huguet, T., and Burstin, J. (2006). Functional mapping in pea, as an aid to the candidate gene selection and for investigating synteny with the model legume *Medicago truncatula*. Theoretical and Applied Genetics **112,** 1024-1041.

Aukerman, M.J., and Sakai, H. (2003). Regulation of flowering time and floral organ identity by a microRNA and its *APETALA2*-like target genes. The Plant Cell **15,** 2730-2741.

Avila, C.M., Satovic, Z., Sillero, J.C., Nadal, S., Rubiales, D., Moreno, M.T., and Torres, A.M. (2005). QTL detection for agronomic traits in faba bean (*Vicia faba L.*). Agriculturae Conspectus Scientificus (Poljoprivredna Znanstvena Smotra) **70,** 65-73.

Axelsson, T., Shavorskaya, O., and Lagercrantz, U. (2001). Multiple flowering time QTLs within several *Brassica* species could be the result of duplicated copies of one ancestral gene. Genome **44,** 856-864.

Barak, S., Tobin, E.M., Andronis, C., Sugano, S., and Green, R.M. (2000). All in

good time: the *Arabidopsis* circadian clock. Trends in Plant Science **5,** 517-522.

Barber, H.N. (1959). Physiological genetics of *Pisum*. II. The genetics of photoperiodism and vernalisation. Heredity **13,** 33-60.

Baudry, A., Ito, S., Song, Y.H., Strait, A.A., Kiba, T., Lu, S., Henriques, R., Pruneda-Paz, J.L., Chua, N.-H., Tobin, E.M., Kay, S.A., and Imaizumi, T. (2010). F-Box proteins FKF1 and LKP2 act in concert with ZEITLUPE to control Arabidopsis clock progression. The Plant Cell **22,** 606-622.

Baulcombe, D.C. (1999). Fast forward genetics based on virus-induced gene silencing. Current Opinion in Plant Biology **2,** 109-113.

Baurle, I., and Dean, C. (2006). The timing of developmental transitions in plants. Cell **125,** 655-664.

Bernier, G., and Périlleux, C. (2005). A physiological overview of the genetics of flowering time control. Plant Biotechnology Journal **3,** 3-16.

Beveridge, C.A., and Murfet, I.C. (1996). The *gigas* mutant in pea is deficient in the floral stimulus. Physiologia Plantarum **96,** 637-645.

Blair, M.W., Iriarte, G., and Beebe, S. (2006). QTL analysis of yield traits in an advanced backcross population derived from a cultivated Andean * wild common bean (*Phaseolus vulgaris L.*) cross. TAG Theoretical and Applied Genetics **112,** 1149-1163.

Blazquez, M.A., Trenor, M., and Weigel, D. (2002). Independent control of gibberellin biosynthesis and flowering time by the circadian clock in *Arabidopsis*. Plant Physiology **130,** 1770-1775.

Boersma, J.G., Li, C., Lesniewska, K., Krishnapillai, S., and Yang, H. (2008). Identification of quantitative trait loci (QTLs) influencing early vigour, height, flowering date, and seed size and their implications for breeding of narrow-leafed lupin (*Lupinus angustifolius L.*). Australian Journal of Agricultural Research **59,** 527-535.

Bond, D.M., Dennis, E.S., Pogson, B.J., and Finnegan, E.J. (2009). Histone Acetylation, *VERNALIZATION INSENSITIVE 3*, *FLOWERING LOCUS C*, and the vernalization response. Molecular Plant **2,** 724-737.

Boss, P.K., Bastow, R.M., Mylne, J.S., and Dean, C. (2004). Multiple pathways in the decision to flower: enabling, promoting, and resetting. The Plant Cell **16,** S18-S31.

Burch-Smith, T.M., Anderson, J.C., Martin, G.B., and Dinesh-Kumar, S.P. (2004). Applications and advantages of virus-induced gene silencing for gene function studies in plants. The Plant Journal **39,** 734-746.

Caicedo, A.L., Stinchcombe, J.R., Olsen, K.M., Johanna Schmitt, and Purugganan, M.D. (2004). Epistatic interaction between *Arabidopsis FRI* and *FLC* flowering time genes generates a latitudinal cline in a life history trait. Proceedings of the National Academy of Sciences **101,** 15670–15675.

Cao, S., Ye, M., and Jiang, S. (2005). Involvement of GIGANTEA gene in the regulation of the cold stress response in Arabidopsis. Plant Cell Reports **24,** 683-690.

Carre, I.A. (2002). *ELF3*: a circadian safeguard to buffer effects of light. Trends in Plant Science **7,** 4-6.

Cerdan, P.D., and Chory, J. (2003). Regulation of flowering time by light quality. Nature **423,** 881-885.

Chaïlakhyan, M.K. (1985). Hormonal regulation of reproductive development in higher plants. Biologia Plantarium **27,** 292-302.

Chardon, F., Virlon, B., Moreau, L., Falque, M., Joets, J., Decousset, L., Murigneux, A., and Charcosset, A. (2004). Genetic architecture of flowering time in maize as inferred from quantitative trait loci meta-analysis and synteny conservation with the rice genome. Genetics **168,** 2169-2185.

Chen, M., and Ni, M. (2006a). RFI2, a RING-domain zinc finger protein, negatively regulates *CONSTANS* expression and photoperiodic flowering. The Plant Journal **46,** 823-833.

Chen, M., and Ni, M. (2006b). RED AND FAR-RED INSENSITIVE 2, a RING-domain zinc finger protein, mediates phytochrome-controlled seedling deetiolation responses. Plant Physiology **140,** 457-465.

Chen, X., and Meyerowitz, E.M. (1999). *HUA1* and *HUA2* are two members of the floral homeotic *AGAMOUS* pathway. Molecular Cell **3,** 349-360.

Cheng, X.-F., and Wang, Z.-Y. (2005). Overexpression of *COL9*, a *CONSTANS-LIKE* gene, delays flowering by reducing expression of *CO* and *FT* in *Arabidopsis thaliana*. The Plant Journal **43,** 758-768.

Choi, H.K., Mun, J.H., Kim, D.J., Zhu, H., Baek, J.M., Mudge, J., Rob, J., Ellis, N., Doyle, J., and Kiss, G.B. (2004). Estimating genome conservation between crop and model legume species. Proceedings of the National Academy of Sciences of the United States of America **101,** 15289-15294.

Chouard, P. (1960). Vernalization and its relations to dormancy. Annual Review of Plant Physiology **11,** 191-238.

Clement, M., Posada, D., and Crandall, K.A. (2000). TCS: a computer program to estimate gene genealogies. Molecular Ecology **9,** 1657-1659.

Cober, E.R., Tanner, J.W., and Voldeng, H.D. (1996). Genetic control of

photoperiod response in early-maturing, near-isogenic soybean lines. Crop Science **36,** 601-605.

Cobos, M.J., Rubio, J., Fernandez-Romero, M.D., Garza, R., Moreno, M.T., Millan, T., and Gil, J. (2007). Genetic analysis of seed size, yield and days to flowering in a chickpea recombinant inbred line population derived from a Kabuli * Desi cross. Annals of Applied Biology **151,** 33-42.

Corbesier, L., Vincent, C., Jang, S., Fornara, F., Fan, Q., Searle, I., Giakountis, A., Farrona, S., Gissot, L., Turnbull, C., and Coupland, G. (2007). FT protein movement contributes to long-distance signaling in floral induction of *Arabidopsis*. Science **316,** 1030-1033.

Covington, M., Maloof, J., Straume, M., Kay, S., and Harmer, S. (2008). Global transcriptome analysis reveals circadian regulation of key pathways in plant growth and development. Genome Biology **9,** R130.

Covington, M.F., and Harmer, S.L. (2007). The circadian clock regulates auxin signaling and responses in Arabidopsis. PLoS Biology **5,** e222.

Covington, M.F., Panda, S., Liu, X.L., Strayer, C.A., Wagner, D.R., and Kay, S.A. (2001). ELF3 modulates resetting of the circadian clock in *Arabidopsis*. The Plant Cell **13,** 1305-1316.

Dalmais, M., Schmidt, J., Signor, C.L., Moussy, F., Burstin, J., Savois, V., Aubert, G., Brunaud, V., Oliveira, Y.d., Guichard, C., Thompson, R., and Bendahmane, A. (2008). UTILLdb, a *Pisum sativum* in silico forward and reverse genetics tool. Genome Biology **9,** R43.

Daniel, X., Sugano, S., and Tobin, E.M. (2004). CK2 phosphorylation of CCA1 is necessary for its circadian oscillator function in *Arabidopsis*. Proceedings of the National Academy of Sciences of the United States of America **101,** 3292-3297.

Davis, S.J. (2009). Integrating hormones into the floral-transition pathway of *Arabidopsis thaliana*. Plant, Cell and Environment **32,** 1201-1210.

Devlin, P.F., and Kay, S.A. (2000). Cryptochromes are required for phytochrome signaling to the circadian clock but not for rhythmicity. The Plant Cell **12,** 2499-2510.

Ding, Z., Millar, A.J., Davis, A.M., and Davis, S.J. (2007). *TIME FOR COFFEE* encodes a nuclear regulator in the *Arabidopsis thaliana* circadian clock The Plant Cell **19,** 1522-1536.

Dodd, A.N., Salathia, N., Hall, A., Kevei, E., Toth, R., Nagy, F., Hibberd, J.M., Millar, A.J., and Webb, A.A.R. (2005). Plant circadian clocks increase photosynthesis, growth, survival, and competitive advantage. Science **309,**

630-633.

Dodda, A.N., Loveb, J., and Webba, A.A.R. (2004). The plant clock shows its metal: circadian regulation of cytosolic free Ca2+. Trends in Plant Science **10,** 15-21.

Dowson-Day, M.J., and Millar, A.J. (1999). Circadian dysfunction causes aberrant hypocotyl elongation patterns in *Arabidopsis*. The Plant Journal **17,** 63-71.

Doyle, M.R., Bizzell, C.M., Keller, M.R., Michaels, S.D., Song, J., Noh, Y.-S., and Amasino, R.M. (2005). *HUA2* is required for the expression of floral repressors in *Arabidopsis thaliana*. The Plant Journal **41,** 376-385.

Doyle, M.R., Davis, S.J., Bastow, R.M., McWatters, H.G., Kozma-Bognar, L., Nagy, F., Millar, A.J., and Amasino, R.M. (2002). The *ELF4* gene controls circadian rhythms and flowering time in *Arabidopsis thaliana*. Nature **419,** 74-77.

Ducrocq, S., Madur, D., Veyrieras, J.-B., Camus-Kulandaivelu, L., Kloiber-Maitz, M., Presterl, T., Ouzunova, M., Manicacci, D., and Charcosset, A. (2008). Key impact of *Vgt1* on flowering time adaptation in maize: evidence from association mapping and ecogeographical information. Genetics **178,** 2433-2437.

Dunlap, J.C. (1999). Molecular bases of circadian clocks. Cell **96,** 271-290.

Edwards, K.D., and Millar, A.J. (2007). Analysis of circadian leaf movement rhythms in *Arabidopsis thaliana*, pp. 103-113.

Edwards, K.D., Anderson, P.E., Hall, A., Salathia, N.S., Locke, J.C., Lynn, J.R., Straume, M., Smith, J.Q., and Millar, A.J. (2006). *FLOWERING LOCUS C* mediates natural variation in the high-temperature response of the *Arabidopsis* circadian clock. The Plant Cell **18,** 639-650.

Ellis, T.H.N., Turner, L., Hellens, R.P., Lee, D., Harker, C.L., Enard, C., Domoney, C., and Davies, D.R. (1992). Linkage Maps in Pea. Genetics **130,** 649-663.

Eriksson, M.E., and Millar, A.J. (2003). The circadian clock. A plant's best friend in a spinning world. Plant Physiology **132,** 732-738.

Farré, E.M., Harmer, S.L., Harmon, F.G., Yanovsky, M.J., and Kay, S.A. (2005). Overlapping and Distinct Roles of PRR7 and PRR9 in the Arabidopsis Circadian Clock. Current Biology **15,** 47-54.

Faure, S., Higgins, J., Turner, A., and Laurie, D.A. (2007). The *FLOWERING LOCUS T-Like* Gene Family in Barley (*Hordeum vulgare*). Genetics **176,** 599-609.

Fornara, F., Panigrahi, K.C.S., Gissot, L., Sauerbrunn, N., Ruhl, M., Jarillo, J.A., and Coupland, G. (2009). *Arabidopsis* DOF transcription factors act

redundantly to reduce *CONSTANS* expression and are essential for a photoperiodic flowering response. Developmental Cell **11,** 75-86.

Foucher, F., Morin, J., Courtiade, J., Cadioux, S., Ellis, N., Banfield, M.J., and Rameau, C. (2003). *DETERMINATE* and *LATE FLOWERING* are two *ERMINAL FLOWER1/CENTRORADIALIS* homologs that control two distinct phases of flowering initiation and development in Pea. The Plant Cell **15,** 2742-2754.

Fowler, S., Lee, K., Onouchi, H., Samach, A., Richardson, K., Morris, B., Coupland, G., and Putterill, J. (1999). *GIGANTEA*: A circadian clock-controlled gene that regulates photoperiodic flowering in Arabidopsis and encodes a protein with several possible membrane-spanning domains. The EMBO Journal **18,** 4679-4688.

Garner, W.W., and Allard, H.A. (1920). Effects of the relative length of night and day and other factors of the environment on growth and reproduction in plants. Journal of Agricultural Research **18,** 553-606.

Gendall, A.R., Levy, Y.Y., Wilson, A., and Dean, C. (2001). The *VERNALIZATION 2* gene mediates the epigenetic regulation of vernalization in *Arabidopsis*. Cell **107,** 525-535.

Gondo, T., Sato, S., Okumura, K., Tabata, S., Akashi, R., and Isobe, S. (2007). Quantitative trait locus analysis of multiple agronomic traits in the model legume *Lotus japonicus*. Genome **50,** 627-637.

Gould, P.D., Diaz, P., Hogben, C., Kusakina, J., Salem, R., Hartwell, J., and Hall, A. (2009). Delayed fluorescence as a universal tool for the measurement of circadian rhythms in higher plants. The Plant Journal **58,** 893-901.

Gould, P.D., Locke, J.C.W., Larue, C., Southern, M.M., Davis, S.J., Hanano, S., Moyle, R., Milich, R., Putterill, J., Millar, A.J., and Hall, A. (2006). The molecular basis of temperature compensation in the *Arabidopsis* circadian clock. The Plant Cell **18,** 1177-1187.

Green, R.M., and Tobin, E.M. (1999). Loss of the circadian clock-associated protein 1 in *Arabidopsis* results in altered clock-regulated gene expression. Proceedings of the National Academy of Sciences of the United States of America **96,** 4176-4179.

Green, R.M., Tingay, S., Wang, Z.-Y., and Tobin, E.M. (2002). Circadian rhythms confer a higher level of fitness to *Arabidopsis* plants. Plant Physiology **129,** 576-584.

Gu, W., Zhu, J., Wallace, D.H., Singh, S.P., and Weeden, N.F. (1998). Analysis of genes controlling photoperiod sensitivity in common bean using DNA markers.

Euphytica **102,** 125-132.

Halaban, R. (1968). The flowering response of *Coleus* in relation to pohotoperiod and the circadian rhythm of leaf movement. Plant Physiology **43,** 1894-1898.

Hall, A., Bastow, R.M., Davis, S.J., Hanano, S., McWatters, H.G., Hibberd, V., Doyle, M.R., Sung, S., Halliday, K.J., Amasino, R.M., and Millar, A.J. (2003). The *TIME FOR COFFEE* gene maintains the amplitude and timing of *Arabidopsis* circadian clocks. The Plant Cell **15,** 2719-2729.

Hall, K.J., Parker, J.S., Ellis, T.H.N., Turner, L., Knox, M.R., Hofer, J.M.I., Lu, J., Ferrandiz, C., Hunter, P.J., Taylor, J.D., and Baird, K. (1997). The relationship between genetic and cytogenetic maps of pea. II. Physical maps of linkage mapping populations. Genome **40,** 755-769.

Hames, C., Ptchelkine, D., Grimm, C., Thevenon, E., Moyroud, E., Gerard, F., Martiel, J.-L., Benlloch, R., Parcy, F., and Muller, C.W. (2008). Structural basis for LEAFY floral switch function and similarity with helix-turn-helix proteins. The EMBO Journal **27,** 2629-2637.

Harmer, S.L., and Kay, S.A. (2005). Positive and negative factors confer phase-specific circadian regulation in transcription of *Arabidopsis* The Plant Cell **17,** 1926-1940.

Harmer, S.L., Hogenesch, J.B., Straume, M., Chang, H.-S., Han, B., Zhu, T., Wang, X., Kreps, J.A., and Kay, S.A. (2000). Orchestrated transcription of key pathways in *Arabidopsis* by the circadian clock. Science **290,** 2110-2113.

Hartmann, U., Hohmann, S., Nettesheim, K., Wisman, E., Saedler, H., and Huijser, P. (2000). Molecular cloning of *SVP*: a negative regulator of the floral transition in Arabidopsis. The Plant Journal **21,** 351-360.

Hayama, R., and Coupland, G. (2004). The molecular basis of diversity in the photoperiodic flowering responses of *Arabidopsis* and rice. Plant Physiology **135,** 677-684.

Hayama, R., Izawa, T., and Shimamoto, K. (2002). Isolation of rice genes possibly involved in the photoperiodic control of flowering by a fluorescent differential display method. Plant and Cell Physiology **43,** 494-504.

Hayama, R., Agashe, B., Luley, E., King, R., and Coupland, G. (2007). A circadian rhythm set by dusk determines the expression of *FT* homologs and the short-day photoperiodic flowering response in Pharbitis. The Plant Cell **19,** 2988-3000.

Hazen, S.P., Schultz, T.F., Pruneda-Paz, J.L., Borevitz, J.O., Ecker, J.R., and Kay, S.A. (2005). *LUX ARRHYTHMO* encodes a Myb domain protein essential for circadian rhythms. Proceedings of the National Academy of Sciences of the

United States of America **102,** 10387-10392.

Hazen, S.P., Naef, F., Quisel, T., Gendron, J.M., Chen, H., Ecker, J.R., Borevitz, J.O., and Kay, S.A. (2009). Exploring the transcriptional landscape of plant circadian rhythms using genome tiling arrays. Genome Biology **10,** R17.

He, Y., Michaels, S.D., and Amasino, R.M. (2003). Regulation of flowering time by histone acetylation in *Arabidopsis*. Science **302,** 1751-1754.

Hecht, V., Knowles, C.L., Vander Schoor, J.K., Liew, L.C., Jones, S.E., Lambert, M.J.M., and Weller, J.L. (2007). Pea *LATE BLOOMER1* is a *GIGANTEA* ortholog with roles in photoperiodic flowering, deetiolation, and transcriptional regulation of circadian clock gene homologs. Plant Physiology **144,** 648-661.

Hecht, V., Laurie, R.E., Vander Schoor, J.K., Ridge, S., Knowles, C.L., Liew, L.C., Sussmilch, F.C., Murfet, I.C., Macknight, R.C., and Weller, J.L. (2011). The pea *GIGAS* gene is a *FLOWERING LOCUS T* homolog necessary for graft-transmissible specification of flowering but not for responsiveness to photoperiod. The Plant Cell**,** tpc.110.081042.

Hecht, V., Foucher, F., Ferrandiz, C., Macknight, R., Navarro, C., Morin, J., Vardy, M.E., Ellis, N., Beltran, J.P., Rameau, C., and Weller, J.L. (2005). Conservation of Arabidopsis flowering genes in model legumes. Plant Physiology **137,** 1420-1434.

Heintzen, C., Nater, M., Apel, K., and Staiger, D. (1997). AtGRP7, a nuclear RNA-binding protein as a component of a circadian-regulated negative feedback loop in *Arabidopsis thaliana*. Proceedings of the National Academy of Sciences of the United States of America **94,** 8515-8520.

Hellens, R.P., Moreau, C., Lin-Wang, K., Schwinn, K.E., Thomson, S.J., Fiers, M.W.E.J., Frew, T.J., Murray, S.R., Hofer, J.M.I., Jacobs, J.M.E., Davies, K.M., Allan, A.C., Bendahmane, A., Coyne, C.J., Timmerman-Vaughan, G.M., and Ellis, T.H.N. (2010). Identification of Mendel's white flower character. PLoS ONE **5,** e13230.

Hicks, K.A., Albertson, T.M., and Wagner, D.R. (2001). *EARLY FLOWERING3* encodes a novel protein that regulates circadian clock function and flowering in *Arabidopsis*. The Plant Cell **13,** 1281-1292.

Hicks, K.A., Millar, A.J., Carre, I.A., Somers, D.E., Straume, M.D., Meeks-Wagner, R., and Kay, S.A. (1996). Conditional circadian dysfunction of the *Arabidopsis early-flowering 3* mutant. Science **274,** 790-792.

Hou, C.-J., and Yang, C.-H. (2009). Functional analysis of *FT* and *TFL1* orthologs from Orchid (*Oncidium* Gower Ramsey) that regulate the vegetative to

reproductive transition. Plant and Cell Physiology **50,** 1544-1557.

Hsu, C.Y., Liu, Y., Luthe, D.S., and Yuceer, C. (2006). Poplar FT2 shortens the juvenile phase and promotes seasonal flowering. The Plant Cell **18,** 1846 - 1861.

Igasaki, T., Watanabe, Y., Nishiguchi, M., and Kotoda, N. (2008). The *FLOWERING LOCUS T/TERMINAL FLOWER 1* Family in Lombardy Poplar. Plant and Cell Physiology **49,** 291-300.

Imaizumi, T., Tran, H.G., Swartz, T.E., Briggs, W.R., and Kay, S.A. (2003). FKF1 is essential for photoperiodic-specific light signalling in *Arabidopsis*. Nature **426,** 302-306.

Imaizumi, T., Schultz, T.F., Harmon, F.G., Ho, L.A., and Kay, S.A. (2005). FKF1 F-box protein mediates cyclick degradation of a repressor of *CONSTANS* in *Arabidopsis*. Science **309,** 293-297.

Ishikawa, M., Kiba, T., and Chua, N.H. (2006). The *Arabidopsis SPA1* gene is required for circadian clock function and photoperiodic flowering. The Plant Journal **46,** 736-746.

Ito, S., Niwa, Y., Nakamichi, N., Kawamura, H., Yamashino, T., and Mizuno, T. (2008). Insight into missing genetic links between two evening-expressed pseudo-response regulator genes *TOC1* and *PRR5* in the circadian clock-controlled circuitry in *Arabidopsis thaliana*. Plant and Cell Physiology **49,** 201-213.

Izawa, T., Takahashiy, Y., and Yanoz, M. (2003). Comparative biology comes into bloom: genomic and genetic comparison of flowering pathways in rice and *Arabidopsis*. Current Opinion in Plant Biology **6,** 113-120.

Izawa, T., Oikawa, T., Sugiyama, N., Tanisaka, T., Yano, M., and Shimamoto, K. (2002). Phytochrome mediates the external light signal to repress *FT* orthologs in photoperiodic flowering of rice. Genes and Development **16,** 2006-2020.

Jacobsen, S.E., and Olszewski, N.E. (1993). Mutations at the *SPINDLY* locus of Arabidopsis alter gibberellin signal transduction. The Plant Cell **5,** 887-896.

Jaeger, K.E., and Wigge, P.A. (2007). FT protein acts as a long-range signal in *Arabidopsis*. Current Biology **17,** 1-5.

Jang, S., Marchal, V., Panigrahi, K.C., Wenkel, S., Soppe, W., Deng, X.-W., Valverde, F., and Coupland, G. (2008). Arabidopsis COP1 shapes the temporal pattern of CO accumulation conferring a photoperiodic flowering response. The EMBO Journal **27,** 1277-1288.

Jimenez-Gomez, J.M., Wallace, A.D., and Maloof, J.N. (2010). Network analysis identifies *ELF3* as a QTL for the shade avoidance response in arabidopsis.

PLoS Genetics **6,** e1001100.

Jing, R., Vershinin, A., Grzebyta, J., Shaw, P., Smýkal, P., Marshall, D., Ambrose, M.J., Ellis, T.N., and Flavell, A.J. (2010). The genetic diversity and evolution of field pea (*Pisum*) studied by high throughput retrotransposon based insertion polymorphism (RBIP) marker analysis. BMC Evolutionary Biology **10,** 1471-2148.

Johanson, U., West, J., Lister, C., Michaels, S., Amasino, R., and Dean, C. (2000). Molecular analysis of *FRIGIDA*, a major determinant of natural variation in *Arabidopsis* flowering time. Science **290,** 344-347.

Johnson, E., Bradley, M., Harberd, N.P., and Whitelam, G.C. (1994). Photoresponses of light-grown *phyA* mutants of *Arabidopsis* (Phytochrome A is required for the perception of daylength extensions). Plant Physiology **105,** 141-149.

Jones, H., Leigh, F.J., Mackay, I., Bower, M.A., Smith, L.M.J., Charles, M.P., Jones, G., Jones, M.K., Brown, T.A., and Powell, W. (2008). Population-based resequencing reveals that the flowering time adaptation of cultivated barley originated east of the fertile crescent. Molecular Biology and Evolution **25,** 2211-2219.

Jones, S.E. (2004). Genetic and hormonal control of flowering in pea and *Arabidopsis*. In School of Plant Science (Sandy Bay: University of Tasmania).

Jung, J.-H., Seo, Y.-H., Seo, P.J., Reyes, J.L., Yun, J., Chua, N.-H., and Park, C.-M. (2007). The *GIGANTEA*-regulated microRNA172 mediates photoperiodic flowering independent of *CONSTANS* in Arabidopsis. The Plant Cell **19,** 2736-2748.

Kaldis, A.D., and Prombona, A. (2006). Synergy between the light-induced acute response and the circadian cycle: a new mechanism for the synchronization of the *Phaseolus vulgaris* clock to light. Plant Molecular Biology **61,** 883-895.

Kalo, P., Seres, A., Taylor, S.A., Jakab, J., Kevei, Z., Kereszt, A., Endre, G., Ellis, T.H.N., and Kiss, G.B. (2004). Comparative mapping between *Medicago sativa* and *Pisum sativum*. Molecular Genetics and Genomics **272,** 235-246.

Kardailsky, I., Shukla, V.K., Ahn, J.H., Dagenais, N., Christensen, S.K., Nguyen, J.T., Chory, J., Harrison, M.J., and Weigel, D. (1999). Activation tagging of the floral inducer FT. Science **286,** 1962 - 1965.

Karimi, M., Inze, D., and Depicker, A. (2002). GATEWAY^{TM} vectors for *Agrobacterium*-mediated plant transformation. . Trends in Plant Science **7,** 193-195.

Kelly, M.O., and Spanswick, R.M. (1997). Maternal, single-gene regulation of

assimilate partitioning in pea. Plant Physiology **114,** 1055-1059.

Kevei, E., Gyula, P., Feher, B., Toth, R., Viczian, A., Kircher, S., Rea, D., Dorjgotov, D., Schafer, E., Millar, A.J., Kozma-Bognar, L., and Nagy, F. (2007). *Arabidopsis thaliana* circadian clock is regulated by the small GTPase LIP1. Current Biology **17,** 1-9.

Khanna, R., Kikis, E.A., and Quail, P.H. (2003). *EARLY FLOWERING 4* functions in phytochrome B-regulated seedling de-etiolation. Plant Physiology **133,** 1530-1538.

Kiba, T., Henriques, R., Sakakibara, H., and Chua, N.-H. (2007). Targeted degradation of PSEUDO-RESPONSE REGULATOR5 by a SCF^{ZTL} complex regulates clock function and photomorphogenesis in *Arabidopsis thaliana*. The Plant Cell **19,** 2516-2530.

Kikis, E.A., Khanna, R., and Quail, P.H. (2005). ELF4 is a phytochrome-regulated component of a negative-feedback loop involving the central oscillator components CCA1 and LHY. The Plant Journal **44,** 300-313.

Kim, H.-J., Hyun, Y., Park, J.-Y., Park, M.-J., Park, M.-K., Kim, M.D., Kim, H.-J., Lee, M.H., Moon, J., Lee, I., and Kim, J. (2004). A genetic link between cold responses and flowering time through *FVE* in *Arabidopsis thaliana*. Nature Genetics **36,** 167-171.

Kim, J., and Somers, D.E. (2010). Rapid assessment of gene function in the circadian clock using artificial microRNA in Arabidopsis mesophyll protoplasts. Plant Physiology **154,** 611-621.

Kim, J., Kim, Y., Yeom, M., Kim, J.-H., and Nam, H.G. (2008). FIONA1 is essential for regulating period length in the *Arabidopsis* circadian clock. The Plant Cell **20,** 307-319.

Kim, M.Y., Lee, S., Van, K., Kim, T.-H., Jeong, S.-C., Choi, I.-Y., Kim, D.-S., Lee, Y.-S., Park, D., Ma, J., Kim, W.-Y., Kim, B.-C., Park, S., Lee, K.-A., Kim, D.H., Kim, K.H., Shin, J.H., Jang, Y.E., Kim, K.D., Liu, W.X., Chaisan, T., Kang, Y.J., Lee, Y.-H., Kim, K.-H., Moon, J.-K., Schmutz, J., Jackson, S.A., Bhak, J., and Lee, S.-H. (2010). Whole-genome sequencing and intensive analysis of the undomesticated soybean (Glycine soja Sieb. and Zucc.) genome. Proceedings of the National Academy of Sciences **107,** 22032-22037.

Kim, W.-Y., Fujiwara, S., Suh, S.-S., Kim, J., Kim, Y., Han, L., David, K., Putterill, J., Nam, H.G., and Somers, D.E. (2007). ZEITLUPE is a circadian photoreceptor stabilized by GIGANTEA in blue light. Nature **449,** 356-362.

Kim, W.Y., Hicks, K.A., and Somers, D.E. (2005). Independent roles for *EARLY*

FLOWERING 3 and *ZEITLUPE* in the control of circadian timing, hypocotyl length, and flowering time. Plant Physiology **139,** 1557-1569.

King, W.M., and Murfet, I.C. (1985). Flowering in *Pisum*: a sixth locus, *Dne*. Annals of Botany **56,** 835-846.

Kinoshita, T., Doi, M., Suetsugu, N., Kagawa, T., Wada, M., and Shimazaki, K.-i. (2001). phot1 and phot2 mediate blue light regulation of stomatal opening. Nature **414,** 656-660.

Knott, J.E. (1934). Effect of localized photoperiod on spinach. Proceedings of the American Society for Horticultural Science **32,** 152-154.

Kobayashi, Y., Kaya, H., Goto, K., Iwabuchi, M., and Araki, T. (1999). A pair of related genes with antagonistic roles in mediating flowering signals. Science **286,** 1960-1962.

Kolmos, E., Nowak, M., MWerner, a., Fischer, K., Schwarz, G., Mathews, S., Schoof, H., Nagy, F., Bujnicki, J.M., and Davis, S.J. (2009). Integrating *ELF4* into the circadian system through combined structural and functional studies. HFSP Journal **3,** 350-366

Kong, F., Liu, B., Xia, Z., Sato, S., Kim, B., Watanabe, S., Yamada, T., Tabata, S., Kanazawa, A., Harada, K., and Abe, J. (2010). Two coordinately regulated homologs of *FLOWERING LOCUS T* are involved in the control of photoperiodic flowering in soybean. Plant Physiology **154,** 1220-1231.

Kumar, J., and Rheenen, H.A.v. (2000). A major gene for time of flowering in chickpea. Journal of Heredity **91,** 67-68.

Kwak, M.H., Velasco, D., and Gepts, P. (2008). Mapping homologous sequences for determinacy and photoperiod sensitivity in common bean (*Phaseolus vulgaris*). Journal of Heredity **99,** 283-291.

Laucou, V., Haurogne., K., Ellis, N., and Rameau, C. (1998). Genetic mapping in pea. 1. RAPD-based genetic linkage map of *Pisum sativum*. Theoretical and Applied Genetics **97,** 905-915.

Laurie, D.A., and Devos, K.M. (2002). Trends in comparative genetics and their potential impacts on wheat and barley research. Plant Molecular Biology **48,** 729-740.

Ledger, S., Strayer, C., Ashton, F., Kay, S.A., and Putterill, J. (2001). Analysis of the function of two circadian-regulated *CONSTANS-LIKE* genes. The Plant Journal **26,** 15-22.

Lee, H., Xiong, L., Gong, Z., Ishitani, M., Stevenson, B., and Zhu, J.-K. (2001). The Arabidopsis *HOS1* gene negatively regulates cold signal transduction and encodes a RING finger protein that displays cold-regulated

nucleo-cytoplasmic partitioning. Genes and Development **15,** 912-924.

Lee, I., Aukerman, M.J., Gore, S.L., Lohman, K.N., Michaels, S.D., Weaver, L.M., John, M.C., Feldmann, K.A., and Amasino, R.M. (1994). Isolation of *LUMINIDEPENDENS*: a gene involved in the control of flowering time in *Arabidopsis*. The Plant Cell **6,** 75-83.

Lee, J., and Lee, I. (2010). Regulation and function of SOC1, a flowering pathway integrator. Journal of Experimental Botany **61,** 2247-2254.

Lejeune-Hénaut, I., Bourion, V., Eteve, G., Cunot, E., Delhaye, K., and Desmyter, C. (1999). Floral initiation in field-grown forage peas is delayed to a greater extent by short photoperiods, than in other types of European varieties. Euphytica **109,** 201-211.

Lejeune-Hénaut, I., Hanocq, E., Béthencourt, L., Fontaine, V., Delbreil, B., Morin, J., Petit, A., Devaux, R., Boilleau, M., Stempniak, J.-J., Thomas, M., Lainé, A.-L., Foucher, F., Baranger, A., Burstin, J., Rameau, C., and Giauffret, C. (2008). The flowering locus *Hr* colocalizes with a major QTL affecting winter frost tolerance in *Pisum sativum L.* . Theoretical and Applied Genetics **116,** 1105-1116.

Lester, D.R., Ross, J.J., Davies, P.J., and Reid, J.B. (1997). Mendels stem length gene (Le) encodes a gibberellin 3B-hydroxylase. The Plant Cell **9,** 1435-1443.

Levy, Y.Y., Mesnage, S., Mylne, J.S., Gendall, A.R., and Dean, C. (2002). Multiple roles of *Arabidopsis VRN1* in vernalization and flowering time control. Science **297,** 243-246.

Li, D., Liu, C., Shen, L., Wu, Y., Chen, H., Robertson, M., Helliwell, C.A., Ito, T., Meyerowitz, E., and Yu1, H. (2008). A repressor complex governs the integration of flowering signals in *Arabidopsis*. Developmental Cell **15,** 110-120.

Lidder, P., Gutierrez, R.A., Salome, P.A., McClung, C.R., and Green, P.J. (2005). Circadian control of messenger RNA stability. Association with a sequence-specific messenger RNA decay pathway. Plant Physiology **138,** 2374-2385.

Liew, L.C., Hecht, V., Weeden, N., and Weller, J.L. (2009a). Isolation of *Pseudo Response Regulator* genes and evaluation as candidate gens for photoperiod response loci. Pisum Genetics **41,** 21-25.

Liew, L.C., Hecht, V., Laurie, R.E., Knowles, C.L., Vander Schoor, J.K., Macknight, R.C., and Weller, J.L. (2009b). *DIE NEUTRALIS* and *LATE BLOOMER 1* contribute to regulation of the pea circadian clock. The Plant Cell **21,** 3198-3211.

Lifschitz, E., and Eshed, Y. (2006). Universal florigenic signals triggered by *FT* homologues regulate growth and flowering cycles in perennial day-neutral tomato. Journal of Experimental Botany **57,** 3405-3414.

Lifschitz, E., Eviatar, T., Rozman, A., Shalit, A., Goldshmidt, A., Amsellem, Z., Alvarez, J.P., and Eshed, Y. (2006). The tomato *FT* ortholog triggers systemic signals that regulate growth and flowering and substitute for diverse environmental stimuli. Proceedings of the National Academy of Sciences **103,** 6398-6403.

Lim, M.-H., Kim, J., Kim, Y.-S., Chung, K.-S., Seo, Y.-H., Lee, I., Kim, J., Hong, C.B., Kim, H.-J., and Park, C.-M. (2004). A new Arabidopsis gene, *FLK*, encodes an RNA binding protein with K homology motifs and regulates flowering time via *FLOWERING LOCUS C*. The Plant Cell **16,** 731-740.

Liu, C., Chen, H., Er, H.L., Soo, H.M., Kumar, P.P., Han, J.-H., Liou, Y.C., and Yu, H. (2008a). Direct interaction of *AGL24* and *SOC1* integrates flowering signals in *Arabidopsis*. Development **135,** 1481-1491.

Liu, H., Wang, H., Gao, P., Xü, J., Xü, T., Wang, J., Wang, B., Lin, C., and Fu, Y.-F. (2009). Analysis of clock gene homologs using unifoliolates as target organs in soybean (*Glycine max*). Journal of Plant Physiology **166,** 278-289.

Liu, J., Yu, J., McIntosh, L., Kende, H., and Zeevaart, J.A. (2001a). Isolation of a *CONSTANS* ortholog from Pharbitis nil and its role in flowering. Plant Physiology **125,** 1821-1830.

Liu, L.-J., Zhang, Y.-C., Li, Q.-H., Sang, Y., Mao, J., Lian, H.-L., Wang, L., and Yang, H.-Q. (2008b). COP1-mediated ubiquitination of CONSTANS is implicated in cryptochrome regulation of flowering in *Arabidopsis*. The Plant Cell **20,** 292-306.

Liu, X.L., Covington, M.F., Fankhauser, C., Chory, J., and Wagner, D.R. (2001b). *ELF3* encodes a circadian clock-regulated nuclear protein that functions in an *Arabidopsis PHYB* signal transduction pathway. The Plant Cell **13,** 1293-1304.

Locke, J.C.W., Southern, M.M., Kozma-Bognar, L., Hibberd, V., Brown, P.E., Turner, M.S., and Millar, A.J. (2005). Extension of a genetic network model by iterative experimentation and mathematical analysis. Molecular Systems Biology **1,** E1-E9.

Locke, J.C.W., Kozma-Bognar, L., Gould, P.D., Feher, B., Kevei, E., Nagy, F., Turner, M.S., Hall, A., and Millar, A.J. (2006). Experimental validation of a predicted feedback loop in the multi-oscillator clock of Arabidopsis thaliana. Molecular Systems Biology **2,** 59.

Loridon, K., McPhee, K., Morin, J., Dubreuil, P., Pilet-Nayel, M.L., Aubert, G.,

Rameau, C., Baranger, A., Coyne, C., Lejeune-He`naut, I., and Burstin, J. (2005). Microsatellite marker polymorphism and mapping in pea (*Pisum sativum L.*). Theoretical and applied genetics**,** 1022-1031.

Love, J., Dodd, A.N., and Webb, A.A.R. (2004). Circadian and diurnal Calcium oscillations encode photoperiodic information in Arabidopsis. The Plant Cell **16,** 956-966.

Lu, S.X., Knowles, S.M., Andronis, C., Ong, M.S., and Tobin, E.M. (2009). CIRCADIAN CLOCK ASSOCIATED 1 and LATE ELONGATED HYPOCOTYL function synergistically in the circadian clock of Arabidopsis. Plant Physiology **150,** 834-843.

Macknight, R., Bancroft, I., Page, T., Lister, C., Schmidt, R., Love, K., Westphal, L., Murphy, G., Sherson, S., Cobbett, C., and Dean, C. (1997). *FCA*, a gene controlling flowering time in Arabidopsis, encodes a protein containing RNA-binding domains Cell **89,** 737-745.

Makino, S., Matsushika, A., Kojima, M., Yamashino, T., and Mizuno, T. (2002). The *APRR1/TOC1* quintet implicated in circadian rhythms of *Arabidopsis thaliana*: I. characterization with *APRR1*-overexpressing plants. Plant and Cell Physiology **43,** 58-69.

Martin-Tryon, E.L., and Harmer, S.L. (2008). *XAP5 CIRCADIAN TIMEKEEPER* coordinates light signals for proper timing of photomorphogenesis and the circadian clock in *Arabidopsis*. The Plant Cell **20,** 1244-1259.

Martinez-Garcia, J.F., Virgos-Soler, A., and Prat, S. (2002). Control of photoperiod-regulated tuberization in potato by the *Arabidopsis* flowering-time gene *CONSTANS*. Proceedings of the National Academy of Sciences of the United States of America **99,** 15211-15216.

Más, P. (2005). Circadian clock signaling in *Arabidopsis thaliana*: from gene expression to physiology and development. International Journal of Developmental Biology **49,** 491-500.

Más, P. (2008). Chromatin remodelling and the Arabidopsis biological clock. Plant Signaling and Behaviour **3,** 121-123.

Más, P., Kim, W.-Y., Somers, D.E., and Kay, S.A. (2003a). Targeted degradation of TOC1 by ZTL modulates circadian function in *Arabidopsis thaliana*. Nature **426,** 567-570.

Más, P., Alabadi, D., Yanovsky, M.J., Oyama, T., and Kay, S.A. (2003b). Dual role of *TOC1* in the control of circadian and photomorphogenic responses in *Arabidopsis*. The Plant Cell **15,** 223-236.

Matsushika, A., Makino, S., Kojima, M., and Mizuno, T. (2000). Circadian waves

of expression of the APRR1/TOC1 family of pseudo-response regulators in *Arabidopsis thaliana*: Insight into the plant circadian clock. Plant and Cell Physiology **41,** 1002-1012.

Matsushika, A., Murakami, M., Ito, S., Nakamichi, N., Yamashino, T., and Mizuno, T. (2007). Characterization of circadian-associated pseudo-response regulators: I. Comparative studies on a series of transgenic lines misexpressing five distinctive PRR genes in *Arabidopsis thaliana*. Bioscience, Biotechnology and Biochemistry **71,** 527-534.

McWatters, H.G., Bastow, R.M., Hall, A., and Millar, A.J. (2000). The *ELF3* zeitnehmer regulates light signalling to the circadian clock. Nature **408,** 716-720.

McWatters, H.G., Kolmos, E., Hall, A., Doyle, M.R., Amasino, R.M., Gyula, P., Nagy, F., Millar, A.J., and Davis, S.J. (2007). *ELF4* is required for oscillatory properties of the circadian clock. Plant Physiology **144,** 391-401.

Menéndez, C.M., Hall, A.E., and Gepts, P. (1997). A genetic linkage map of cowpea (*Vigna unguiculata*) developed from a cross between two inbred, domesticated lines. Theoretical and Applied Genetics **95,** 1210-1217.

Michael, T.P., and McClung, C.R. (2002). Phase-specific circadian clock regulatory elements in *Arabidopsis*. Plant Physiology **130,** 627-638.

Michael, T.P., and McClung, C.R. (2003). Enhancer trapping reveals widespread circadian clock transcriptional control in Arabidopsis. Plant Physiology **132,** 629-639.

Michael, T.P., Salome, P.A., Yu, H.J., Spencer, T.R., Sharp, E.L., McPeek, M.A., Alonso, J.M., Ecker, J.R., and McClung, C.R. (2003). Enhanced fitness conferred by naturally occurring variation in the circadian clock. Science **302,** 1049-1053.

MIchael, T.P., Mockler, T.C., Breton, G., McEntee, C., Byer, A., Trout, J.D., Hazen, S.P., Shen, R., Priest, H.D., Sullivan, C.M., Givan, S.A., Yanovsky, M., Hong, F., Kay, S.A., and Chory, J. (2008). Network discovery pipeline elucidates conserved time-of-day–specific cis-regulatory modules. PLoS Genetics **4,** e14.

Michaels, S.D., Ditta, G., Gustafson-Brown, C., Pelaz, S., Yanofsky, M., and Amasino, R.M. (2003). *AGL24* acts as a promoter of flowering in *Arabidopsis* and is positively regulated by vernalization. The Plant Journal **33,** 867-874.

Millar, A.J., Short, S.R., Chua, N.H., and Kay, S.A. (1992). A novel circadian phenotype based on firefly Luciferase expression in transgenic plants. The Plant Cell **4,** 1075-1087.

Millar, A.J., Carre, I.A., Strayer, C.A., Chua, N.-H., and Kay, S.A. (1995). Circadian clock mutants in *Arabidopsis* identified by luciferase imaging. Science **267,** 1161-1163.

Miwa, K., Serikawa, M., Suzuki, S., Kondo, T., and Oyama, T. (2006). Conserved expression profiles of circadian clock-related genes in two *Lemna* species showing long-day and short-day photoperiodic flowering responses. Plant and Cell Physiology **47,** 601-612.

Mizoguchi, T., and Coupland, G. (2000). *ZEITLUPE* and *FKF1*: novel connections between flowering time and circadian clock control. Trends in Plant Science **5,** 409-411.

Mizoguchi, T., Wheatley, K., Hanzawa, Y., Wright, L., Mizoguchi, M., Song, H.-R., Carre, I.A., and Coupland, G. (2002). *LHY* and *CCA1* are partially redundant genes required to maintain circadian rhythms in *Arabidopsis*. Developmental Cell **2,** 629-641.

Mizoguchi, T., Wright, L., Fujiwara, S., Cremer, F., Lee, K., Onouchi, H., Mouradov, A., Fowler, S., Kamada, H., Putterill, J., and Coupland, G. (2005). Distinct roles of *GIGANTEA* in promoting flowering and regulating circadian rhythms in *Arabidopsis*. The Plant Cell **17,** 2255-2270.

Montaigu, A.d., Toth, R., and Coupland, G. (2010). Plant development goes like clockwork. Trends in Genetics **26,** 296-306.

Mouhu, K., Hytönen, T., Folta, K., Rantanen, M., Paulin, L., Auvinen, P., and Elomaa, P. (2009). Identification of flowering genes in strawberry, a perennial SD plant. BMC Plant Biology **9,** 1-16.

Mouradov, A., Cremer, F., and Coupland, G. (2002). Control of flowering time: interacting pathways as a basis for diversity. The Plant Cell **14** S111-S130.

Murakami, M., Yamashino, T., and Mizuno, T. (2004). Characterization of circadian-associated APRR3 pseudo-response regulator belonging to the APRR1/TOC1 quintet in Arabidopsis thaliana. Plant and Cell Physiology **45,** 645-650.

Murakami, M., Nakamichi, N., Yamashino, T., and Mizuno, T. (2002). The APRR3 component of the clock-associated APRR1/TOC1 quintet is phosphorylated by a novel protein kinase belonging to the WNK family, the gene for which is also transcribed rhythmically in *Arabidopsis thaliana*. Plant and Cell Physiology **43,** 675-683.

Murakami, M., Tago, Y., Yamashino, T., and Mizuno, T. (2007). Comparative overviews of clock-associated genes of *Arabidopsis thaliana* and *Oryza sativa*. Plant and Cell Physiology **48,** 110-121.

Murakami, M., Ashikari, M., Miura, K., Yamashino, T., and Mizuno, T. (2003). The evolutionarily conserved *Os*PRR Quintet: rice Pseudo-Response Regulators implicated in circadian rhythm. Plant and Cell Physiology **44,** 1229-1236.

Murakami, M., Matsushika, A., Ashikari, M., Yamashino, T., and Mizuno, T. (2005). Circadian-associated rice Pseudo Response Regulators (*Os*PRRs): insight into the control of flowering time. Bioscience, Biotechnology, and Biochemistry **69,** 410-414.

Murfet, I.C. (1971a). Flowering in Pisum . Three distinct phenotypic classes determined by the interaction of a dominant early and a dominant late gene Heredity **26,** 243-257.

Murfet, I.C. (1971b). Flowering in *Pisum*: reciprocal grafts between known genetypes. Australian Journal of Biological Science **24,** 1089-1101.

Murfet, I.C. (1971c). Flowering in *Pisum*: a three gene system. Heredity **27,** 93-110.

Murfet, I.C. (1973). Flowering in Pisum. *Hr*, a gene for high response to photoperiod. Heredity **31,** 157-164.

Murfet, I.C. (1977). The physiological genetics of flowering. In The physiology of the garden pea, J.F. Sutcliffe and J.S. Pate, eds (London: Academic Press), pp. 385-430.

Murfet, I.C. (1982). Flowering in the garden pea: expression of gene *Sn* in the field and use of multiple characters to detect segregation. Crop Science **22,** 923-926.

Murfet, I.C. (1988). Internode length in *Pisum*: variation in response to a daylength extension with incandescent light. Annals of Botany **61,** 331-345.

Murfet, I.C. (1992). Garden pea and allies: an update from Hobart. Flowering Newsletter **13,** 10-20.

Murfet, I.C., and Reid, J.B. (1973). Flowering in *Pisum*: evidence that gene *Sn* controls a graft-transmissible inhibitor. Australian Journal of Biological Sciences **26,** 675-677.

Murfet, I.C., and Sherriff, L.J. (1996). Confirmation that the *sn* locus is between *Aldo* and *Gal2* in linkage group VII of pea. Pisum Genetics **28,** 13-14.

Murfet, I.C., and Taylor, S.A. (1999). Flowering gene *Ppd* in pea: map position and disturbed segregation of allele *ppd-2*. Journal of Heredity **90,** 548-550.

Mutasa-Gottgens, E., and Hedden, P. (2009). Gibberellin as a factor in floral regulatory networks. Journal of Experimental Botany **60,** 1979-1989.

Mylne, J.S., Barrett, L., Tessadori, F., Mesnage, S.p., Johnson, L., Bernatavichute, Y.V., Jacobsen, S.E., Fransz, P., and Dean, C. (2006). *LHP1,* the

Arabidopsis homologue of *HETEROCHROMATIN PROTEIN1*, is required for epigenetic silencing of *FLC*. Proceedings of the National Academy of Sciences of the United States of America **103,** 5012-5017.

Nelson, D.C., Lasswell, J., Rogg, L.E., Cohen, M.A., and Bartel, B. (2000). *FKF1*, a clock-controlled gene that regulates the transition to flowering in *Arabidopsis*. Cell **101,** 331-340.

Ni, M., Tepperman, J.M., and Quail, P.H. (1998). PIF3, a phytochrome-interacting factor necessary for normal photoinduced signal transduction, is a novel basic helix-loop-helix protein. Cell **95,** 657-667.

Ni, M., Tepperman, J.M., and Quail, P.H. (1999). Binding of phytochrome B to its nuclear signalling partner PIF3 is reversibly induced by light. Nature **400,** 781-784.

Noh, Y.-S., and Amasino, R.M. (2003). *PIE1*, an *ISWI* family gene, is required for *FLC* activation and floral repression in *Arabidopsis*. The Plant Cell **15,** 1671-1682.

Oliverio, K.A., Crepy, M., Martin-Tryon, E.L., Milich, R., Harmer, S.L., Putterill, J., Yanovsky, M.J., and Casal, J.J. (2007). GIGANTEA regulates phytochrome A-mediated photomorphogenesis independently of its role in the circadian clock. Plant Physiology **144,** 495-502.

Onai, K., and Ishiura, M. (2005). *PHYTOCLOCK 1* encoding a novel GARP protein essential for the *Arabidopsis* circadian clock. Genes to Cells **10,** 963-972.

Onouchi, H., Igeno, M.I., Perilleux, C., Graves, K., and Coupland, G. (2000). Mutagenesis of plants overexpressing *CONSTANS* demonstrates novel interactions among *Arabidopsis* flowering-time genes. The Plant Cell **12,** 885-900.

Or, E., Hovav, R., and Abbo, S. (1999). A major gene for flowering time in chickpea. Crop Science **39,** 315-322.

Osborn, T.C., Kole, C., Parkin, I.A.P., and Sharpe, A.G. (1997). Comparison of flowering time genes in *Brassica rapa*, *B. napus* and *Arabidopsis thaliana*. Genetics **146,** 1123 - 1129.

Panda, S., Poirier, G.G., and Kay, S.A. (2002). *tej* defines a role for Poly(ADP-Ribosyl)ation in establishing period length of the *Arabidopsis* circadian oscillator. Developmental Cell **3,** 51-61.

Para, A., Farre, E.M., Imaizumi, T., Pruneda-Paz, J.L., Harmon, F.G., and Kay, S.A. (2007). PRR3 is a vascular regulator of TOC1 stability in the *Arabidopsis* circadian clock The Plant Cell **19,** 3462-3473.

Park, D.H., Somers, D.E., Kim, Y.S., Choy, Y.H., Lim, H.K., Soh, M.S., Kim, H.J.,

Kay, S.A., and Nam, H.G. (1999). Control of circadian rhythms and photoperiodic flowering by the *Arabidopsis GIGANTEA* gene. Science **285,** 1579-1582.

Paton, D.M., and Barber, H.N. (1955). Physiological genetics of *Pisum*. I. Grafting experiments between early and late varieties. Australian Journal of Biological Science **8,** 231-240.

Phan, H.T.T., Ellwood, S.R., Adhikari, K., Nelson, M.N., and Oliver, R.P. (2007). The first genetic and comparative map of white lupin (*Lupinus albus L.*): Identification of QTLs for anthracnose resistance and flowering time, and a locus for alkaloid content. DNA Research **14,** 59-70.

Pittendrigh, C.S. (1972). Circadian surfaces and the diversity of possible roles of circadian organisation in photoperiodic induction. Proceedings of the National Academy of Sciences USA **69,** 2734-2737.

Pruneda-Paz, J.L., Breton, G., Para, A., and Kay, S.A. (2009). A functional genomics approach reveals CHE as a component of the *Arabidopsis* circadian clock. Science **323,** 1481-1485.

Putterill, J., Laurie, R., and Macknight, R. (2004). It's time to flower: the genetic control of flowering time. Bioessays **26,** 363-373.

Putterill, J., Sobson, F., Lee, K., Simon, R., and Coupland, G. (1995). The *CONSTANS* gene of Arabidopsis promotes flowering and endcodes a protein showing similarities to zinc finger transcription factors. Cell **80,** 847-857.

Quecini, V., Zucchi, M.I., Baldin, J., and Vello, N.A. (2007). Identification of soybean genes involved in circadian clock mechanism and photoperiodic control of flowering time by *in silico* analyses. Journal of Integrative Plant Biology **49,** 1640-1653.

Quesada, V., Macknight, R., Dean, C., and Simpson, G.G. (2003). Autoregulation of *FCA* pre-mRNA processing controls Arabidopsis flowering time. The EMBO Journal **22,** 3142-3152.

Rameau, C., Denoue, D., Fraval, F., Haurogne, K., Josserand, J., Laucou, V., Batge, S., and Murfet, I.C. (1998). Genetic mapping in pea. 2. Identification of RAPD and SCAR markers linked to genes affecting plant architecture. Theoretical and applied genetics **97,** 916-928.

Reed, J.W., Nagpal, P., Bastow, R.M., Solomon, K.S., Dowson-Day, M.J., Elumalai, R.P., and Millar, A.J. (2000). Independent action of ELF3 and phyB to control hypocotyl elongation and flowering time. Plant Physiology **122,** 1149-1160.

Reid, J.B. (1979a). Flowering in Pisum: the effect of age on the gene *Sn* and the sit of

action of gene *Hr*. Annals of Botany **44,** 163-173.

Reid, J.B. (1979b). Red-far red reversibility of flower development and apical senescence in *Pisum*. Zeitschrift fur Pflanzenphysiologie **93,** 297-301.

Reid, J.B. (1980). Apical senescence in *Pisum*: a direct or indirect role for the flowering genes? Annals of Botany **45,** 195-201.

Reid, J.B., and Murfet, I.C. (1975). Flowering in *Pisum*: the sites and possible mechanisms of the vernalization response. Journal of Experimental Botany **26,** 860-867.

Reid, J.B., and Murfet, I.C. (1977). Flowering in *Pisum*: the effect of light quality on the genotype *If e Sn Hr*. Journal of Experimental Botany **28,** 1357-1364.

Reid, J.B., and Murfet, I.C. (1984). Flowering in Pisum: a fifth locus, *Veg*. Annals of Botany **53,** 369-382.

Ross, J.J., and Murfet, I.C. (1985). A comparison of the flowering and branching control systems in *Lathyrus odoratus L.* and *Pisum sativum L*. Annals of Botany **56,** 847-856.

Salome, P.A., and McClung, C.R. (2005a). What makes the Arabidopsis clock tick on time? A review on entrainment. Plant, Cell and Environment **28,** 21-38.

Salome, P.A., and McClung, C.R. (2005b). *PSEUDO-RESPONSE REGULATOR 7* and *9* are partially redundant genes essential for the temperature responsiveness of the *Arabidopsis* circadian clock. The Plant Cell **17,** 791-803.

Samach, A., Onouchi, H., Gold, S.E., Ditta, G.S., Schwarz-Sommer, Z., Yanofsky, M.F., and Coupland, G. (2000). Distinct roles of CONSTANS target genes in reproductive development of *Arabidopsis*. Science **288,** 1613-1616.

Sarker, A., Erskine, W., Sharma, B., and Tyagi, M.C. (1999). Inheritance and linkage relationship of days to flower and morphological loci in lentil (*Lens culinaris* Medikus subsp. *culinaris*). Journal of Heredity **90,** 270-275.

Satter, R.L., and Galston, A.W. (1981). Mechanisms of control of leaf movements. Annual Review of Plant Physiology **32,** 83-110.

Sawa, M., Nusinow, D.A., Kay, S.A., and Imaizumi, T. (2007). FKF1 and GIGANTEA complex formation is required for day-length measurement in *Arabidopsis*. Science **318,** 261-265.

Schaffer, R., Landgraf, J., Accerbi, M., Simon, V., Larson, M., and Wisman, E. (2001). Microarray analysis of diurnal circadian-regulated genes in *Arabidopsis*. The Plant Cell **13,** 113-123.

Schaffer, R., Ramsay, N., Samach, A., Corden, S., Putterill, J., Carre, I.A., and Coupland, G. (1998). The *late elongated hypocotyl* mutation of *Arabidopsis* disrupts circadian rhythms and the photoperiodic control of flowering. Cell **93,**

1219-1229.

Schomburg, F.M., Patton, D.A., Meinke, D.W., and Amasino, R.M. (2001). *FPA*, a gene involved in floral induction in *Arabidopsis*, encodes a protein containing RNA-recognition motifs. The Plant Cell **13,** 1427-1436.

Schultz, T.F., Kiyosue, T., Yanovsky, M., Wada, M., and Kay, S.A. (2001). A role for LKP2 in the circadian clock of *Arabidopsis*. The Plant Cell **13,** 2659-2670.

Searle, I., and Coupland, G. (2004). Induction of flowering by seasonal changes in photoperiod. The EMBO Journal **23,** 1217-1222.

Searle, I., He, Y., Turck, F., Vincent, C., Fornara, F., Krober, S., Amasino, R.A., and Coupland, G. (2006). The transcription factor FLC confers a flowering response to vernalization by repressing meristem competence and systemic signaling in Arabidopsis. Genes and Development **20,** 898-912.

Silverstone, A.L., Mak, P., Martinez, E.C., and Sun, T. (1997). The new *RGA* locus encodes a negative regulator of gibberellin response in *Arabidopsis Thaliana*. Genetics **146,** 1087–1099.

Simpson, G.G., and Dean, C. (2002). Arabidopsis, the rosetta stone of flowering time? Science **296,** 285-289.

Simpson, G.G., Dijkwel, P.P., Quesada, V., Henderson, I., and Dean, C. (2003). FY Is an RNA 3´ end-processing factor that interacts with FCA to control the *Arabidopsis* floral transition Cell **113,** 777-787.

Slotte, T., Holm, K., McIntyre, L.M., Lagercrantz, U., and Lascoux, M. (2007). Differential expression of genes important for adaptation in *Capsella bursa-pastoris* (Brassicaceae). Plant Physiology **145,** 160-173.

Somers, D.E., Devlin, P.F., and Kay, S.A. (1998a). Phytochromes and cryptochromes in the entrainment of the *Arabidopsis* circadian clock. Science **282,** 1488-1490.

Somers, D.E., Webb, A.A.R., Pearson, M., and Kay, S.A. (1998b). The short-period mutant, *toc1-1*, alters circadian clock regulation of multiple outputs throughout development in *Arabidopsis thaliana*. Development **125,** 485-494.

Somers, D.E., Schultz, T.F., Milnamow, M., and Kay, S.A. (2000). *ZEITLUPE* encodes a novel clock-associated PAS protein from *Arabidopsis*. Cell **101,** 319-329.

Staiger, D., Zecca, L., Kirk, D.A.W., Apel, K., and Eckstein, L. (2003a). The circadian clock regulated RNA-binding protein AtGRP7 autoregulates its expression by influencing alternative splicing of its own pre-mRNA. The Plant Journal **33,** 361-371.

Staiger, D., Allenbach, L., Salathia, N., Fiechter, V., Davis, S.J., Millar, A.J.,

Chory, J., and Fankhauser, C. (2003b). The Arabidopsis *SRR1* gene mediates phyB signaling and is required for normal circadian clock function. Genes and Development **17,** 256-268.

Strayer, C., Oyama, T., Schultz, T.F., Raman, R., and al, e. (2000). Cloning of the *Arabidopsis* clock gene *TOC1*, an autoregulatory response regulator homolog. Science **289,** 768-771.

Suarez-Lopez, P., Wheatley, K., Robson, F., Onouchi, H., Valverde, F., and Coupland, G. (2001). *CONSTANS* mediates between the circadian clock and the control of flowering in *Arabidopsis*. Nature **410,** 1116-1120.

Sung, S., and Amasino, R.M. (2004). Vernalization in *Arabidopsis thaliana* is mediated by the PHD finger protein VIN3. Nature **427,** 159-164.

Tadege, M., Wen, J., He, J., Tu, H., Kwak, Y., Eschstruth, A., Cayrel, A., Endre, G., Zhao, P.X., Chabaud, M., Ratet, P., and Mysore, K.S. (2008). Large-scale insertional mutagenesis using the *Tnt1* retrotransposon in the model legume Medicago truncatula. The Plant Journal **54,** 335-347.

Takahashi, Y., Teshima, K.M., Yokoi, S., Innan, H., and Shimamoto, K. (2009). Variations in Hd1 proteins, *Hd3a* promoters, and *Ehd1* expression levels contribute to diversity of flowering time in cultivated rice. Proceedings of the National Academy of Sciences **106,** 4555-4560.

Tamaki, S., Matsuo, S., Wong, H.L., Yokoi, S., and Shimamoto, K. (2007). Hd3a protein s a mobile flowering signal in rice. Science **316,** 1033-1036.

Taylor, S.A., and Murfet, I.C. (1993). Flowering in pea: a mutation from Lf_d to lf_a and a summary of induced *Lf* mutations. Pisum Genetics **25,** 60-63.

Taylor, S.A., and Murfet, I.C. (1994). A short day mutant in pea is deficient in the floral stimulus. Flowering Newsletter **18,** 39-43.

Taylor, S.A., and Murfet, I.C. (1996). Flowering in *Pisum*: Identification of a new *ppd* allele and its physiological action as revealed by grafting. Physiologia Plantarum **97,** 719-723.

Templeton, A.R., Crandall, K.A., and Sing, C.F. (1992). A cladistic-analysis of phenotypic associations with haplotypes inferred from restriction endonuclease mapping and DNA-sequence data. III. Cladogram estimation. Genetics **132,** 619-633.

Thines, B., and Harmon, F.G. (2010). Ambient temperature response establishes *ELF3* as a required component of the core Arabidopsis circadian clock. Proceedings of the National Academy of Sciences **107,** 3257-3262.

Thines, B., and Harmon, F.G. (2011). Four easy pieces: mechanisms underlying circadian regulation of growth and development. Current Opinion in Plant

Biology **14,** 31-37.

Thompson, J.D., Gibson, T.J., Plewniak, F., Jeanmougin, F., and Higgins, D.G. (1997). The ClustalX windows interface: flexible strategies for multiple sequence alignment aided by quality analysis tools. Nucleic Acids Research **24,** 4876-4882.

Trevaskis, B., Hemming, M.N., Peacock, W.J., and Dennis, E.S. (2006). *HvVRN2* responds to daylength, whereas *HvVRN1* is regulated by vernalization and developmental status. Plant Physiology **140,** 1397-1405.

Triques, K., Piednoir, E., Dalmais, M., Schmidt, J., Signor, C.L., Sharkey, M., Caboche, M., Sturbois, B., and Bendahmane, A. (2008). Mutation detection using ENDO1: Application to disease diagnostics in humans and TILLING and Eco-TILLING in plants. BMC Molecular Biology **9,** 42.

Tseng, T.S., Salome, P.A., McClung, C.R., and Olszewski, N.E. (2004). SPINDLY and GIGANTEA interact and act in *Arabidopsis thaliana* pathways involved in light responses, flowering, and rhythms in cotyledon movements. The Plant Cell **16,** 1550-1563.

Tullu, A., Tar'an, B., Warkentin, T., and Vandenberg, A. (2008). Construction of an intraspecific linkage map and QTL analysis for earliness and plant height in lentil. Crop Science **48,** 2254-2264.

Turck, F., Fornara, F., and Coupland, G. (2008). Regulation and identity of florigen: FLOWERING LOCUS T moves center stage. Annual Review of Plant Biology **59,** 573 - 594.

Turner, A., Beales, J., Faure, S., Dunford, R., and Laurie, D. (2005). The pseudo-response regulator *ppd-h1* provides adaptation to photoperiod in barley. Science **310,** 1031-1034.

Ueda, H.R. (2006). Systems biology flowering in the plant clock field. Molecular System Biology **2,** 60-61.

Valverde, F., Mouradov, A., Soppe, W., Ravenscroft, D., Samach, A., and Coupland, G. (2004). Photoreceptor regulation of CONSTANS protein in photoperiodic flowering. Science **303,** 1003-1006.

Wang, H., Ma, L.-G., Jin-Ming, Zhao, H.-Y., and Deng, X.W. (2001). Direct interaction of *Arabidopsis* cryptochromes with COP1 in light control development. Science **294,** 154-158.

Wang, J., Long, Y., Wu, B., Liu, J., Jiang, C., Shi, L., Zhao, J., King, G., and Meng, J. (2009). The evolution of *Brassica napus FLOWERING LOCUST* paralogues in the context of inverted chromosomal duplication blocks. BMC Evolutionary Biology **9,** 271.

Wang, Q., Sajja, U., Rosloski, S., Humphrey, T., Kim, M.C., Bomblies, K., Weigel, D., and Grbic, V. (2007). *HUA2* caused natural variation in shoot morphology of *A. thaliana*. Current Biology **17,** 1513-1519.

Wang, Z.-Y., and Tobin, E.M. (1998). Constitutive expression of the *CIRCADIAN CLOCK ASSOCIATED 1 (CCA1)* gene disrupts circadian rhythms and suppresses its own expression. Cell **93,** 1207-1217.

Wang, Z.-Y., Kenigsbuch, D., Sun, L., Harel, E., Ong, M.S., and Tobin, E.M. (1997). A Myb-related transcription factor is involved in the Phytochrome regulation of an *Arabidopsis Lhcb* gene. The Plant Cell **9,** 491-507.

Webb, A.A.R. (1998). Stomatal rhythms. In Biological rhythms and photoperiodism in plants, P.J. Lumsden and A.J. Millar, eds (Oxford: BIOS Scientific Publishers), pp. 69-80.

Webb, A.A.R. (2003). The physiology of circadian rhythms in plants. New Phytologist **160,** 281-303.

Weeden, N.F. (2007). Genetic changes accompanying the domestication of *Pisum sativum*: Is there a common genetic basis to the 'domestication syndrome' for legumes? Annals of Botany **100,** 1017-1025.

Weeden, N.F., Kneen, B.E., and Murfet, I.C. (1988). Pisum Newsletter **20,** 49-51.

Weeden, N.F., Muehlbauer, F.J., and Ladizinsky, G. (1992). Extensive conservation of linkage relationships between pea and lentil genetic maps. Journal of Heredity **83,** 123-129.

Weeden, N.F., Ellis, T.H.N., Timmerman-Vaughan, G.M., Swiecicki, W.K., Rozov, S.M., and Berdnikov, V.A. (1998). A consensus linkage map for *Pisum sativum*. Pisum Genetics **30,** 1-4.

Weller, J.L. (2005). Mobile flowering signals in pea. Flowering Newsletter **36,** 15-24.

Weller, J.L. (2007). Update on the genetics of flowering. Pisum Genetics **39,** 1-8.

Weller, J.L., Murfet, I.C., and Reid, J.B. (1997a). Pea mutants with reduced sensitivity to far-red light define an important role for Phytochrome A in day-length detection. Plant Physiology **114,** 1225-1236.

Weller, J.L., Reid, J.B., Taylor, S.A., and Murfet, I.C. (1997b). The genetic control of flowering in pea. Trends in Plant Science **2,** 412-418.

Weller, J.L., Nagatani, A., Kendrick, R.E., Murfet, I.C., and Reid, J.B. (1995). New *lv* mutants of pea are deficient in Phytochrome B. Plant Physiology **108,** 525-532.

Weller, J.L., Batge, S.L., Smith, J.J., Kerckhoffs, L.H.J., Sineshchekov, V.A., Murfet, I.C., and Reid, J.B. (2004). A dominant mutation in the pea *PHYA* gene confers enhanced responses to light and impairs the light-dependent

degradation of Phytochrome A. Plant Physiology **135,** 2186-2195.

Weller, J.L., Hecht, V., Liew, L.C., Sussmilch, F.C., Wenden, B., Knowles, C.L., and Vander Schoor, J.K. (2009). Update on the genetic control of flowering in garden pea. Journal of Experimental Botany **60,** 2493-2499.

Willige, B.C., Ghosh, S., Nill, C., Zourelidou, M., Dohmann, E.M.N., Maier, A., and Schwechheimer, C. (2007). The DELLA domain of *GA INSENSITIVE* mediates the interaction with the *GA INSENSITIVE DWARF1A* gibberellin receptor of Arabidopsis. The Plant Cell **19,** 1209-1220.

Xing, D., Zhao, H., Xu, R., and Li, Q.Q. (2008). Arabidopsis PCFS4, a homologue of yeast polyadenylation factor Pcf11p, regulates *FCA* alternative processing and promotes flowering time. The Plant Journal **54,** 899-910.

Yakir, E., Hilman, D., Harir, Y., and Green, R.M. (2007). Regulation of output from the plant circadian clock. Febs Journal **274,** 335-345.

Yamaguchi, A., Kobayashi, Y., Goto, K., Abe, M., and Araki, T. (2005). *TWIN SISTER OF FT* (*TSF*) acts as a floral pathway integrator redundantly with *FT*. Plant and Cell Physiology **46,** 1175-1189.

Yan, L., Loukoianov, A., Tranquilli, G., Helguera, M., Fahima, T., and Dubcovsky, J. (2003). Positional cloning of the wheat vernalization gene *VRN1*. Proceedings of the National Academy of Sciences of the United States of America **100,** 6263-6268.

Yan, L., Loukoianov, A., Blechl, A., Tranquilli, G., Ramakrishna, W., SanMiguel, P., Bennetzen, J.L., Echenique, V., and Dubcovsky, J. (2004). The wheat *VRN2* gene is a flowering repressor down-regulated by vernalization. Science **303,** 1640-1644.

Yan, L., Fu, D., Li, C., Blechl, A., Tranquilli, G., Bonafede, M., Sanchez, A., Valarik, M., Yasuda, S., and Dubcovsky, J. (2006). The wheat and barley vernalization gene *VRN3* is an orthologue of *FT*. Proceedings of the National Academy of Sciences **103,** 19581-19586.

Yano, M., Katayose, Y., Ashikari, M., Yamanouchi, U., Monna, L., Fuse, T., Baba, T., Yamamoto, K., Umehara, Y., Nagamura, Y., and Sasaki, T. (2000). *Hd1,* a major photoperiod sensitivity quantitative trait locus in rice, is closely related to the *Arabidopsis* flowering time gene *CONSTANS*. The Plant Cell **12,** 2473-2484.

Yanovsky, M., and Kay, S. (2003). Living by the calendar: how plants know when to flower. Nature Reviews: Molecular Cell Biology **4,** 265-275.

Yanovsky, M.J., Mazzella, M.A., and Casal, J.J. (2000). A quadruple photoreceptor mutant still keep track of time. Current Biology **10,** 1013-1015.

Yoshida, R., Fekih, R., Fujiwara, S., Oda, A., Miyata, K., Tomozoe, Y., Nakagawa, M., Niinuma, K., Hayashi, K., Ezura, H., Coupland, G., and Mizoguchi, T. (2009). Possible role of EARLY FLOWERING 3 (ELF3) in clock-dependent floral regulation by SHORT VEGETATIVE PHASE (SVP) in *Arabidopsis thaliana*. New phytologist **182,** 838-850.

Yu, J.-W., Rubio, V., Lee, N.-Y., Bai, S., Lee, S.-Y., Kim, S.-S., Liu, L., Zhang, Y., Irigoyen, M.L., Sullivan, J.A., Zhang, Y., Lee, I., Xie, Q., Paek, N.-C., and Deng, X.W. (2008). COP1 and ELF3 control circadian function and photoperiodic flowering by regulating GI stability. Molecular Cell **32,** 617-630.

Zagotta, M.T., Hicks, K.A., Jacobs, C.I., Young, J.C., Hangarter, R.P., and Meeks-Wagner, D.R. (1996). The Arabidopsis *ELF3* gene regulates vegetative photomorphogenesis and the photoperiodic induction of flowering. The Plant Journal **10,** 691-702.

Zeilinger, M.N., Farre, E.M., Taylor, S.R., Kay, S.A., and Doyle, F.J. (2006). A novel computational model of the circadian clock in *Arabidopsis* that incorporates PRR7 and PRR9. Molecular System Biology **2,** 58.

Zhang, H., Ransom, C., Ludwig, P., and van Nocker, S. (2003). Genetic analysis of early flowering mutants in Arabidopsis defines a class of pleiotropic developmental regulator required for expression of the flowering-time switch *Flowering Locus C*. Genetics **164,** 347-358.

Zhou, Y., Sun, X.-D., and Ni, M. (2007). Timing of photoperiodic flowering: light perception and circadian clock. Journal of Integrative Plant Biology **49,** 28-34.

Zhu, H., Choi, H.-K., Cook, D.R., and Shoemaker, R.C. (2005). Bridging model and crop legumes through comparative genomics. Plant Physiology **137,** 1189-1196.

Appendix

Appendix 1 – Primers

Primers used for gene isolation

GENE	NAME	SEQUENCE	Tm (°C)	Description
ELF3	ELF3-D1F	GGWGGRCCAAGAGCWCCWCCYAGGAAY AAR ATG G	60	degenerated primer to isolate Pea orthologous gene
	ELF3-D2R	AAC TCA AAC ACT TGG ACW GCA AAC ACT CTC TGT TG	60	degenerated primer to isolate Pea orthologous gene
	ELF3-D3F	CAA GTK TTT GAR YTG CAT AGA CTG ATH AAR GTN CA	60	degenerated primer to isolate Pea orthologous gene
	ELF3-D4R	CCT TCR GAA GGW GAC ATN ACA GGA ATT AAC CAY TG	60	degenerated primer to isolate Pea orthologous gene
	ELF3-1F	ACC TCC CAG GAA CAA AAT GG	60	Specific Pea primer for sequencing and qPCR
	ELF3-2R	AAC TCA AAC ACT TGG ACT GC	58	Specific Pea primer for sequencing and qPCR
	ELF3-GW1	GGA ATA CTA AAT TGC TCA TAC AAA GCC	67	Specific Pea primer for Genome Walking
	ELF3-GW2	GTT CCT GGG AGG TGC TCT TGG CCC TCC	67	Specific Pea primer for Genome Walking
	ELF3-GW3	AGA TTG TCA ACA GGT GAA AAT TTC TCC	67	Specific Pea primer for Genome Walking
	ELF3-GW4	GCA GTA ATA GGC CAA AAA CAT TTC GG	67	Specific Pea primer for Genome Walking and qPCR
	ELF3-3F	AGG GTT CCT GTA TAT GTT CG	58	Specific Pea primer for sequencing
	ELF3-3R	CCA TGC TGT CTT GGA TCC	56	Specific Pea primer for isolation intron 1
	ELF3-I2F	GCC AAA AAC AAA AGC CTG AA	56	Specific Pea primer for marker CHAMP x TER
	ELF3-I2R	TCC AAC GTA TAT CCC TAG TAG T	60	Specific Pea primer for marker CHAMP x TER
	ELF3-4F	GCC ACT CCA CCC GAA TAC T	60	Specific Pea primer for intron 1 isolation

	ELF3-4R	GTT TCC CAG CCT GAC GAA T	58	Specific Pea primer for intron 2 isolation
	ELF3-5F	ACC AGT CCA ACC CAG GCT AT	62	Specific Pea primer for RACE
	ELF3-6F	ACA GCA TTT CCA AGA TCT CCA G	64	Specific Pea primer for RACE
	ELF3-7F	TGT TTG CAG TCC AAG TGT TTG	58	Specific Pea primer for intron 3 isolation
	ELF3-7R	CGA TCC GGC AAT TAG TTG TT	58	Specific Pea primer for intron 3 isolation
	ELF3-5UF	TTC CTA ACA CTC TTT CTC TCT CTC	62	Specific Pea primer for 5' Genome walking
	ELF3-3UF	CGA CGC ACT GTA GTG GTG TA	60	Specific Pea primer for 3' Genome walking
	ELF3-3UR	ACC AGC TTT TGA CCA TCC TG	60	Specific Pea primer for 3' Genome walking
	ELF3-FLF	GGG ATG AAA AGA GGG AAT GA	58	Specific Pea primer for full length cDNA
	ELF3-FLR	CAC CAC TAC AGT GCG TCG TA	62	Specific Pea primer for full length cDNA
	ELF3-F	GATTGTGTTGTGGAAGTGTA	56	Specific Pea primer for 5'UTR
	ELF3-R	GATAACTCAACAAGCACCAT	56	Specific Pea primer for 3'UTR
	ELF3-FF	GTTTAGAGTTTAGGATAGAAAAGGGGTAGG	80	Specific Pea primer for 5'UTR
	ELF3-RR	GATCCTCCATGTCAATATACACCACTAC	76	Specific Pea primer for 3'UTR
	ELF3-GW-1F	AAATTGTTATCATTCCGAACACA	60	Specific Pea primer for 5'UTR
	ELF3-8R	TGCAAACTAATTGCCAAATTAAA	58	Specific Pea primer within intron 1 for mutation identification
ELF4	DELF4.1	CAG TCG GTG CTT GAC AGG AAC AGA GCA ATA ATH CAR CAR GT	61	degenerated primer to isolate Pea orthologous gene
	DELF4.2	GAG ATC AGA ATA AAG AGA AGC AAC CTT TGA AAT RTT NCC RTT	61	degenerated primer to isolate Pea orthologous gene
	ELF4P.1F	GTG CTT GAC AGG AAC AGA GC	62	Specific Pea primer to sequence and for marker
	ELF4P.1R	CAG AAT AAA GAG AAG CAA CC	56	Specific Pea primer to sequence and for marker
	ELF4P-2F	CAA TCT AGA ATG CCT GAT AAC ATG G	54	Specific Pea primer for IPCR
	ELF4P-2R	ACA CGT TTT TCA CCA TGT TAT CAG G	54	Specific Pea primer for IPCR
	ELF4-GSP1	TCA GTC GGT GCT TGA CAG GAA CAG AGC	67	Specific primer for Genome Walking

	ELF4-GSP2	TGA GAT CAG AAT AAA GAG AAG CAA CCT TTG	67	Specific primer for Genome Walking
	ELF4-153.1	GTT GTG ATG GTA GTT TTG AGG	60	Specific primer for 3' end of ELF4 (GenWalking clone 153)
	ELF4-153.2	GTA CAA GAT TGA AGC AGA AGG	60	Specific primer for 3' end of ELF4 (GenWalking clone 153)
	ELF4-AluI	GTA TTT AAC AAA TTT TGC ACC CTT TCT AGC	80	dCAPS primer for mapping
	ELF4-153.3	AAA GGG GCA TTT ATA CCC TTA CA	64	primer for mapping using wirh ELF4-TaqI
	ELF4-TaqI	ATG TTG TCA TCA ATT ATG TCT TTG AAT TCG	80	dCAPS primer for mapping
	ELF4-FLF	CAC AAA CCA AGA ACA AAA CAT AAT TG	68	primer for full length cDNA
	ELF4-FLR	ACT ACT ACT ACA TAA CAA CAA GAG G	68	primer for full length cDNA
HUA2	HUA2-1F	GCGATCTTGTCCTTGCTAAG	60	Medicago primer for isolation Pea ortholog
	HUA2-1R	TGAATATCTGTGGGTGCAAC	58	Medicago primer for isolation Pea ortholog
	HUA2-2F	CGTGATGCTTTTGAAGGAAT	56	Medicago primer for isolation Pea ortholog
	HUA2-2R	TTCCGAATGAGAAGTTCAAC	56	Medicago primer for isolation Pea ortholog
	HUA2-3F	TCTTGTTGATTCTATCACCC	56	Medicago primer for isolation Pea ortholog
	HUA2-3R	TTTTCCTCTCAAGCCACAAC	58	Medicago primer for isolation Pea ortholog
LUX	LUX-1F	TTGATCCCACCGGAGCTCGC	66	Medicago primer for isolation Pea ortholog
	LUX-2F	GTGTGGACCCCACAGTTACA	62	Medicago primer for isolation Pea ortholog
	LUX-1R	ACCCTTCAACATTCATCAAC	56	Medicago primer for isolation Pea ortholog
	LUX-3F	CTAATGATAGTAATAAATAA	46	Medicago primer for isolation Pea ortholog
	LUX-2R	GCTACTACCAACAATCAAAC	56	Medicago primer for isolation Pea ortholog
	LUX-4F	GAACAGAAACGACGCTGAAACG	60	Pea specific primers
	LUX-5F	AAGAGATTCGTCGACGTTGTGG	60	Pea specific primers
	LUX-4R	CAGCGTCGTTTCTGTTCTAACC	60	Pea specific primers
	LUX-5R	GGTTGACGTCGATGAGTGTACG	60	Pea specific primers

	LUX-6F	GCCTCACCGTACACTCATCG	64	Pea specific primers
	LUX-FLF	AACGGTTAGAAGAAGTGAATGG	58	Pea specific primers
	LUX-7F	TGAATTCTCATTCGCAATCG	56	Pea specific primers
	LUX-FLR	AGCAAATACAACTCGGATGC	58	Pea specific primers
	LUX-Q1F	TTCTCACCCTCACATGTCTCC	62	Pea specific primers for real-time PCR around intron in 3'UTR
	LUX-Q1R	TGGACGAAGTCACAATCAACA	58	Pea specific primers for real-time PCR around intron in 3'UTR
	LUX-7R	GTTGGAAAGACCTTGCATCC	60	Pea specific primers
	LUX-8R	GGCCGTTTCAGCGTCGTTTC	64	Pea specific primers
	LUX-SN1	CGGTTAGACGCTGAAACGGC	64	Allele specific primer for sn1 mutation
	LUX-dSN4	ACAGACGAAGAGCGTGTAACGGACT	60	dCAPS primer for sn4 mutation
	LUX-SN1.2	CGGATTCGGCGGTTAGACGC	66	Allele specific primer for sn1 mutation
	LUX-9F	CGGGACAAATCACCAAACG	62	Primer around sn1 and sn2 mutations- play with HRM
	LUX-9R	TCGACGAATCTCTTGTGAAGC	60	Primer around sn1 and sn2 mutations- play with HRM
MYB1	MYB1P-1F	GAG AGG TGT TAC CCC AAA GC	62	Specific Pea primer designed on F.Foucher sequence
	MYB1P-1R	TTG GGG TAA CAC CTC TCT GG	62	Specific Pea primer designed on F.Foucher sequence
	MYB1P-2R	CTG GTT TCC TTC GCT TCT AC	60	Specific Pea primer designed on F.Foucher sequence
	MYB1-GSP1	GGA CGA CTT GCG TTT CGG GCT CTA TTC TCC	67	Specific primer for Genome Walking
	MYB1-GSP2	CTT AAG ACT CGT CGA ACA GGG TTT AAA CC	67	Specific primer for Genome Walking
	MYB1-GSP3	CGT ATC CTC TTG GGA CCT GTC TCT TCA AC	67	Specific primer for Genome Walking
	MYB1-GSP4	CTT TTG TAA GGT TTA AAC CCT GTT CGA CG	67	Specific primer for Genome Walking
	MYB1-2F	GCA ACA TTC TTG ATT CTT GG	56	Specific primer for amplification intron7
	MYB1-3'END	ACT TAA TGT TTC TTC TCT AAT GC	60	Specific primer for amplification 3'UTR
	MYB1-GSP5	CGG AGG TGA ACC AAT TTG TCT AGA TGG	67	Specific primer for Genome Walking

	MYB1-GSP6	GGA GGA AAT GAT TGA GGA ATA GAT GAC C	67	Specific primer for Genome Walking
	MYB1-5'F1	GGT AGT GGC TGA GAT TGG	56	Specific primer for full length cDNA
	MYB1-5'F2	GGC TTT ACT ATT TGC TGT GC	58	Specific primer for full length cDNA
	MYB1-5'R1	AAC CAC TTC TTC ACC AGA GG	60	Specific primer for full length cDNA
	MYB1-3R	CGG ATT TTC TGT GAT TCT ATG C	62	Specific primer for full length cDNA
	MYB1-4R	GAT GCA ACT GCA ATA AGT GG	58	Specific primer for full length cDNA
	MYB1.3F	GGC ACG GTC ATC TAT TCC	56	Specific primer for full length cDNA
	MYB1.4F	CTT TTC CTA CTA CAG AGG	52	Specific primer for full length cDNA
	MYB1.5R	TTC AAC CTC TGT AGT AGG	52	Specific primer for full length cDNA
	MYB1-6F	TGG CAG CGC ATA GAA GAG CAT	64	Specific primer for full length cDNA
	MYB1-6R	GAA TTT TTG CGC ATG GCT CCT G	66	Specific primer for full length cDNA
	MYB1-Q1	GAC GGA TGC GCT AGA GAA GAA TGG	60	Specific primer for real time PCR
	MYB1-Q2	AGA ATA GAG CCC GAA ACG CAA GTC	60	Specific primer for real time PCR
MYB2	MYB2P-1F	GGT GGA CAG ATG AAG AAC	54	Specific Pea primer designed on F.Foucher sequence
	MYB2P-2F	CAT GTT GGC ACA AAG ACT GC	60	Specific primer for RACE
	MYB2P-1R	CTT CTG AGC ATG ACT TCG	54	Specific Pea primer designed on F.Foucher sequence
	MYB2P-2R	AAT TGA CTC CAC CAA TGT CGT	60	Specific primer for RACE
	MYB2P-3R	TGA CCA AAA TCT AAC GAC CCA AGA G	64	Specific primer for 5'RACE
PRR37	DPR-F37	CAT RTT GTB HCT GCW YTG YTW MGS AAT TGT RGY TA	60	degenerated primer to isolate Pea orthologous genes
	DPR-R37	CCA VAG GTT BTT AAG YTC RTT CYT BCK WAT NGG YTT	60	degenerated primer to isolate Pea orthologous genes
	PRR37-F	TTG GAT TTG TGC ATT CCT GA	56	Specific Pea primer for full length cDNA
	PRR37.1F	GYT ACG CAA TTG TAG TTA TG	56	Specific primer for RACE
	PRR37.2F	CAA GCG TGG AAA GCT CTA GAA GAT CC	76	Specific primer for RACE

	PRR37.3F	TGT GCA AGA TCA TGA GCC ACA TAG C	74	Specific primer for RACE
	PRR37.1R	GCT TTC CAC GCT TGA AGA CCA TTG G	74	Specific primer for RACE
	PRR37.2R	GAC AAT ACC CAT AGA ATC GTG AGA TGA C	80	Specific primer for RACE
	PRR37.4F	GAC GAT GAT GAT TCC ACA CG	60	Specific primer for mapping (intron)
	PRR37.5F	TGG CAA CAT GTT TGG AGA AG	58	Specific primer for mapping (intron)
	PRR37.6F	GGA AGC AGA GGC TTG AGT GT	62	Specific primer for mapping (intron)
	PRR37.3R	GTT GAG CAT GCT CGA CTT GG	62	Specific primer for mapping (intron)
	PRR37.4R	GTG GCT CAT GAT CTT GCA CA	60	Specific primer for mapping (intron)
	PRR37.5R	ACA CTC AAG CCT CTG CTT CC	62	Specific primer for mapping (intron)
	PRR37.6R	GAT TGT TTA CGA GGG CTG CT	60	Specific primer for mapping (intron)
	PRR37.7F	TGA TAT AGA TGG TAT GCA GC	56	Specific primer for sequencing cDNA from RACE
	PRR37-FLF	AAG GGA TCG ACT CAA ATC CA	58	Specific primer for isolating full length cDNA
	PRR37-FLR	TAA AAA TGG ACG CCT GCC TA	58	Specific primer for isolating full length cDNA
	PRR37-8F	CTG AAC TCC AAG TCG TGC AA	60	Specific primer for isolating full length cDNA
	PRR37-8R	GGA TCA GCA ATT TGG ATT GG	58	Specific primer for isolating full length cDNA
PRR59	DPR-F59	TTR YWG CDG TTB STG ATG GNT TRA ANG CNT GGG	60	degenerated primer to isolate Pea orthologous genes
	DPR-R59	MGACRT CATTAT RACAGG AATRTT TTTRCA AATDTS ATGCTC CATNA	60	degenerated primer to isolate Pea orthologous genes
	DCCT-F359	MGR GAA GCH GCH YTR RHV AAR TTY CGD HTR AAR MGN AAR GA	60	degenerated primer to isolate Pea orthologous genes
	DCCT-R359	YKH ACA AAY TGN CCY YTN AYN CGD GGN CGB TKN TC	60	degenerated primer to isolate Pea orthologous genes
	PRR59.1F	CTC AAG GGA AGA CCG CGG AAT TTC G	78	Specific primer for RACE
	PRR59.2F	GGT ATC TGG CTA TGC ACT TCT CTC G	76	Specific primer for RACE
	PRR59.1R	TAA GAT CGA AAT TCC GCG GTC TTC C	70	Specific primer for RACE
	PRR59.2R	ATA GCC AGA TAC CGA TGG CAA ATC G	72	Specific primer for RACE

	PRR59.3F	ATG CAT GTT GAG AGG TGC AG	60	Specific primer for mapping (introns)
	PRR59.3R	AGC TTC CAT GTT TGG CTT TG	58	Specific primer for mapping (introns)
	PRR59.4R	CAA ACA TGC TGC CAC AGA TT	58	Specific primer for mapping (introns)
	PRR59.4F	GGG CTT TTG AGA TGG GAG A	58	Specific primer for mapping (introns)
	PRR59.5F	AAA GGA AGT GAT GCA CAG AGC	62	Specific primer for mapping (introns)
	PRR59.5R	TCC TCT CCC CTG AGT CAC AT	62	Specific primer for mapping (introns)
	PRR59.6F	GTG CTT TTG GTT GAA GCT GA	58	Specific primer for mapping (introns)
	PRR59.6R	GATCAATGTCTGGCCTAAACG	62	Specific primer
	PRR59.7R	GCTTGTCTCTCCATTTTTGTGG	64	Specific primer
PsTIC	TIC-D1	ATG GAT AGA ATC AGA GAA GCT AGA AGA	55	degenerate primer
	TIC-D2	CGG AAA CTC CGA TCA TYT CRT C	55	degenerate primer
	TIC-D3	TGG AAA GCC GCY GAT GAA ATG AT	54	degenerate primer
	TIC-D4	CAC TGG TCT CGG TYT YTT NCT CTT	56	degenerate primer
	TIC-D5	GCC GAA GTA TTG TAC GGN ATG ATG AG	59	degenerate primer
	TIC-D6	TTT TGG GAC GGG GTT GAT TRA A	52	degenerate primer
	TIC-D7	ACC GAG ACC AGT GAA GYA YGA RGA	58	degenerate primer
	TIC-D8	GGT ATT GGA AAT GGG TAA SCR TTA TTC TG	58	degenerate primer
	TIC-D9	GCA TGG ACC GAC TTT CAT HTT CCC	58	degenerate primer
	TIC-D10	GCT GCA TTT GCA TGC CAW ART TCT GGC C	62	degenerate primer
	TIC-D12	CTG GTG GTT GGT TCC GSY YTG NAC YTG	64	degenerate primer
	TIC-D13	CAA TGG TTC TTT TTA TCC TTC NCA AAT GAT	55	degenerate primer
	TIC-D14	TGC TCT GCT GGC TTC ACY TGA ACT GC	62	degenerate primer
	TIC-D15	GCC AGA ACT ATG GCA TGC MAA TGC A	58	degenerate primer

	TIC-D17	CCT CAA AGC CTA GTA CAG ASS AGY AAC A	61	degenerate primer
	TIC-1F	GAA GAT CAT CTA CCA ACG GAT T	62	Pea specific primer
	TIC-1R	CCT GGT CTC GGT CTT TTA CTC T	66	Pea specific primer
	TIC-2F	CGA GAT AGA GAT CGC CGA AG	62	Pea specific primer
	TIC-2R	TGG CAA AGA CTT CAC AGA TCC	62	Pea specific primer
	TIC-3F	GAT CGC CGA AGT ATT GTA CGG	64	Pea specific primer for 5839 x Terese marker
	TIC-d3R	GCC ATC ACT AGC AGA AGA TTT ATT ATT ATC	80	Pea specific primer for 5839 x Terese marker
TOC1	DTOC1.1	CATGACATTTGCAAAAACATTCCTGTNATHATGATG	60	degenerated primer to isolate Pea orthologous gene
	DTOC1.2	GAACTTAGAAAYTTGTGGCAACAYRTNTGGMG	61	degenerated primer to isolate Pea orthologous gene
	DTOC1.3	AGTTGATAGGAGAGAAGCAGCATTGHTNAARTTYMG	62	degenerated primer to isolate Pea orthologous gene
	DTOC1.4	GATCCA CATTAATACCATTCAACTTHCTGACRAAYTGNCC	64	degenerated primer to isolate Pea orthologous gene
	TOC1P-6F	GGCAATTCGTCAGTAAGTTGAATGG	56	Specific Pea primer for IPCR
	TOC1P-6R	TCTGTCTGAATTTAAGCAATGCTGC	54	Specific Pea primer for IPCR
	TOC1P-3	CAGAAAAGAAAAGAGCGCTGC	52	Specific Pea primer for real time PCR
	TOC1P-4	AACACGAGGCCGCCTTTCTGC	68	Specific Pea primer for real time PCR
	TOC1-GSP1	AGTTGATAGGAGAGAAGCAGCATTGC	67	Specific primer for Genome Walking
	TOC1-GSP2	ATACCATTCAACTTACTGACGAATTGC	67	Specific primer for Genome Walking
	TOC1-7F	TATCCCGATGCTGGAATCTC	60	Specific primer for Genome Walking
	TOC1-7R	GCTCCTCAATAACAGCAGCA	60	Specific primer for Genome Walking
	TOC1-9F	GCAATAATCCCGAGGCTGG	60	Specific primer for Genome Walking
	TOC1-9R	CCAGCCTCGGGATTATTGC	60	Specific primer for Genome Walking
	TOC1-10F	GCTAGTATTGCCACTGCTGC	62	Specific primer for Genome Walking
	TOC1-10R	GCAGCAGTGGCAATACTAGC	62	Specific primer for Genome Walking

TOC1-8F	TTCTCTGATGACACAGACGAC	62	Medicago primer for isolation Pea ortholog
TOC1-8R	GACATAAGTGAAAAAGGCTGA	58	Medicago primer for isolation Pea ortholog

Primers used for mapping and genotyping

GENE	Primers	SEQUENCE	Tm (°C)	Restriction	Mapping population
ACETISOM	ACETISOM-F1	GATGGCAGGGCTACTAATGTTGC	60	MseI	Torsdag x Terese
	ACETISOM-R2	GGGGAAATGCAGGCAGACCCTC			
ALDO	Aldo-F	GAGAATTCCCCCTGCTGTCC	65	-	Torsdag x Terese (size marker)
	Aldo-R	CAGCATAATACTCAGTAGCACC			
CLPSER	CLP-F	GTATTGGAGGAGGATTTTAGGG	58	-	Torsdag x Terese (size marker)
	CLP-R	GCTTATGAGTTTGGAGGGGAGGGG			
IVDH	IVDH-2F	AGTATGGAGGGCTTGGTCTA	52	PciI	JI281 x JI399
	IVDH-2R	CCATTAGTACACCACATCTT			
Phot1b	Ps.Phot1b.F1	GTGGTGGTAGTGGTTCGAGG	58	NspI	Torsdag x Terese
	Ps.Phot1b.R1	CAATCCGTTGGGACGCAGCA			
PCFS4	PCFS4-2F	GTACGGTCCACCAGTTTTGC	52	BtgI	JI1794 x 5839
	PCFS4-2R	GGATCAAACTCAATGCCAAC			
TOE	TOE-3F	GAAGAGCGTCATTCTTTACGG	58	MlyI	Torsdag x Terese
	TOE-3R	TGACCTGGCCATTACTTTGC			

U131248	U131248-2F	GAGGATGATATGCTTTATCG	54	RsaI	Torsdag x Terese
	U131248-3R	GTCATCCGTGCTGTAGTTGC			
PEPTRANS	PEPTRANS-F1	GCCGTGATTCGGATCTGATGG	60	PciI	Torsdag x Terese
	PEPTRANS-R1	CGGTCGTATAAAGGAATGACTAC			
PUTTIP	PutTIP-F	CATGCTTTCTCACTATTTGCCGC	57	HpyCh4IV	Torsdag x Terese
	PutTIP-R	GCAACCAAAGGTTGATGTTGAGG			
THIOLP	ThiolP-F	CCGAAGAGGATTACCCCTAYCGTGC	55	MboII	Torsdag x Terese
	ThiolP-R	GCTTCTCCCCAGCTACCACCCC			
COLb	CO1P-1F	AGACGGAGTTGTGCCGGTGC	60	HphI	JI1794 x 5839
	CO1P-2R	ACGAATTGTCTTCTCGAACC			
ELF3	ELF3.GW4	GCAGTAATAGGCCAAAAACATTTCGG	62	TaqI	JI1794 x SLOW
	ELF3-2R	AACTCAAACACTTGGACTGC			
	ELF3-5GW-1F	AAATTGTTATCATTCCGAACACA	60	SpeI/HaeIII	5839 X 1794/1771
	ELF3-GW1	GGAATACTAAATTGCTCATACAAAGCC			
ELF4	ELF4-AluI	GTATTTAACAAATTTTGCACCCTTTCTAGC	50	AluI	JI281 x JI399
	ELF4.153.2	GTACAAGATTGAAGCAGAAGG			
	ELF4-GSP1	TCAGTCGGTGCTTGACAGGAACAGAGC	58	BfuAI	Torsdag x Terese (*dne-1* mutation)
	ELF4-GSP2	TGAGATCAGAATAAAGAGAAGCAACCTTTG			
HUA2	HUA2-3F	TCTTGTTGATTCTATCACCC	54	SspI	Torsdag x Terese
	HUA2-3R	TTTTCCTCTCAAGCCACAAC			
LUX	LUX-FLF	AACGGTTAGAAGAAGTGAATGG	58	-	ASP marker in Torsdag x Terese (*sn-1* mutation)

	LUX-SN1.2	CGGATTCGGCGGTTAGACGC			
	LUX-7R	GTTGGAAAGACCTTGCATCC			
	LUX8R	GGCCGTTTCAGCGTCGTTTC			
MYB1	MYB1.5'F1	GGTAGTGGCTGAGATTGG	60	TaqI	JI281 x JI399
	MYB1.5'R1	AACCACTTCTTCACCAGAGG			
PRR37	PRR37-5F	TGGCAACATGTTTGGAGAAG	58	TaqI	JI281 x JI399
	PRR37-5R	ACACTCAAGCCTCTGCTTCC			
	PRR37-5F	TGGCAACATGTTTGGAGAAG	60	XmnI	JI1794 x SLOW/5839
	PRR37-5R	ACACTCAAGCCTCTGCTTCC			
PRR59	PRR59-3F	ATGCATGTTGAGAGGTGCAG	60	RsaI	JI1794xSLOW
	PRR59-3R	AGCTTCCATGTTTGGCTTTG			
TIC	TIC-3F	GATCGCCGAAGTATTGTACGG	54	TaqI	Torsdag x Terese
	TIC-d3R	GCCATCACTAGCAGAAGATTTATTATTATC			

Primers used for RT-PCR

GENE	PRIMER	SEQUENCE	Tm('C)
ACT	ACT-F	GTG TCT GGA TTG GAG GAT CAA TC	59
	ACT-R	GGC CAC GCT CAT CAT ATT CA	
ELF4	ELF4P.1F	GTG CTT GAC AGG AAC AGA GC	56
	ELF4P.1R	CAG AAT AAA GAG AAG CAA CC	

MYB1	MYB1-Q1	GAC GGA TGC GCT AGA GAA GAA TGG	60
	MYB1-Q2	AGA ATA GAG CCC GAA ACG CAA GTC	
TOC1	DTOC1.3	AGT TGA TAG GAG AGA AGC AGC ATT GHT NAA RTT YMG	57
	DTOC1.4	GAT CCA CAT TAA TAC CAT TCA ACT THC TGA CRA AYT GNC C	
LATE1	GI-GSP4	GTT TCC CTA CTA TGG CAC AAG TTG ATT GC	60
	GI-12R	CCT TGG CTA TCC AGG GTT GC	
PRR37	PRR37-5F	TGG CAA CAT GTT TGG AGA AG	60
	PRR37-5R	ACA CTC AAG CCT CTG CTT CC	
PRR59	PRR59-2F	GGT ATC TGG CTA TGC ACT TCT CTC G	60
	PRR59-4R	CAA ACA TGC TGC CAC AGA TT	
ELF3	ELF3-GW4	GCA GTA ATA GGC CAA AAA CAT TTC GG	60
	ELF3-2R	AACTCA AACACTTGGACTGC	
LUX	LUX-Q1F	TTCTCACCCTCACATGTCTCC	56
	LUX-Q1R	TGGACGAAGTCACAATCAACA	
MYB2	MYB2P-1F	GGTGGACAGATG AAGAAC	56
	MYB2P-1R	CTTCTGAGCATGACTTCG	
PIM	PIM-4F	GCTTCAGAGTTTGGAACAGC	58
	PIM-6R	GACTCCATGGTGGTTTGG	
FTLa	FTLA-6F	GCCCAAGCAACCCTACTTTT	60
	FTL-A-2R	CCATCCTGGAGCGTAAACCC	
FTLb	FTL-B-3F	GGAAATGACCCCGTGATCTA	60

	FTL-B-5R	TGAATCCCTAAGTTGGGTCG	
FTLc	FTL.L1.8F	GATATTCCAGCCACAACAAGC	60
	FTL.L1.7R	TTATGACGCCACTCTGGAGCAA	
FTLe1	FTLe-1-F4	CCTTGTAATCCTCATATGAGAG	62
	FTLe-1-R5	CGTTGTTCCTGTAGTTGCTGG	
FTLe2	FTLe-2-F7	CGACTACCGGGACAGCATTT	62
	FTLe-2-R7	CAGGTGAACCAAGGTTATAAAC	

Other primers

GENE	NAME	SEQUENCE	Tm (°C)	Description
PGEM-T	PGEMT-F	GCC CGA CGT CGC ATG CTC C	55	Primers for pGEMT and pGEMT-easy plasmid
	PGEMT-R	GAG CTC TCC CAT ATG GTC G	55	Primers for pGEMT and pGEMT-easy plasmid
RACE-PCR	SMART.A	AAGCAGTGGTATCAACGCAGAGTACGCGGG	66	SMART-RACE PCR from Clontech
	3-CDS	AAGCAGTGGTATCAACGCAGAGTACTTTTTTTTTTTTTTTTTTTTTTTTTTTTT	62	SMART-RACE PCR from Clontech
	5-CDS	TTTTTTTTTTTTTTTTTTTTTTTT	38	SMART-RACE PCR from Clontech
	LUPA	CTAATACGACTCACTATAGGGCAAGCAGTGGTATCAACGCAGAGT	69	SMART-RACE PCR from Clontech

	SUP	CTAATACGACTCACTATAGGGC	53	SMART-RACE PCR from Clontech
	NUP	AAGCAGTGGTATCAACGCAGAGT	55	SMART-RACE PCR from Clontech
TOPO-GW	TOPO-GW-F	CGACGGCCAGTCTTAAGCTCGG	64	Primers for pCR8/GW/TOPO plasmid
	TOPO-GW-R	CACTATAGGGGATATCAGCTGG	60	Primers for pCR8/GW/TOPO plasmid
	TOPO-1F	CGCTAGCATGGATGTTTTCC	60	Primers for pCR8/GW/TOPO plasmid
	TOPO-1R	AGGGGATATCAGCTGGATGG	62	Primers for pCR8/GW/TOPO plasmid
ADAPTORS	GW-KA1	GCGCTGCAGGCATGCGAGCTCCCAAGCTTGATCG	72	Adaptor primer EcoRI for Genome Walking (KK)
	GW-KA2	AATTCGATCAAGCTTGGGAGCTCGCATGCCTGCAGCGC	71	Adaptor primer EcoRI for Genome Walking (KK)
	GW-KA3	GCGCTGCAGGCATGCGAGCTCCCA	66	Adaptor primer HindIII for Genome Walking (KK)
	GW-KA4	AGCTTGGGAGCTCGCATGCCTGCAGCGC	69	Adaptor primer HindIII for Genome Walking (KK)
	GW-KP1	GCGCTGCAGGCATGCGAGCTC	62	Primer for PCR for Genome Walking (KK)
	GW-AP1	GTAATACGACTCACTATAGGGC	60	Primer for PCR for Genome Walking (CLontech)
	GW-AP2	ACTATAGGGCACGCGTGGT	60	Primer for PCR for Genome Walking (CLontech)
	GW-ADAPT-1	GTAATACGACTCACTATAGGGCACGCGTGGTCGACGGCCCGGGCTGGT	76	Primer for Adaptor for Genome Walking (CLontech)
	GW-ADAPT-2	PO4-ACCAGCCC-NH2	36	Primer for Adaptor for Genome Walking (CLontech)

OLIGO dT	dT-A	TTTTTTTTTTTTTTA	Oligo dT primer for Reverse transcription
	dT-C	TTTTTTTTTTTTTTG	Oligo dT primer for Reverse transcription
	dT-G	TTTTTTTTTTTTTTC	Oligo dT primer for Reverse transcription

Appendix 2 – Referred publications

Liew, L. C., Hecht, V., Laurie, R. E., Knowles, C. L., Vander Schoor, J. K., Macknight, R. C., Weller, J. L., 2009. DIE NEUTRALIS and LATE BLOOMER 1 contribute to regulation of the pea circadian clock, The plant cell, 21(10), 3198-3211

Isolation of *Pseudo Response Regulator* genes and evaluation as candidate genes for photoperiod response loci

Lim Chee Liew[1], Valerie Hecht[1], Norman Weeden[2], James L Weller[1]

[1]School of Plant Science, University of Tasmania, Hobart, Tasmania 7001 Australia
[2]Department of Plant Science and Plant Pathology, Montana State University, Bozeman MT, USA

Introduction

The genetic control of flowering in pea has been studied for more than five decades, and several loci affecting photoperiod response are known (1). Mutations at the *Sn*, *Dne*, *Ppd* or *Hr* loci result in early-flowering under short-day conditions (2-5) whereas loss-of-function mutations in the *PhyA* or *Late1* genes cause late flowering under long-day conditions (6, 7). In Arabidopsis, many genes that affect photoperiodic flowering have a primary role in regulation of the circadian clock, and we recently showed that *Late1* is the pea ortholog of the clock-related Arabidopsis gene *GIGANTEA (GI)* (7). This study also showed that *Late1* interacts genetically with *Sn*, and that *sn* mutant impairs the diurnal expression rhythm of *Late1* (7). This provides the first direct evidence that *Sn* might be involved in the clock mechanism in some way.

One potential route to the identification of the *Sn* gene could be to assess homologs of Arabidopsis circadian clock-related genes as candidates. We previously isolated several clock-related genes in pea (8), but found that none of them mapped close to known photoperiod response loci. However, the list of potential candidate genes for these loci has been extended with recent identification of additional clock-related genes in Arabidopsis. Isolation of the corresponding pea genes has been greatly assisted by recent progress in sequencing of the Medicago genome and advances in comparative genome analysis between Medicago and pea (9-11).

Several recent studies have examined the contribution of the *PSEUDO RESPONSE REGULATOR* (*PRR*) gene family to the circadian clock mechanism (12-15). This family includes the core clock gene *TIMING OF CAB EXPRESSION 1* (*TOC1)* and four other members; *PRR9*, *PRR7*, *PRR5*, and *PRR3*. All five genes show diurnal and circadian regulation, with distinct peaks of expression that occur sequentially every 2 hours after dawn (12). This finding has suggested that like TOC1, other members of the "*PRR* quintet" might also form part of the central oscillator. We recently observed that the effect of the *sn* mutant on the expression of *LATE1* is similar to the effect of the *prr5 prr7 prr9* triple mutant on *GI* in Arabidopsis (16), raising the possibility that in some respects *Sn* might act similarly to *PRR* genes. We therefore set out to isolate *PRR* genes in pea, in order to examine their potential role within the pea circadian clock, and also their potential identity as candidate genes for photoperiod response loci.

Materials and Methods

Sequences of *PRR* homologs from *Medicago truncatula* and other species were obtained using tBLASTn searches of the Genbank database (http://www.ncbi.nlm.gov) and the Medicago EST database at http://compbio.dfci.harvard.edu. To isolate members of the *PRR* gene family in pea, degenerate primers were designed within conserved domains using the CODEHOP strategy (http://blocks.fhcrc.org/codehop.html) (17). The full length *PsPRR37* and partial *PsPRR59* cDNA were obtained by 5' and 3' RACE-PCR using the BD-SMART RACE cDNA amplification kit (CLONTECH). Protein alignments of various PRRs were performed with ClustalX (18) and adjusted using GENEDOC (Nicholas et al. 1997; http://www.psc.edu/biomed/genedoc). Relationships among PRR amino acid sequences were determined using phylogenetic analyses in PAUP* 4.0b10 (http://paup.csit.fsu.edu).

The origin of the WT line NGB5839 (cv. Torsdag *le-3*) and the *sn-2 and sn-4* mutants have been described previously (7, 19). The *sn-3* mutant is an additional recessive mutant isolated in the same screen as *sn-4* (7). All plants were grown in the Hobart phytotron, using previously-described growth media, light sources and phytotron conditions (7).

Information and approximate map positions of pea genes in the bottom half of LGVII was obtained from several published maps (20-22). To identify Medicago homologs of pea genes in this region, tBLASTx searches were performed against the Medicago genomic database at the J. Craig Venter Institute (http://www.jcvi.org/cgi-bin/medicago/index.cgi). The map positions of relevant genes were obtained by using Medicago Genome Browser (http://gbrowse.jcvi.org/cgi-bin/gbrowse/medicago_imgag/).

Results and Discussion

Identification of PRR homologs in Medicago truncatula

PRR proteins are characterized by two conserved domains; the Pseudo-regulator (PR) domain and the CONSTANS, CONSTANS-LIKE, and TOC1 (CCT) domain (12). Several reports have identified PRR genes in a number of species including rice (23), Lemna (24) and Populus (25). Phylogenetic analysis shows that these genes fall into three major groups, which can be designated as *PRR1*, *PRR59* and *PRR37*, on the basis of the Arabidopsis sequences they include (**Figure 1**). Two accessions from Lemna and one from rice (*OsPRR59)* show affinity to the *PRR59* clade at the sequence level, but fall outside this group in the phylogenetic analysis, most probably because they do not contain complete sequences for both conserved domains.

BLAST searches of the *Medicago truncatula* genomic (NCBI) and EST databases identified seven distinct *PRR* sequences, including three genomic and four ESTs. Additional EST contigs corresponding to three of the genomic sequences were also identified. Four of these sequences were predicted to encode full-length PRR proteins, including two in the *PRR59* clade and two in the *PRR37* clade. The remaining three EST sequences were only partial. Two distinct ESTs from the 5' region grouped with the partial pea *TOC1* sequence described previously, while the other from the 3' region did not show a clear relationship to any other PRR.

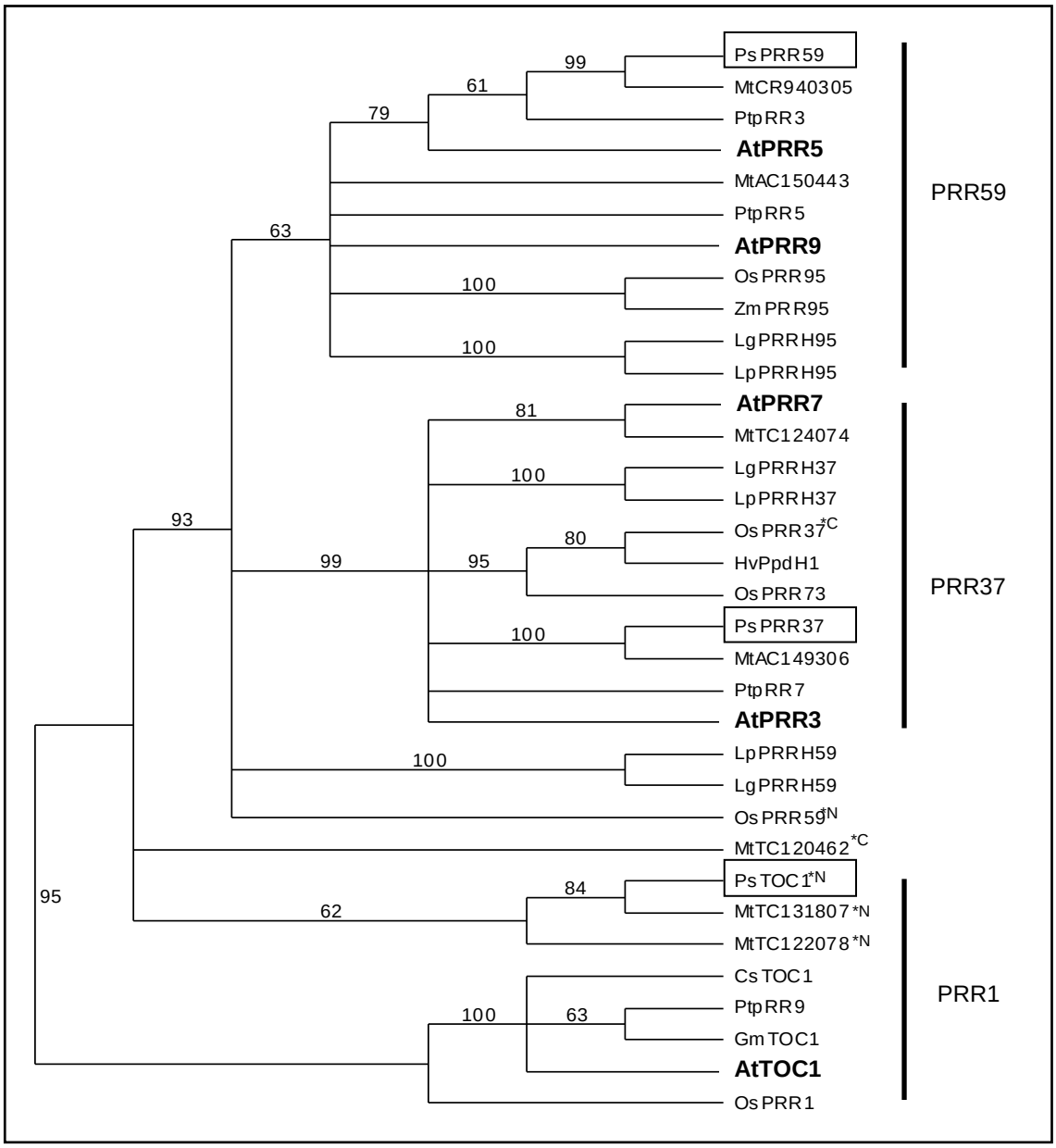

Figure 2. Phylogenic tree of PRRs. Amino acid sequences of PRR and CCT domains were aligned and used to produce the neighbour-joining tree as described in materials and methods. The bootstrap values are indicated as a percentage above each branch. Ps, *Pisum sativum*; Mt, *Medicago truncatula*; At, *Arabidopsis thaliana*; Lg, *Lemna gibba*; Lp, *Lemna paucicostata*; Os, *Oryza sativa*; Hv, *Hordeum vulgare*; Pt, *Populus trichocarpa*; Cs, *Castanea sativa*; Zm, *Zea mays*; Gm, *Glycine max*. ^C: sequence contains C-terminal; ^N: sequence contains N-terminal.

The three Medicago BAC contigs containing the genomic *PRR* sequences have all been assigned map positions (www.medicago.org), on chromosome 3 (CR940305), 7 (AC150443) and 4 (AC149306). These positions predict positions for the corresponding pea sequences in the middle of LGIII, near the top of LGV, and in the bottom half of LGVII, respectively. We noted in particular that AC149306 was located in a region of chromosome 4 corresponding to the region of pea LGVII known to contain the *Sn* locus. *Sn* was previously reported to show close linkage with the amylase locus *Amy1* (26) and was mapped between isozyme loci *Aldo* and *Gal2* (27) on the lower section of pea

linkage group VII. The similar positions of *MtPRR59* (CR940305) and the *Dne* locus also suggested a possible candidate gene relationship.

Isolation of PRR homologs from pea

Using degenerate primers targeting the PR and CCT domains two distinct fragments from the PR domain were amplified by PCR. These sequences were extended to both 5' and 3' ends using RACE PCR to obtain one partial (70%) and one full-length coding sequence. Phylogenetic analysis showed that these sequences belonged the *PRR59* and *PRR37* clades, respectively, and they were designated as *PsPRR59* and *PsPRR37*. Figure 1 shows that these sequences are apparent orthologs of the Medicago *PRR* genes on CR940305 and AC149306.

Mapping of PRR genes and evaluation of PsPRR37 as a candidate for Sn

Sequencing of *PRR59* and *PRR37* from mapping parents JI1794 and "Slow" identified polymorphisms that were used to map both genes in the RIL population derived from these parents (22). The results confirmed positions for *PRR59* in LGIII near *Dne* and for *PRR37* in LGVII, consistent with the positions predicted by the location of the orthologous Medicago genes. The relationship between *PRR59* and *Dne* was not explored further, as *Dne* as been identified as the pea ortholog of the Arabidopsis *ELF4* gene (28). However, for *PRR37*, no recombination was detected with the Amy locus on LGVII, and as *Amy* was previously noted to be tightly linked to *Sn* (26), this indicated that *PRR37* is in the region of *Sn*.

In order to carry out fine mapping of *Sn*, we also generated a new mapping population derived from a cross between the *sn-4* mutant in the NGB5839 background and cv, Térèse. Unfortunately, we found that the coding region of *PRR37* was identical in NGB5839 and Térèse, precluding the straight-forward mapping of *PRR37* relative to *Sn* in this cross. Instead, the entire coding sequence of *PRR* was determined from the three known induced *sn* mutants and from their isogenic wild-type lines Borek (*sn-2*) and NGB5839 (*sn-3* and *sn-4*). In all three cases the *PRR37* coding sequence was identical in mutant and wild-type, indicating that the *sn* phenotype does not result from a mutation that affects *PRR37* protein structure. It will obviously be of interest in future to isolate flanking sequence of *PRR37* and identify an appropriate polymorphism that will allow the cosegregation of *PRR37* and *Sn* to be directly tested.

A comparative map of the Sn *region*

As an aid to future mapping studies in the region of *Sn*, we generated a comparative map using markers anchored in published pea linkage maps and the Medicago physical map (**Figure 2**). This identified a broad region likely to contain *Sn*, bounded approximately by the *Aldo* and *Sod9* genes. In Medicago, the physical map of this region is estimated to span approximately 5Mb, although it still contains several gaps where adjacent BAC contigs are not yet joined. We are now using this information as a basis for the design of additional markers for the mapping of *Sn* and for the identification of other potential candidate genes. The first step will be the mapping of *Sn* relative to other markers shown.

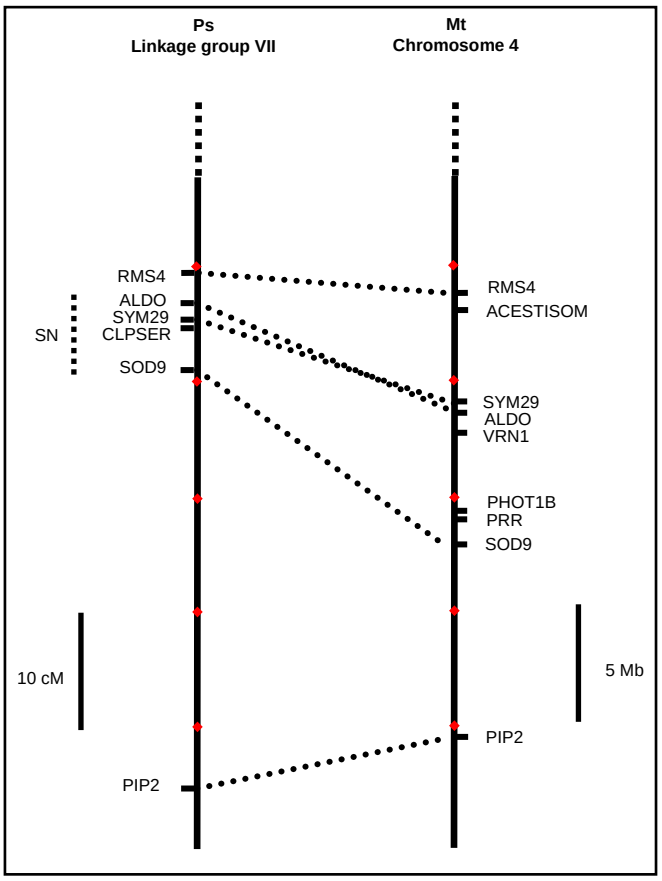

Figure 2. Comparative map between pea(Ps) and Medicago(Mt). Orthologous genes in the two species are joined by a dash line. The scale on the left give approximate recombination distances(cM) for pea linkage group VII whereas the scale on the right give approximate physical distance (Mb) for Medicago chromosome 4. Actual map postions of Medicago genes are as follows: *RMS4* (AC174294_7; 23.07), *ACETISOM* (AC135231_13; 22.98), *SYM29* (C149637_40; 19.15), *ALDO* (AC174316_9; 18.60), *VRN1* (AC137825_7; 17.85), *PHOT1B* (AC148218_19; 14.85), *PRR* (AC149306_58; 14.76), *SOD9* (AC126007_11; 13.63), *PIP2* (AC153003_20; 4.81)

1. Weller, J.L., *Update on the genetics of flowering.* Pisum Genetics, 2007. **39**: p. 1-8.
2. Murfet, I.C., *Flowering in Pisum: a three gene system.* Heredity, 1971. **27**: p. 93-110.
3. King, W.M. and I.C. Murfet, *Flowering in Pisum: a sixth locus, Dne.* Annals of Botany, 1985. **56**: p. 835-846.
4. Murfet, I.C. and S.A. Taylor, *Flowering gene Ppd in pea: map position and disturbed segregation of allele ppd-2.* Journal of Heredity, 1999. **90**(5): p. 548-550.
5. Murfet, I.C., *Flowering in Pisum. Hr, a gene for high response to photoperiod.* Heredity, 1973. **31**(2): p. 157-164.
6. Weller, J.L., et al., *A dominant mutation in the pea PHYA gene confers enhanced responses to light and impairs the light-dependent degradation of Phytochrome A.* Plant Physiology, 2004. **135**(4): p. 2186-2195.
7. Hecht, V., et al., *Pea LATE BLOOMER1 is a GIGANTEA ortholog with roles in photoperiodic flowering, deetiolation, and transcriptional regulation of circadian clock gene homologs.* Plant Physiology, 2007. **144**(2): p. 648-661.
8. Hecht, V., et al., *Conservation of Arabidopsis flowering genes in model legumes.* Plant Physiology, 2005. **137**(4): p. 1420-1434.
9. Choi, H.K., et al., *Estimating genome conservation between crop and model legume species.* Proceedings of the National Academy of Sciences of the United States of America, 2004. **101**: p. 15289-15294.

10. Kalo, P., et al., *Comparative mapping between Medicago sativa and Pisum sativum.* Molecular Genetics and Genomics, 2004. **272**: p. 235-246.
11. Zhu, H., et al., *Bridging model and crop legumes through comparative genomics.* Plant Physiology, 2005. **137**(4): p. 1189-1196.
12. Matsushika, A., et al., *Circadian waves of expression of the APRR1/TOC1 family of pseudo-response regulators in Arabidopsis thaliana: Insight into the plant circadian clock.* Plant and Cell Physiology, 2000. **41**(9): p. 1002-1012.
13. Matsushika, A., et al., *Characterization of circadian-associated pseudo-response regulators: I. Comparative studies on a series of transgenic lines misexpressing five distinctive PRR genes in Arabidopsis thaliana.* Bioscience, Biotechnology and Biochemistry, 2007. **71**(2): p. 527-534.
14. Nakamichi, N., et al., *Arabidopsis clock-associated Pseudo-Response Regulators PRR9, PRR7 and PRR5 coordinately and positively regulate flowering time through the canonical CONSTANS-dependent photoperiodic pathway.* Plant and Cell Physiology, 2007. **48**: p. 822-832.
15. Salome, P.A. and C.R. McClung, *PSEUDO-RESPONSE REGULATOR 7 and 9 are partially redundant genes essential for the temperature responsiveness of the Arabidopsis circadian clock.* The Plant Cell, 2005. **17**(3): p. 791-803.
16. Nakamichi, N., et al., *PSEUDO-RESPONSE REGULATORS, PRR9, PRR7 and PRR5, together play essential roles close to the circadian clock of Arabidopsis thaliana.* Plant and Cell Physiology, 2005. **46**(5): p. 686-698.
17. Rose, T.M., et al., *Consensus-degenerate hybrid oligonucleotide primers for amplification of distantly related sequences.* Nucleic Acids Research, 1998. **26**(7): p. 1637-1644.
18. Thompson, J.D., et al., *The ClustalX windows interface: flexible strategies for multiple sequence alignment aided by quality analysis tools.* Nucleic Acids Research, 1997. **24**: p. 4876-4882.
19. Arumingtyas, E.L. and I.C. Murfet, *Flowering in Pisum: a further gene controlling response to photoperiod.* Journal of Heredity, 1994. **85**: p. 12-17.
20. Aubert, G., et al., *Functional mapping in pea, as an aid to the candidate gene selection and for investigating synteny with the model legume Medicago truncatula.* Theoretical and Applied Genetics 2006. **112**: p. 1024-1041.
21. Laucou, V., et al., *Genetic mapping in pea. 1. RAPD-based genetic linkage map of Pisum sativum.* Theoretical and Applied Genetics, 1998. **97**: p. 905-915.
22. Weeden, N.F., et al., *A consensus linkage map for Pisum sativum.* Pisum Genetics, 1998. **30**: p. 1-4.
23. Murakami, M., et al., *The evolutionarily conserved OsPRR Quintet: rice Pseudo-Response Regulators implicated in circadian rhythm.* Plant and Cell Physiology, 2003. **44**(11): p. 1229-1236.
24. Miwa, K., et al., *Conserved expression profiles of circadian clock-related genes in two Lemna species showing long-day and short-day photoperiodic flowering responses.* Plant and Cell Physiology, 2006. **47**(5): p. 601-12.
25. Tuskan, G.A., et al., *The Genome of Black Cottonwood, Populus trichocarpa (Torr. & Gray).* Science, 2006. **313**(5793): p. 1596-1604.
26. Weeden, N.F., B.E. Kneen, and I.C. Murfet, Pisum Newsletter, 1988. **20**: p. 49-51.
27. Murfet, I.C. and L.J. Sherriff, *Confirmation that the sn locus is between Aldo and Gal2 in linkage group VII of pea.* Pisum Genetics, 1996. **28**: p. 13-14.
28. Liew, L.C., et al., *DIE NEUTRALIS and LATE BLOOMER 1 contribute to regulation of the pea circadian clock.* The Plant Cell, 2009. **21**: p. 3198-3211.